

JUNE 1974

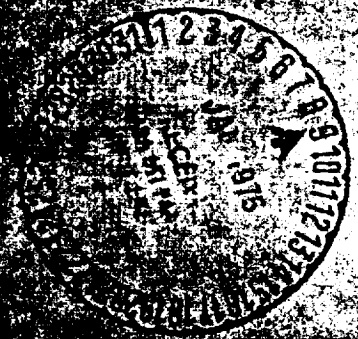
NASA CR-

140386

VOLUME 1 CHARACTERIZATION AND OPTIMIZATION OF FILTRATION DEVICES

FINAL REPORT  
SHUTTLE  
FILTER  
STUDY


|  |              |
|--|--------------|
| (NASA-CR-140386) SHUTTLE FILTER STUDY.   | N75-13913    |
| VOLUME 1: CHARACTERIZATION AND OPTIMIZATION OF FILTRATION DEVICES Final Report (Wintec Corp., Los Angeles, Calif.) 158 p HC \$6.25 | Unclas 05005 |
| CSCL 22B   | G3/18        |



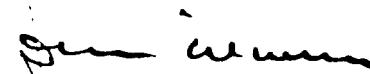
VOLUME I CHARACTERIZATION AND OPTIMIZATION OF FILTRATION DEVICES

**FINAL REPORT**  
**SHUTTLE**  
**FILTER**  
**STUDY**

Approved



J.R. Buckingham  
Program Manager



John Winzen  
Technical Director

Prepared for

National Aeronautics and Space Administration  
Lyndon B. Johnson Space Center  
Houston, Texas

Prepared by

WINTEC DIVISION  
BRUNSWICK CORPORATION  
Los Angeles, California

## FOREWORD

The original program, "Cryogenic Filter Study," was initiated in September, 1971, and was amended in June, 1971, and June, 1972, to include the broader aspects of overall contaminant management of all Space Shuttle related fluid systems. The program was conducted by the Wintec Corporation, Los Angeles, California, for the NASA - Johnson Space Center, Houston, Texas, under Contract NAS 9-11264. The effort was performed under the technical direction of the NASA - JSC project manager, Mr. James W. Akkerman, of the Propulsion and Power Division. The Wintec program manager was Mr. James R. Buckingham. Performance of the program was actually conducted at two locations: Wintec Corporation, Los Angeles, California, and the NASA - JSC White Sands Test Facility.

Support and assistance was furnished by Messrs. Brian A. Wilson, Frank B. Jones and Raymond Perrone, of the Wintec Engineering Department. A number of the filter materials tested were furnished free of charge by the manufacturer, in particular, G. Bopp & Company, Zurich, Switzerland, and Tobler, Ernst and Traber, Elmsford, New York.

Acknowledgement is also made of other major contributors to this program. Dr. Craig Smith, of Applied Nucleonics, conducted the development of the radioactive tracer techniques and performed the component wear analyses. Messrs. J. Brewer and J. Horner, of the UCLA Nuclear Energy Laboratory, assisted with the irradiations. Mr. Rod Bailey, of Moog, Inc., assisted with planning the component sensitivity test program of a bi-propellant valve. In addition, Rocketdyne Division of Rockwell International, Consolidated Controls Corporation, Parker Aircraft and NASA - KSC made available components for tests conducted during the Contaminant Generation Analysis phase of the program.

Finally, acknowledgement is made of the substantial assistance provided by Messrs. I.D. Smith and R. Tillet, of the NASA - JSC White Sands Test Facility, where certain portions of the test program were conducted.

## ABSTRACT

This report covers the results of a program to develop a new technology base for filtration equipment and comprehensive fluid particulate contamination management techniques, as related to the NASA - JSC Space Shuttle and Space Station projects. The scope of the program was divided into the following three basic task categories.

### I. Characterization and Optimization of Filtration Devices.

This task included an evaluation of state of the art literature, definition of technology gaps, evaluation of candidate filter media, testing of these media in various liquids and gases, selection and standardization of the optimum media, formulation of mathematical models or design guides for predicting filter performance, definition of standardized filter configurations and the development of a new type of filter - monitoring device.

### II. Characterization of Contaminant Generation and Contaminant Sensitivity at the Component Level.

This task included contaminant generation, or wear analysis studies of typical spacecraft components using radioactive tracer techniques. In addition, components were tested to determine their susceptibility to particulate contamination.

### III. Development of a Comprehensive Particulate Contamination Management Plan For Space Shuttle Fluid Systems.

This task comprised the preparation of a document which establishes the general contamination management requirements for flight vehicle and associated ground support equipment for the Shuttle program. This document contains procedures and specifications for the prevention and control of particulate contamination as developed during tasks I and II.

## CONTENTS OF FINAL REPORT

The report covering the work performed under this contract has been divided into three separate volumes as shown below.

VOLUME I: FILTER CHARACTERIZATION

VOLUME II: COMPONENT STUDIES  
Contaminant Generation  
Contaminant Sensitivity

VOLUME III: APPENDIX  
Test Data Tables  
Test Graphs  
Test Procedures  
Contaminant Adder  
WSTF Tests

CONTENTS OF VOLUME I

|  | <u>Page</u> |
|--|-------------|
| SECTION 1: INTRODUCTION .....  | 1           |
| SECTION 2: SUMMARY .....   | 2           |
| SECTION 3: TASK I, CHARACTERIZATION AND OPTIMIZATION OF FILTRATION DEVICES ..... | 5           |
| 3.1 Objectives of Task I .....   | 5           |
| 3.2 Evaluation of Existing Literature .....                                      | 5           |
| 3.3 Terminology and Definitions .....  | 7           |
| 3.4 Description of Test Media .....  | 7           |
| 3.5 Filter Media Tests - Flow Resistance .....                                   | 8           |
| 3.5.1 Liquid Flow Resistance Tests .....   | 8           |
| 3.5.2 Gaseous Flow Resistance Tests .....  | 22          |
| 3.5.3 Etched Disc Flow Resistance Tests .....                                    | 28          |
| 3.6 Filter Media Tests - Contaminant Tolerance .....                             | 33          |
| 3.6.1 Contaminant Tolerance Criteria .....                                       | 33          |
| 3.6.2 Evaluation of Test Fixture System and Methods .....                        | 34          |
| 3.6.3 Contaminant Tolerance Tests - Gas .....                                    | 41          |
| 3.6.4 Contaminant Tolerance Tests - Liquids .....                                | 50          |
| 3.7 Filter Media Tests - Filtration Rating .....                                 | 72          |
| 3.7.1 General Criteria .....   | 72          |
| 3.7.2 Retention Index Tests .....  | 72          |
| 3.7.3 Transmission Tests .....   | 78          |
| 3.7.4 Bubble Point Tests .....   | 80          |
| 3.7.5 Boiling Pressure Tests .....   | 81          |
| 3.8 Mathematical Models for Flow Resistance .....                                | 84          |
| 3.8.1 Liquid Flow .....  | 84          |
| 3.8.2 Gas Flow .....   | 106         |
| 3.9 Filter Performance Design Guides .....                                       | 114         |
| 3.9.1 Specific Flow Index .....  | 114         |
| 3.9.2 Glass Bead Rating Versus Specific Flow Index .....                         | 114         |
| 3.9.3 Contaminant Tolerance Index .....  | 114         |
| 3.9.4 Contaminant Tolerance Index Versus Specific Flow Index .....               | 116         |
| 3.9.5 Filter Area Requirement .....  | 118         |
| 3.10 Filter Design Optimization .....  | 121         |
| 3.10.1 Filter Configurations .....   | 121         |
| 3.10.2 Filter Media .....  | 128         |
| 3.10.3 Filter Cleanliness .....  | 129         |
| 3.11 Prototype Filter Development .....  | 130         |
| SECTION 4: TASK II, CONTAMINANT GENERATION AND SENSITIVITY TESTS .....           | 133         |
| 4.1 Contaminant Generation Tests .....   | 133         |
| 4.2 Contaminant Sensitivity Tests .....  | 133         |
| SECTION 5: TASK III, CONTAMINATION MANAGEMENT PLAN .....                         | 135         |
| SECTION 6: CONCLUSIONS AND RECOMMENDATIONS .....                                 | 137         |
| SECTION 7: REFERENCES .....  | 139         |
| 7.1 Terminology and Definitions .....  | 139         |
| 7.2 List of Publications .....   | 143         |

**TABLES**

| <u>Table<br/>Number</u> | <u>Title</u>   | <u>Page</u> |
|-------------------------|--|-------------|
| 1                       | Summary of Standardized Fluid Cleanliness Levels and Filter Media.....                             | 3           |
| 2                       | Spacecraft Fluids and Operational Parameters.....  | 6           |
| 3                       | Physical Properties of Porous Media.....   | 9           |
| 4                       | List of Figures for Flow Resistance Tests.....   | 12          |
| 5                       | Density and Viscosity of Gases at 75°F.....  | 22          |
| 6                       | Initial Bubble Point Pressure for Etched Disc Filter.....  | 29          |
| 7                       | System Recovery Test Data.....   | 36          |
| 8                       | Figure Numbers for Contaminant Tolerance Tests with Gas.....                                       | 41          |
| 9                       | Particle Size Distribution: AC Test Dust.....  | 54          |
| 10                      | Particle Size Distribution AC Coarse Dust - Number of Particles.....                               | 54          |
| 11                      | Particle Size Distribution and Content: Mixture 310-FTP.....                                       | 59          |
| 12                      | Contaminant Tolerance Index Data for Various Media and Fluids.....                                 | 65          |
| 13                      | Total Area Fraction of Limiting Orifices: TDDW and PDSW.....                                       | 68          |
| 14                      | Retention Index Test Data.....   | 74          |
| 15                      | Retention Index of TDDW Wire Cloth.....  | 74          |
| 16                      | Retention Index of TDDW Wire Cloth.....  | 76          |
| 17                      | Retention Index of Plain Dutch Single Weave Wire Cloth.....  | 76          |
| 18                      | Retention Index of Dutch Weave Media.....  | 77          |
| 19                      | Composition and Size Distribution: AC Coarse Dust - Zinc Sulfide<br>Mixture.....                   | 78          |
| 20                      | Largest Particle of Zinc Sulfide Transmitted Through Various Filter<br>Media.....                  | 79          |
| 21                      | Reynolds Number Through Filter Media.....  | 87          |
| 22                      | Calculated vs. Empirical Values for Flow Constant "a".....   | 92          |
| 23                      | Calculated vs. Empirical Values for Flow Constant "b".....   | 96          |
| 24                      | Physical Properties of Dutch Weave Wire Cloth Relative to Calculation<br>of Flow Constant "a"..... | 99          |
| 25                      | Empirical Values of Tortuosity Factor and Number of Major Flow Paths<br>for Various Media.....     | 100         |
| 26                      | Physical Properties of Dutch Weave Wire Cloth Relative to Calculation<br>of Flow Constant "b"..... | 101         |
| 27                      | Basic Flow Resistance Equations for Various Media.....   | 102         |
| 28                      | Flow Resistance Equations for Nitrogen at 50 PSIA.....   | 106         |
| 29                      | Basic Flow Resistance Equations for Gas.....   | 109         |
| 30                      | Contaminant Flow Factor vs. Area Flow Factor: 325 X 2300 TDDW.....                                 | 118         |
| 31                      | Contaminant Tolerance Index for 325 X 2300 TDDW.....   | 120         |
| 32                      | Recommended Filter Media.....  | 128         |

## ILLUSTRATIONS

| <u>Figure<br/>Number</u> | <u>Title</u>   | <u>Page</u> |
|--------------------------|--|-------------|
| 1                        | Liquid Flow Resistance Test Housing.....                   | 10          |
| 2                        | Liquid Flow Test Schematic.....                            | 10          |
| 3                        | Flow Resistance of TDDW Wire Cloth in Water.....           | 13          |
| 4                        | Flow Resistance of PDSW Wire Cloth in Water.....           | 13          |
| 5                        | Flow Resistance of BMT Wire Cloth in Water.....            | 14          |
| 6                        | Flow Resistance of TSW Wire Cloth in Water.....            | 14          |
| 7                        | Flow Resistance of PSW Wire Cloth in Water.....            | 15          |
| 8                        | Flow Resistance of Synthetic Cloth in Water.....           | 15          |
| 9                        | Flow Resistance of Metal Fiber Structures.....             | 16          |
| 10                       | Flow Resistance of Powdered Metal Structures in Water..... | 16          |
| 11                       | Flow Resistance of Membranes in Water.....                 | 17          |
| 12                       | Flow Resistance of TDDW Wire Cloth in Mil-H-5606.....      | 17          |
| 13                       | Flow Resistance of PDSW Wire Cloth in Mil-H-5606.....      | 18          |
| 14                       | Flow Resistance of PSW Wire Cloth in Mil-H-5606.....       | 18          |
| 15                       | Flow Resistance of Various Filter Media in JP-4.....       | 19          |
| 16                       | Flow Resistance of TDDW & PDSW in Water - Glycol.....      | 19          |
| 17                       | Flow Resistance of TDDW in Liquid Nitrogen.....            | 20          |
| 18                       | Flow Resistance of PDSW in Liquid Nitrogen.....            | 20          |
| 18A                      | Flow Resistance of TDDW in Liquid Oxygen.....              | 20A         |
| 18B                      | Flow Resistance of PDSW in Liquid Oxygen.....              | 20A         |
| 18C                      | Flow Resistance of TDDW in Liquid Hydrogen.....            | 20B         |
| 18D                      | Flow Resistance of PDSW in Liquid Hydrogen.....            | 20B         |
| 19                       | Effect of Medium Type on Flow Resistance.....              | 21          |
| 20                       | Effect of Fluid Characteristics on Flow Resistance.....    | 21          |
| 21                       | Gas Flow Test Fixture.....                                 | 23          |
| 22                       | Gas Flow Test Schematic.....                               | 23          |
| 23                       | Comparative Flow Resistance of TDDW in Nitrogen.....       | 24          |
| 24                       | Flow Resistance of TDDW in Oxygen (SCFM).....              | 24          |
| 25                       | Flow Resistance of TDDW in Oxygen (ACFM).....              | 25          |
| 26                       | Flow Resistance of TDDW in Helium (SCFM).....              | 25          |
| 27                       | Flow Resistance of TDDW in Helium (ACFM).....              | 26          |
| 28                       | Flow Resistance of TDDW in Hydrogen (SCFM).....            | 26          |
| 29                       | Flow Resistance of TDDW in Hydrogen (ACFM).....            | 27          |
| 30                       | Effect of Gas Characteristics on Flow Resistance.....      | 27          |



| <u>Figure Number</u> | <u>Title</u>   | <u>Page</u> |
|----------------------|--|-------------|
| 31                   | Etched Labyrinth Disc Filter Pattern.....                                      | 30          |
| 32                   | Comparative Flow Resistance, Etched Labyrinth Disc in Water.....               | 30          |
| 33                   | Comparative Flow Resistance, Etched Labyrinth Disc in Isopropanol.....         | 31          |
| 34                   | Comparative Flow Resistance, 10 Micron Etched Labyrinth Disc in Nitrogen.....  | 31          |
| 35                   | Comparative Flow Resistance, 20 Micron Etched Labyrinth Disc in Nitrogen.....  | 32          |
| 36                   | Comparative Flow Resistance, 40 Micron Etched Labyrinth Disc in Nitrogen.....  | 32          |
| 37                   | Contaminant Addition Manifold.....   | 35          |
| 38                   | Contaminant Addition Port.....   | 35          |
| 39                   | Flow Fixture Evaluation.....   | 38          |
| 40                   | Effect of Add Rate.....  | 38          |
| 41                   | Effect of Add Size.....  | 39          |
| 42                   | Effect of Dry vs. Slurry Adds.....   | 39          |
| 43                   | Effect of Dry vs. Slurry Adds at High Flow Rates.....                          | 40          |
| 44                   | Effect of Add Size and Interval at High Flow Rates.....                        | 40          |
| 45                   | Contaminant Tolerance of 30 x 250 TDDW Flowing Gaseous Oxygen (50 psi).....    | 42          |
| 46                   | Contaminant Tolerance of 80 x 700 TDDW Flowing Gaseous Oxygen (50 psi).....    | 42          |
| 47                   | Contaminant Tolerance of 165 x 1400 TDDW Flowing Gaseous Oxygen (50 psi).....  | 43          |
| 48                   | Contaminant Tolerance of 325 x 2300 TDDW Flowing Gaseous Oxygen (50 psi).....  | 43          |
| 49                   | Contaminant Tolerance of 80 x 700 TDDW Flowing Gaseous Oxygen (400 psi).....   | 44          |
| 50                   | Contaminant Tolerance of 165 x 1400 TDDW Flowing Gaseous Oxygen (400 psi)..... | 44          |
| 51                   | Contaminant Tolerance of 325 x 2300 TDDW Flowing Gaseous Oxygen (400 psi)..... | 45          |
| 52                   | Contaminant Tolerance of 30 x 250 TDDW Flowing Hydrogen (50 psi).....          | 45          |
| 53                   | Contaminant Tolerance of 80 x 700 TDDW Flowing Hydrogen (50 psi).....          | 46          |
| 54                   | Contaminant Tolerance of 165 x 1400 TDDW Flowing Hydrogen (50 psi).....        | 46          |
| 55                   | Contaminant Tolerance of 325 x 2300 TDDW Flowing Hydrogen (50 psi).....        | 47          |
| 56                   | Contaminant Tolerance of 30 x 250 TDDW Flowing Hydrogen (400 psi).....         | 47          |
| 57                   | Contaminant Tolerance of 80 x 700 TDDW Flowing Hydrogen (400 psi).....         | 48          |
| 58                   | Contaminant Tolerance of 165 x 1400 TDDW Flowing Hydrogen (400 psi).....       | 48          |
| 59                   | Contaminant Tolerance of 325 x 2300 TDDW Flowing Hydrogen (400 psi).....       | 49          |
| 60                   | GO <sub>2</sub> and GH <sub>2</sub> Test System (WSTF).....                    | 49          |
| 61                   | Contaminant Tolerance Comparison.....  | 51          |
| 62                   | Contaminant Tolerance Comparison.....  | 51          |
| 63                   | Contaminant Tolerance Comparison.....  | 53          |
| 64                   | Contaminant Tolerance of TDDW Wire Cloth (Water).....                          | 53          |
| 65                   | Contaminant Tolerance of 325 x 2300 TDDW in Water, AC Coarse Dust.....         | 55          |
| 66                   | Contaminant Tolerance of 325 x 2300 TDDW in Water, AC Fine Dust.....           | 55          |

| <u>Number</u> | <u>Title</u>  | <u>Page</u> |
|---------------|---|-------------|
| 67            | Contaminant Capacity of 325 x 2300 TDDW.....  | 57          |
| 68            | Contaminant Tolerance of 325 x 2300 TDDW, Water and PPO.....                                | 57          |
| 69            | Contaminant Tolerance of 325 x 2300 TDDW, Water and WSTF Dust.....                          | 58          |
| 70            | Contaminant Type Effect on Contaminant Tolerance.....                                       | 58          |
| 71            | Contaminant Tolerance vs. Flow Rate for $\Delta P$ Increases.....                           | 60          |
| 72            | Contaminant Tolerance of 30 x 150 PDSW in Various Fluids.....                               | 60          |
| 73            | Contaminant Tolerance of 80 x 400 PDSW in Various Fluids.....                               | 61          |
| 74            | Contaminant Tolerance of 2 x 120 x 650 PDSW in Various Fluids.....                          | 61          |
| 75            | Contaminant Tolerance of 165 x 800 PDSW in Various Fluids.....                              | 62          |
| 76            | Contaminant Tolerance of 165 x 1400 TDDW in Various Fluids.....                             | 62          |
| 77            | Contaminant Tolerance of 325 x 2300 TDDW in Various Fluids.....                             | 63          |
| 78            | Density of Mil-H-5606 and JP-4.....   | 63          |
| 79            | Viscosity of Water, JP-4 and Mil-H-5606.....  | 66          |
| 80            | Effect of Pleating on Contaminant Tolerance.....  | 66          |
| 81            | Contaminant Tolerance of 325 x 2300 TDDW.....   | 69          |
| 82            | Contaminant Tolerance Comparison Pleated Element vs. Flat Screen.....                       | 69          |
| 83            | Pleated Conical Filter.....   | 71          |
| 84            | Retention Index.....  | 75          |
| 85            | Boiling Point Test, TDDW.....   | 83          |
| 86            | Flow Resistance Curve Comparison, O.S.U. Equation.....                                      | 85          |
| 87            | Flow Resistance of 325 x 2300 TDDW.....   | 85          |
| 88            | Test Data Comparison to Calculated Curve of Flow Resistance (325 x 2300).....               | 104         |
| 89            | Test Data Comparison to Calculated Curve of Flow Resistance (165 x 1400).....               | 104         |
| 90            | Test Data Comparison to Calculated Curve of Flow Resistance (80 x 400).....                 | 105         |
| 91            | Test Data Comparison to Calculated Curve of Flow Resistance (Liquid Nitrogen).....          | 105         |
| 92            | Flow Resistance of 325 x 2300 TDDW (Nitrogen).....  | 107         |
| 93            | Flow Resistance of 165 x 1400 TDDW (Nitrogen).....  | 107         |
| 94            | Flow Resistance of 80 x 700 TDDW (Nitrogen).....  | 108         |
| 95            | Flow Resistance of 30 x 250 TDDW (Nitrogen).....  | 108         |
| 96            | Viscosity of Gases.....   | 110         |
| 97            | Correlation of Calculated Gas Flow Resistance to Actual Data Points 325 x<br>2300 TDDW..... | 112         |
| 98            | Correlation of Calculated Gas Flow Resistance to Actual Data Points 165 x<br>1400 TDDW..... | 112         |
| 99            | Correlation of Calculated Gas Flow Resistance to Actual Data Points 80 x<br>700 TDDW.....   | 113         |

| <u>Figure Number</u> | <u>Title</u>  | <u>Page</u> |
|----------------------|---|-------------|
| 100                  | Correlation of Calculated Gas Flow Resistance to Actual Data Points<br>30 x 250 TDDW.....                         | 113         |
| 101                  | Glass Bead Rating vs. Specific Flow Index.....  | 115         |
| 102                  | Glass Bead Rating vs. Contaminant Tolerance Index.....  | 115         |
| 103                  | Glass Bead Rating vs. Contaminant Tolerance Index.....  | 117         |
| 104                  | Contaminant Tolerance Index vs. Specific Flow Index.....  | 117         |
| 105                  | Area Required for Specific Filtration Requirements.....   | 119         |
| 106                  | Area Required for Specific Filtration Requirements.....   | 119         |
| 107                  | Contaminant Tolerance vs. Unit Flow Rate for $\Delta P$ Increase Above Clean Condition<br>325 x 2300 TDDW.....    | 122         |
| 108                  | Contaminant Tolerance vs. Unit Flow Rate for $\Delta P$ Increase Above Clean Condition<br>165 x 1400 TDDW.....    | 122         |
| 109                  | Contaminant Tolerance vs. Unit Flow Rate for $\Delta P$ Increase Above Clean Condition<br>80 x 700 TDDW.....      | 123         |
| 110                  | Contaminant Tolerance vs. Unit Flow Rate for $\Delta P$ Increase Above Clean Condition<br>30 x 250 TDDW.....      | 123         |
| 111                  | Contaminant Tolerance vs. Unit Flow Rate for $\Delta P$ Increase Above Clean Condition<br>2 x 120 x 650 PDSW..... | 124         |
| 112                  | Contaminant Tolerance vs. Unit Flow Rate for $\Delta P$ Increase Above Clean Condition<br>80 x 400 PDSW.....      | 124         |
| 113                  | Contaminant Tolerance vs. Unit Flow Rate for $\Delta P$ Increase Above Clean Condition<br>30 x 160 PDSW.....      | 125         |
| 114                  | Contaminant Tolerance vs. Unit Flow Rate for $\Delta P$ Increase Above Clean Condition<br>30 x 150 PDSW.....      | 125         |
| 115                  | Type I Spacecraft/GSE Interface Filter.....   | 126         |
| 116                  | Type III Component Filter.....  | 127         |
| 117                  | Prototype Sequential Strip Filter.....  | 132         |

## SECTION 1

### INTRODUCTION

With the conclusion of the Apollo program, the National Aeronautics and Space Administration has initiated the Space Shuttle program which includes, as its major objective, the development of a reusable space transportation system, and of long-life orbiting space stations. This program is predicated on multiple mission reusability of a spacecraft, implementation of simplified launch support operations and rapid turnaround refurbishment of the spacecraft orbiters. Maximum service life, reusability, commonality and maintainability of components and systems are prime prerequisites for this program, in order to achieve the economic and operational levels required for future space missions.

With the advent of reusable, long-life vehicles in space transportation, any problems encountered in previous one-mission systems, such as component failure caused by uncontrolled particulate contamination in the various fluid systems, will become considerably more critical.

Contamination particles existing in a typical fluid system originate from three different sources. These are:

1. Residual manufacturing debris in the fluid tankage and other fluid systems.
2. Contaminate particles in the on-loaded fluids.
3. System generated particles from the wear of components in normal operation.

All three of these sources will be significant on the space shuttle vehicle. Since a new drop tank will be coupled to a reusable orbiter and other new fluids loaded for each mission, the concentration of contaminants in the orbiter after a number of flights may be much higher than with the single burn vehicle. Also, since the number of operating cycles, which will be accomplished by the components in the orbiter system, will be greater than those for a one-use vehicle, the system generated contamination level is expected to increase proportionally. Finally, additional contamination will be introduced during overhaul and maintenance operations.

Present spacecraft and Ground Support systems, developed for the Apollo program, employ, for the most part, in-line filters which are brazed, welded, or mechanically connected into the fluid system. The design of these filters was seldom based on known fluid contamination levels or fluid characteristics, but rather on arbitrary parameters having little, if any, relation to actual fluid conditions or mission duty cycle requirements. The resultant size and performance efficiency of these filters varied considerably between systems and often added unnecessary weight, cost, complexity and failure modes.

Experience gained during the Apollo program, therefore, indicates a need for advanced contamination management planning so that components are protected from contamination to the degree that their contaminant sensitivity warrants, throughout their entire useful service life.

This program was initiated in order to provide an adequate technology base for the formulation of a logical, total contamination management plan to be implemented early in the design phase of the Shuttle program.

## SECTION 2

### SUMMARY

A program was completed to develop a new technology base for filtration equipment and comprehensive fluid particulate contamination management techniques, to be employed in the Space Shuttle program. The program included the following tasks:

- I. Characterization and Optimization of Filter Media and Filter Configurations
- II. Characterization of Contaminant Generation and Contaminant Sensitivity at the Component Level
- III. Development of a Comprehensive Particulate Contamination Management Plan For Onboard and GSE Fluid Systems

During Task I, a literature search was conducted and existing technology gaps were identified. A test matrix was developed and pertinent terminology and performance parameters were defined. Ten different types of filter media, in up to eight filtration ratings each, were selected and subjected to flow resistance, filtration capability and contaminant tolerance tests. The test data were reduced to mathematical models and design guides for predicting filter performance were developed. From this data, and from information furnished by NASA - JSC, four standard filtration ratings, or fluid cleanliness levels, were established for all Shuttle fluid systems (See Table 1). Evaluation of the performance characteristics of the various media tested resulted in standardization of four grades, of two types, of media which were recommended for application in all Space Shuttle fluid Systems. These media were selected because they provide the necessary degree of protection in terms of maximum particle size cut-off, while providing the best characteristics of flow resistance and tolerance to system contamination. Using these standardized media, three different types, or configurations, of filters were selected for specific installation points or utilization in a fluid system. Table 1 contains a summary of the standardized fluid cleanliness levels, applicable selected filter media and filter types.

Task II consisted of testing selected flight components to determine their sensitivity to fluid contamination and their self-generation characteristics. During this task, a technique using radioactive tracers for determining the contaminant generation characteristics of operating components was developed. This method involves irradiation of the critical wear parts of the component, followed by filtration of the effluent fluid from the operating component and analysis of generated matter by radiation measurement of the material on the filter. Only the radioactive matter, traceable to the component, is detected and measured, and this measurement is unaffected by the presence of extraneous particulate matter which may be in the system and collected on the filter. In addition, a procedure was developed for determining the degree of sensitivity of a component to particulate matter in the operating fluid. The method involves placing the standardized media upstream from the component and utilizing a pre-contaminated operating fluid. A series of tests is conducted using progressively coarser filter media until failure of the component occurs. This technique established the maximum filtration rating necessary to assure the planned operational life of the component in a contaminated system. The tests conducted during this phase of the program were reduced to standard procedures which are included in the report, and which make it possible to develop information relative to the selection of the proper filter medium to

be used for protective filtration, as well as, the correct size of the filter and optimum placement within the system.

During Task III, comprehensive contamination management requirements were established for flight vehicle and associated ground support equipment for the Space Shuttle program. The resultant Contamination Management Plan requires the contractor to generate and implement procedures to determine the proper size, type and location of filters to provide the necessary degree of protection for sensitive components. In addition, studies of component contaminant generation are suggested, in order to determine the type and amount of contaminant released into the fluid by the operating components. Surface cleanliness levels, assembly methods and test fluid controls commensurate with the requirements of the most sensitive component within the system are to be established by the contractor.

**TABLE 1**  
**SUMMARY OF STANDARDIZED FLUID CLEANLINESS LEVELS AND FILTER MEDIA**

| System Fluid Cleanliness Level | Maximum Particle Size (microns) * | Standard Filter Medium And Grade | SUGGESTED MEDIA FOR INSTALLATION SHOWN |                         |                                |
|--------------------------------|-----------------------------------|----------------------------------|--|-------------------------|--------------------------------|
|                                |                                   |                                  | S.C./GSE Interface (Type I)            | System Filter (Type II) | Component Interface (Type III) |
| A                              | 10 X 25                           | TDDW 325 X 2300                  | X                                      |                         |                                |
| B                              | 20 X 50                           | TDDW 165 X 1400                  |  | X                       |                                |
| C                              | 40 X 100                          | PDSW 80 X 400                    |  |                         | X                              |
| D                              | 100 X 250                         | PDSW 30 X 160                    |  |                         | X                              |

\* The maximum particle size expression consists of two numbers, the first being equivalent to the Glass Bead Rating (GBR) of the filter, and the second being a measure of the largest dimension of an unevenly shaped particle (MPR).

### SECTION 3

## CHARACTERIZATION AND OPTIMIZATION OF FILTRATION DEVICES

### TASK I

#### 3.1 OBJECTIVES OF TASK I

The objectives of Task I of this study were as follows:

- To determine the characteristics of currently available porous media so as to make it possible to standardize and optimize performance, maintainability and reliability of filtration devices to be used in flight or launch servicing systems.
- To determine the minimum number of distinct types of filtration devices required to provide maximum commonality of design and interchangeability between systems.
- To develop a means of continuous in-service monitoring of system fluid cleanliness trends and a method of determining and signalling the current condition of filters in terms of residual service-life to provide information necessary for planned maintenance.

The program was planned to meet these objectives after a limited review and evaluation of existing literature. Major effort was placed in the testing and development phases to maximize the availability of correlateable data to form a basis for the Integrated Contamination Management Plan described in Task III.

Certain guidelines were established during the early stages of the study to ensure applicability to the Space Shuttle program. The types of propellants and other operational fluids, and the proposed flow rates, pressures, temperatures and total quantity expended per mission, were set forth. These parameters are shown in Table 2.

#### 3.2 EVALUATION OF EXISTING LITERATURE

During the initial stages of the program, an effort was made to compile a list of published reports, books and articles, which could provide information relative to the objectives of the study. Two sources of information were utilized during this search: the Wintec Library of articles, books and reports, and the NASA, AIAA, and Engineering Index Files. Material from the latter sources was retrieved by computer under a program managed by WESRAC under a contract to NASA.

The computer search yielded a large number of titles associated with filters and filtration. Examination of the abstracts indicated that 36 merited further study. The Wintec Library, also, provided a large number of articles related to filter design, however, only 13 additional pieces of literature were found to contain material applicable to the program. A list of these 49 items, along with a brief discussion of the contents of each, is contained in Section 6 of this report.

Review of the published literature and reports shows that the work done by others can be classified in several distinct categories. For example, there is the classical work by A.E. Scheidegger, which concerns itself solely with the development of mathematical formulations of Flow Through Porous Media. In another category, are various articles by manu-



TABLE 2  
SPACECRAFT FLUIDS AND OPERATIONAL PARAMETERS

| Fluid                        | Subsystem  | Flow Rate   | Pressure  | Temp. | Total Flow/Mission          |
|------------------------------|--|-------------|-----------|-------|-----------------------------|
| LH <sub>2</sub>              | Attitude Control   | 4 lb/sec    | 30 psia   | 50°R  | 1000 lbs                    |
|                              | Orbital Man-<br>euvering Sys.  | 15 lb/sec   | 30 psia   | 50°R  | 4000 lbs                    |
|                              | Main Propulsion<br>System  | 400 lb/sec  | 30 psia   | 50°R  | 100,000 lbs                 |
|                              | Power System   | .2 lb/sec   | 30 psia   | 50°R  | 500 lbs                     |
| LO <sub>2</sub>              | Attitude Control   | 16 lb/sec   | 30 psia   | 175°R | 4000 lbs                    |
|                              | Orbital Man-<br>euvering Svs.  | 90 lb/sec   | 30 psia   | 175°R | 20,000 lbs                  |
|                              | Main Propulsion<br>System  | 2500 lb/sec | 30 psia   | 175°R | 500,000 lbs                 |
|                              | Power System   | .2 lb/sec   | 30 psia   | 175°R | 500 lbs                     |
| GH <sub>2</sub>              | Attitude Control   | 4 lb/sec    | 1500 psia | 300°R | 1000 lbs                    |
|                              | Fuel Cells   | 2.3 lb/sec  | 100 psia  | 540°R | 200 lbs                     |
| CO <sub>2</sub>              | Attitude Control   | 16 lb/sec   | 1500 psia | 350°R | 4000 lbs                    |
|                              | Fuel Cells   | 19 lb/hr    | 100 psia  | 540°R | 1500 lbs                    |
|                              | Breathing  | 15 lb/hr    | 50 psia   | 540°R | 100 lbs                     |
| He                           | Pressurization<br>(mainstage)  | 2 lb/sec    | 3000 psia | 540°R | 250 lbs                     |
|                              | Pressurization<br>(JP4)  | .001 lb/sec | 3000 psia | 540°R | 3 lbs                       |
|                              | Pressurization<br>(OAMS)   | .20 lb/sec  | 3000 psia | 40°R  | 40 lbs                      |
| H <sub>2</sub> O             | Life Support   | .1 lb/sec   | 20 psia   | 540°R | 300 lbs                     |
| Water-<br>Glycol             | Environmental  | .4 lb/sec   | 50 psia   | 540°R | Continuous<br>Recirculation |
| Flush-<br>ing Sol-<br>vents  | Not established at this time - expected to simulate spacecraft fluids and flow rates - only pressure reduced |             |           |       |                             |
| MIL-5606<br>Hydraulic<br>Oil | Controls   | 10 lb/sec   | 3000 psi  | 735°R | 1000 lbs                    |
| GN <sub>2</sub>              | Breathing  | 7.5 lb/sec  | 50 psia   | 540°R | 100 lbs                     |
| JP-4                         | Jet Engines  | 5 lb/sec    | 20 psia   | 540°R | 3000 lbs                    |

facturers of porous media, or other media, which cover the more narrow field of their flow resistance in a single fluid medium. Another category consists of application oriented reports, which concern themselves with specific products, such as surface tension devices, bubble separators, etc. Finally, there is considerable literature published by the filter industry regarding filter performance in fluid (mostly hydraulic oil) and employing specific filter media, artificial contaminants, and laboratory test methods designed to differentiate between various filter media, filter designs or manufacturers.

The reports, therefore, failed to provide characterization data on porous media performance, which could be applied to the fluids, products or system conditions of the Shuttle program.

### 3.3 TERMINOLOGY AND DEFINITIONS

The filter industry, over the years, has originated a number of terms and expressions relative to the performance characteristics of porous media and filter assemblies. Many of these terms, such as "absolute" or "nominal" filter rating, or "dirt holding capacity" are not sufficiently descriptive and, in many cases, are completely misleading as to their true meaning within the industry. A comprehensive list of terminology and definitions was, therefore, prepared in an effort to provide a common ground for communication between the filter designer and the user. This list is included in Section 6 of this report.

### 3.4 DESCRIPTION OF TEST MEDIA

Many types of porous media are currently available and are used for filtration of fluids. The various media can be segregated into several general classes, which are briefly described below.

#### Membranes

These media, generally, consist of thin sheets of organic material, such as cellulose esters, polyethylene, Teflon, etc., with closely controlled size pores. Manufacturing methods are generally proprietary.

#### Sintered Metal Powders

Powder metallurgy has developed several types of media that fall in this class. Originally, these materials were used as oil impregnated bearing materials, but their porosity and permeability characteristics were soon recognized by the filter industry as adaptable to filter media. In general, the manufacturing process consists of providing a mixture of spherical shaped particles chosen to provide the desired pore size. The mixture of particles is placed in a die or mold, compressed to the desired density, and then sintered to provide matrix integrity.

#### Fiber Felt

This material is formed by deposition of a mixture of fibers on a moving porous belt. The filtration rating is determined by the fiber size, the density and thickness of the felted material. In the case of the metal fiber felts, the deposited material is compressed to a pre-determined thickness and density, and sintered. This joins the intermixed fibers at all points of contact and minimizes migration of media from the filter sheet. Micron size rating is determined by selecting a proper fiber diameter and length and controlling the density and thickness of the finished product. Very fine filtration (down to 2 or 3 micron GBR) can be provided, coupled with relatively large contaminant tolerance caused by the ingestion of the fine particles within the body of the media. This type of medium, characteristically, filters out a much larger percentage of particles smaller than the glass bead rating or cut-off particle size of the medium.

### Square Weave Cloth

This material may be woven from strands of metal or synthetic material. A wide choice of material of construction is available. The type of weave may be Plain Square Weave, in which the strands pass over and under each other in alternating sequence, or Twilled Square Weave, in which the strands pass "over two, under two" in a staggered pattern. In both cases, the resultant pore is square shaped. The twilled construction is generally used for screens with wire counts in excess of 250 wires per inch.

### Dutch Weave Wire Cloth

These media differ from the Square Weave materials in that the warp wires are usually larger than the shute wires, and there are considerably more shute wires than warp wires. The Dutch Weaves are manufactured in two general types: Plain Weave and Twilled Weave. In both cases, the shute wires are always driven up together to minimize wire shift and loss of filtration rating. In the Plain Dutch Single Weave media, the shute wires pass over, then under, successive warp wires with each successive shute wire alternating the order. Thus, each warp wire has a series of shute wires above and below. The flow passage is formed by the intersection of two shute wires and the warp wire, and is triangular in shape. Twilled Dutch Single Weave is similar in construction, except that each shute wire passes over and under two warp wires in alternating succession. This type of weave is often called Broad Mesh Twill, and provides a generally looser weave (with resultant loss of filtration rating control) than provided by the Plain Dutch Single Weave. Twilled Dutch Double Weave is a complex type of woven mesh used to provide the finest filtration possible with wire mesh. It is similar in construction to the Twilled Dutch Single Weave, except that twice as many shute wires are used and each shute wire is slightly distorted to provide room for another shute wire beside it. While the shute wires in the Plain Dutch Weaves appear straight when viewed at right angles to the face of the screen, the Twilled Dutch Double Weave media show the distorted "zig-zag" appearance of the shute wires. There is always a shute wire directly above and below each warp wire, and the number of shute wires per inch is approximately twice that for Plain Dutch Single Weave for an equal filtration rating. All shute wires are driven up tight, which prevents wire shift and loss of filtration rating. As compared to the flow path provided by the Plain Dutch Single Weaves, the pore shape is also triangular, but the degree of tortuosity is approximately twice as great and the fluid must change direction several times in passing through. It is this degree of tortuosity that provides excellent control of the length dimension of particles.

Table 3 contains a summary of the physical characteristics of all ten (10) basic types of media, and their specific filtration grades which were tested during this program.

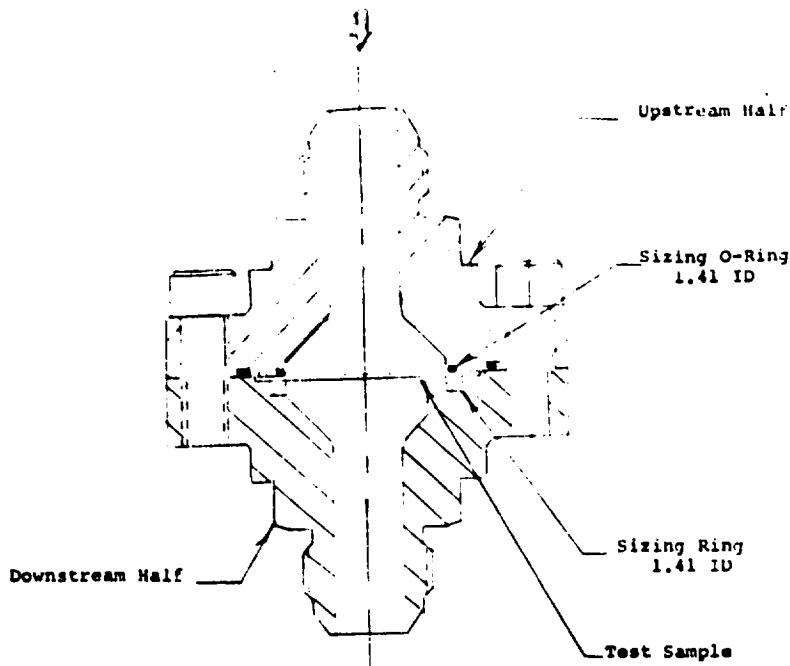
## 3.5 FILTER MEDIA TESTS - FLOW RESISTANCE TESTS

### 3.5.1 Liquid Flow Resistance Tests

Samples of the various porous media were tested in deionized water, hydraulic fluid (Mil-H-5606), JP-4 fuel, LN<sub>2</sub>, LO<sub>2</sub>, LH<sub>2</sub>, and a mixture of ethylene glycol and water (35%/65% by weight). The purpose of these tests was to determine the relationship between pressure drop and unit flow rate (GPM/in<sup>2</sup>) for the various media using fluids of widely differing physical characteristics.

Each sample of medium was cut in circular form to fit into a sample holder as shown in Figure 1. A "sizing ring" located beneath the sample of porous medium was used in conjunction with a sealing O-Ring above the sample to provide an exposed flow area of 1.584 square inches (1.41 diameter). Secondary O-Rings located outside the sample circumference serve to





POROUS MEDIA FLOW RESISTANCE  
TEST HOUSING

FIGURE 1

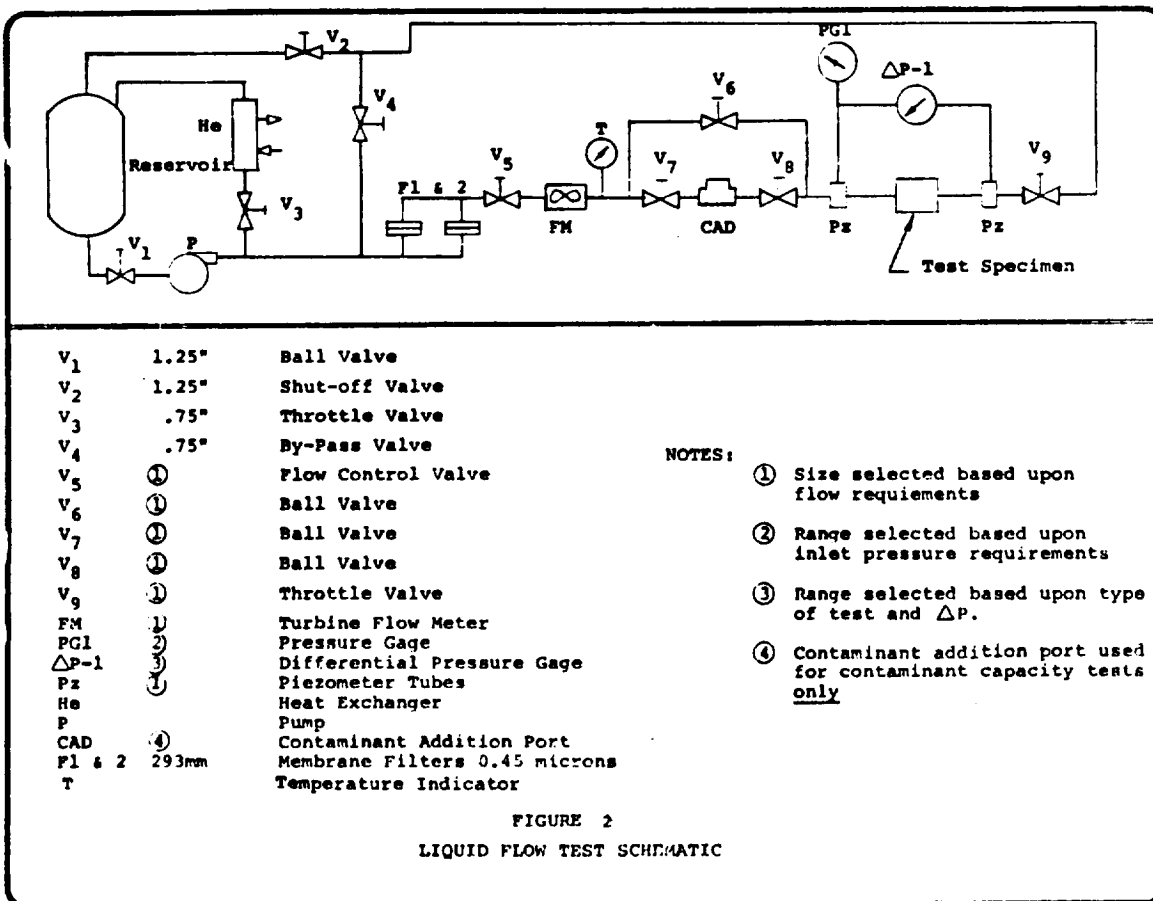


FIGURE 2

LIQUID FLOW TEST SCHEMATIC

seal the test fixture against external leakage.

During the flow resistance tests, no support was provided beneath the test sample, and differential pressures were limited to those values which would not cause distortion or "bellying" of the medium.

The sample test housing was mounted in a flow system as shown schematically in Figure 2. Initial tests were made at a series of flow rates with the test sample omitted from the housing. Pressure differential measurements were taken across the piezometer pick-up points at each flow rate to establish the system pressure drop, or "tare."

The sample of the porous medium was then cleaned and placed in the fixture. Flow was initiated and pressure differential across the piezometer pick-up was measured at several flow points. The "tare" values of pressure drop at each flow rate were then subtracted from the corresponding "gross" values to obtain the net pressure differential across the sample. The flow rates were then reduced to unit area, which allowed presentation of the data in terms of GPM/in<sup>2</sup> of exposed specimen area. Graphs showing the relationship between unit flow rate (GPM/in<sup>2</sup>) and pressure differential (psid) for each type of filter medium and each test liquid were plotted and are included as Figures 3 through 18 in this section of the report.

Table 4 summarizes all of the tests conducted and references the various figures containing the graphical presentations. Tables of the test data, from which the graphs were drawn, are included in the appendix, together with Test Procedure, TP-1, which describes, in detail, the method employed for these tests.

Figure Numbers 3 through 18 illustrate the effects of the physical characteristics of the test fluid on flow resistance. The slopes of the curves vary from 45° (slope of 1.0) to just above 63° (slope of 2.0) depending on the type of medium, the unit flow rate (GPM/in<sup>2</sup>) and the characteristics of the fluid.

Four factors can cause the slope to reach in excess of 1.0: a fluid with low viscosity or high density, a high unit flow rate and a simple nontortuous flow path. On the other hand, high viscosity, low density, low flow rate and high degrees of tortuosity of the flow path all tend to cause the slope to be lower.

These factors are illustrated by Figure 19, plotted from the previous curves, which shows the general effect of type of medium on the flow resistance curve. The curves all show flow resistance with water, and all media are rated at 20 microns glass bead rating (GBR). The two less complex structures, 2 X 120 X 650 and 850 X 850, both show higher slopes at the low end of the flow rate scale than the more tortuous materials, 165 X 1400 or sintered fiber felt (Dynalloy X-7). As the flow rate increases, however, all of the slopes approach 2.0.

Figure 20, also plotted from the previous curves, shows the effect of the fluid characteristics on flow resistance. The 165 X 1400 TDDW medium flow resistance is shown in Mil-H-5606 (sp. gr. 0.75, viscosity 10 cp), Water - Glycol (sp. gr. 1.05, viscosity 2.3 cp), Water (sp. gr. 1.0, viscosity 0.75 cp), and JP-4 fuel (sp. gr. 0.75, viscosity 0.62 cp). Here, it can be seen that not only is the total pressure differential affected by the fluid, but the shape of the curve is also affected. While the high viscosity of Mil-H-5606 raises the total pressure differential throughout the flow rate range, the same high viscosity causes the slope of the curve to be depressed.

The water - glycol mixture, with a density slightly more than water and one fourth that of Mil-H-5606, shows a pressure drop between the two and a slope higher than water, but lower

TABLE 4

LIST OF FIGURES - FLOW RESISTANCE TESTS

| Type of Medium                    | LIQUIDS |          |         |                         |      |                 |                 |                 |                |                | GASES |                |  |  |
|-----------------------------------|---------|----------|---------|-------------------------|------|-----------------|-----------------|-----------------|----------------|----------------|-------|----------------|--|--|
|                                   | Water   | Hyd. Oil | Alcohol | H <sub>2</sub> O-Glycol | JP-4 | LN <sub>2</sub> | LO <sub>2</sub> | LH <sub>2</sub> | N <sub>2</sub> | O <sub>2</sub> | He    | H <sub>2</sub> |  |  |
| Twilled Dutch Double Weave (TDDW) | 3       | 12       | 16      | 16                      | 15   | 17              | 18A             | 18C             | 23             | 24             | 26    | 28             |  |  |
| Plain Dutch Singel Weave (PDSW)   | 4       | 13       | 16      | 16                      | 15   | 18              | 18B             | 18D             | 25             | 27             | 29    |                |  |  |
| Twilled Dutch Single Weave (TDSW) | 5       |          |         |                         |      |                 |                 |                 |                |                |       |                |  |  |
| Plain Square Mesh Weave (PSW)     | 7       | 14       |         |                         | 15   |                 |                 |                 |                |                |       |                |  |  |
| Twilled Square Mesh Weave (TSW)   | 6       |          |         |                         | 15   |                 |                 |                 |                |                |       |                |  |  |
| Synthetic Cloths (PSW(S) )        | 8       |          |         |                         |      |                 |                 |                 |                |                |       |                |  |  |
| Metal Fiber Structures            | 9       |          |         |                         |      |                 |                 |                 |                |                |       |                |  |  |
| Sintered Metal Powder             | 10      |          |         |                         |      |                 |                 |                 |                |                |       |                |  |  |
| Membranes                         | 11      |          |         |                         |      |                 |                 |                 |                |                |       |                |  |  |
| Etched Discs                      | 32      |          |         |                         |      | 33              |                 |                 | 34             |                |       |                |  |  |
|                                   |         |          |         |                         |      |                 |                 |                 | 35             |                |       |                |  |  |
|                                   |         |          |         |                         |      |                 |                 |                 | 36             |                |       |                |  |  |

FIGURE 3

FLOW RESISTANCE OF TWILLED DUTCH DOUBLE WEAVE WIRE CLOTH

Fluid: Deionized Water @ 68-82°F

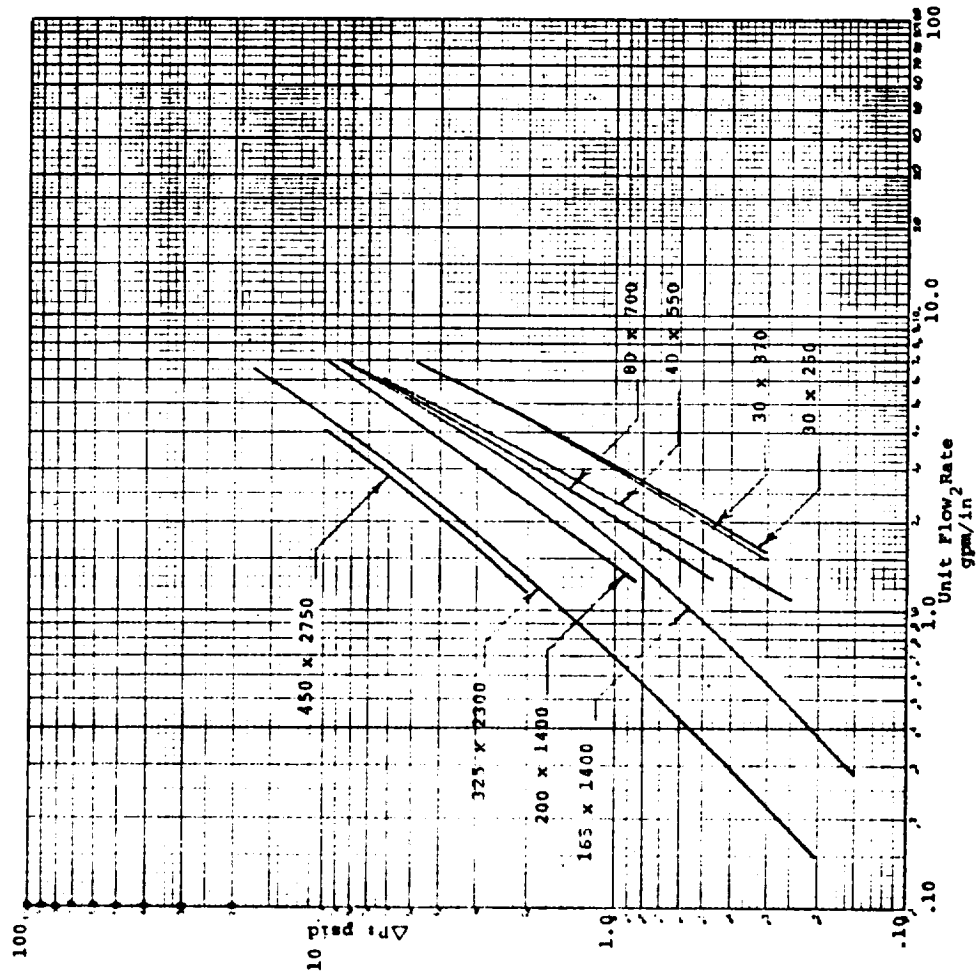


FIGURE 4

FLOW RESISTANCE OF PLAIN DUTCH SINGLE WEAVE WIRE CLOTH

Fluid: Deionized Water @ 65 - 68°F

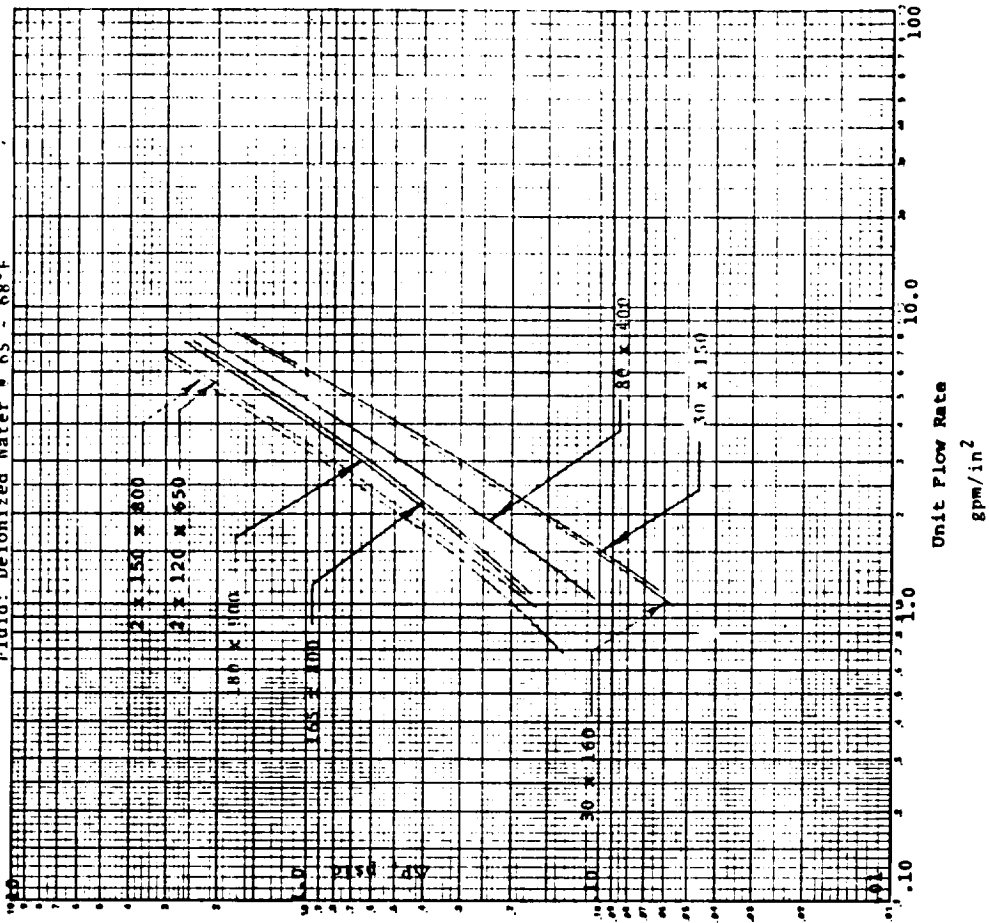




FIGURE 5  
 FLOW RESISTANCE OF 120 x 600 H-B-B BROAD MESH TWILLED  
 WEAVE WIRE CLOTH  
 Fluid: Deionized Water @ 76 - 77°F

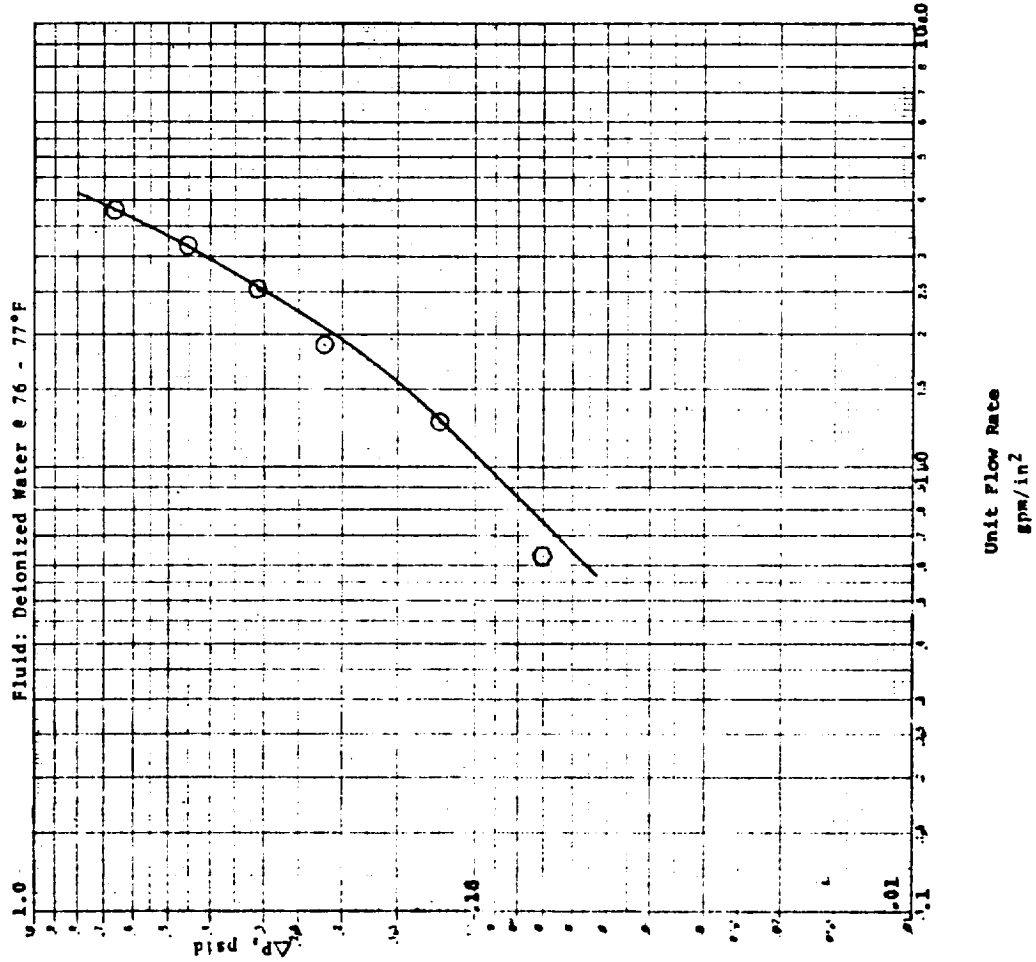


FIGURE 6  
 FLOW RESISTANCE OF TWILLED SQUARE WEAVE WIRE CLOTH  
 Fluid: Deionized Water @ 65-73°F

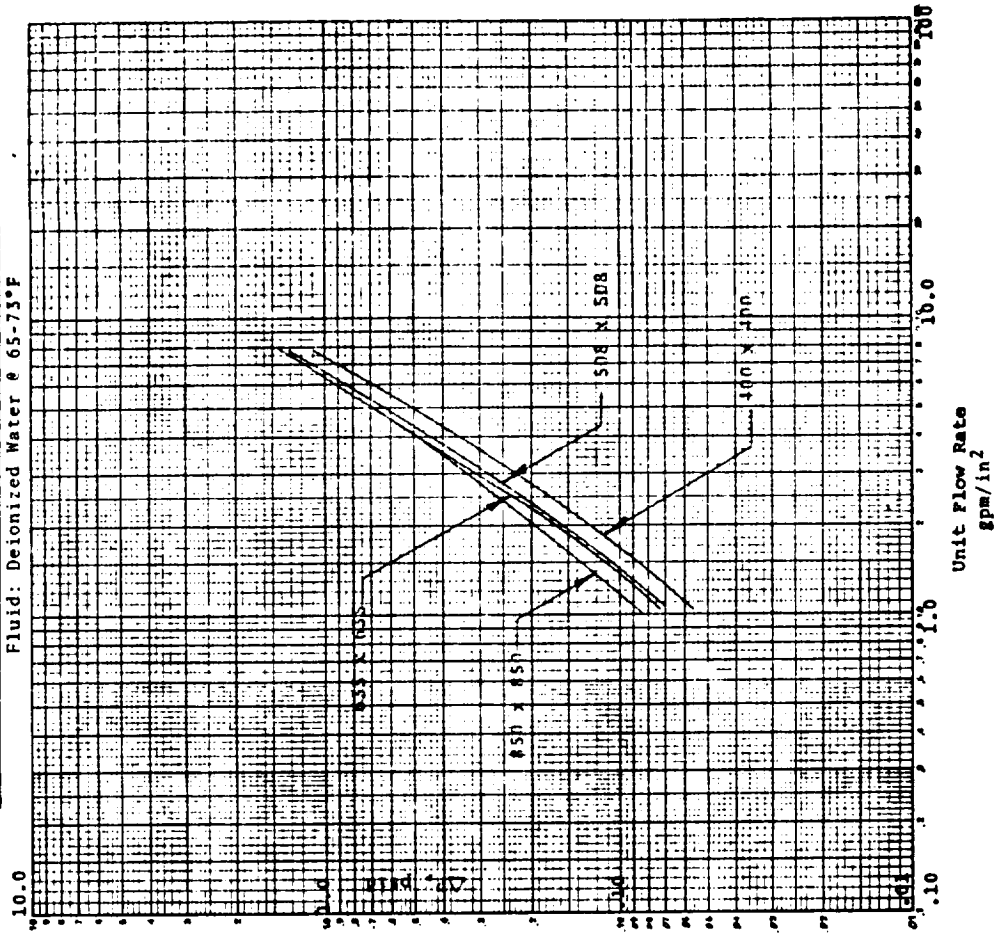


FIGURE 7  
FLOW RESISTANCE OF PLAIN SQUARE WEAVE WIRE CLOTH

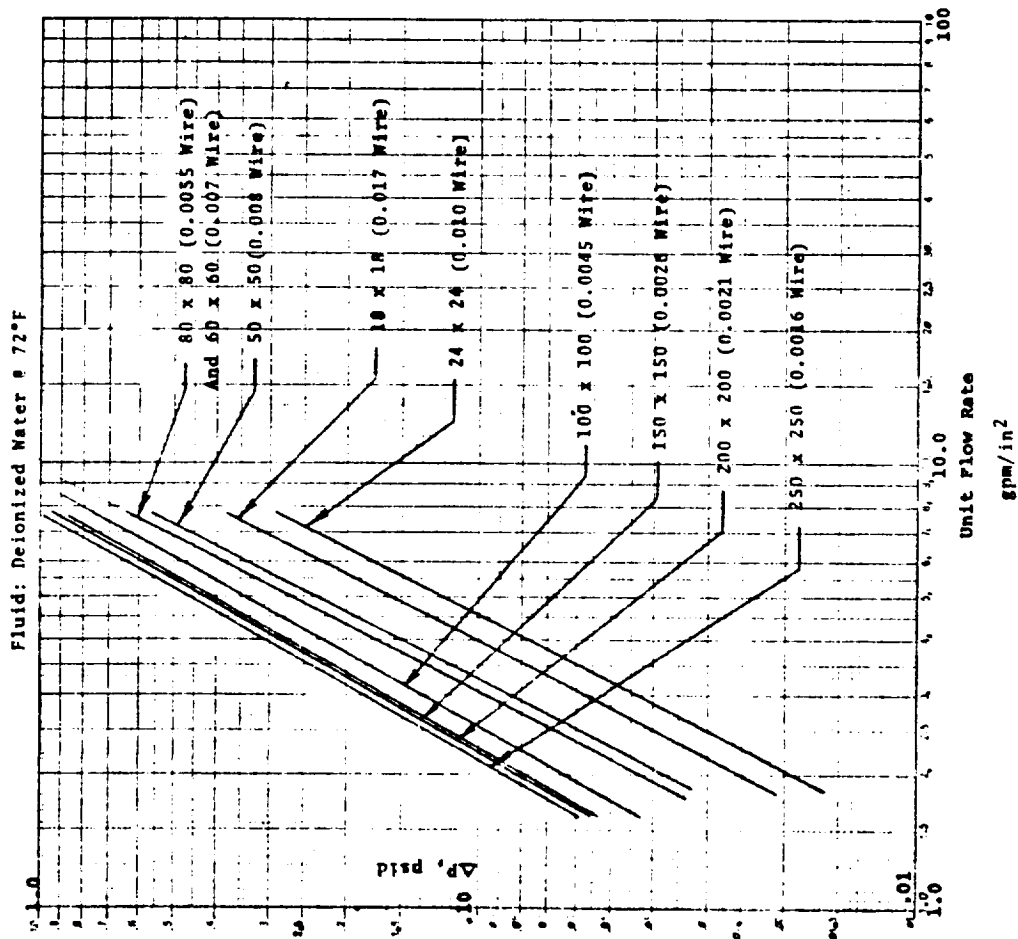


FIGURE 8  
FLOW RESISTANCE OF SYNTHETIC WOVEN CLOTH

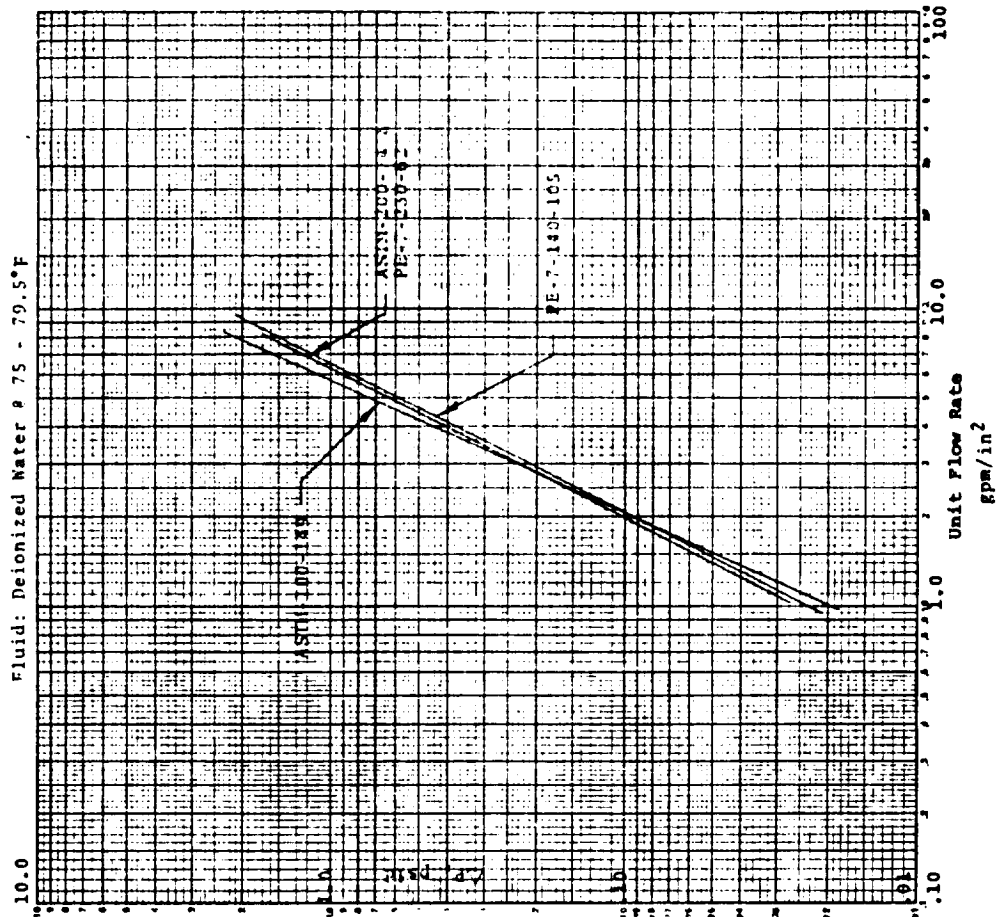


FIGURE 9  
 FLOW RESISTANCE OF METAL FIBER STRUCTURES  
 USING DEIONIZED WATER @ 68°F  
 (Grades are "Dynalloy X")

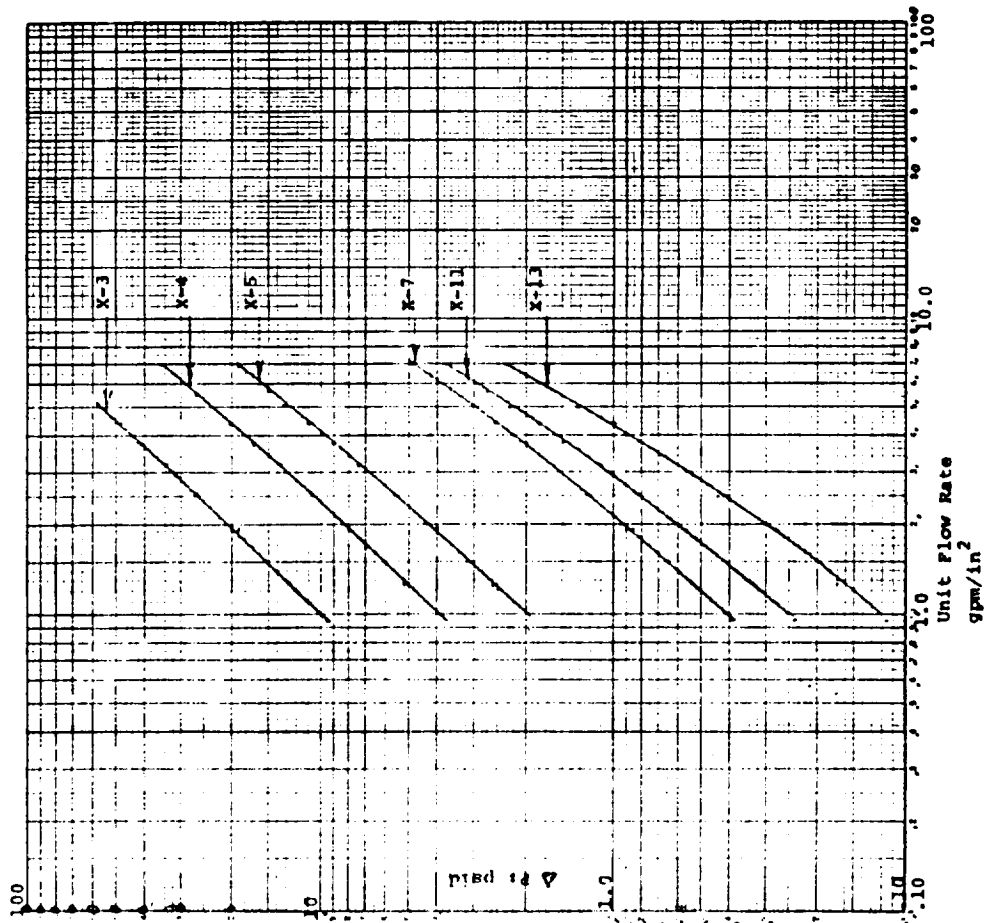


FIGURE 10  
 FLOW RESISTANCE OF POWDERED POROUS METAL STRUCTURES  
 Fluid: Deionized Water @ 78 - 79°F

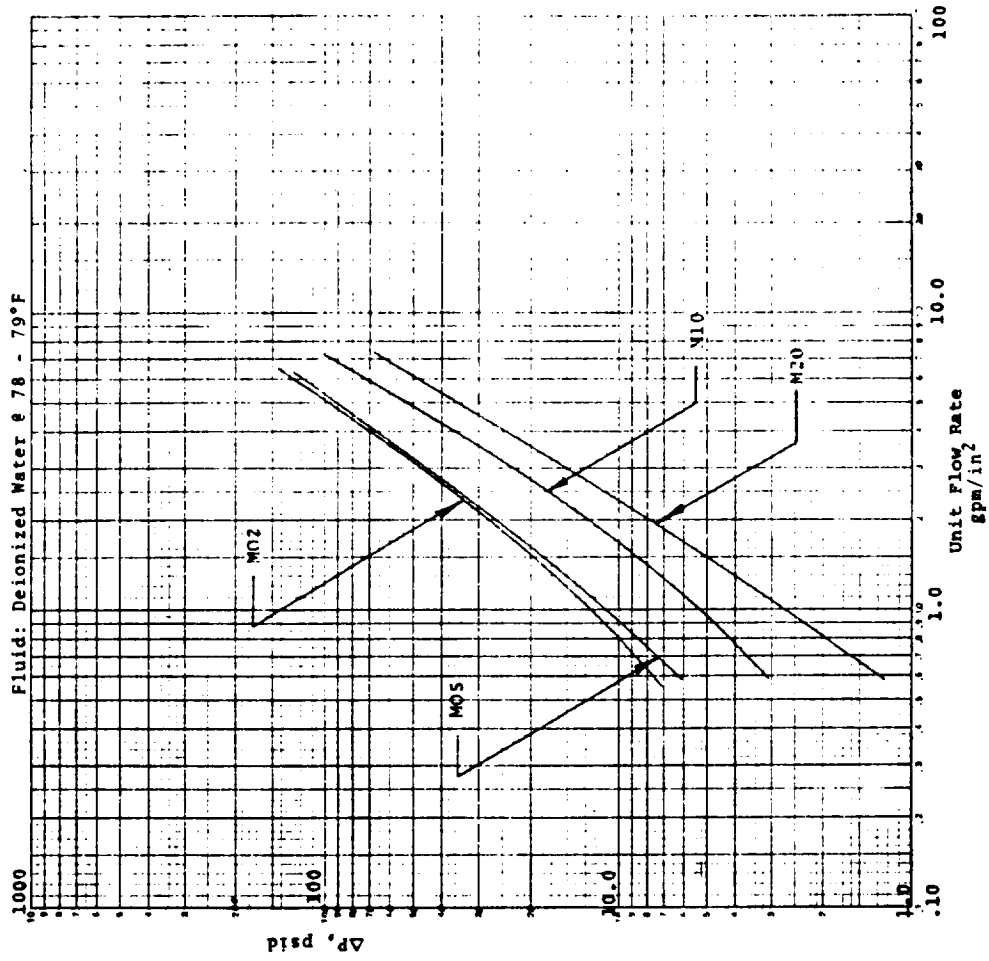


FIGURE 11

FLOW RESISTANCE OF MEMBRANE-FILTERS  
(Composite Curve) Water At 70 - 80°F

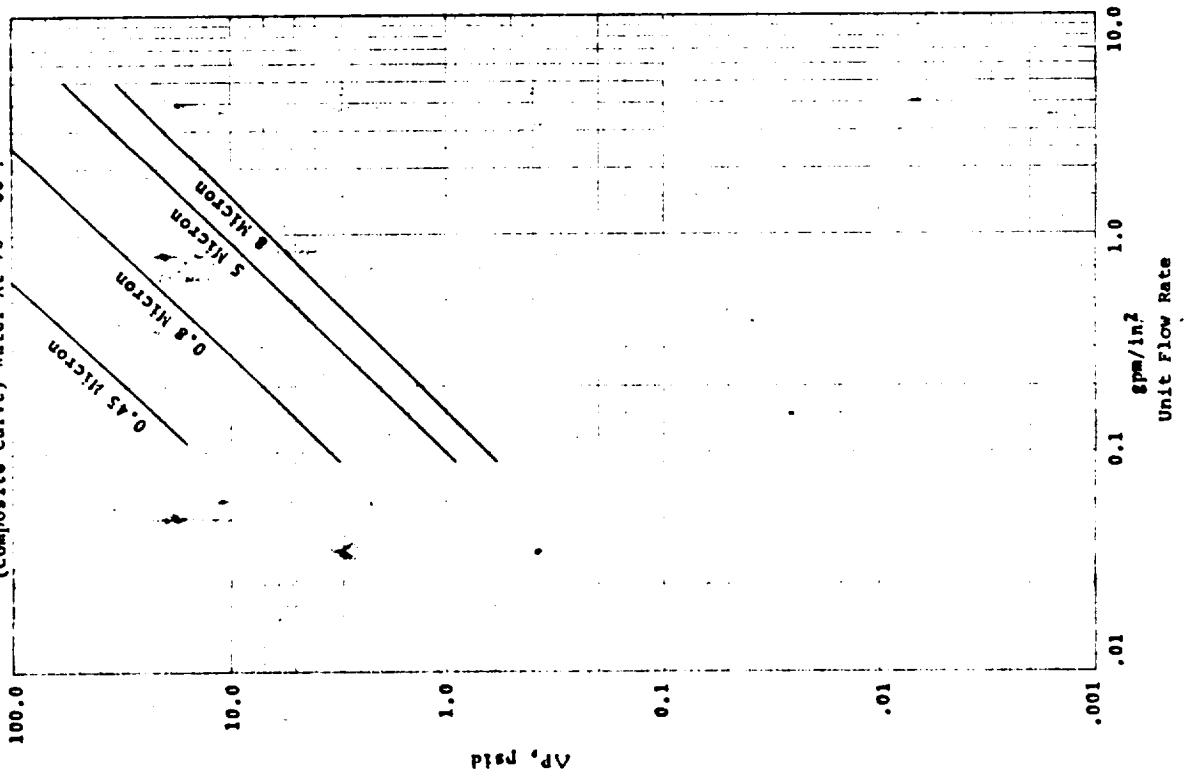


FIGURE 12

FLOW RESISTANCE OF TDDM WIRE CLOTH

Fluid: Mil-H-5606

Temp: 87 - 97° F.

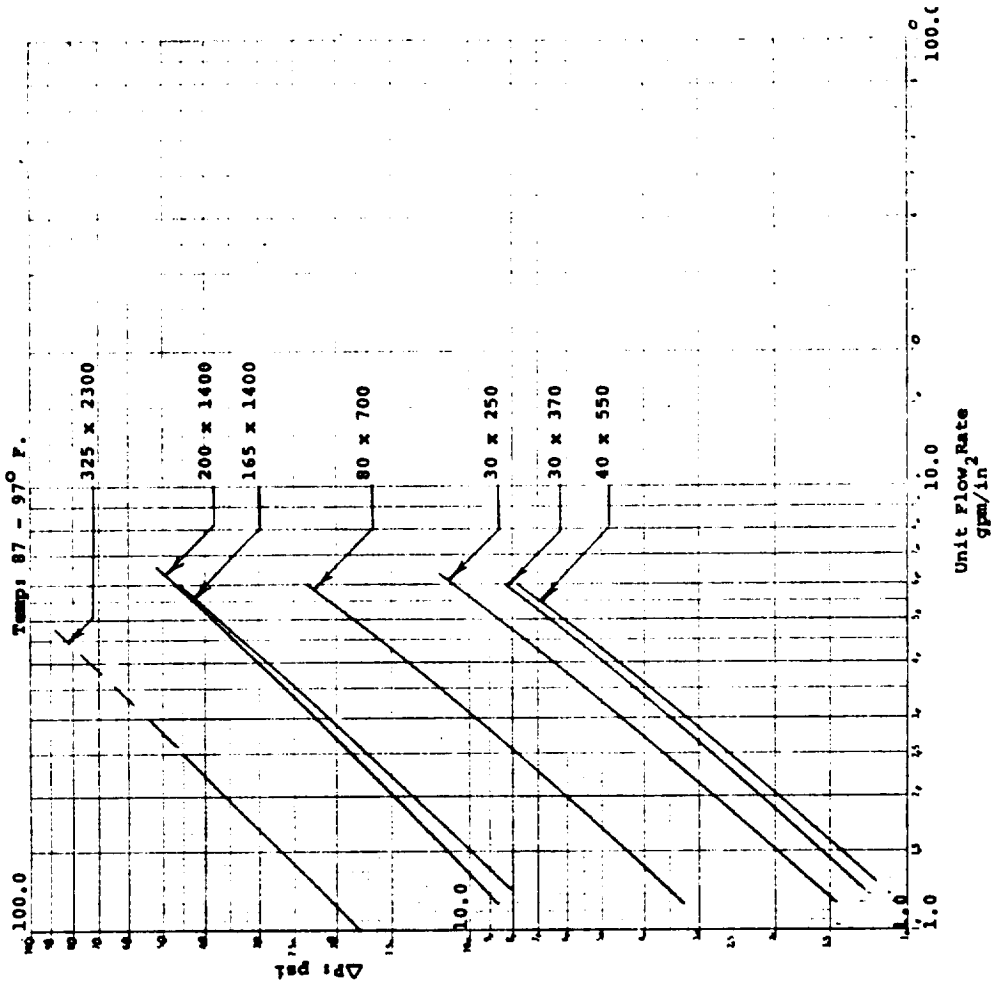


FIGURE 14  
 FLOW RESISTANCE OF PLAIN SQUARE WEAVE WIRE CLOTH

Fluid: MIL-H-5606  
 Temp: 88 - 93 F.

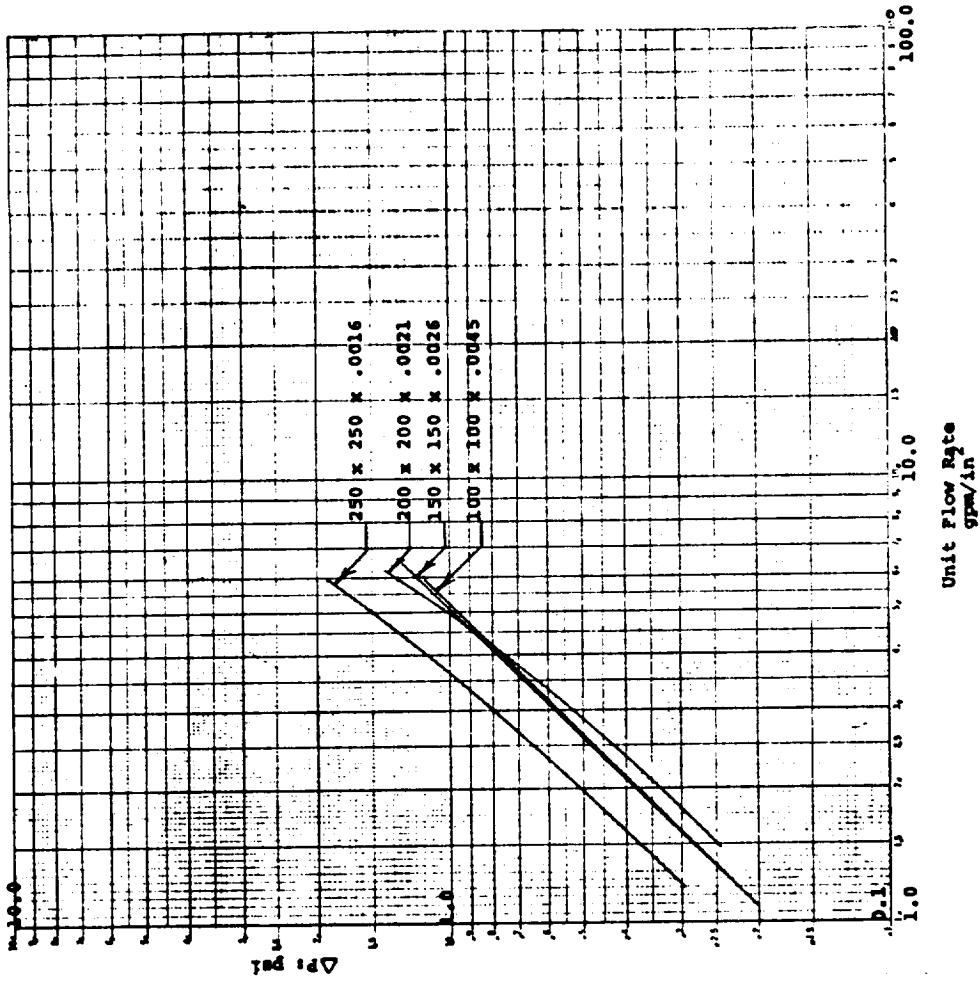
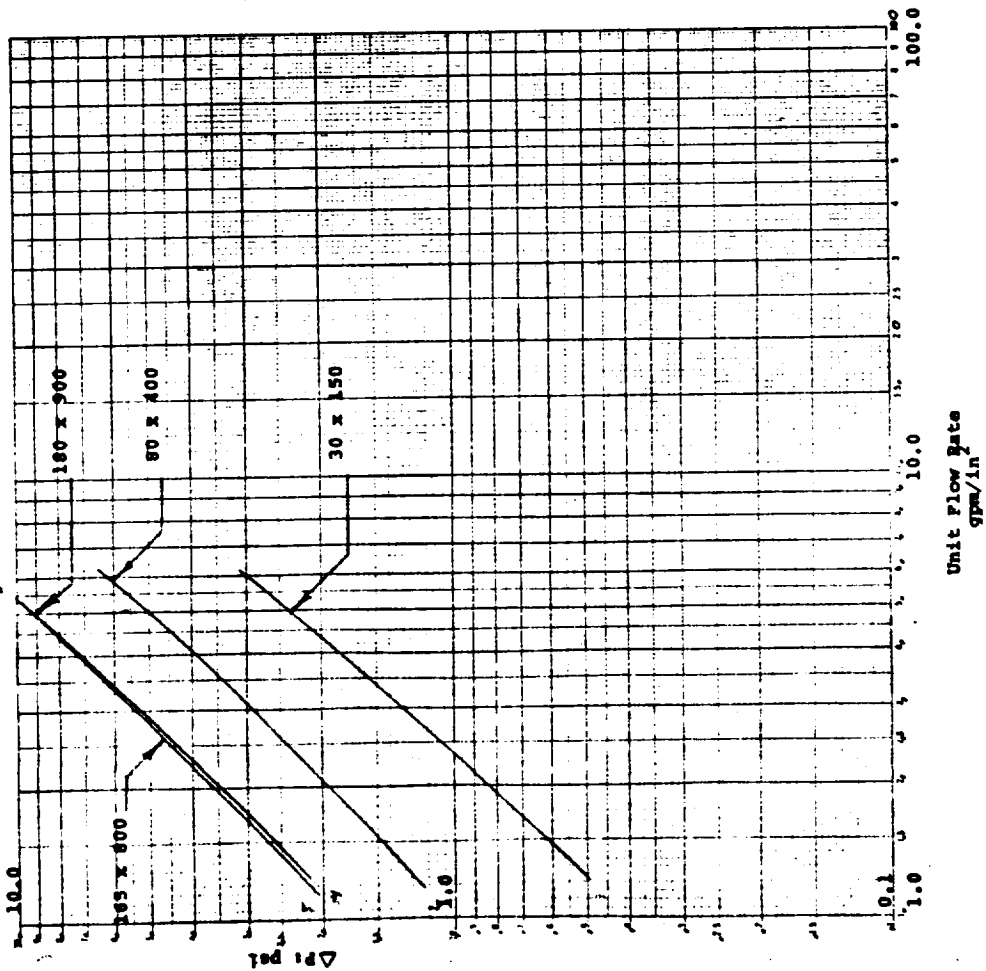
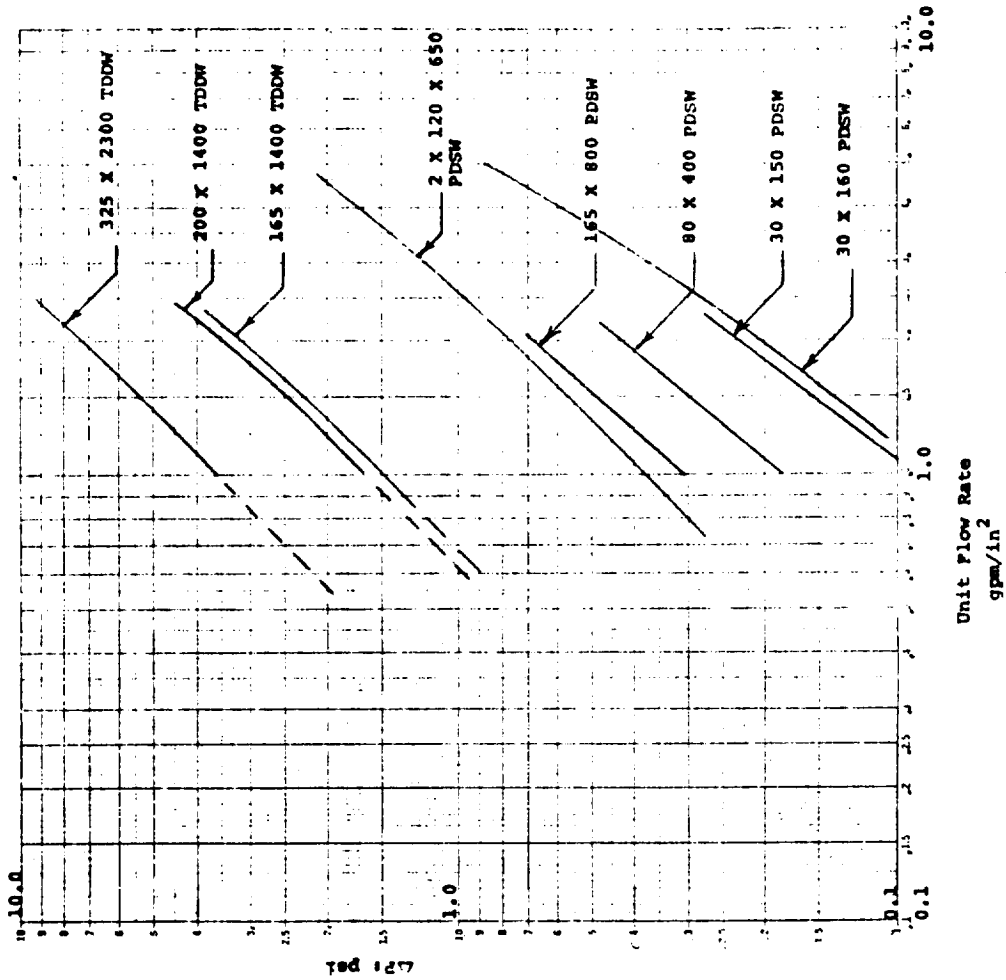


FIGURE 13  
 FLOW RESISTANCE OF PDSM WIRE CLOTH

Fluid: MIL-H-5606  
 Temp: 87 - 97 F.



**FIGURE 16**  
**FLOW RESISTANCE OF TDDM AND PDSM**  
**FLOWING ETHYLENE GLYCOL-WATER**  
**(350/650 by Weight)**



**FIGURE 15**  
**FLOW RESISTANCE OF VARIOUS FILTER MEDIA WITH JP-4 FLUID**  
**Temperature: 80 - 91°F**

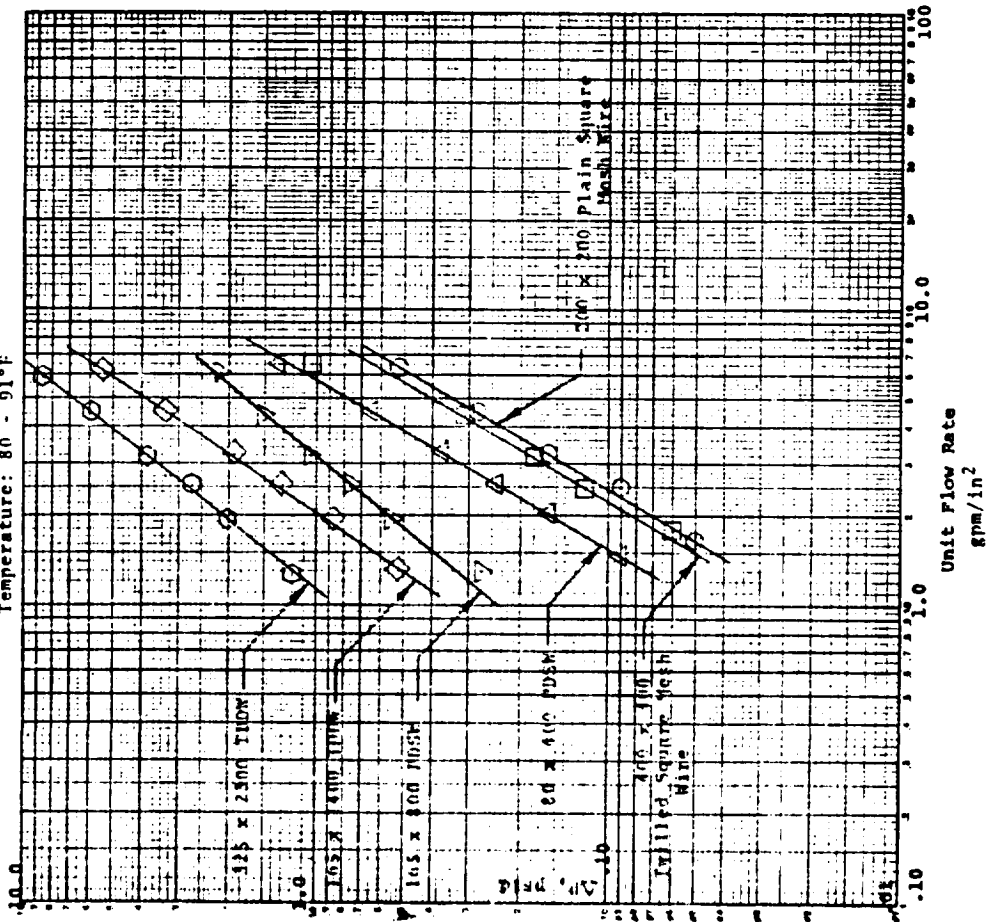


FIGURE 18  
FLOW RESISTANCE OF PDSM WIRE CLOTH

Fluid: Liquid Nitrogen  
Temp: -315° to -319° F.

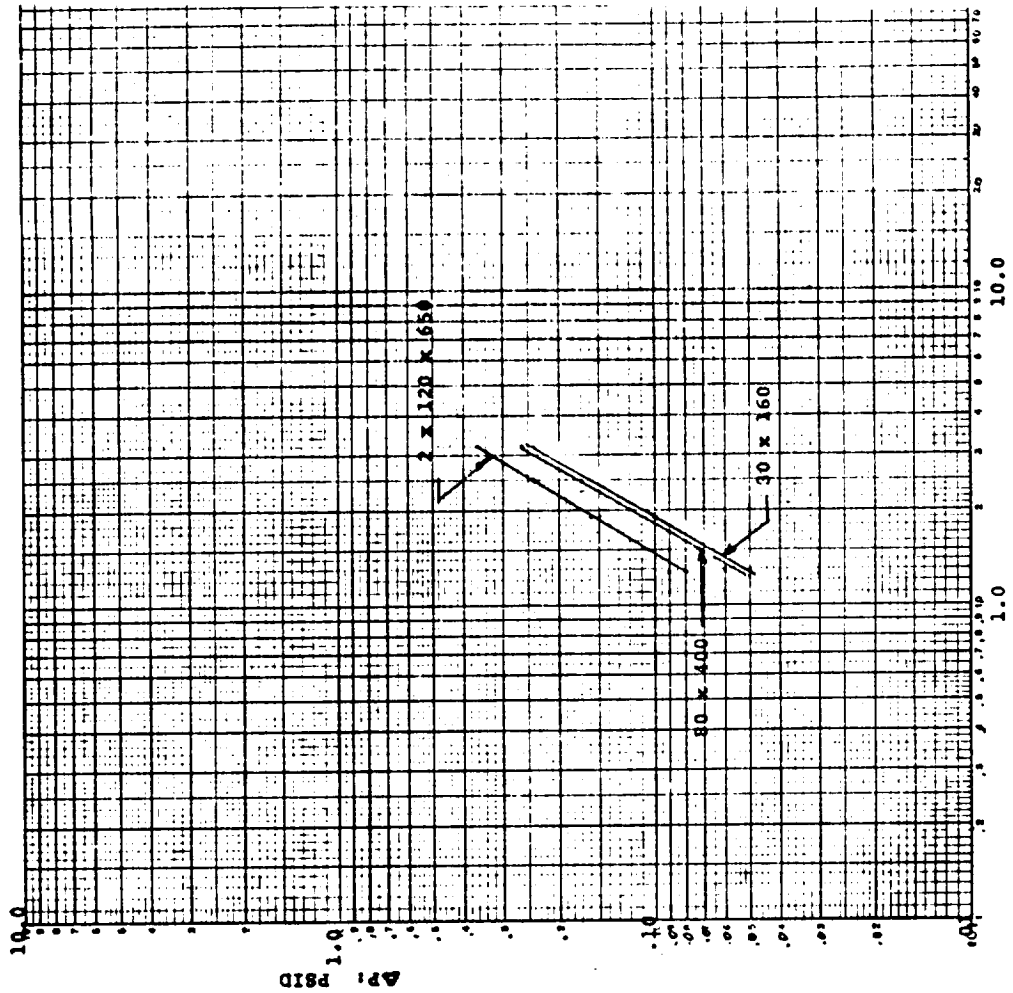


FIGURE 17  
FLOW RESISTANCE OF TDDW WIRE CLOTH

Fluid: Liquid Nitrogen  
Temp: -305° to -317° F.

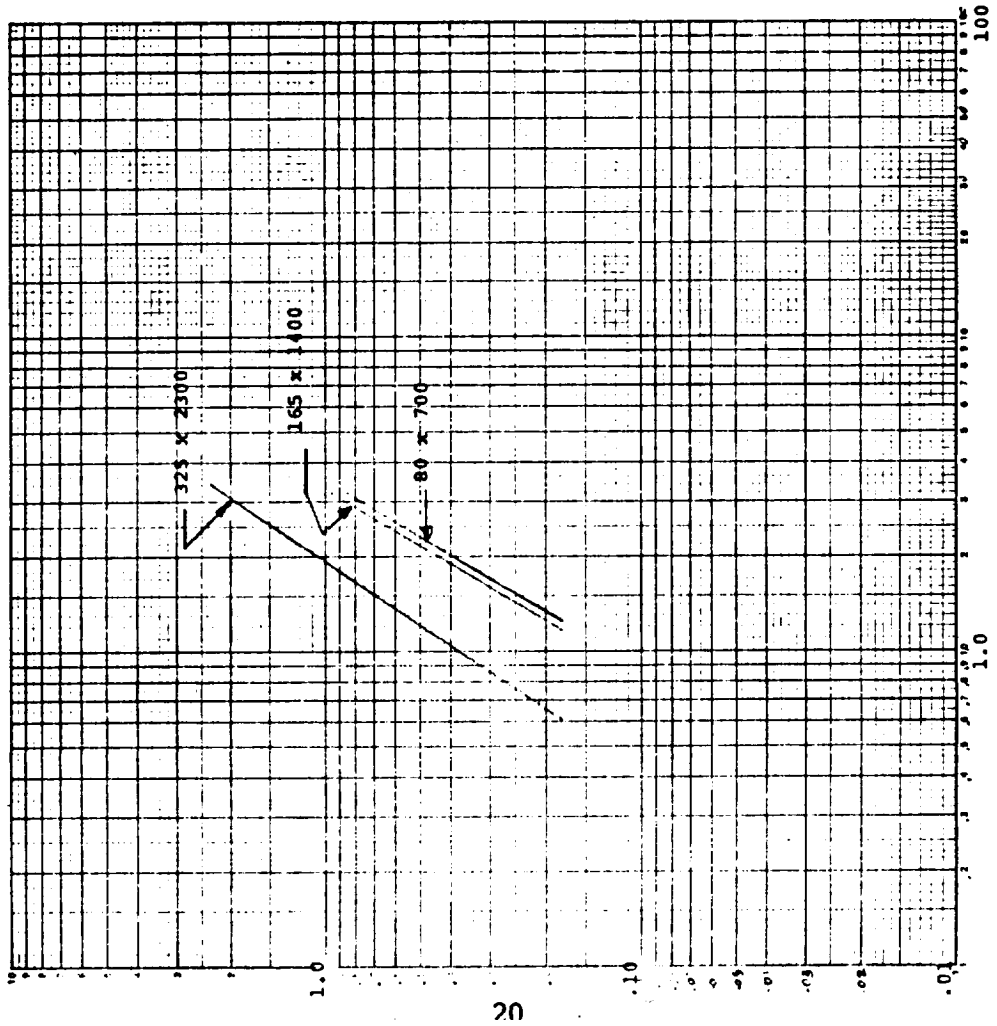


FIGURE 18A

FLOW RESISTANCE OF TDDW WIRE CLOTH

Fluid: Liquid Oxygen  
Temp: -290 to -296°F.

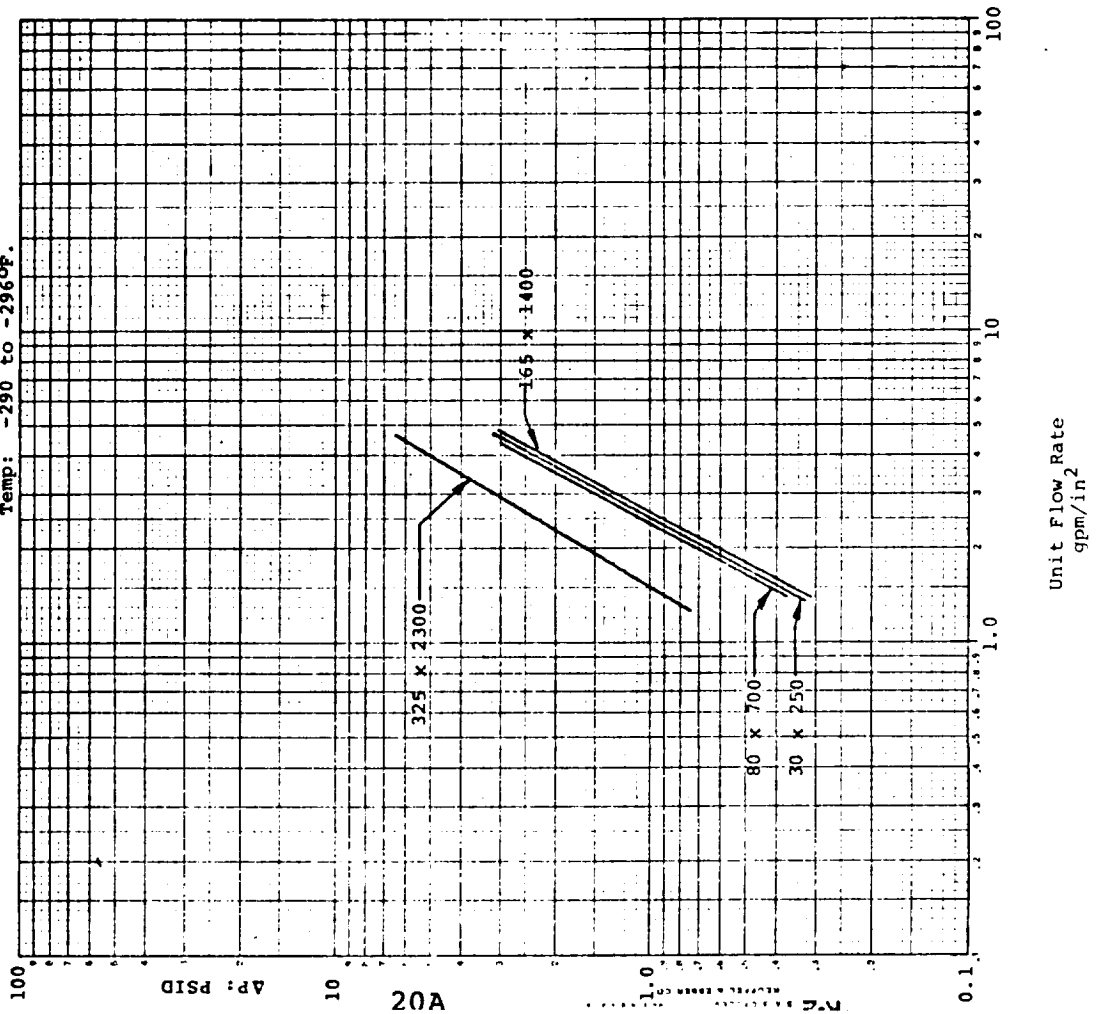


FIGURE 18B

FLOW RESISTANCE OF PDSW WIRE CLOTH

Fluid: Liquid Oxygen  
Temp: -292 to -298°F.

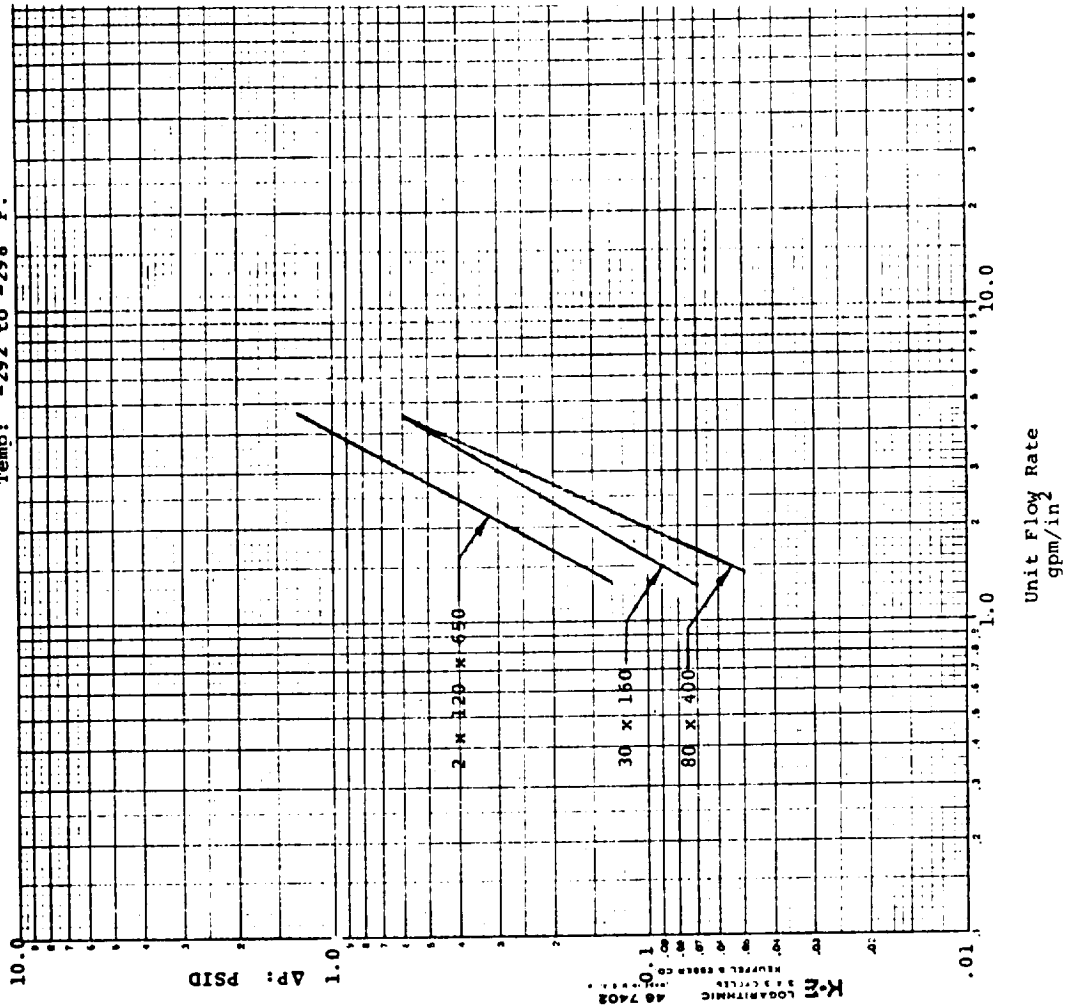




FIGURE 19  
EFFECT OF MEDIUM TYPE  
ON FLOW RESISTANCE  
Fluid: Deionized Water  
Temp: Noted

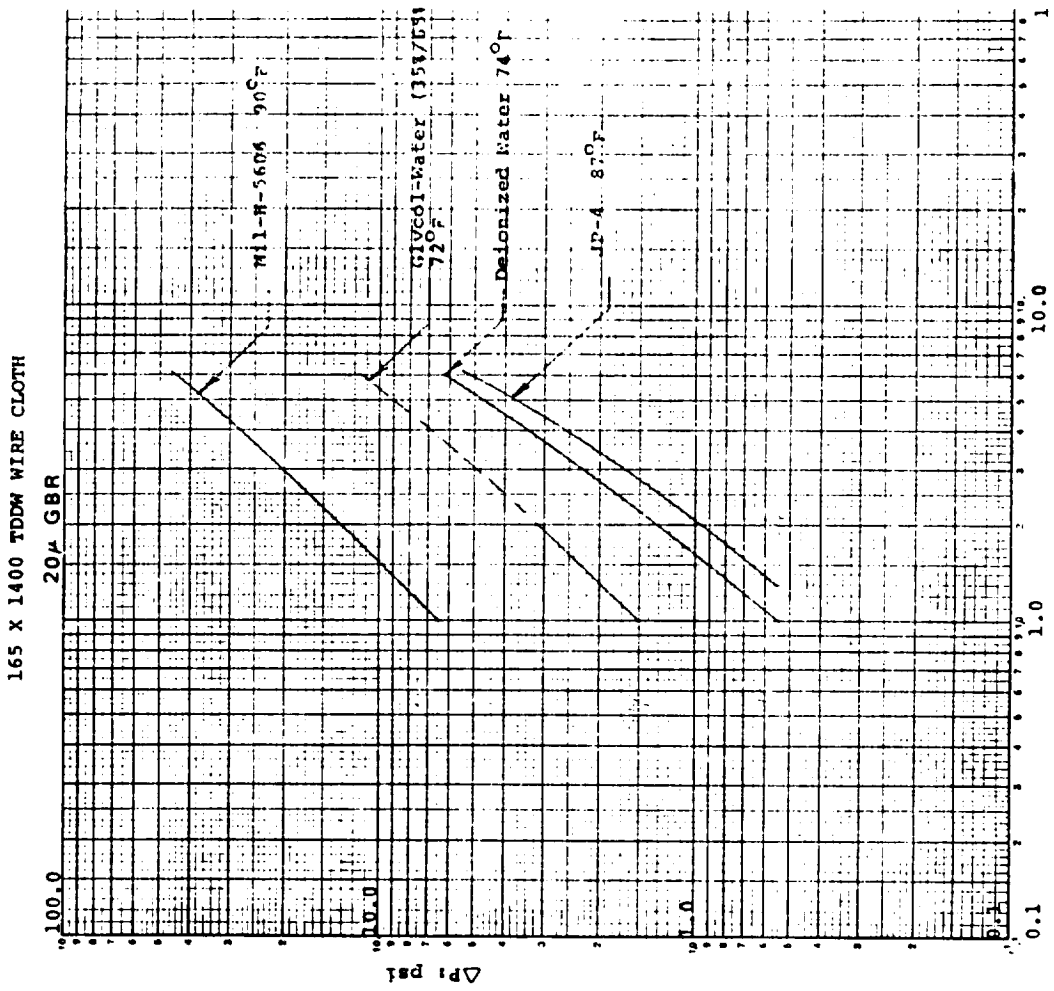
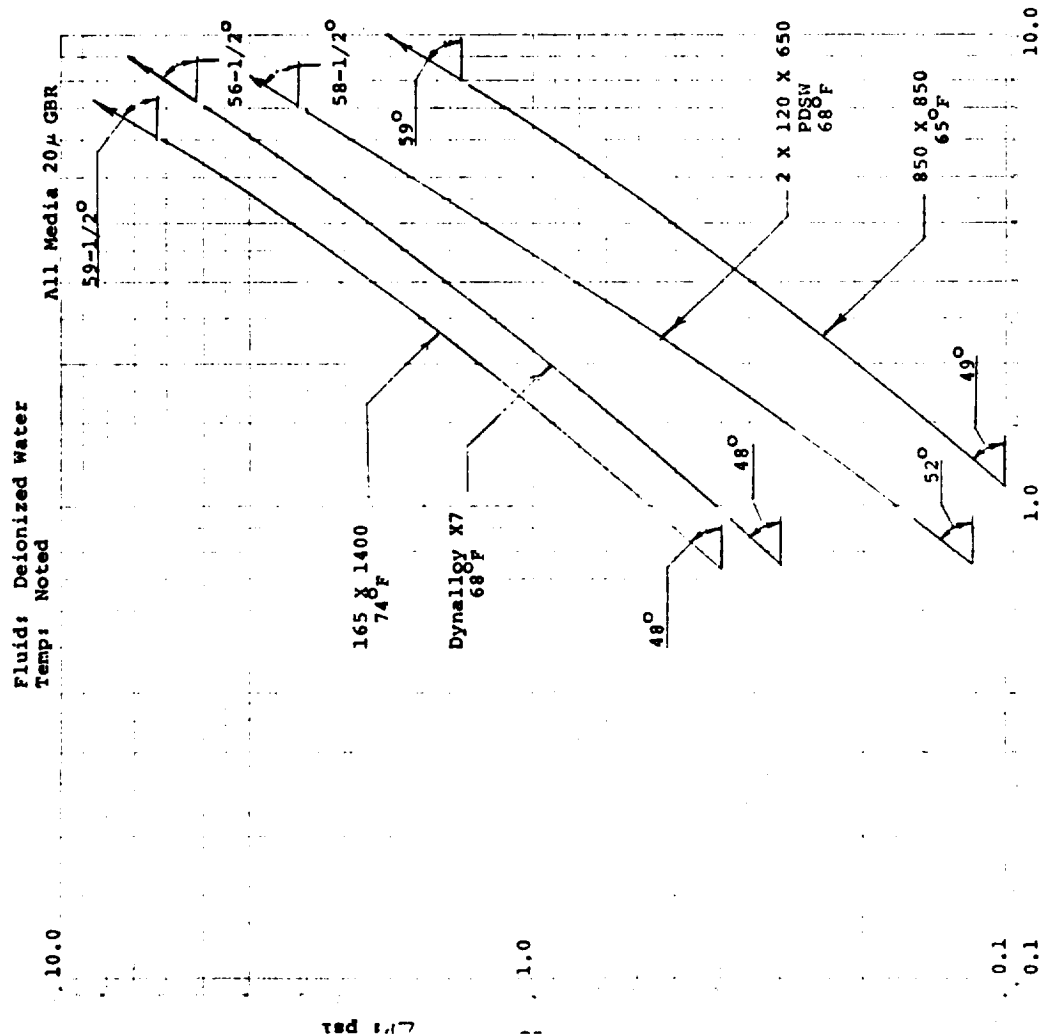


FIGURE 20  
EFFECT OF FLUID CHARACTERISTICS  
ON FLOW RESISTANCE  
165 X 1400 TDDM WIRE CLOTH  
20 μ GBR



than Mil-H-5606.

Finally, JP-4, with both low density and low viscosity, has the lowest pressure drop, but the highest slope.

Note, however, that at the higher unit flow rates, all curves show increasing slope, and if the unit flow rates were to increase further, all would eventually approach  $63^\circ$ . The low viscosity fluids would reach this slope of 2.0 at a lower unit flow rate than any of the other fluids, and the Mil-H-5606 would require the highest flow rate to obtain the high slope.

In a later section (Paragraph 3.8) the mathematical derivation of the equations expressing the relationship between unit flow rate, pressure drop, specific gravity, viscosity and the type of medium are presented, and the effects of all the parameters are discussed in detail.

### 3.5.2 Gaseous Flow Resistance Tests

Flow resistance tests using gaseous nitrogen, oxygen, hydrogen and helium were conducted in a manner similar to that used for liquid tests. The samples of porous media were cut in circles, which when placed in the gas flow test fixture, provided an exposed flow area of 0.332 square inches (0.65 inches diameter). Figure 21 shows the construction of the flow fixture used for gas tests. The back-up screen was not used during the flow resistance tests, and is only required when it is desired that the screen sample be supported against high differential pressure such as in contaminant tolerance tests. The schematic diagram of the test apparatus is shown in Figure 22.

Table 4 lists the figures showing the results of the gas flow resistance tests. The helium and nitrogen gas tests were conducted at Wintec Corporation, while the oxygen and hydrogen gas tests were conducted at the NASA White Sands Test Facility. The test data are plotted on Figures 23 through 39. Two sets of curves are shown, one at 50 psia inlet pressure, and the other at 400 psia. The temperature for the various tests ranged between  $65^\circ$  and  $85^\circ$  F.

As with liquid flow through porous media, it can be seen that the density and viscosity of the gas also affects the slope of the curve as well as the absolute value of pressure drop. The 400 psia curve set illustrates this characteristic quite well. The approximate densities and viscosities of the four gases at 400 psia and an average temperature of  $75^\circ$  F. are listed below in Table 5.

TABLE 5  
DENSITY AND VISCOSITY OF GASES AT  $75^\circ$  F.

| Gas      | Density ( $\#/ft^3$ ) |          | Viscosity (cp) |
|----------|-----------------------|----------|----------------|
|          | 50 psia               | 400 psia |                |
| Oxygen   | 0.268                 | 2.14     | 0.02           |
| Nitrogen | 0.244                 | 1.95     | 0.0175         |
| Helium   | 0.0348                | 0.278    | 0.031          |
| Hydrogen | 0.0173                | 0.138    | 0.0087         |

Again, the 165 X 1400 TDDW medium can be used to show the effects of the various gases on flow resistance. Figure 30, which was developed from Figures 23 through 29, shows pressure drop (psi) vs. actual cubic feet per minute per square inch of medium. This type of presentation provides pressure drop values at the same velocity throughout for the gases, and the density and viscosity effects are quite noticeable. It is apparent from Figure 30 that

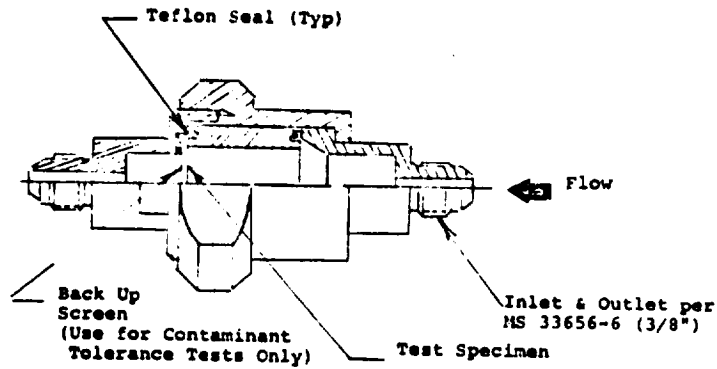


FIGURE 21  
GAS TEST FLOW FIXTURE

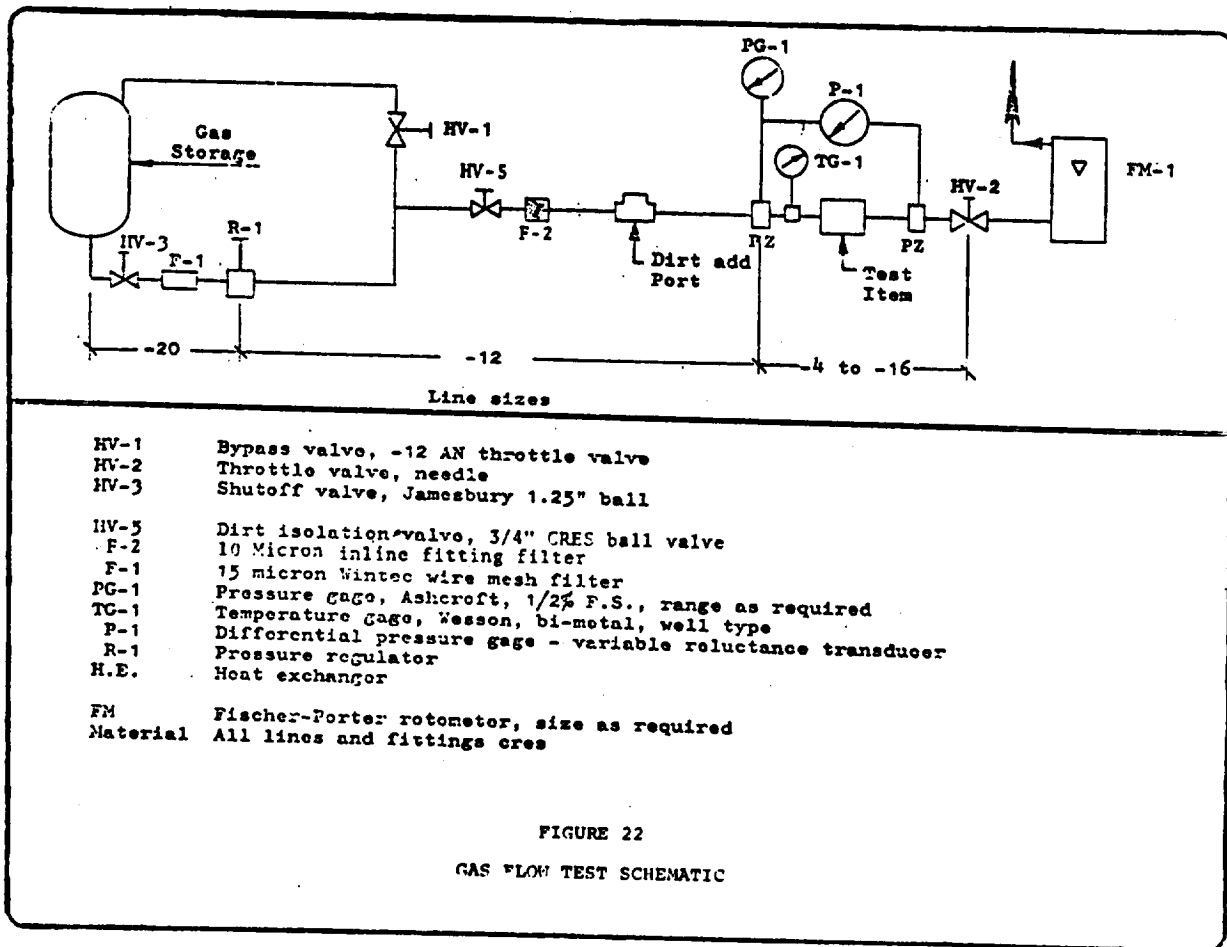
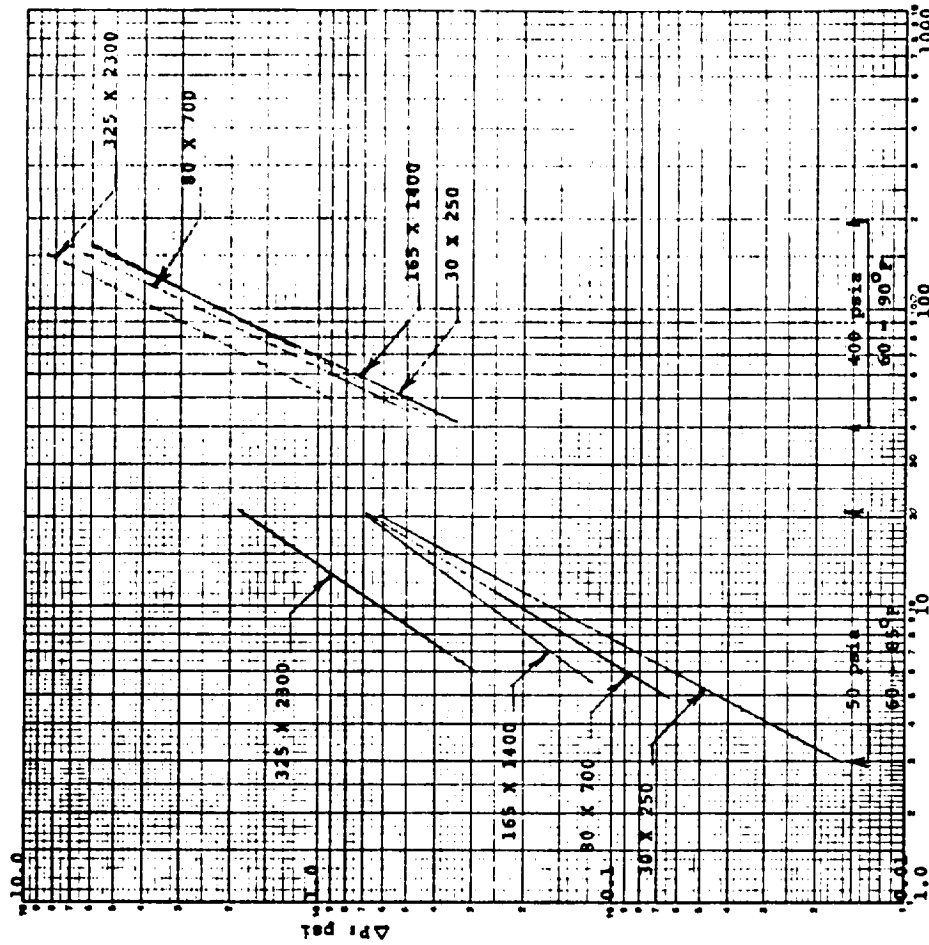


FIGURE 22  
GAS FLOW TEST SCHEMATIC

**FIGURE 24**  
**FLOW RESISTANCE OF TDDM WIRE CLOTH**  
**GASEOUS OXYGEN**  
**SCFM/IN<sup>2</sup> VS ΔP**



**FIGURE 23**  
**COMPARATIVE FLOW RESISTANCE OF TWILLED DUTCH DOUBLE WEAVE WIRE CLOTH**  
**Fluid: Gaseous Nitrogen**

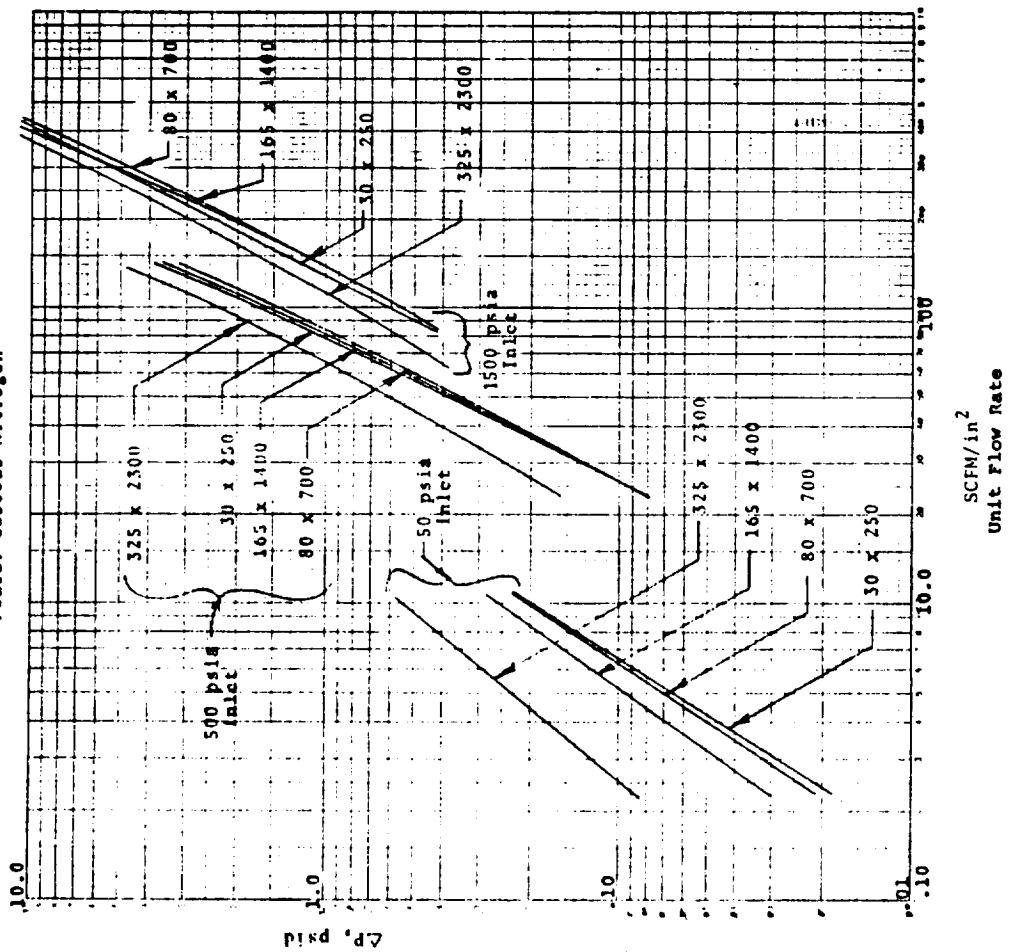


FIGURE 25

FLOW RESISTANCE OF TDDM WIRE CLOTH  
GASEOUS OXYGEN

ACFM/IN<sup>2</sup> VS ΔP

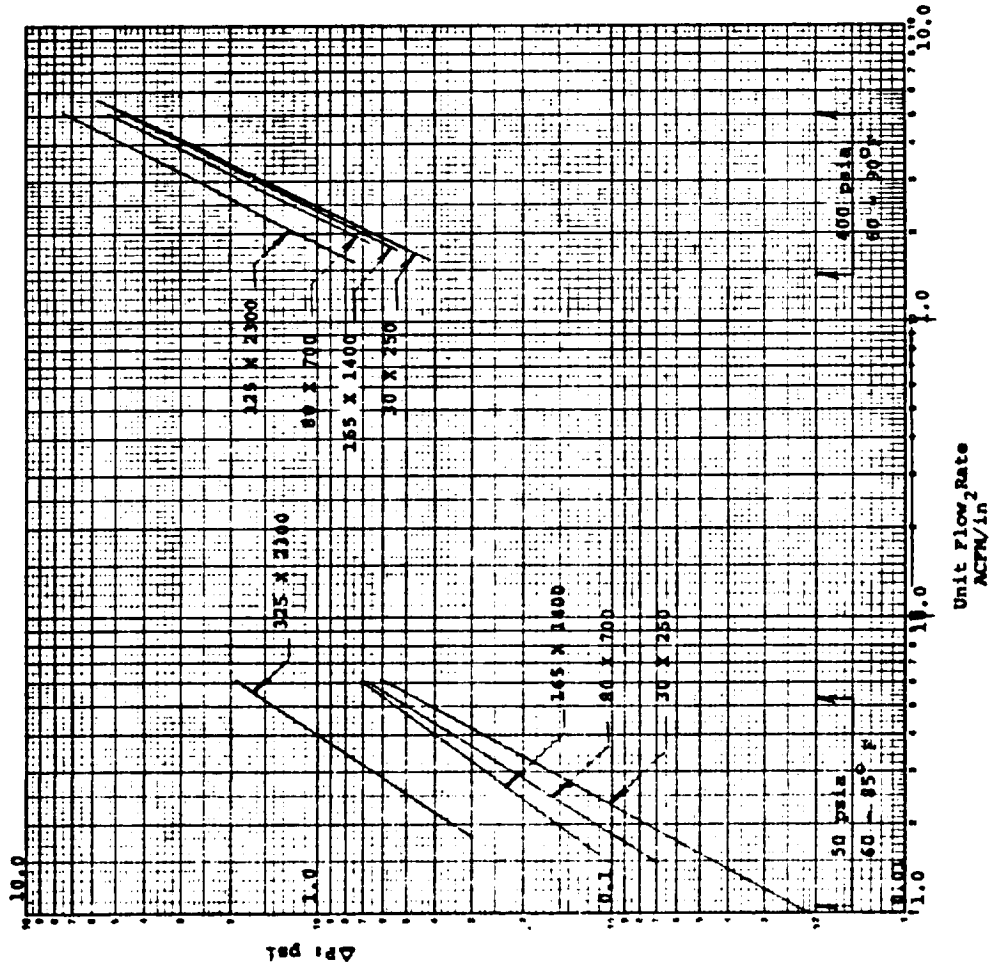


FIGURE 26

FLOW RESISTANCE OF TDDM WIRE CLOTH  
FLOWING GASEOUS HELIUM

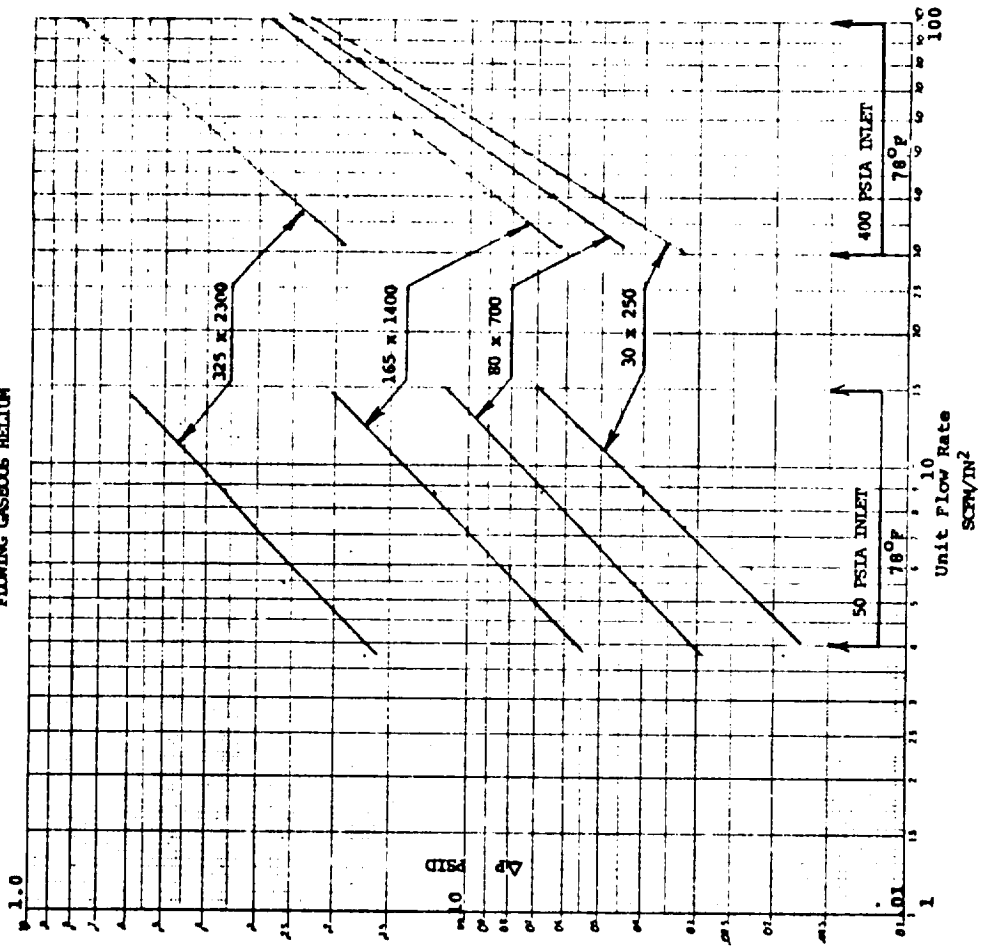


FIGURE 28  
FLOW RESISTANCE OF TDDW WIRE CLOTH  
GASEOUS HYDROGEN  
SCFM/in<sup>2</sup> VS ΔP

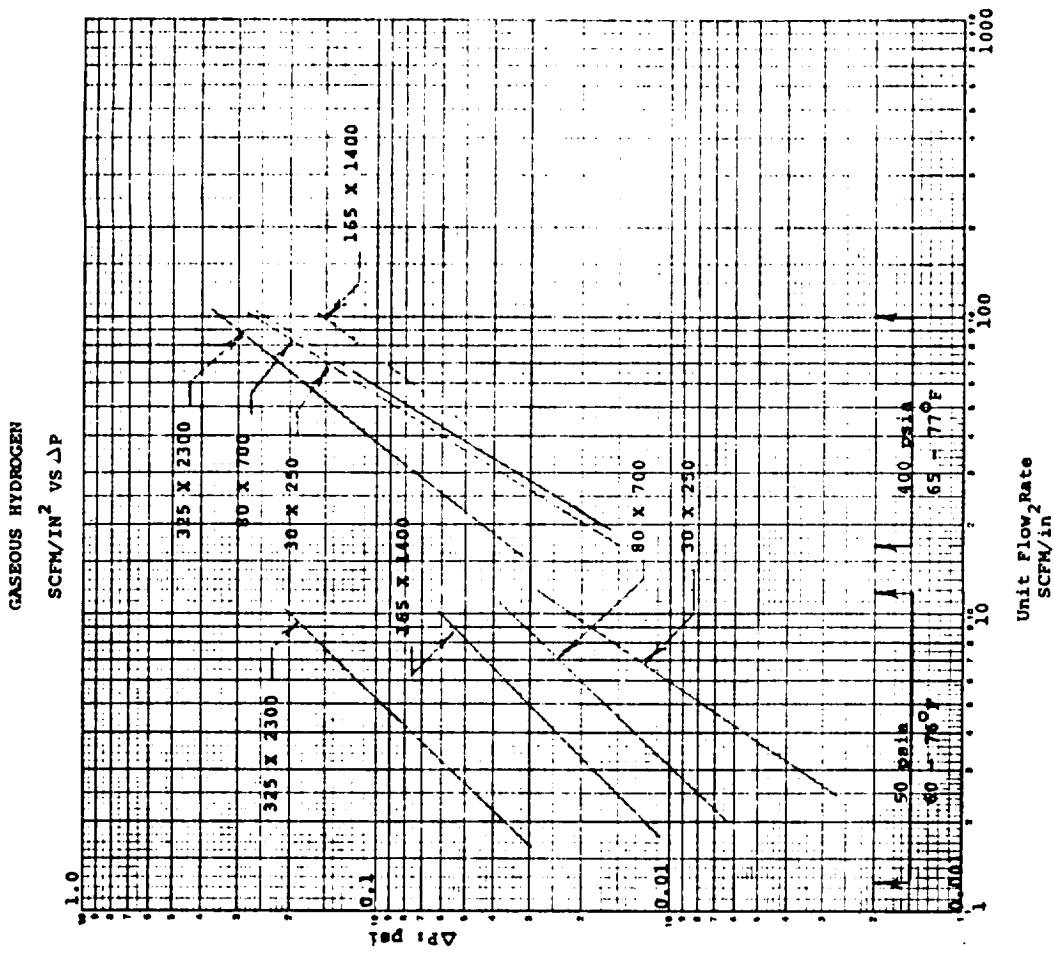


FIGURE 27  
FLOW RESISTANCE OF TDDW WIRE CLOTH  
GASEOUS HELIUM  
ACFM/in<sup>2</sup> VS ΔP

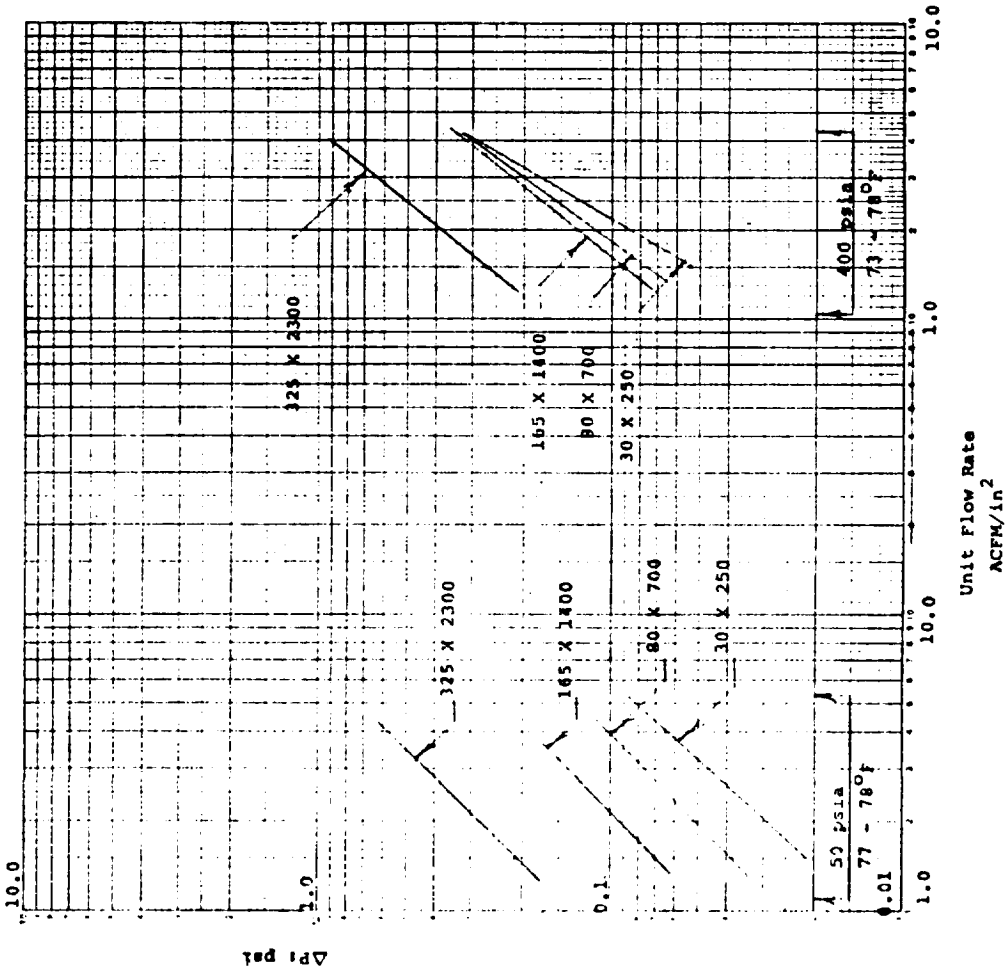


FIGURE 29  
 FLOW RESISTANCE OF TDDM WIRE CLOTH  
 GASEOUS HYDROGEN  
 ACFM/in<sup>2</sup> VS ΔP

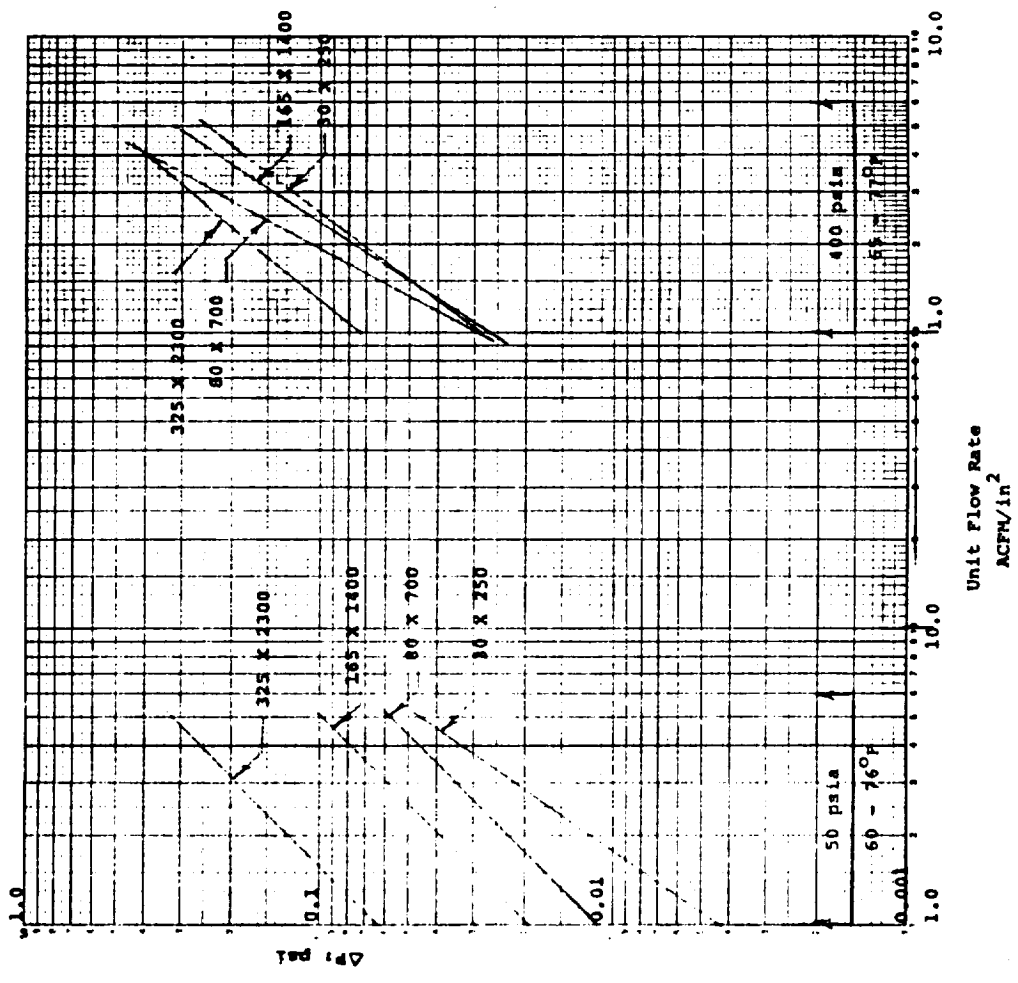
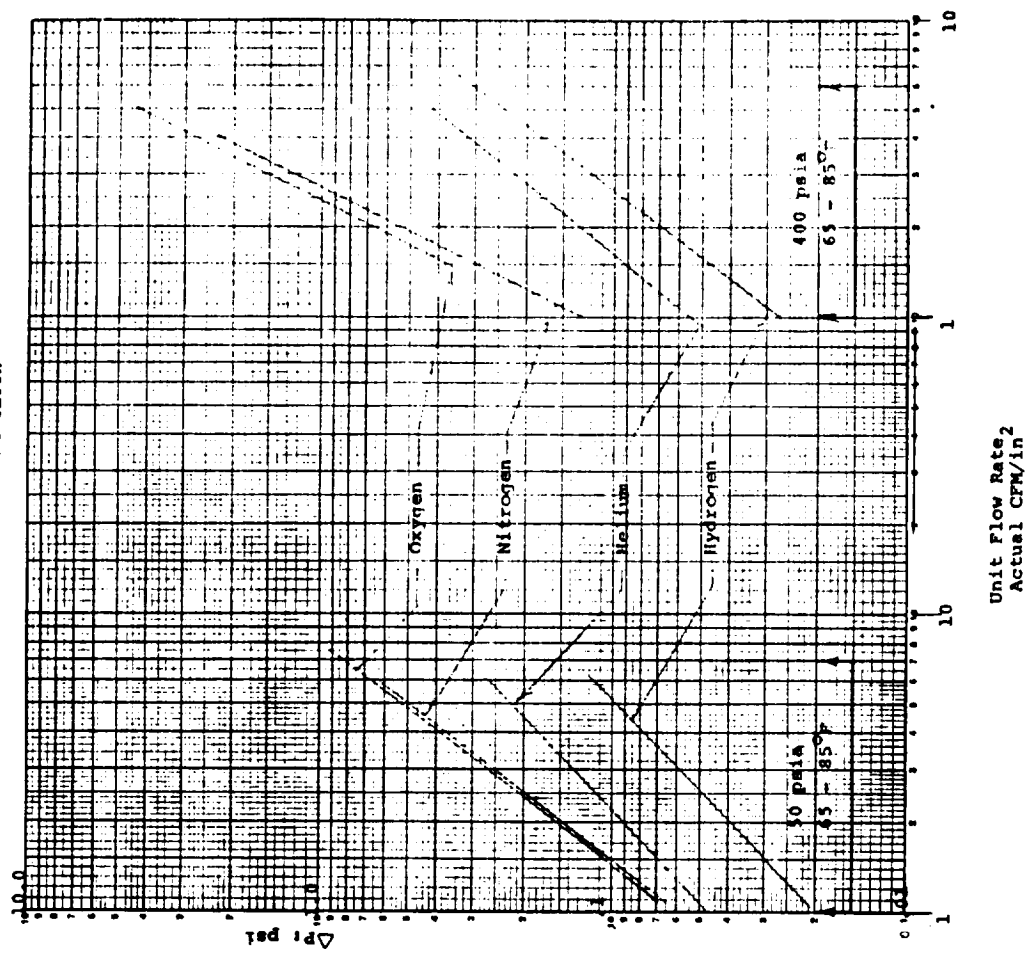


FIGURE 30  
 EFFECT OF GAS CHARACTERISTICS  
 ON FLOW RESISTANCE  
 165 X 1400 TDDM WIRE CLOTH



for gases whose densities are less than approximately 0.24 pounds per cubic foot, the curve slope is not typical of either laminar ( $45^\circ$  slope) or turbulent ( $63-1/2^\circ$  slope) flow. As the gas density increases, the pressure differential rises and the slope of the curve of pressure drop vs. flow velocity increases.

The later section (Paragraph 3.8) on mathematical development of flow equations, considers both the density and the viscosity of the gases and their effects on the curves..

The data obtained in determining flow resistance of the various media to gases showed considerably more scatter than those obtained with liquids. This is due, in part, to the inability to maintain a constant pressure and temperature of the inlet gas throughout the test (which allows a density change to occur), as well as the instrumentation errors inherent in measuring very low pressure differentials. The "tare" value of the system pressure drop is so large a percentage of the "gross" pressure drop with the sample installed that subtraction of the tare from the gross to obtain "net" pressure drop values provides the probability of relatively large errors in the net values. The curves shown represent "average" values of the various tests.

### 3.5.3 Etched Disc Flow Resistance Tests

While most of the tests conducted under this program involved wire mesh or depth type filters, other types of filter media can be fabricated which will provide relatively closely controlled flow passage dimensions. Perhaps, the most interesting of these is the etched disc filter which consists of a stack of thin annular discs, each of which has an etched flow pattern on one side. When the discs are stacked one upon the other with the unetched side of one in contact with the etched side of the next adjacent disc, the etched areas will form minute flow passages. A means of holding the stack of discs tightly compressed completes the formation of a filter element. Its prime advantage is that it can be readily cleaned by releasing the compressive force and separating the discs.

The etched pattern on the disc, of course, controls the flow characteristics of the filter element. The etched pattern tested is shown in Figure 31. This pattern was developed by Jet Propulsion Laboratories for the Mariner program. The labyrinth flow pattern, together with the small "knobs" produces several flow reversals and velocity changes of the fluid, causing particles carried in the fluid stream to be "thrown" to the stagnant areas of the labyrinth. The glass bead rating of the filter is controlled by the etched depth of the pattern, but in theory, the reversing flow pattern and velocity changes will increase the probability of entrapping and removing particles much smaller than the glass bead rating.

The pattern shown in Figure 31 has four entrances and exits and eight separate flow paths, each with four flow reversals. The restricting orifices are formed by the proximity of adjacent knobs and the depth of the etched pattern. The paths are, therefore, rectangular in cross-section with the base of the rectangle equal to 0.010" at the knobs and with a height equal to the etch depth.

The etched discs were fabricated from 0.002 and 0.004 inch thick full-hard AISI 302 stainless steel sheet stock. The 0.002 discs were etched to 10 and 20 microns depth, while the 0.004 material was etched to 40 microns depth.

Stacks of approximately 1000 discs were assembled to form the 10 micron and 20 micron filter element, while 500 discs were used for the 40 micron unit. An internal tension mandrel was used to compress the discs and seal one end of the stack. The element thus formed was sealed in an external case. Flow through the element was from outside to inside.

Flow resistance tests were conducted on the three elements using deionized water, isopropanol



and gaseous nitrogen. Figures 32 through 36 show the data from these tests. As the number of flow passages is directly proportional to the external area of the stack of discs, the flow rate is shown per unit area. The external area of the stack was used in this calculation. Use of this data to predict flow through units of a different diameter, but with the same pattern spacing, is acceptable so long as the disc thickness is consistent with that of the discs tested.

From Figures 32 and 33, it can be seen that the slope of the flow resistance curve at the test flow rates with both water and isopropanol is approximately 1.0. Thus, a linear relationship exists between unit flow rate and pressure differential. However, the pressure drop through these filters was extremely high for the unit flow rates used. This is the penalty that is assessed by the flow reversals and velocity changes of the fluid.

The nitrogen gas tests displayed in Figures 34, 35 and 36 also indicate very high differential pressures must be accepted for this type of filter.

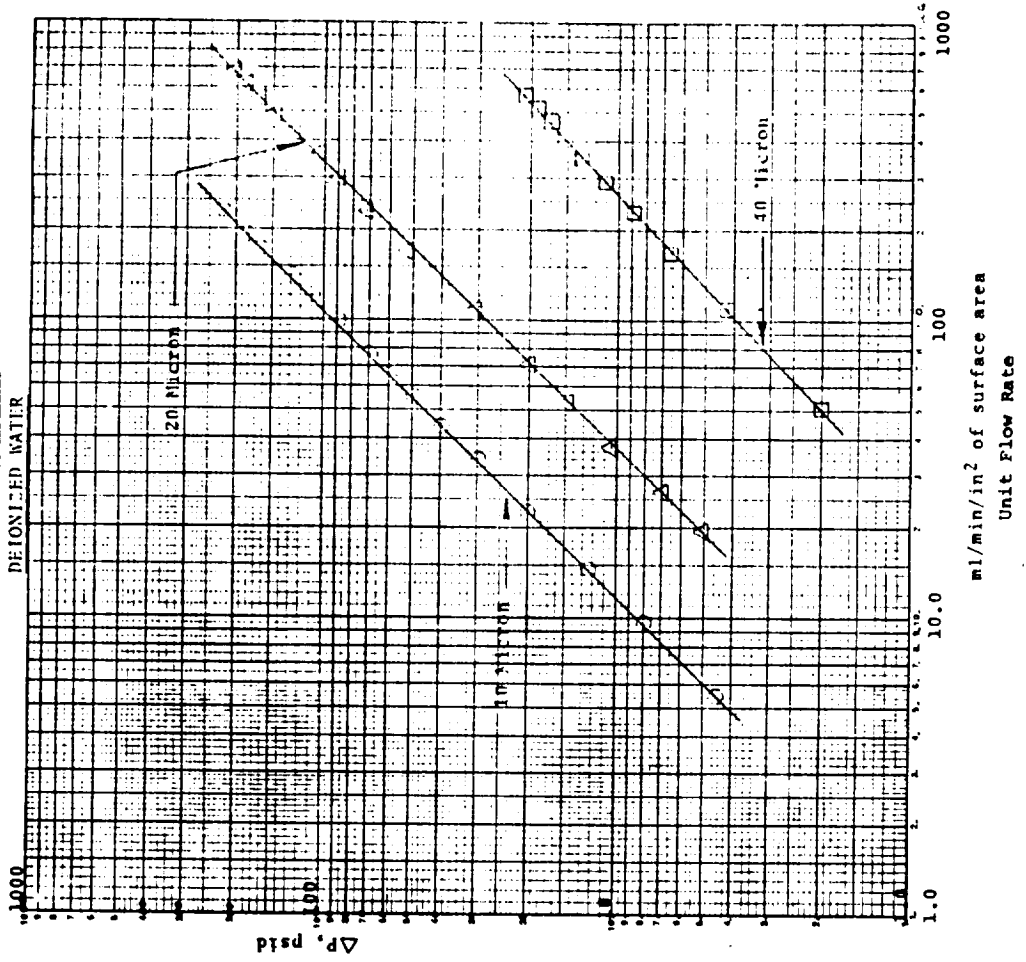
Bubble Point Tests and Glass Bead Tests were conducted on the three elements to develop a bubble point conversion factor applicable to this shape of pore opening. By multiplying the Standard Bubble Point by the diameter of the largest bead found in the glass bead test, an average Bubble Point Conversion Factor of 234 was determined. The data from the glass bead and bubble point tests is shown below in Table 6.

TABLE 6  
INITIAL BUBBLE POINT PRESSURE FOR ETCHED DISC FILTERS

| Disc Stack<br>Micron Rating<br>(microns) | Corrected<br>(Standard)<br>Bubble Point<br>(in. water) | Largest Glass<br>Bead Diameter<br>(microns) | Conversion<br>Factor |
|--|--|---|----------------------|
| 10                                       | 16.58  | 14.2  | 235                  |
| 20                                       | 11.91  | 19.6  | 233                  |
| 40                                       | 6.0  | 39.0  | 234                  |

From the above data, it can be seen that the glass bead rating of the "10 micron" etch depth discs was, in reality, approximately 15 microns, while the 20 and 40 micron etch depth discs closely matched the stated rating.

**FIGURE 32**  
**COMPARATIVE FLOW RESISTANCE, ETCHED LABYRINTH DISC**  
**10, 20 AND 40 MICRON**



**FIGURE 31**  
**ETCHED LABYRINTH DISC PATTERN**

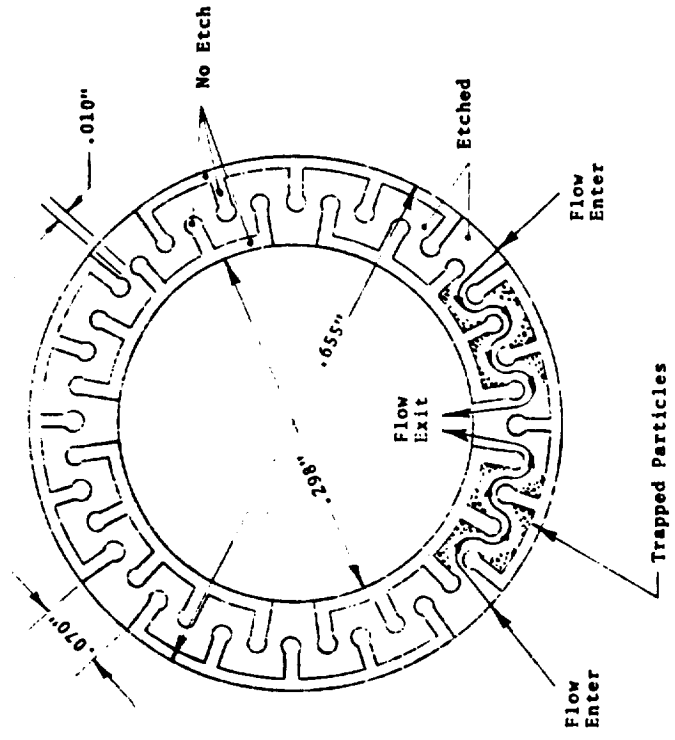


**FIGURE 33**

COMPARATIVE FLOW RESISTANCE, ETCHED LABYRINTH DISC

10, 20 AND 40 MICRON

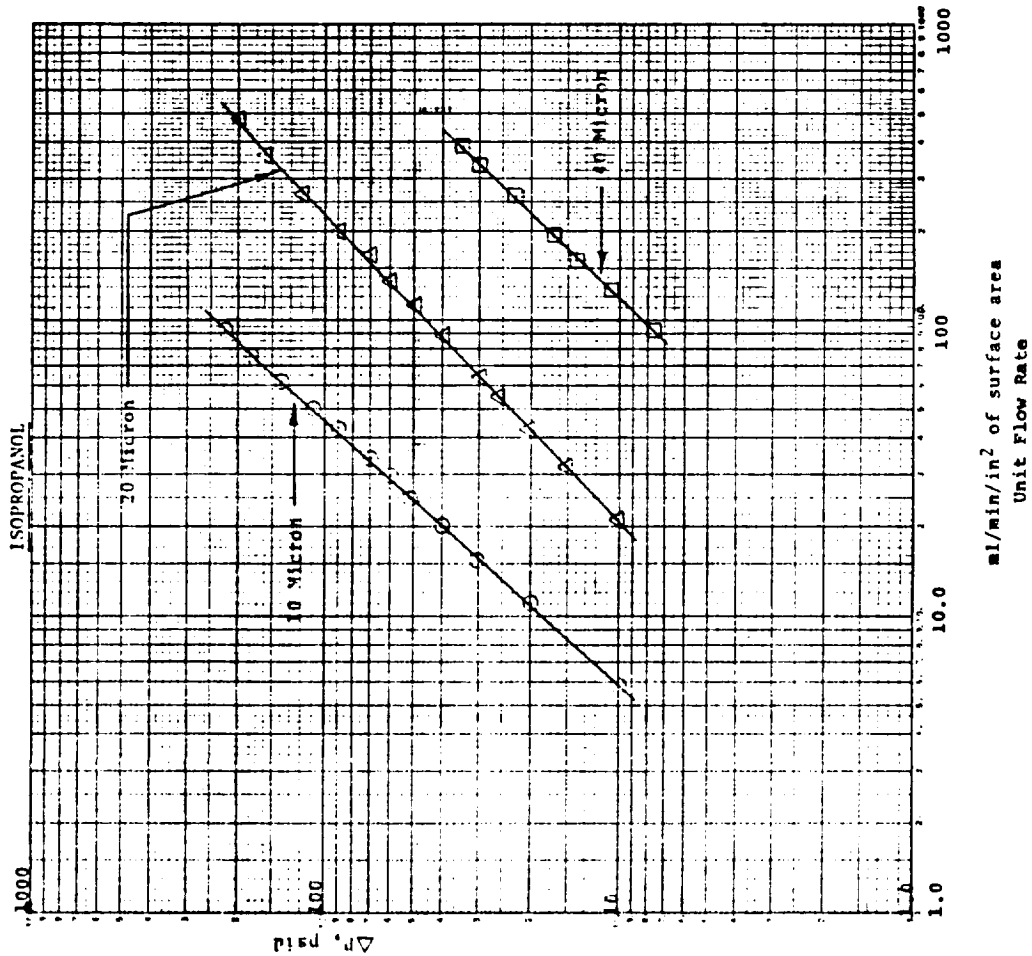


**FIGURE 34**

COMPARATIVE FLOW RESISTANCE, ETCHED LABYRINTH DISC

INLET PRESSURE AT 100, 200 AND 400 PSIG G<sub>2</sub>

10 MICRON DISCS

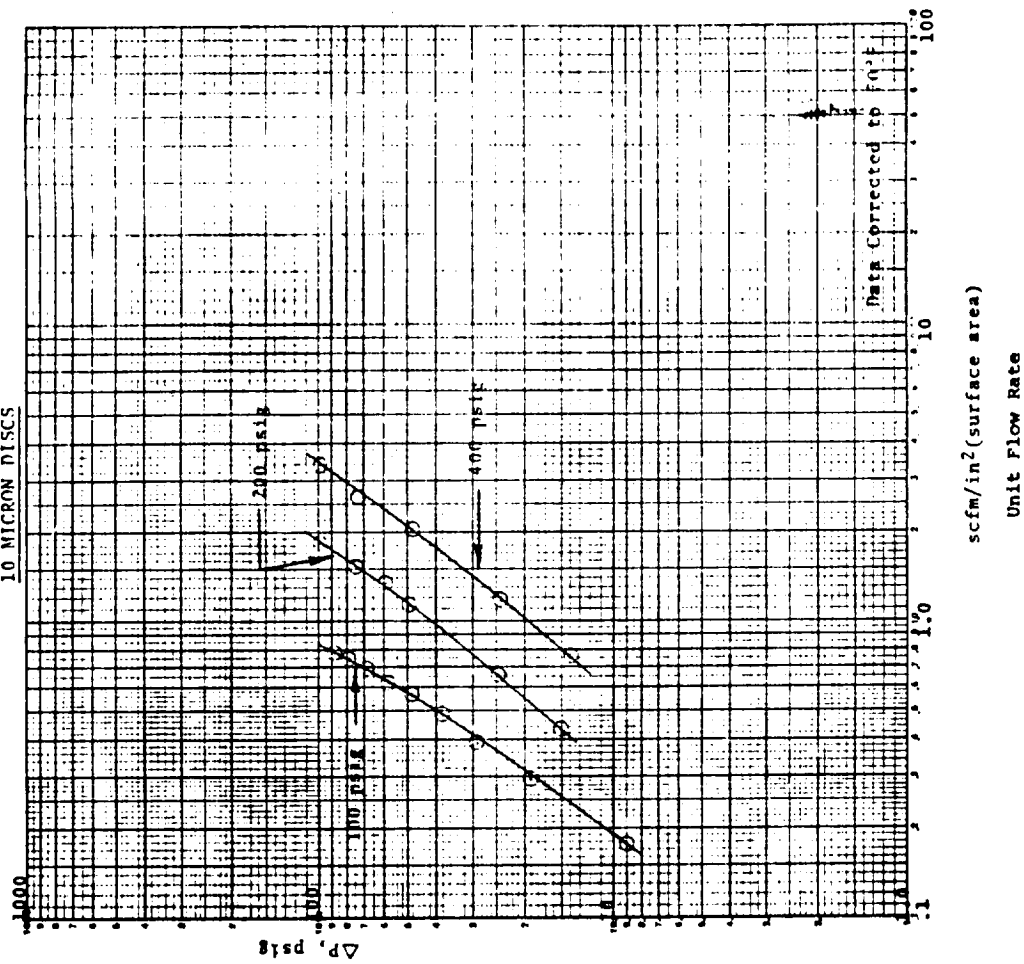


FIGURE 35  
 COMPARATIVE FLOW RESISTANCE, ETCHED LABYRINTH DISC  
 INLET PRESSURES AT 100, 200 AND 400 PSIG GN<sub>2</sub>

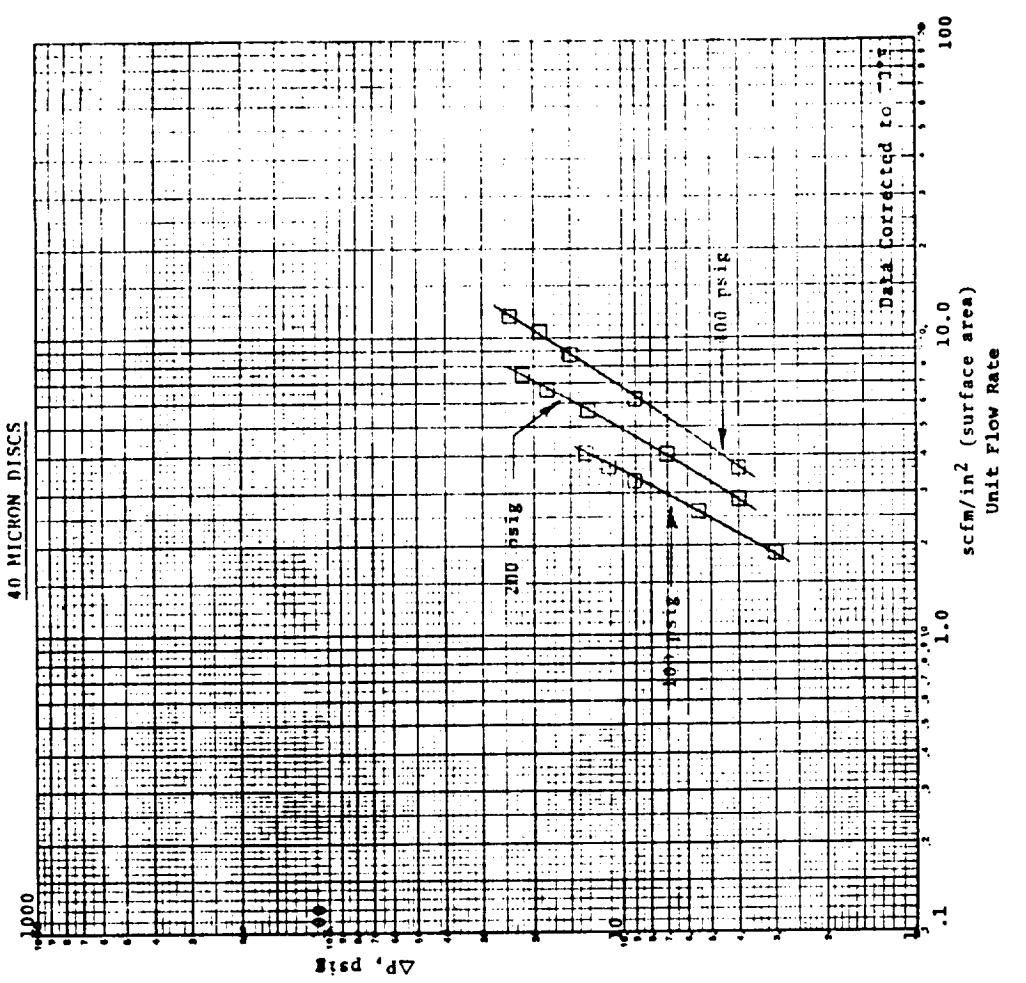
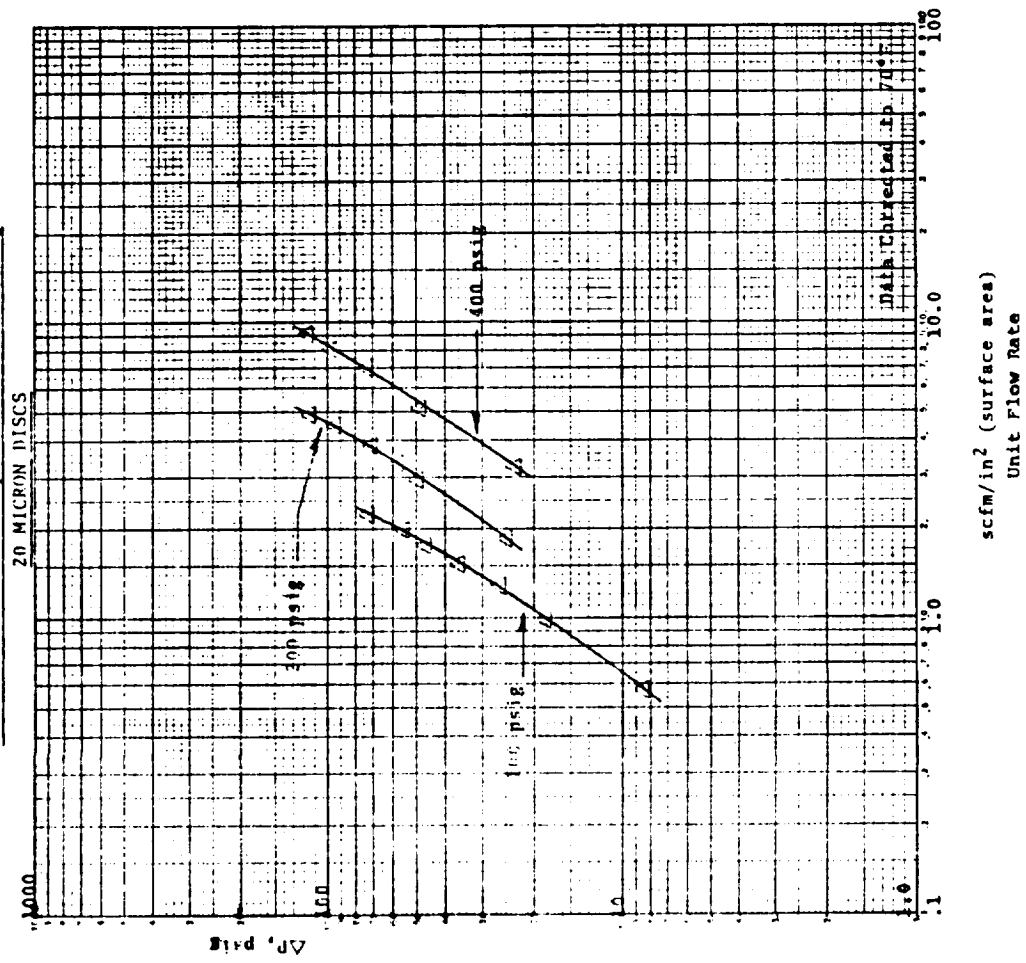


FIGURE 36  
 COMPARATIVE FLOW RESISTANCE, ETCHED LABYRINTH DISC  
 INLET PRESSURES AT 100, 200 AND 400 PSIG GN<sub>2</sub>



### 3.6 FILTER MEDIA TESTS - CONTAMINANT TOLERANCE

#### 3.6.1 Contaminant Tolerance Criteria

The performance of any porous medium installed in a flowing fluid system will be affected by the particulate matter entrained in the fluid. Particles smaller than the pore size of the medium will initially pass through, while larger particles will be blocked. As more and more of the particles are collected by the medium, the pores become either completely or partially blocked, and the "filter cake" will, itself, provide filtration of a finer level than initially provided by the medium. If the flow is held at a constant rate, the pressure drop across the medium will rise, while if the inlet pressure to the medium is held constant, the flow rate will decrease.

By using a specific or "standard" contaminant added to a fluid system flowing at a constant rate, a characteristic curve may be developed showing the effect of known amounts of the specific contaminant on a given medium in terms of pressure drop across the medium. When the pressure drop is plotted as a function of the amount of contaminant added to the upstream fluid per unit area of porous medium, a "Contaminant Tolerance" curve can be obtained. This contaminant tolerance characteristic has, in the past, been termed "dirt holding capacity." This term is entirely misleading, as it is not the amount of contaminant held by the medium that is measured, but rather the amount of contaminant presented to the medium. Thus, if a particular medium provides pores larger than the size of most of the contaminant particles, the particles will pass through and there will be relatively little effect on the medium in terms of increasing pressure drop. This particular medium would be classed as having a high "dirt holding capacity" when, in reality, it exhibits a high dirt passing characteristic relative to the particular contaminant used.

For this reason, the term contaminant tolerance is used throughout this report to describe the effect of a particular contaminant on a porous medium. The contaminant tolerance parameter for a given filter medium may be described in terms of milligrams of contaminant per square inch of medium to produce a specific pressure drop at a specific flow rate. In addition, the type and particle size distribution of the contaminant, as well as the specific fluid and its velocity through the medium must be noted, as each will have a marked effect on the relationship between the weight of contaminant added to the fluid and the resultant pressure drop increase across the medium.

The type of flow system, also, has a pronounced effect on contaminant tolerance. In a recirculating system, such as a typical hydraulic or water - glycol loop in which the same liquid passes through the filter medium many times, the smaller particles which initially pass through the clean medium will be carried by the liquid back to the reservoir and, again, presented to the upstream side of the filter. At this time, the medium has become partially clogged and is functioning as a "finer" filter than when all pores were open. Thus, more fine particles will be trapped, and each successive "pass" of the liquid through the filter will result in increasingly finer filtration. The effect on the filter medium is to cause the pressure drop to rise to a higher level than would be the case if the originally passed particles were never again presented to the filter.

In a non-recirculating system, such as is typically employed with propellants, the fluid passes through the filter only once, and particles that initially pass through are never returned to the face of the medium. Here, a given amount of contaminant in the fluid will produce a lesser pressure drop across the medium than in a recirculating system, and a longer service life will result.

Contaminant tolerance of the various media was determined by injecting pre-weighed increments of AC Coarse Dust (made by General Motors Corporation, Flint, Michigan) upstream of the test sample in a flowing system. With the sample mounted in the flow fixture shown in Figure 1, and with a 100 x 100 mesh back-up screen installed to support the test sample, flow was established at a specific rate and incremental additions of the contaminant were injected into the flowing system. The change in pressure drop across the specimen, resulting from the injection of contaminant, was determined and plotted against the cumulative amount of contaminant injected.

Figure 2 shows the schematic outline of the test system, while Figure 37 shows the details of the flow control valve manifold. The three hand valves used in the flow control manifold allowed the flow to be maintained at a constant rate through the test specimen while incremental additions of contaminant were placed in the contaminant - addition port. After the contaminant was in place, the valves were manipulated to divert flow from the by-pass line through the contaminant additive port and, thence, through the test specimen. Details of the contaminant addition port are shown in Figure 38. The test procedure for conducting contaminant tolerance tests is contained in the Appendix.

For most of the media, contaminant tolerance, or service life, was established using AC Coarse Dust. Although this particular contaminant may not be truly representative of actual contaminant found in spacecraft systems, the relative performance of the various media was established and the ground work laid for determining the effect of real system contaminant when the nature of the material becomes known.

### 3.6.2 Evaluation of Test Fixture, System and Methods

The fixture, in which the test samples were mounted, was used for both flow resistance tests and contaminant tolerance tests. As noted earlier, the flow resistance tests were conducted with the test sample only, (no back-up support was used). For the contaminant tolerance tests, however, a support member consisting of 100 x 100 mesh screen was placed beneath the test medium to provide strength sufficient to allow the imposition of up to 50 psi differential pressure across the medium. The back-up screen was rigidly mounted in a ring of the same internal diameter as the sizing ring used for the flow resistance tests and shown in Figure 1. Thus, the exposed flow area was the same for the contaminant tolerance tests as for the flow resistance tests. Figure 39 shows the results of flow resistance tests with the bare fixture, the fixture with the 100 x 100 mesh back-up and the fixture with the 80 x 700 TDDW with the back-up and without. The addition of the back-up screen appears to have little or no additive affect to the results measured with a test screen alone.

Contaminant tolerance tests were initiated using the test set-up shown schematically in Figure 2. The first tests were conducted with the flow line containing the contaminant addition port and the test sample in a horizontal position. This is typical of the test method called out in MIL-F-8815, and other standard filter specifications for conducting "contaminant holding" tests. It was soon observed, however, that adding contaminant in a horizontal line leads to serious errors and inconsistent results. This is especially true at low fluid velocities when the test contaminant is not thoroughly washed out of the contaminant addition port or settles out in the flow line. The system was modified to provide for positive contaminant addition by changing the position of the flow line from the contaminant addition port to the downstream pressure pick-up piezometer, so that this entire line section was in a vertical position. The test specimen orientation was thus horizontal, and the probability of the contaminant reaching the specimen was greatly improved. At this time, all line sizes were 3/4". These modifications initially appeared to have provided the necessary efficiency

FIGURE 38  
CONTAMINANT ADDITION PORT

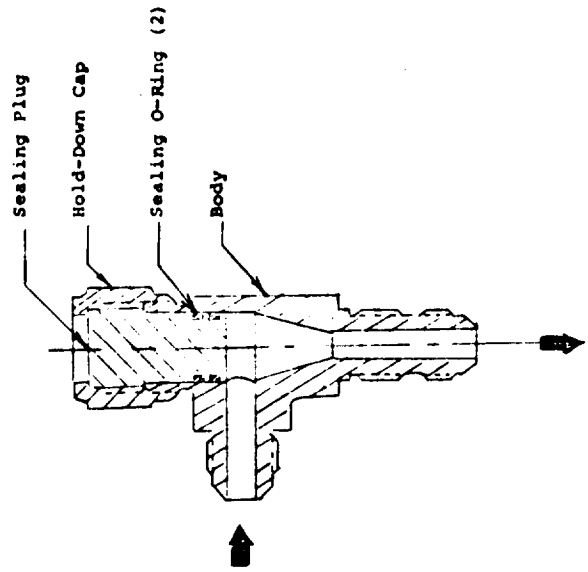
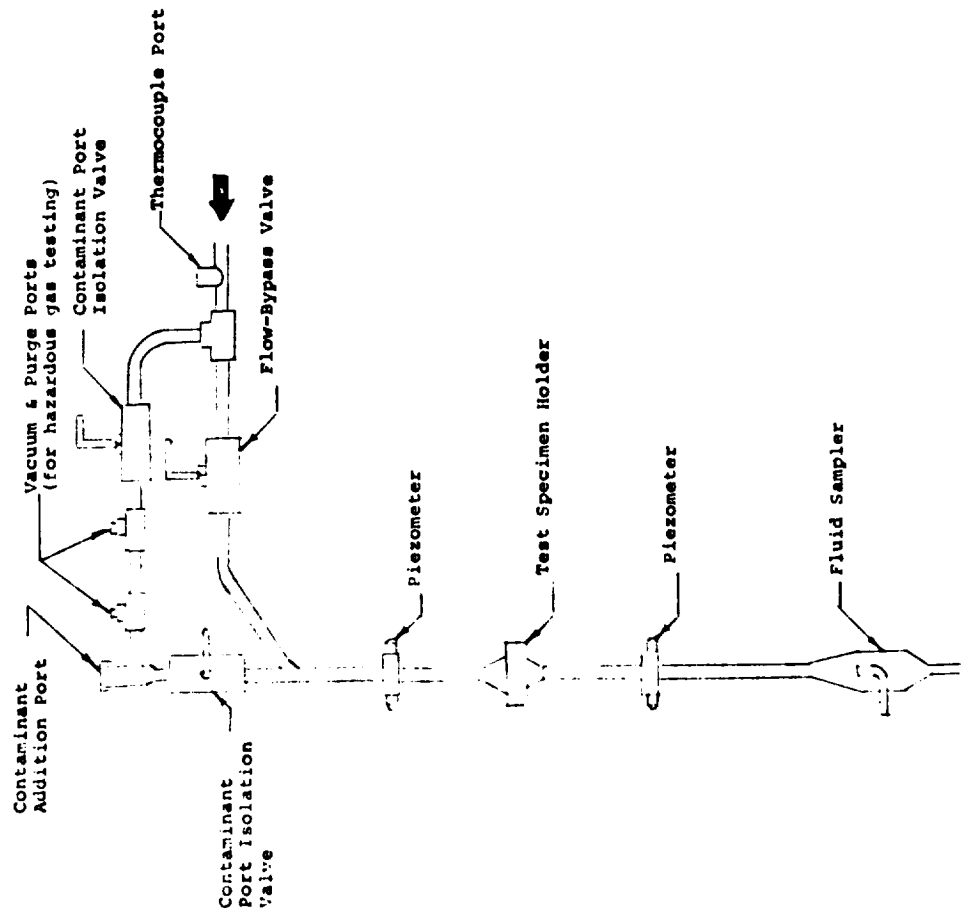


FIGURE 37  
CONTAMINANT ADDITION MANIFOLD



in transmitting injected contaminant to the test medium. Good repeatability was obtained at flow rates of 1.8 GPM and above, but the data scatter at lower flow rates suggested further modification of the flow system would be required. To evaluate the efficiency of the system, a pre-weighed, 0.45 micron membrane filter was installed in place of the screen test media in the test fixture. A standard contaminant tolerance test was conducted in which 30 milligrams of AC Coarse Test Dust was added to the flow system while flowing 0.2 GPM. The contaminant was added in one step, that is, one 30 milligram add. Two minutes after stabilization of differential pressure, the system was shut down, residual fluid was forced through the membrane by nitrogen displacement, and the membrane containing the contaminant was removed, dried and weighed. The weight increase of the contaminated membrane indicated a recovery of only 65 per cent of the added contaminant. On the basis of the recovery test, it was decided to make an additional modification to the system by providing a separate contaminant addition system using 3/8" lines to be used for flow rates of less than 1.8 GPM. The smaller line size provided greater fluid velocity, and greatly increased efficiency in transmitting the test contaminant to the screen media.

In addition to the general line size reduction for low flow rates, the following changes were made in an effort to eliminate entrapment areas and improve system efficiency. The internal surfaces of the fittings and lines and the ball valve bore were polished to remove scratches and provide smooth surfaces. All gaps, steps and voids were eliminated by machining to provide mating, aligned fits. A slight modification was made to the contaminant addition port to minimize air entrapment upon contaminant addition, and to provide a "scouring" effect of the liquid to improve contaminant removal from the addition port. The contaminant addition port by-pass line was changed to provide a 45 degree angle to the specimen inlet flow line. This was done to eliminate any possibility of test contaminant settling in the side entry of the by-pass line.

System recovery tests were then repeated to verify the improved contaminant transmission characteristics of the modified flow system. Following are the results of four (4) recovery tests using 0.45 micron filter membranes in the screen holder at 0.2 GPM flow rate.

TABLE 7  
SYSTEM RECOVERY TEST DATA

|   | Test Number |         |         |         |
|---|-------------|---------|---------|---------|
|   | 1           | 2       | 3       | 4       |
| (1) Weight of Membrane Clean (grams)      | 0.09200     | 0.09070 | 0.09140 | 0.09040 |
| (2) Weight of Membrane After Test (grams) | 0.12085     | 0.12000 | 0.11940 | 0.11830 |
| (3) Weight Gain (2-1) (grams)             | 0.02885     | 0.02930 | 0.02800 | 0.02790 |
| (4) Contaminant Added to System (grams)   | 0.02970     | 0.02980 | 0.02950 | 0.0294  |
| (5) Percentage Recovery (3+4)             | 97.14%      | 98.32%  | 98.64%  | 98.3%   |

The above recovery percentages indicated that the system modifications were successful, and that contaminant tolerance tests could be conducted with the system in an efficient and repetitive manner.

With respect to the procedures for adding contaminants, present standard filter specifications, such as MIL-F-8815 and many aerospace contractor specifications, call for the addition of a specified contaminant (usually AC Coarse or AC Fine Dust) to a flowing system, in dry form, in pre-weighed increments, each 20 per cent of the expected total, at 4 minute intervals.



Obviously, the actual fluid systems, in which filters are used, do not provide contaminant in a series of 5 surges. Rather, the particulate matter will be relatively consistently dispersed throughout the total volume of fluid. Comparatively minor variations in contaminant level will occur as a result of component wear, but the system level does not undergo rapid and dramatic changes as typified by the currently used method of filter evaluation. To more accurately simulate a typical system contamination level, a means of steady, continuous injection of contaminant into the flowing stream would be desirable. Another method would be to contaminate the reservoir of fluid to a predetermined level, provide mixing capability to maintain the mixture, and simply flow the fluid through the filter at the proper flow rate with no return to the reservoir of filtered fluid.

As the tests to be conducted under this program would require incremental additions of contaminant, it was necessary to evaluate the possible effect of varying the incremental addition weight, the time between additions, and adding the contaminant in dry or slurry form. For all tests, the 325 x 2300 TDDW medium, AC Coarse Dust and deionized water were used. Figure 40 shows a comparison of contaminant tolerance curves at  $0.126 \text{ GPM/in}^2$  with 10 milligram increments added at 1 and 2 minute intervals. The variation obtained is well within the limits of repeatability and shows no appreciable deviation caused by a 100 per cent add rate variation. Figure 41 shows the effect of varying the incremental size of contaminant addition from 10 milligrams to 30 milligrams of AC Coarse Dust at a flow rate of  $0.126 \text{ GPM/in}^2$ . Again, the variance between curves is well within repeatability, and it can be concluded that within the limits tested, there is no appreciable difference in contaminant tolerance caused by add size variation. Figures 42 and 43 show the comparative effect of adding the contaminant in dry and slurry form at low ( $0.126 \text{ GPM/in}^2$ ) and high ( $2.21 \text{ GPM/in}^2$ ) flow rates. It was concluded that no appreciable difference occurs. Figure 44 shows that at the highest flow rate planned for testing ( $6.67 \text{ GPM/in}^2$ ) the variations in add size and/or time interval causes no significant variation in contaminant tolerance results.

These tests, therefore, show that contaminant can be added at short time intervals, usually only long enough to allow thorough washing of the contaminant from the addition port. The size of each incremental add need only be small enough to provide a smooth curve for contaminant tolerance, since the add sizes will vary depending on the medium under test and the flow rate of the test fluid.

Although all contaminant tolerance curves in this report are plotted as smooth "curves," the changes in pressure differential actually occur in sharp steps or plateaus with each contaminant addition, followed by a slight secondary rise caused by contaminant which "lagged" the main body of the increment.

As pressure differential readings were taken after stabilization, and just prior to making each add, the abrupt step followed by the slight additional rise, does not show, and a smooth curve has been drawn through the series of data points.

FIGURE 39  
FLOW FIXTURE EVALUATION

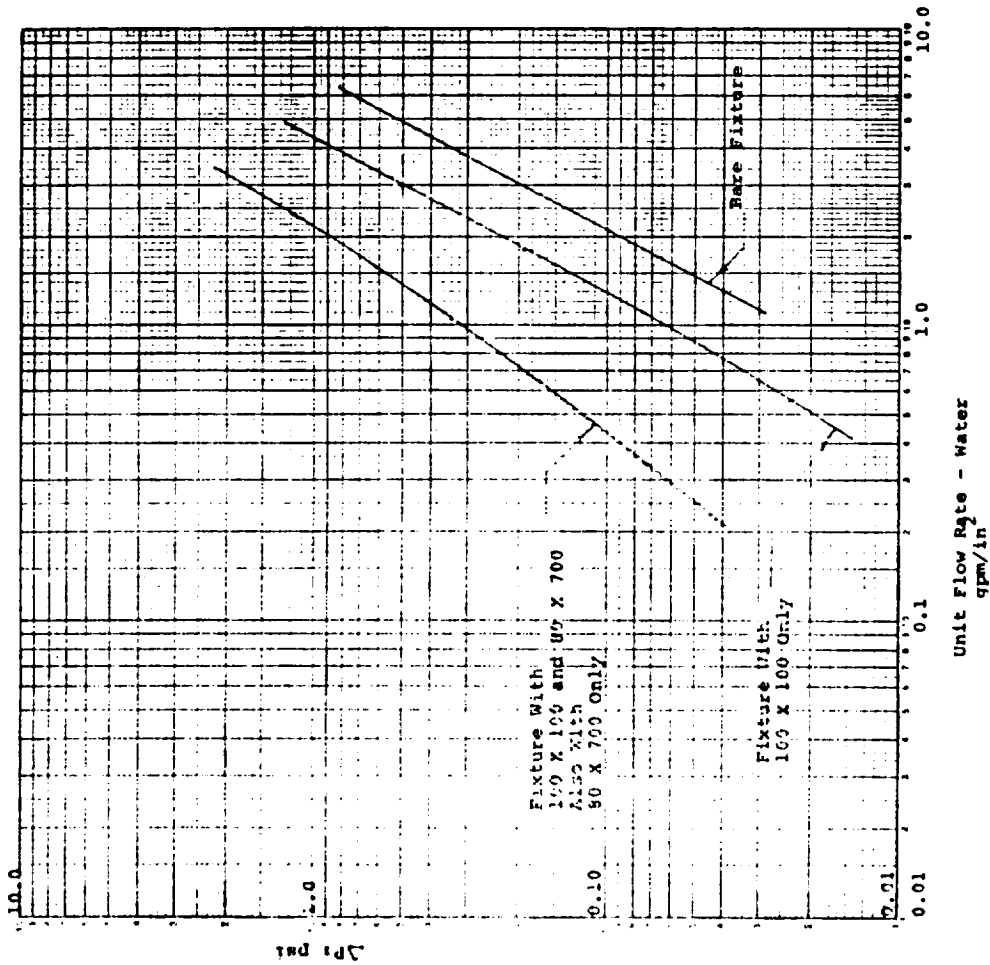


FIGURE 40  
EFFECT OF ADD RATE, 325 X 2300 SCREEN

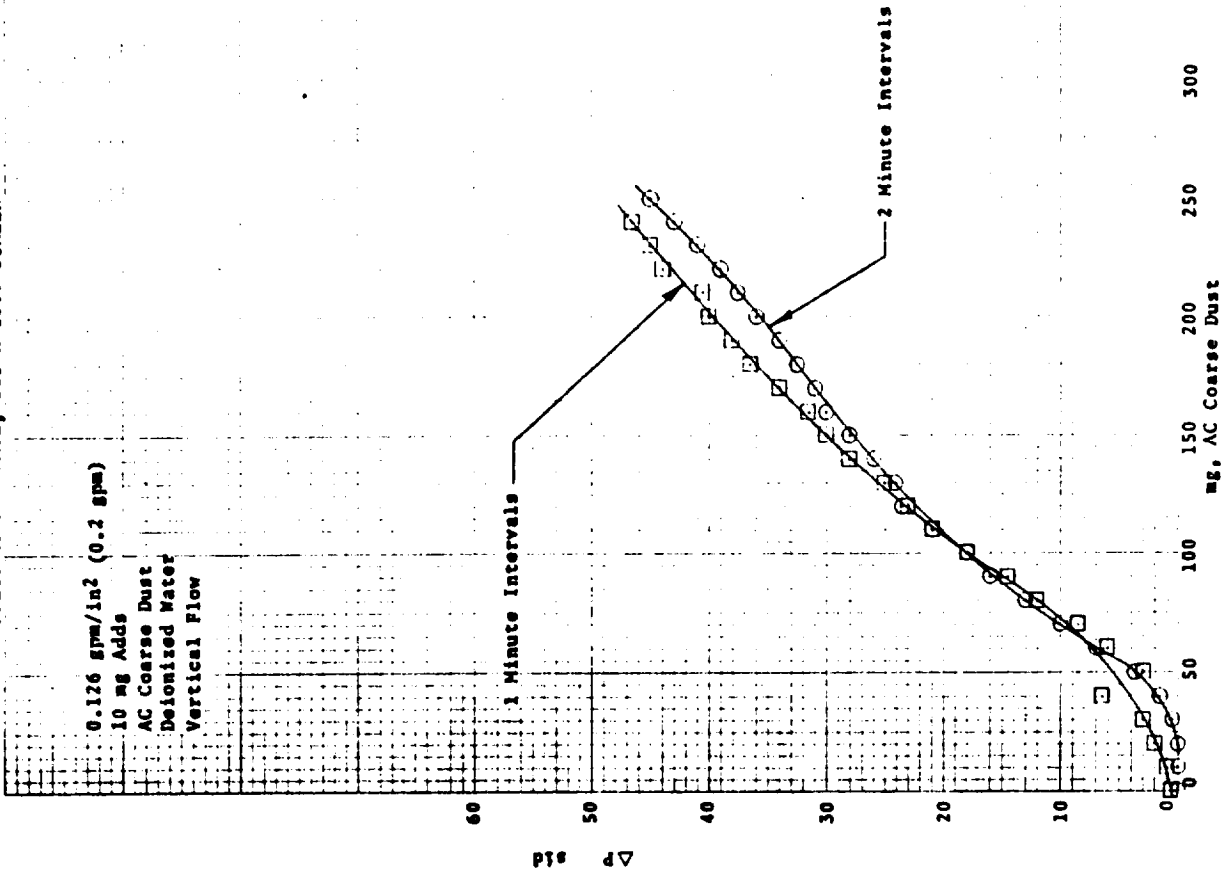


FIGURE 41  
EFFECT OF ADD SIZE, 325 X 2300 SCREEN

0.126 spm/in<sup>2</sup> (0.2 spm)  
1 Minute Intervals  
AC Coarse Dust  
Deionized Water  
Vertical Flow

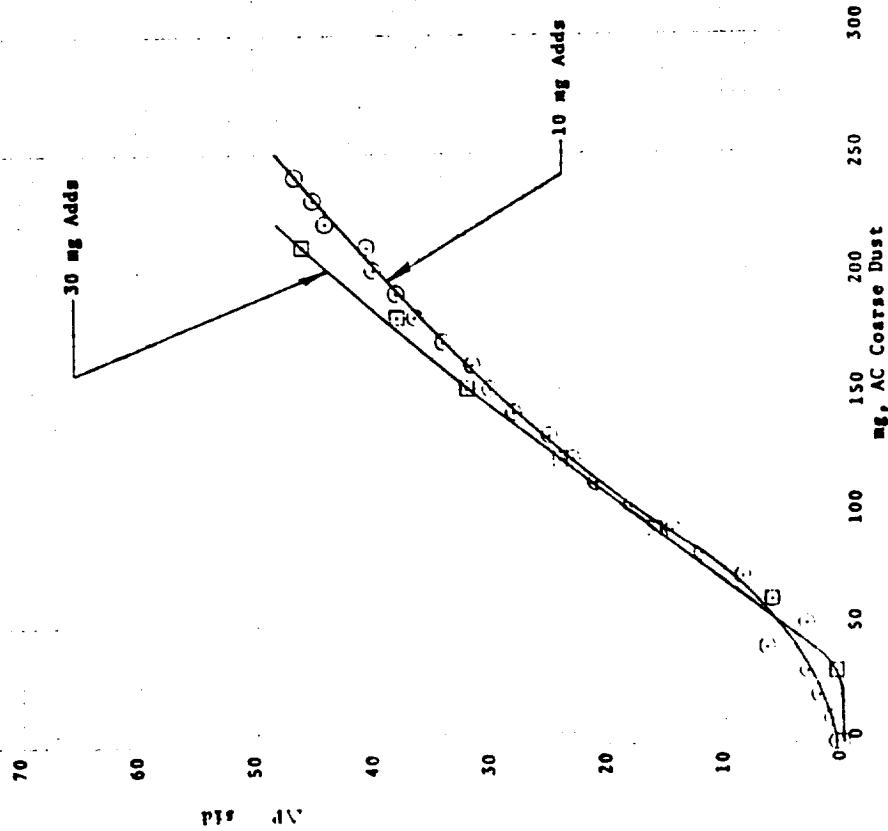


FIGURE 42  
EFFECT OF DRY VS. SLURRY ADDS, 325 X 2300 SCREEN

0.126 spm/in<sup>2</sup> (0.2 spm)  
2 Minute Intervals  
30 mg Adds  
AC Coarse Dust  
Deionized Water  
Vertical Flow

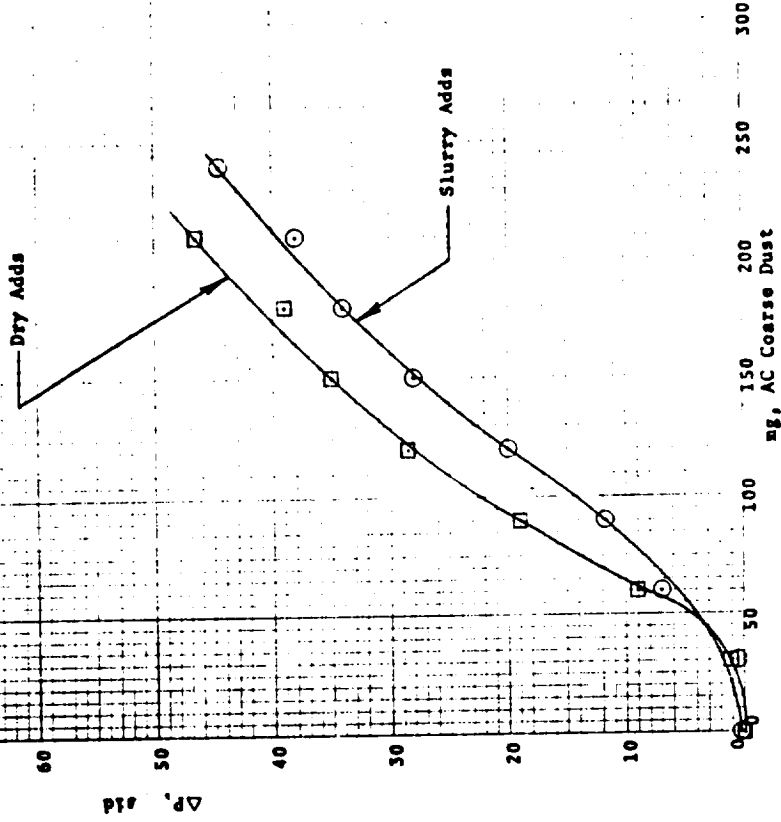


FIGURE 43

EFFECT OF DRY VS. SLURRY ADDS AT HIGH FLOW RATE, 325 X 2300 SCREEN

2.21 gpm/in<sup>2</sup> (3.5 gpm)  
 3 Minute Intervals  
 10.5 mg. Adds  
 AC Coarse Dust  
 Deionized Water  
 Vertical Flow

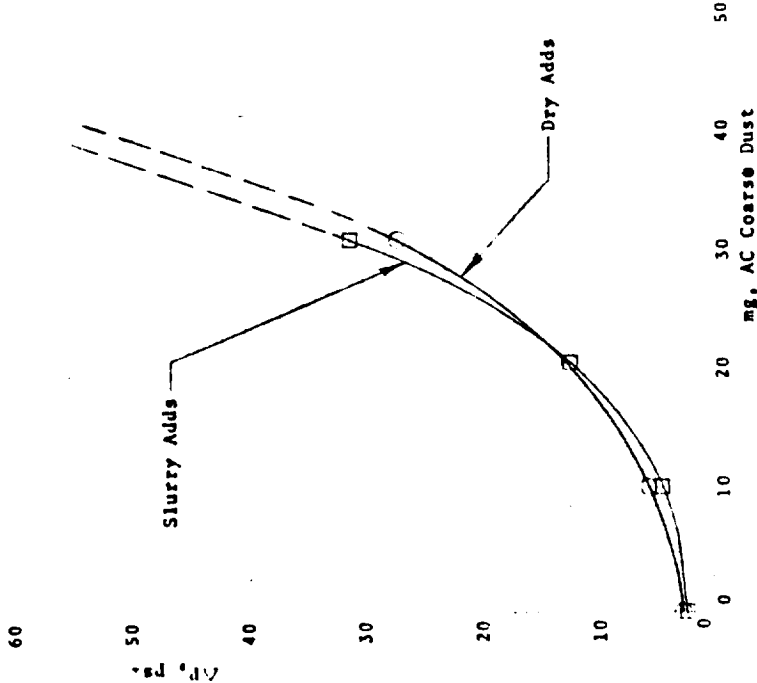
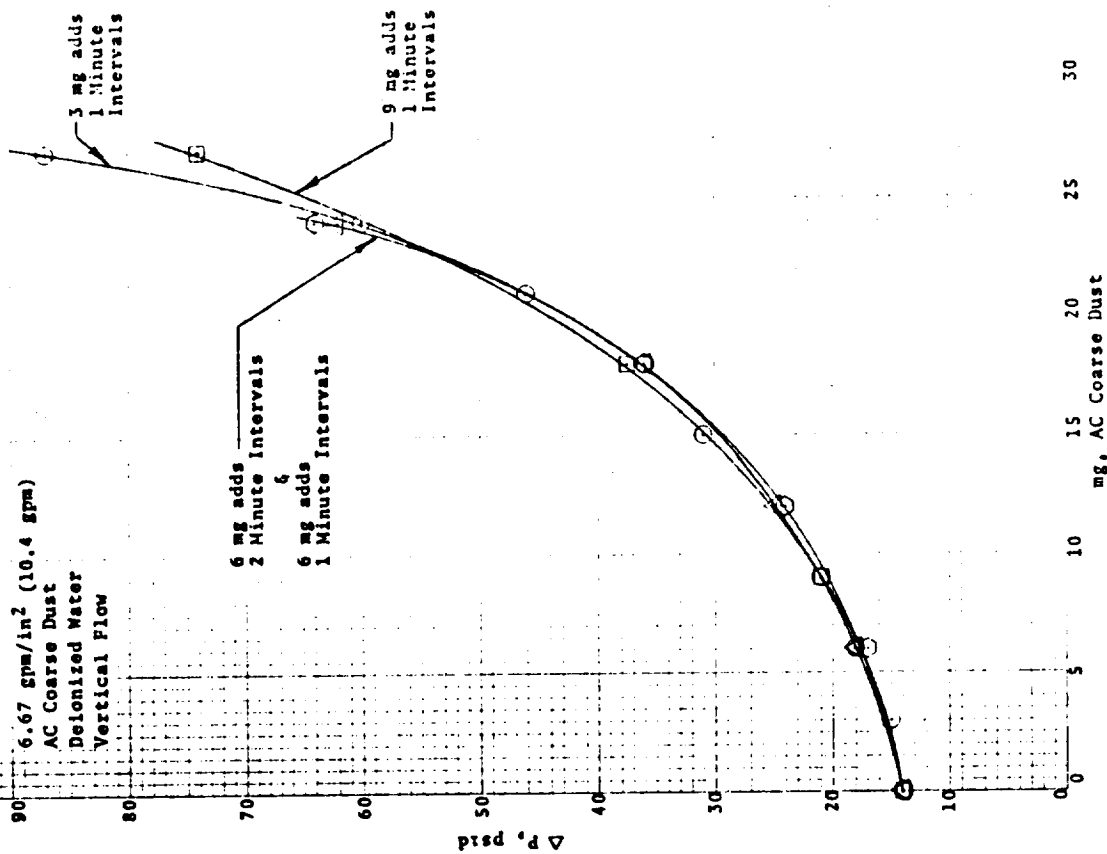


FIGURE 44

EFFECT OF ADD SIZE AND INTERVAL AT HIGH FLOW RATE, 325 X 2500 SCREEN

6.67 gpm/in<sup>2</sup> (10.4 gpm)  
 AC Coarse Dust  
 Deionized Water  
 Vertical Flow



### 3.6.3 Contaminant Tolerance Tests - Gases

The following table lists the figure numbers which show the results of contaminant tolerance tests conducted at the NASA - JSC White Sands Test Facility using gaseous oxygen and hydrogen, and a mixture of AC Coarse Dust with iron pyrite crystals substituted in the size ranges above 40 microns.

TABLE 8  
FIGURE NUMBERS FOR CONTAMINANT TOLERANCE TESTS WITH GAS

|                 | <u>Gaseous Oxygen</u> |                 | <u>Gaseous Hydrogen</u> |                 |
|-----------------|-----------------------|-----------------|-------------------------|-----------------|
|                 | <u>50 psia</u>        | <u>400 psia</u> | <u>50 psia</u>          | <u>400 psia</u> |
| 30 X 250 TDDW   | 45                    |                 | 52                      | 56              |
| 80 X 700 TDDW   | 46                    | 49              | 53                      | 57              |
| 165 X 1400 TDDW | 47                    | 50              | 54                      | 58              |
| 325 X 2300 TDDW | 48                    | 51              | 55                      | 59              |

The contaminant tolerance tests with gas originally used a flow control manifold with by-pass and isolation valves identical to that used in liquid flow resistance tests. Initial tests conducted at WSTF, however, indicated that some Teflon particles were shedding from the non-lubricated stem seal of the control valves and entering the system. As each contaminant addition required closing and opening three valves, the extraneous contamination was not acceptable.

The system was, therefore, modified by removing the by-pass line and the downstream contaminant addition port isolation valve. The schematic diagram of the entire gas testing system, as used at WSTF is shown in Figure 60.

Contaminant tolerance tests with gas are conducted by closing the upstream contaminant isolation valve, opening the contaminant addition port, and dropping the increments of contaminant directly downward into the test specimen. A coarse mesh screen is located at the bottom of the contaminant addition port to break up and distribute the "slug" of contaminant. The isolation valve is then opened allowing gas to sweep the remaining contaminant from the port and screen onto the test specimen. A 10 micron in-line fitting filter was also incorporated immediately downstream of the isolation valve to catch particles of Teflon generated by the valve action. The test fixture used for gas tests was described in the section on flow resistance and shown in Figure 21.

With typical filters operating in a gravity field, the rapid slowing of the gas velocity as it enters the filter case will tend to drop out much of the contaminant it carries. This material will settle out in the void space between the filter element and the housing and will never reach the screen. This accounts in part for the generally "superior" contaminant tolerance of filters in gas use as compared to those in liquid service. In a zero gravity environment, however, the settling forces are not available. Directional changes of the gas prior to contacting the filter elements can be used to take advantage of the momentum of the larger particles, and literally, throw them into a collecting area apart from the screen. For the purpose of these tests, however, it was desired to simulate the worst conditions, hence, a vertical injection - flow line, with a horizontal test specimen, were utilized.

The curves show that the contaminant tolerance is related inversely to the density and velocity of the gas. In all cases, the hydrogen gas provides higher contaminant tolerance; and the tests at 400 psia consistently show less contaminant tolerance than those at 50 psia. In the case of the tests with hydrogen and the lower flow rate tests with oxygen, the initial

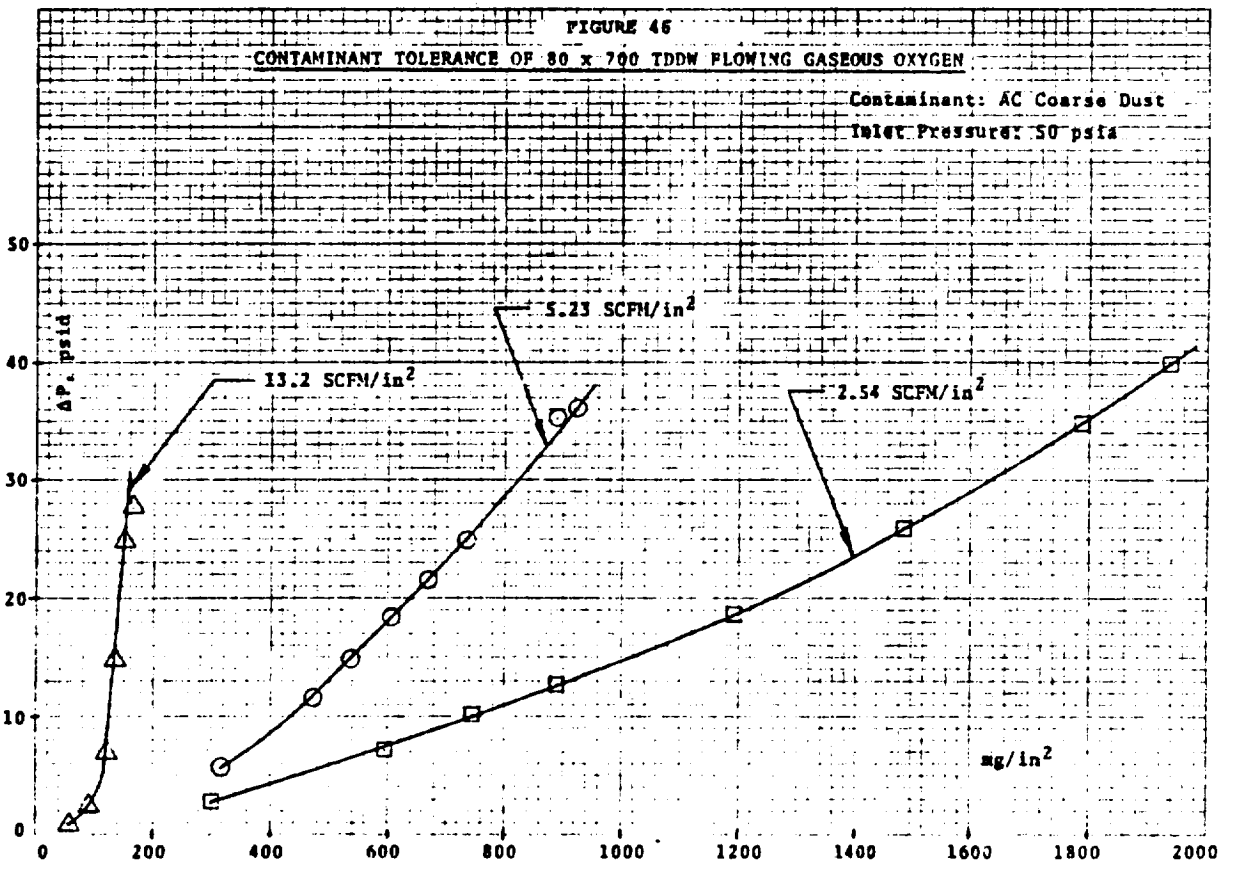
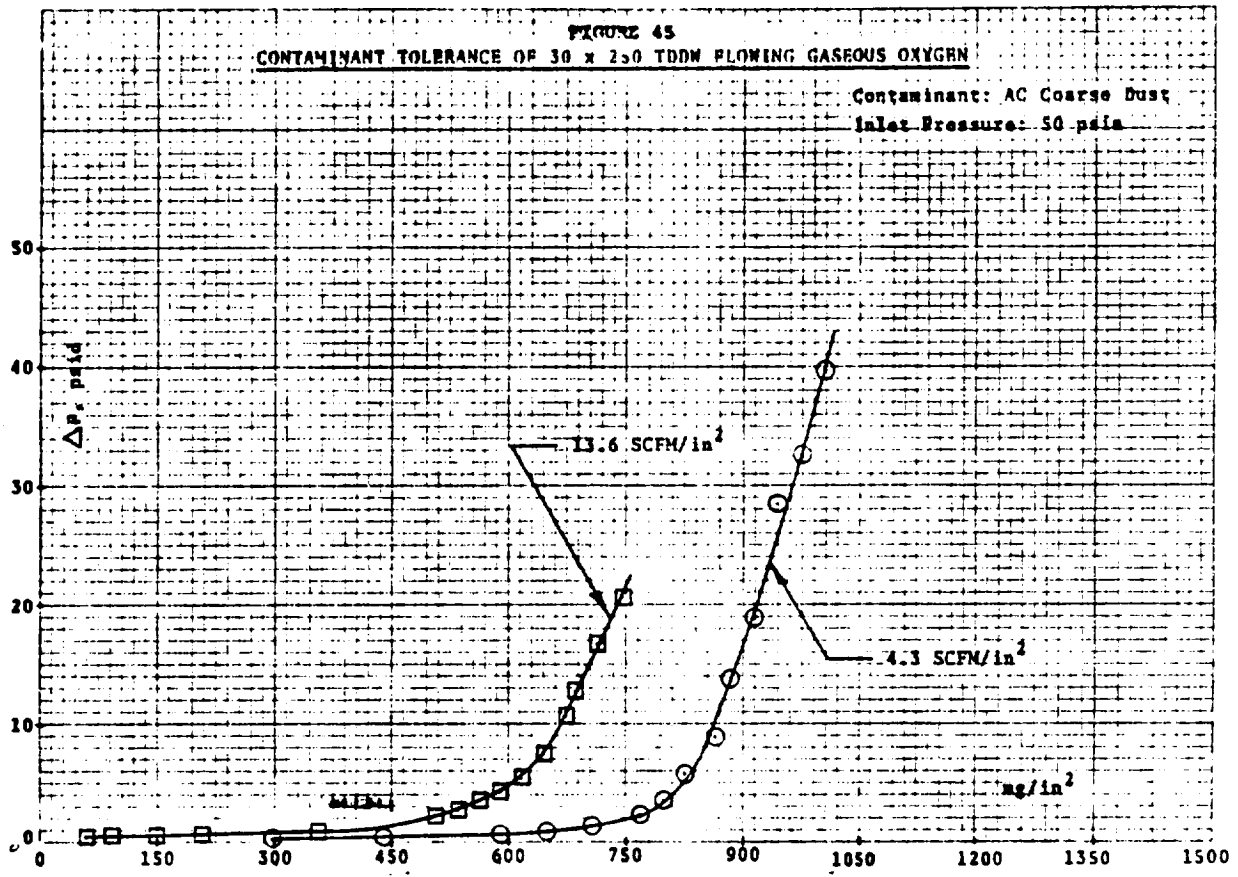


FIGURE 47

CONTAMINANT TOLERANCE OF 165 x 1400 TDDW FLOWING GASEOUS OXYGEN

Contaminant: AC Coarse Dust  
Inlet Pressure: 50 psia

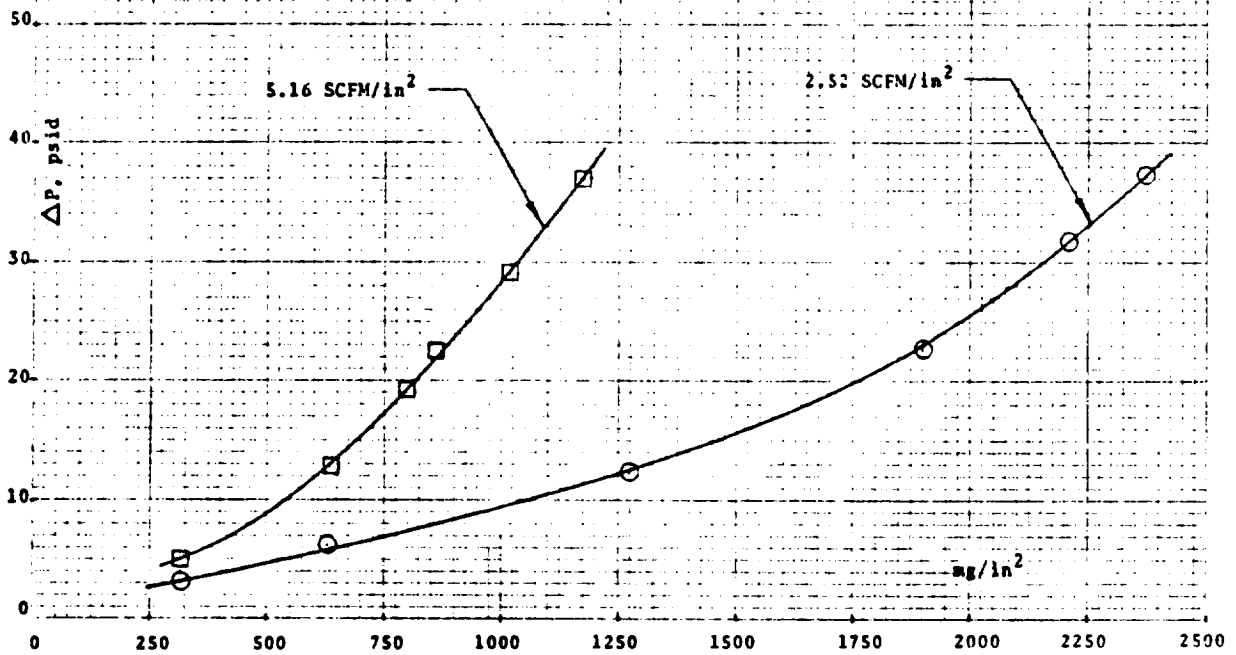
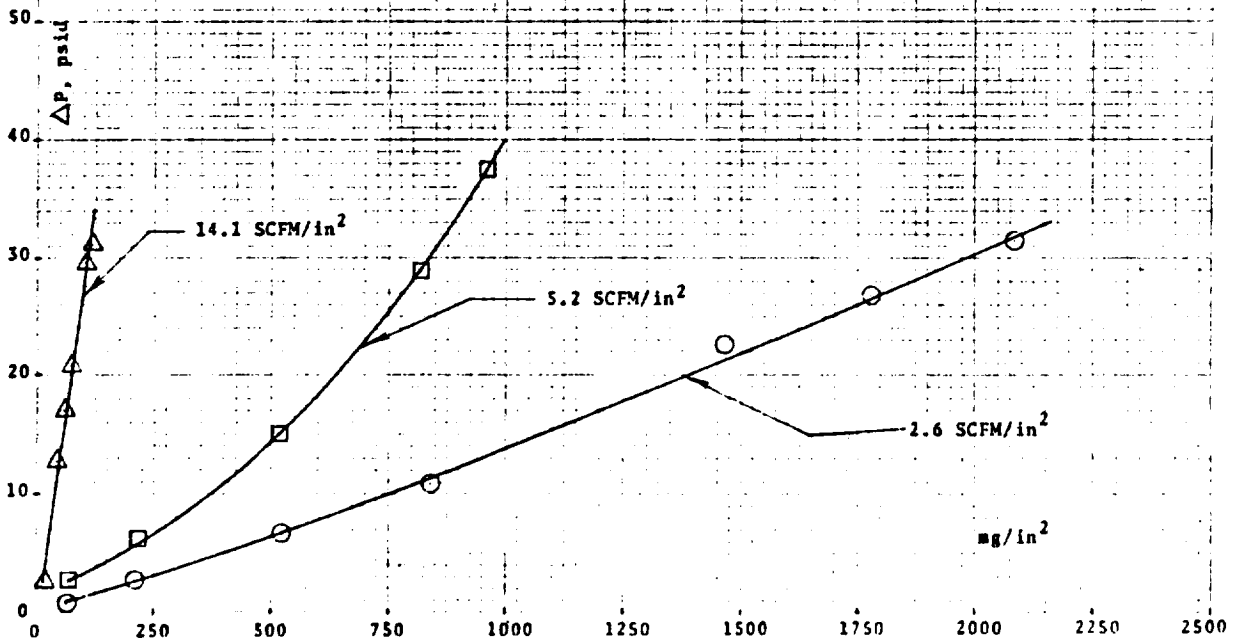
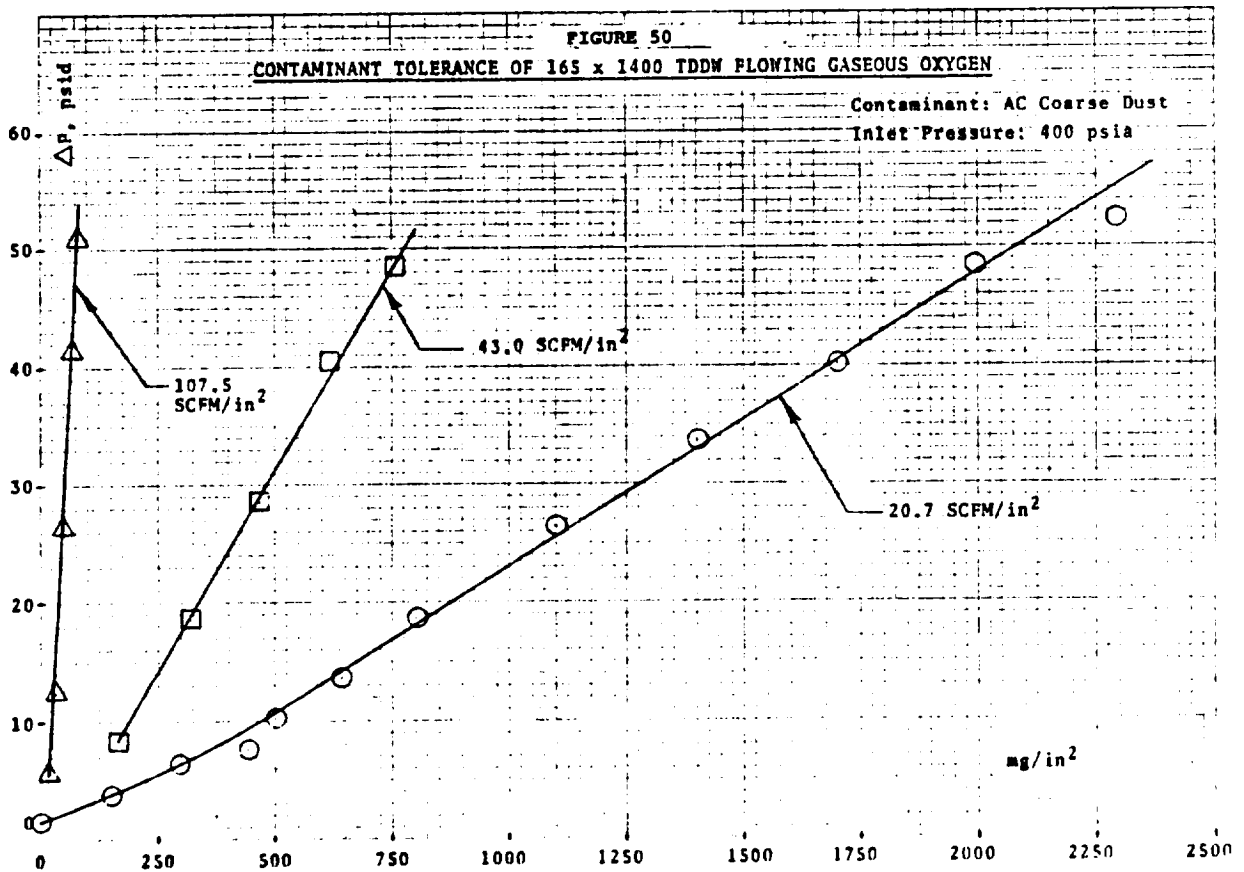
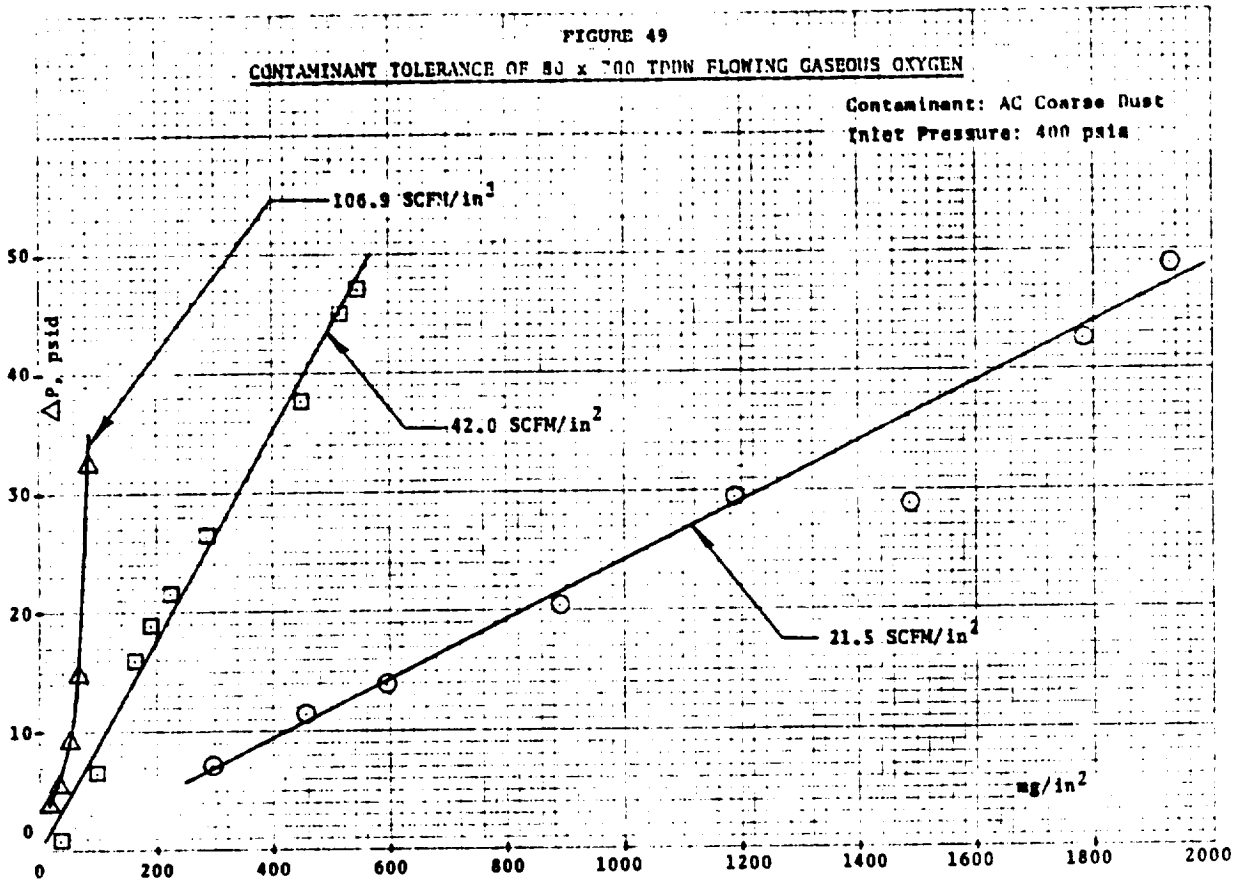


FIGURE 48

CONTAMINANT TOLERANCE OF 325 x 2300 TDDW FLOWING GASEOUS OXYGEN

Contaminant: AC Coarse Dust  
Inlet Pressure: 50 psia







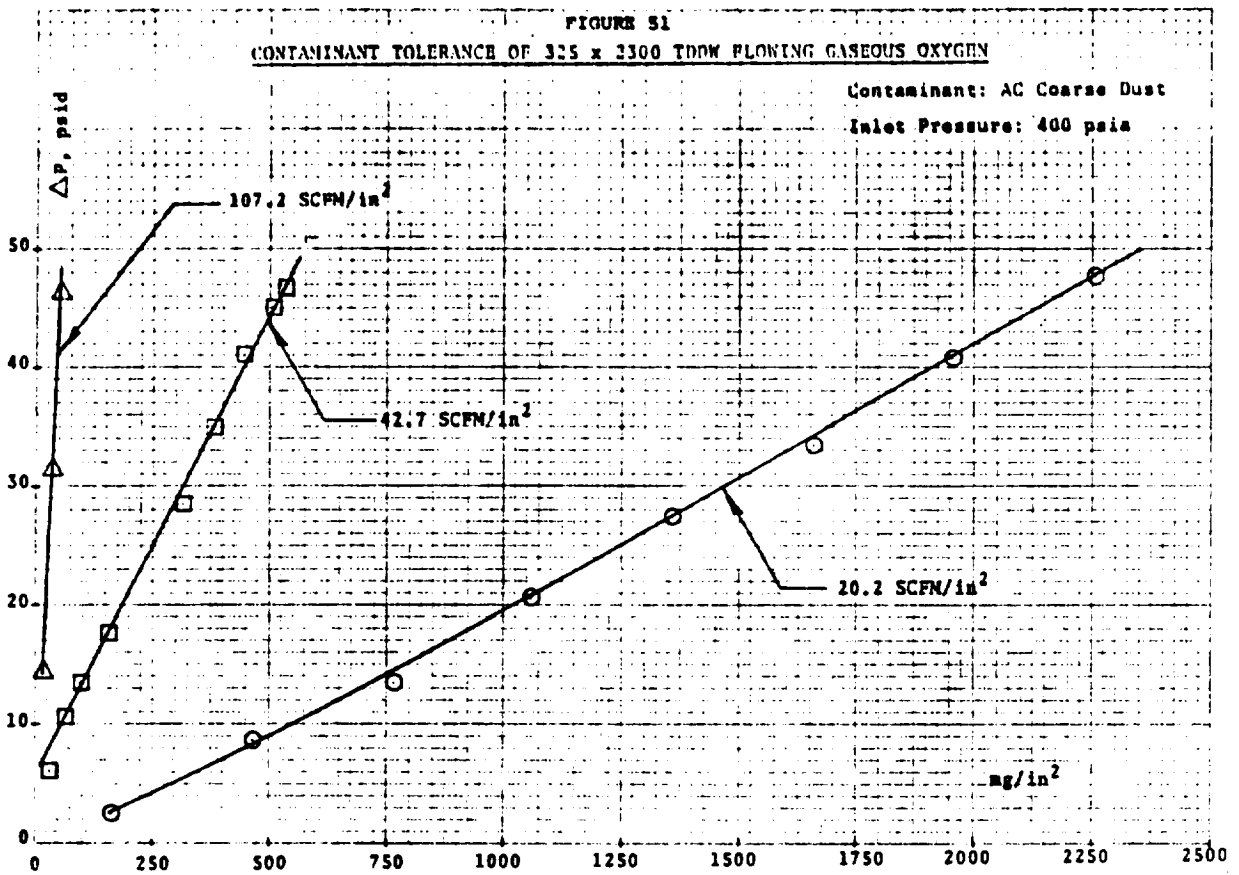


**FIGURE 52**

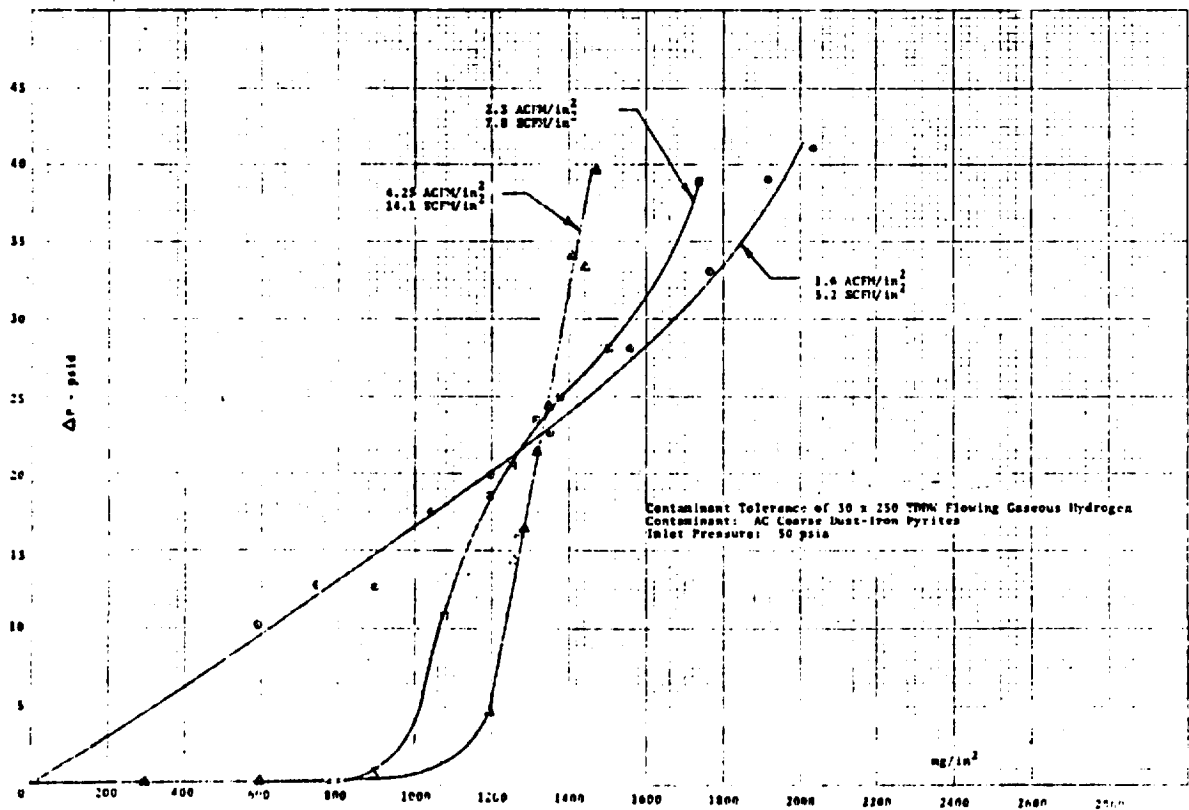


FIGURE 53

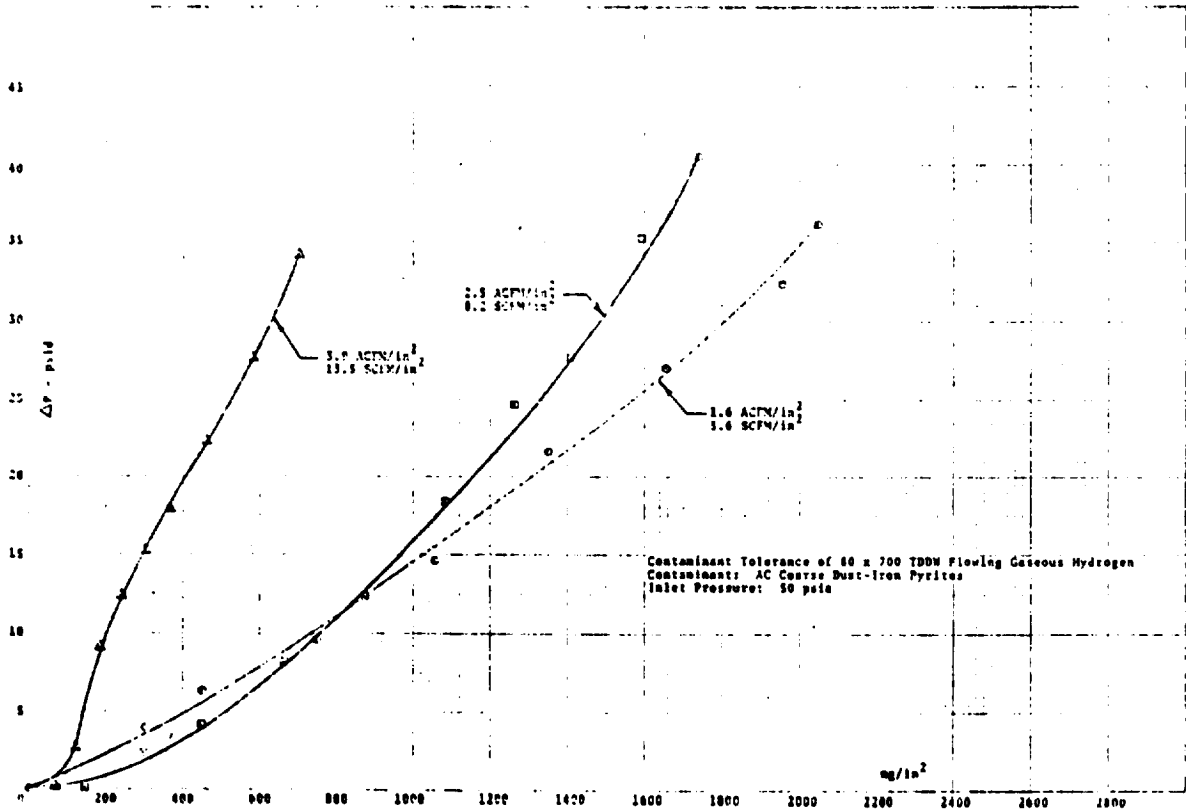


FIGURE 54

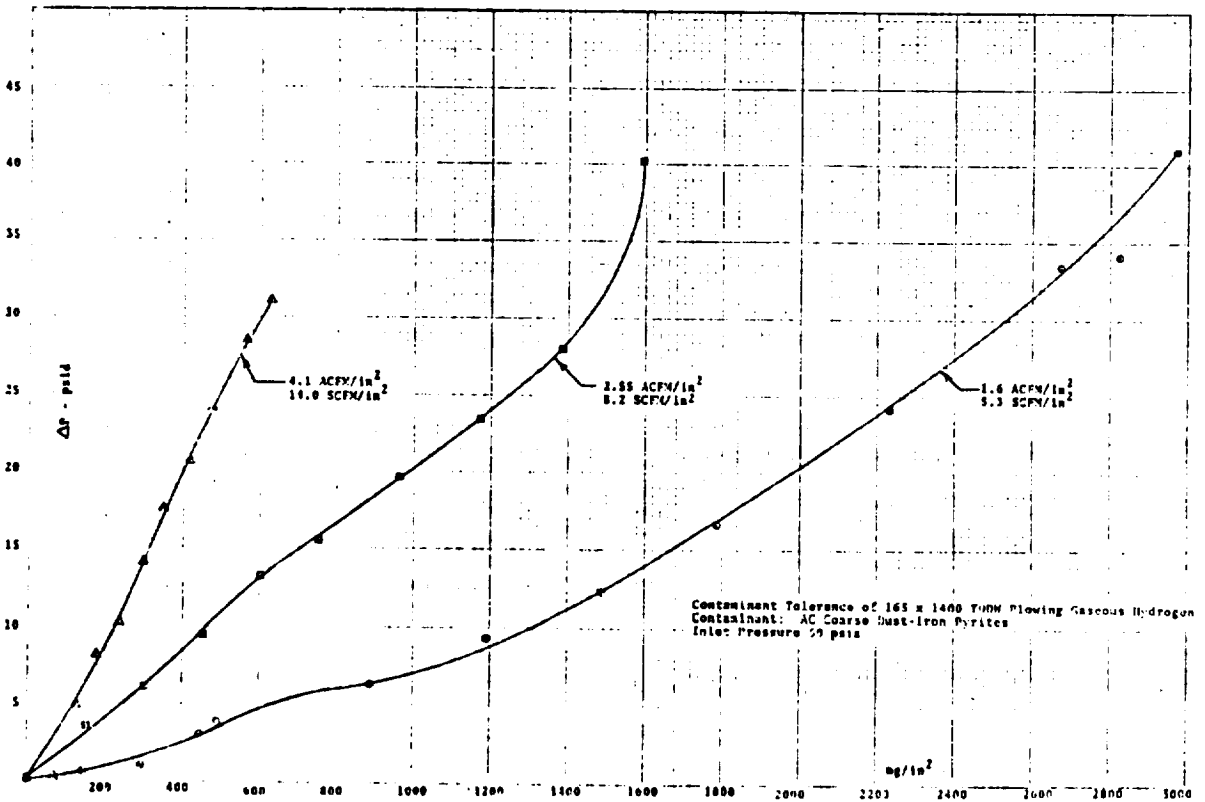


FIGURE 55

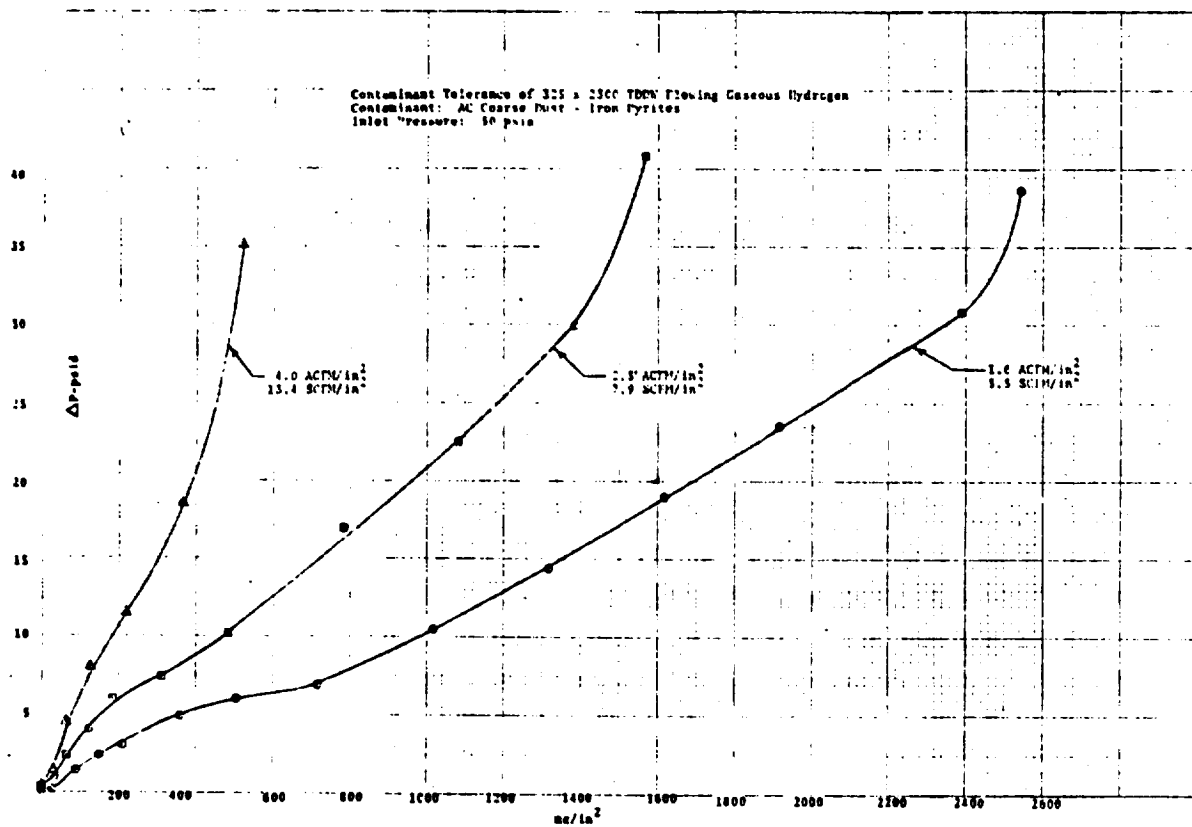


FIGURE 56

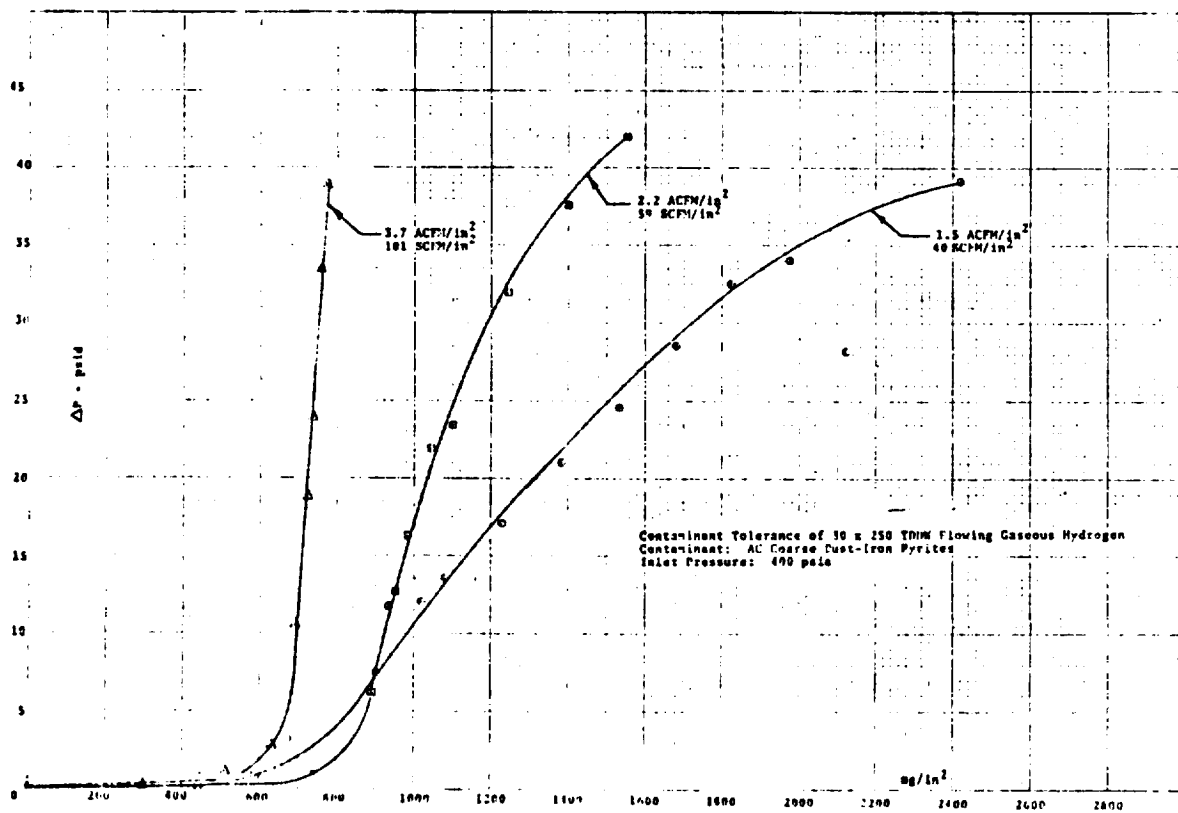


FIGURE 57

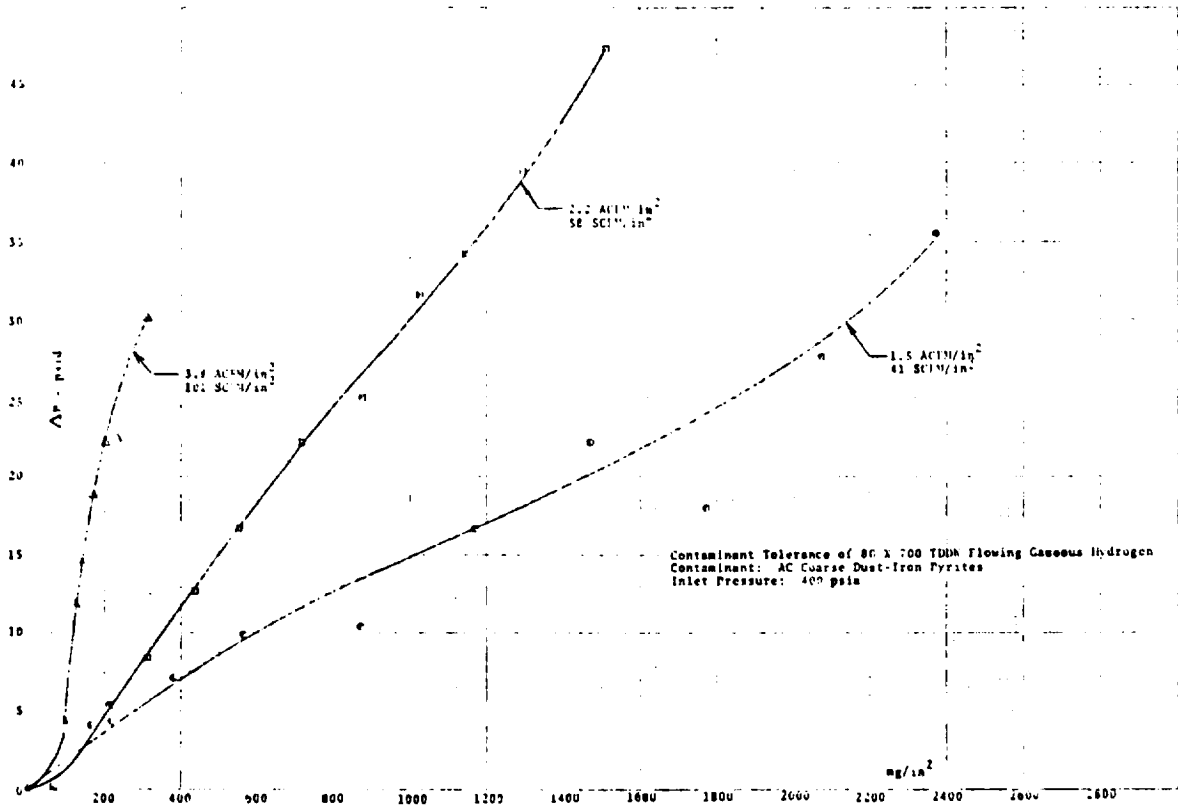


FIGURE 58

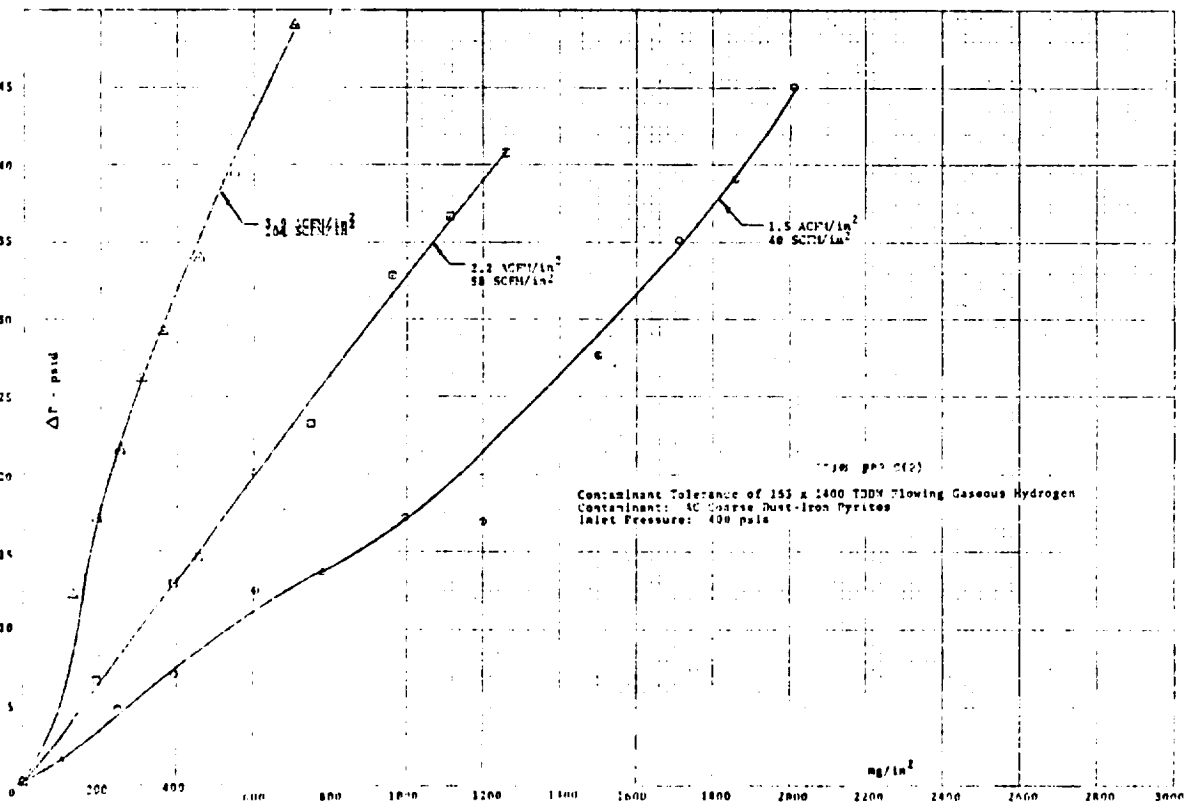


FIGURE 59

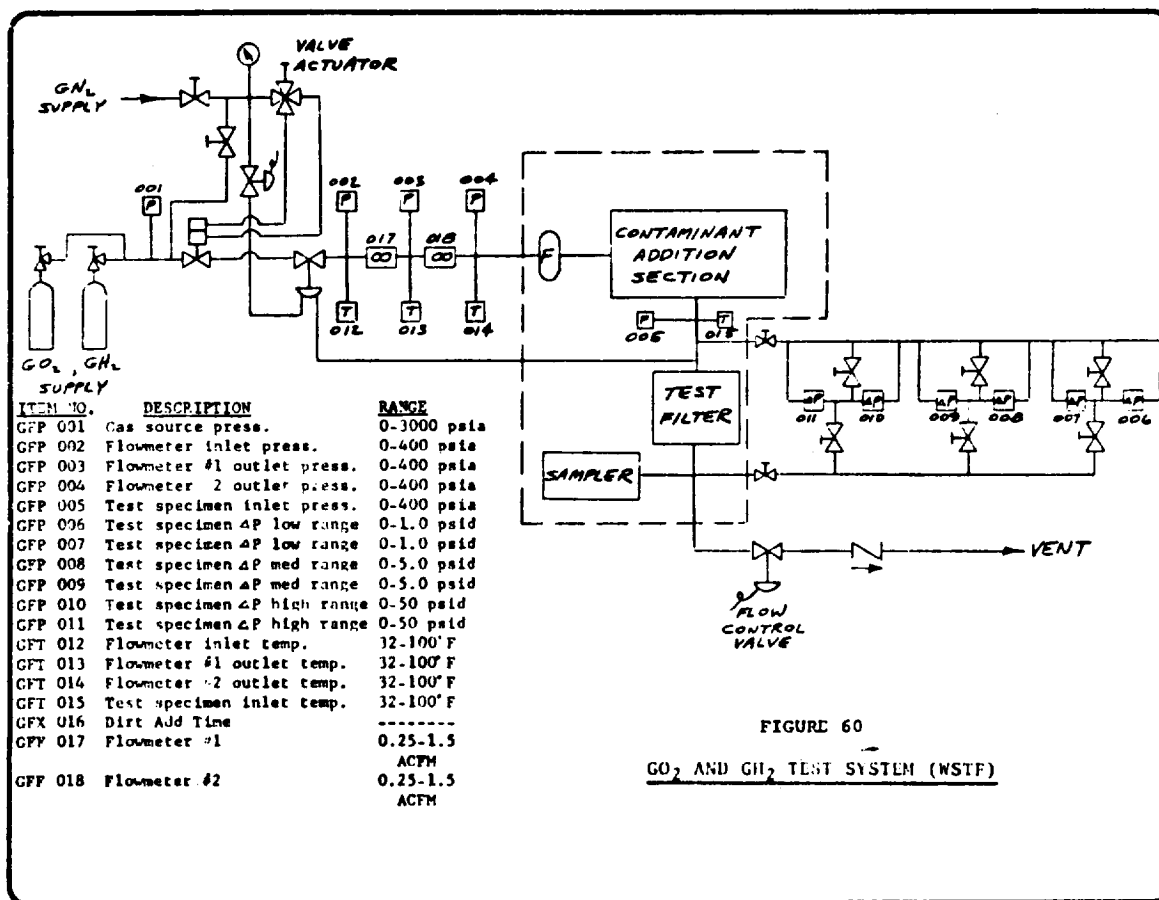
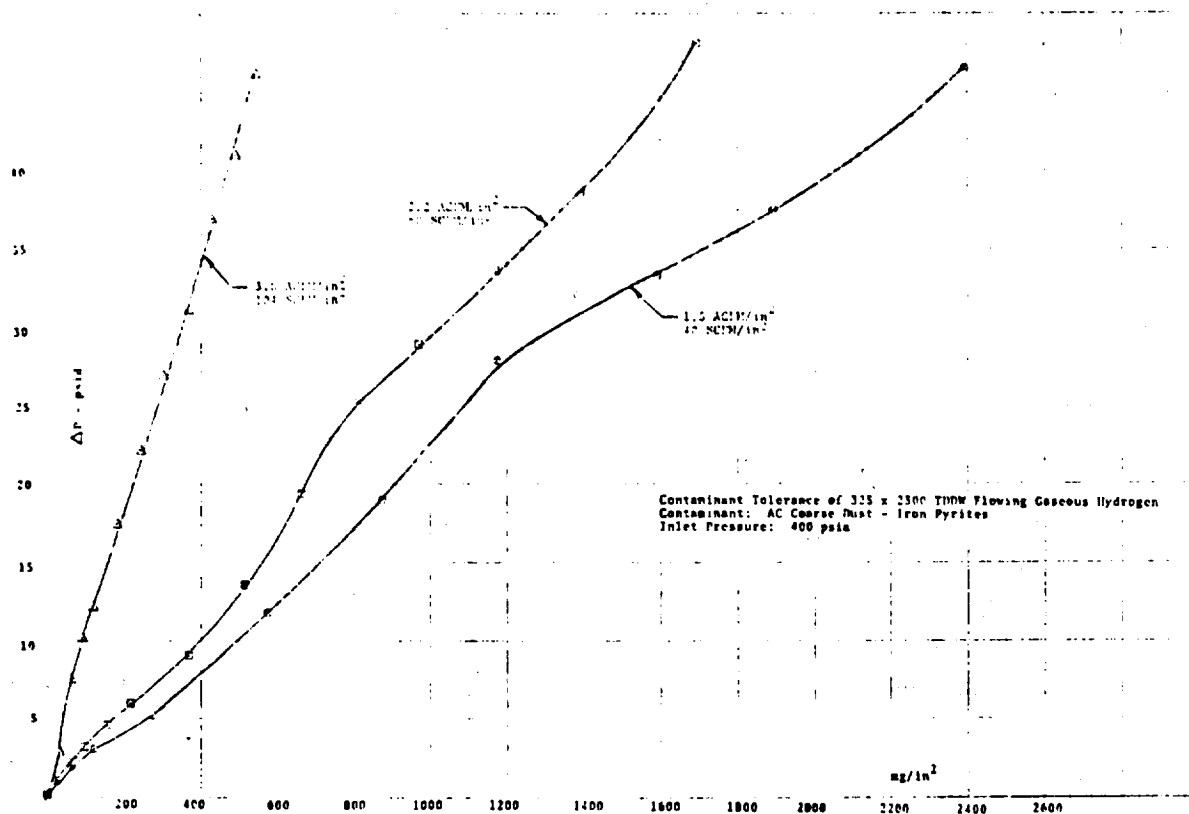


FIGURE 60  
 GO<sub>2</sub> AND GH<sub>2</sub> TEST SYSTEM (NSTF)

contaminant additions cause the typical initial upward sweep of the curve, as experienced in liquid tests (Paragraph 3.6.4). The extended portions of the curves, however, proceed in a relatively straight line. This indicates a silting, or "sand bed," effect, wherein the pressure drop is a function of the contaminant cake thickness, rather than the result of true clogging or plugging of the screen pores.

#### 3.6.4 Contaminant Tolerance Tests - Liquids

Several types and grades of porous media were exposed to incremental additions of various contaminants, using water, hydraulic oil, JP-4 and water - glycol. Because of the large number of tests conducted, the figures and tables resulting from these tests were compiled in a separate Appendix (Volume II) of this report, and only those figures referenced in the following text were included in Volume I.

As noted earlier, each of the media possesses different characteristics, such as size and number of flow paths, configuration of the flow paths and their degree of tortuosity. These characteristics all affect the contaminant tolerance of the media. In addition, the particle size distribution and nature of the contaminant, as well as the physical characteristics of the liquid, have marked effects on pressure differential across the media after ingestion of contaminant. The effect on contaminant tolerance of the various parameters listed below is discussed separately in the following text.

- a) Type of Medium
- b) Filtration Rating of Medium
- c) Flow Velocity
- d) Contaminant Type and Particle Size Distribution
- e) Fluid Characteristics
- f) Element Configuration

##### a) Effect of Type of Medium on Contaminant Tolerance

The contaminant tolerance of a filter medium is affected by the nature of the collective flow paths through the medium, as well as by their size and number per unit area. The cross sectional shape of the flow paths, in wire cloth for instance, vary from the triangular form provided by the dutch weave media, to the square form of the square weaves. The depth type material represented by the sintered fiber felts contains pore shapes of all types caused by the interrelationship of the many metal fibers forming the mat. In general, the medium providing the greatest number of individual flow paths per unit area will provide the greatest contaminant tolerance for a specific filtration rating.

Depth type media, such as the sintered metal fiber felts, provide, by far, the largest number of flow passages and, because of the fact that filtration occurs throughout the body of the material rather than solely on the face of the media, these materials have relatively high contaminant tolerance.

Figure 61 shows a comparison between three types of media, all rated at 40 micron glass bead filtration. The test fluid is deionized water, at 2.21 GPM/in<sup>2</sup>, and the contaminant is AC Coarse Dust. The three media are 80 X 700 Twilled Dutch Double Weave, 80 X 400 Plain Dutch Single Weave, and a sintered metal fiber medium, Dynalloy X-11. Individual graphs and tables are contained in the Appendix. It can be seen that at a pressure drop of 20 psi across the media, the 80 X 400 PDSW shows a contaminant tolerance of 1.8 times that of the 80 X 700 TDDW, while the Dynalloy X-11 shows 2 times that of the 80 X 700 TDDW. Figure 62 shows a similar comparison for 20 micron media, 165 x 1400 TDDW, 2 X 120 X 650 PDSW and Dynalloy X-7. The order of contaminant tolerance is the same as for the 40 micron media. Figure 63 shows an

FIGURE 61

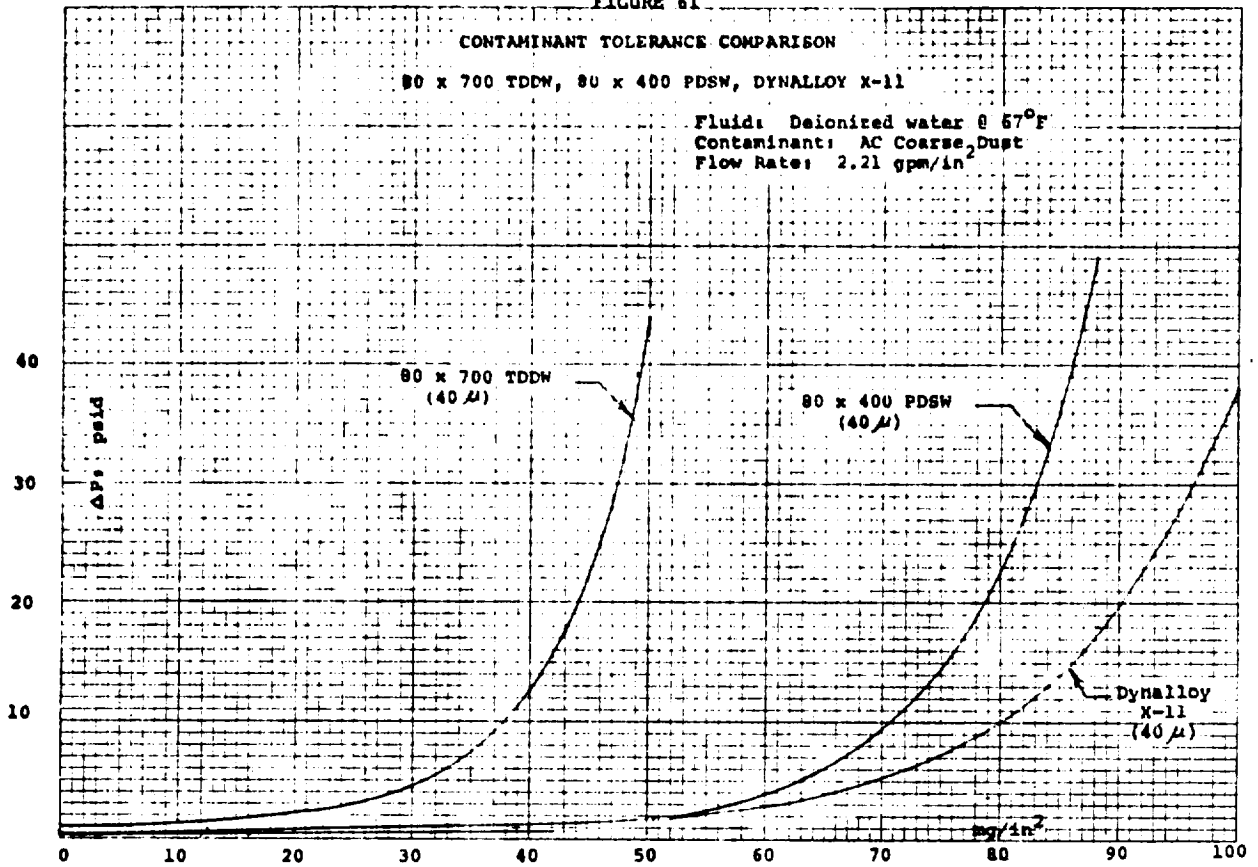
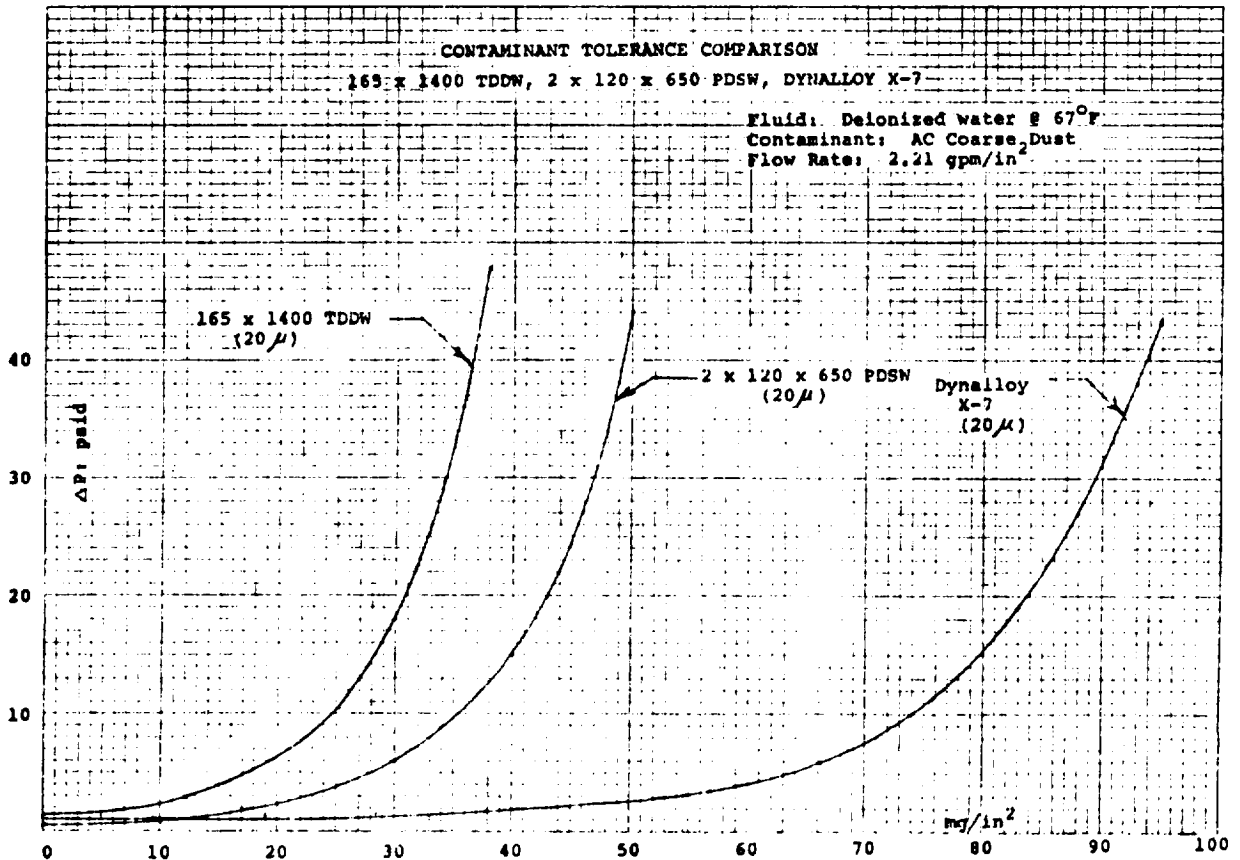


FIGURE 62



apparent reversal of contaminant tolerance for 100 micron rated media, 30 X 250 TDDW, 30 X 160 PDSW and Dynalloy X-13. Here, although the Dynalloy rating is 80 microns, the contaminant tolerance drops due to the Dynalloy's capacity to trap fine particles which pass through the other more open media.

b) Effect of Filtration Rating on Contaminant Tolerance

The filtration rating, or size of largest particle blocked by the medium, generally expressed as the Glass Bead Rating (GBR), also affects the contaminant tolerance of the medium, but this effect will vary depending upon the particle size distribution of the contaminant. Generally, the contaminant tolerance of a specific type of medium to a specific contaminant increases with increasing filtration rating, but it must be emphasized that much of this increase is due to the passing-through of particles smaller than the pore size.

The relationship between contaminant tolerance and filtration rating is shown graphically in Figure 64 for 7 grades of a typical type of porous medium Twilled Dutch Double Weave. Each curve shows the relationship between weight of AC Coarse Dust, introduced to the medium at a water flow rate of 2.21 GPM/in<sup>2</sup>, and the resultant pressure drop across the medium. Individual graphs and tables of data are contained in the Appendix.

Note that all the curves show an initial section of lower slope rising sharply as the pores become clogged. The AC Coarse Dust contains over 80,000 particles per milligram in the size range of 5 - 15 microns and, therefore, has an immediate effect on the finest material, 450 X 2750 TDDW, which blocks all particles in excess of 7 - 8 microns. So even though there are nearly 600,000 pores per square inch of this medium, the blockage of pores occurs rather quickly.

Even the coarse media, such as 30 X 250 rated at 100 microns, eventually traps sufficient particles larger than this rating so that the 3750 pores per square inch of medium become largely blocked. As the particles above the micron rating are trapped, the pores are not completely shut off, but the resultant flow space is reduced to the point where even the very fine particles become lodged in the remaining spaces and the pressure drop rises very sharply.

The curves for the two coarsest screens show an interesting characteristic. The 30 X 250 TDDW is rated at 100 microns GBR, while the 30 X 370 is rated at 95 microns GBR. These two media possess nearly the same micron rating, but the finer material, 30 X 370, shows a greater contaminant tolerance by nearly 30 per cent at 20 psid. This increased tolerance is due to the fact that the different wire diameters used for weaving the 30 X 370 provide a filtration rating approximately equal to the 30 X 250, while providing nearly 50 per cent more flow pores.

This type of data presentation and analysis is necessary to provide the optimization of filter design to provide the best choice of material to accomplish the required system filtration parameters.

c) Effect of Flow Velocity on Contaminant Tolerance

Just as the velocity of fluid flow determines the pressure drop across a specific medium with any fluid, so does flow velocity affect the contaminant tolerance of a porous medium. Figure 65 shows a family of curves for a typical filter medium, 325 X 2300 Twilled Dutch Double Weave, with a filtration rating of 10 microns. The contaminant used is AC Coarse Dust, and the test liquid is deionized water. As the unit flow rate increases, the contaminant tolerance reduces sharply. This is caused by the increased velocity of fluid through the flow passages.



FIGURE 63

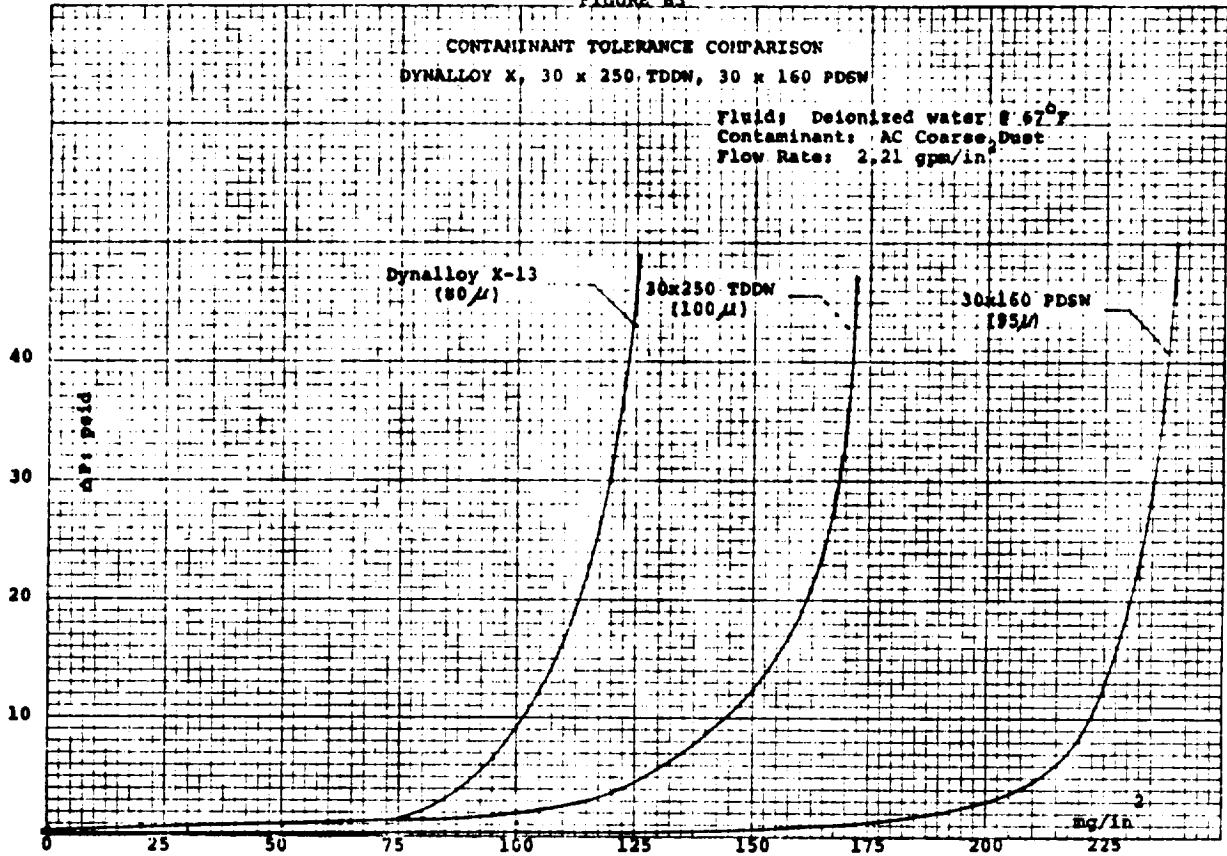
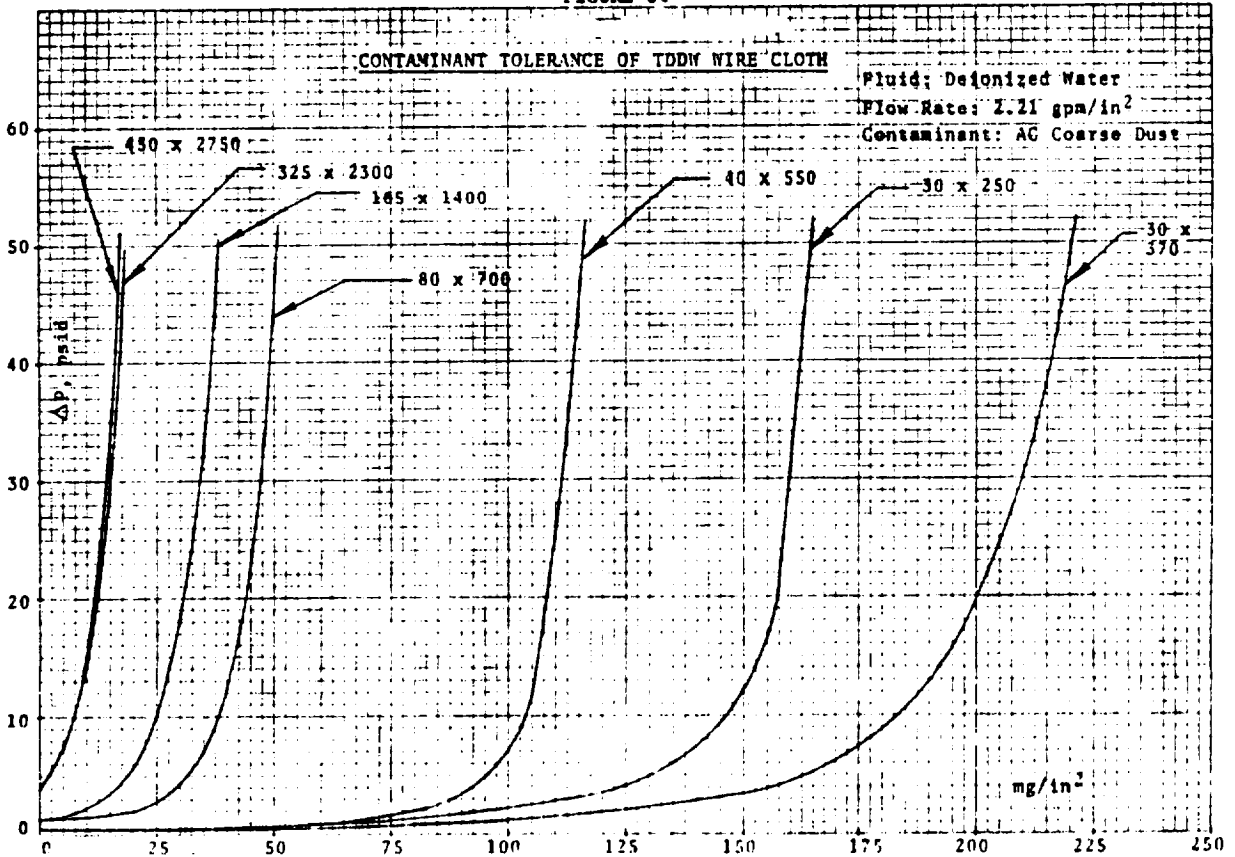


FIGURE 64



From the family of curves shown, each at a specific velocity, a second set of curves can be generated, such as those shown in Figure 66. These curves show the effect of velocity or flow rate very clearly. Each curve represents the flow rate - contaminant exposure relationship to cause a pressure differential increase of a specific amount above the initial clean pressure drop. At very low flow rates, the contaminant tolerance is quite high, but it drops off very sharply as the flow rate increases. The curves then begin to level off at the high unit flow rates where the effect of even small amounts of contaminant is quite severe.

d) Effect of Contaminant Type and Particle Size Distribution

There are many types of contaminants to be found in the various spacecraft systems, but no "typical" contaminant was available in sufficient quantity to test the many types and grades of porous media studied in this program. In order to provide comparative data, it was necessary to utilize a contaminant readily available and consistent in particle size distribution. Therefore, the great majority of contaminant tolerance tests were conducted using AC Coarse Test Dust, consisting of Natural Arizona Dust, supplied by the General Motors Phoenix Laboratory, and classified to a specific particle size distribution by the AC Spark Plug Division of General Motors Corporation, Flint, Michigan. The particle size distribution of this material, and a mixture called AC Fine Test Dust, containing a greater percentage of small particles, is shown in Table 9.

TABLE 9  
PARTICLE SIZE DISTRIBUTION AC TEST DUST

| <u>Micron Size Range</u> | <u>Weight Per Cent</u> |                |
|--------------------------|------------------------|----------------|
|                          | <u>AC Coarse</u>       | <u>AC Fine</u> |
| 0 - 5                    | 12 ± 2%                | 39 ± 2%        |
| 5 - 10                   | 12 ± 3%                | 18 ± 3%        |
| 10 - 20                  | 14 ± 3%                | 16 ± 3%        |
| 20 - 40                  | 23 ± 3%                | 18 ± 3%        |
| 40 - 80                  | 30 ± 3%                | 9 ± 3%         |
| 80 - 200                 | 9 ± 3%                 | 0              |

The above tabulation, provided by the material supplier, does not show the number of particles in the various size ranges, and this information is often required in order to simulate a specified contamination level. To determine the particle size distribution, in terms of numbers of particles, a sample of AC Coarse Test Dust was prepared in a liquid carrier and passed through a Royco Automatic Particle Counter at the Systems Division of TRW, Inc., with the following results:

TABLE 10  
PARTICLE SIZE DISTRIBUTION AC COARSE DUST, NUMBER OF PARTICLES

| <u>Micron Size Range</u> | <u>Number of Particles Per Milligram</u> |
|--------------------------|--|
| 5 - 15                   | $8.3 \times 10^4$                        |
| 16 - 25                  | $3.33 \times 10^4$                       |
| 25 - 50                  | $3.58 \times 10^3$                       |
| 50 - 100                 | 85                                       |
| Over 100                 | 35                                       |

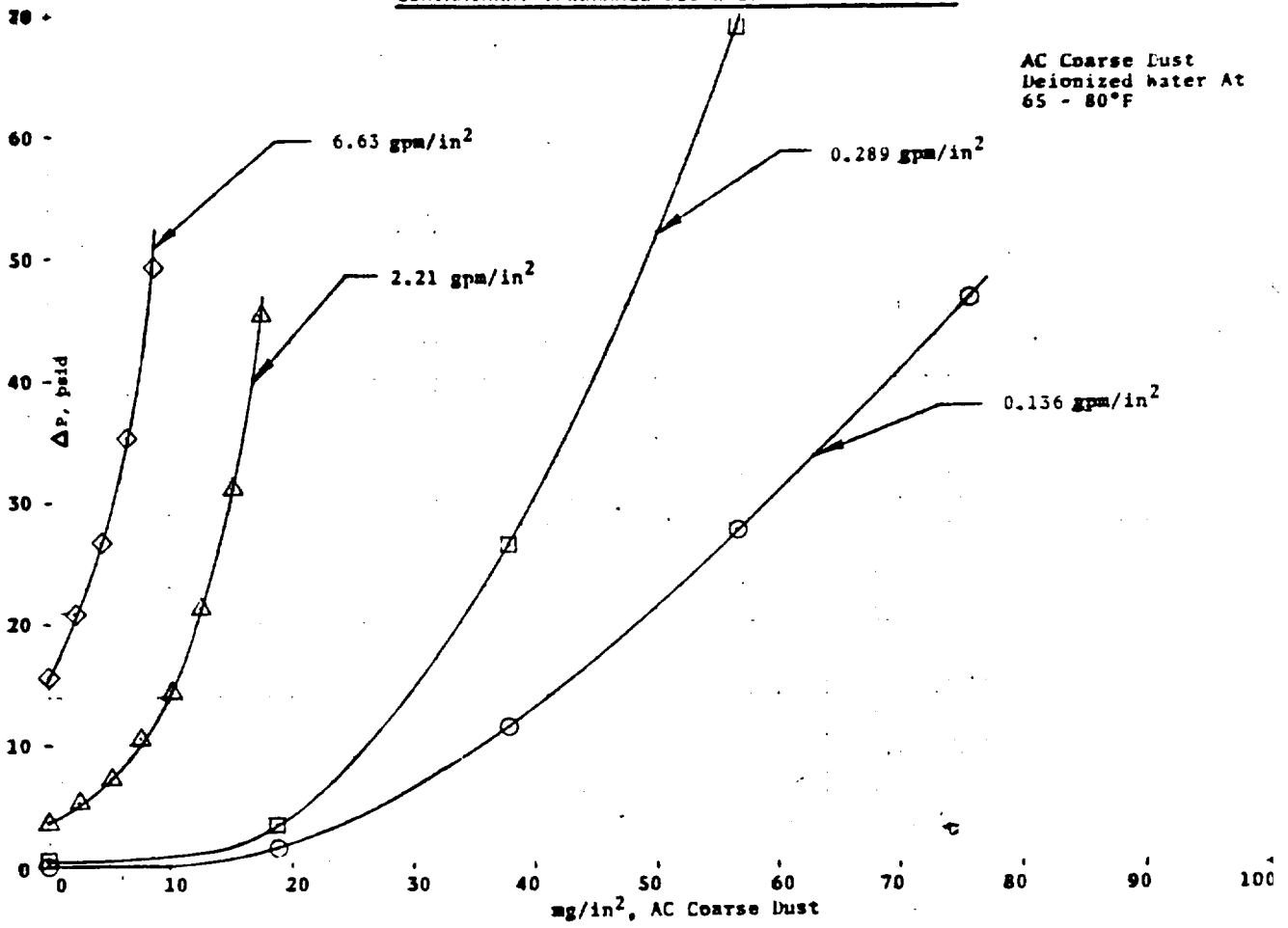
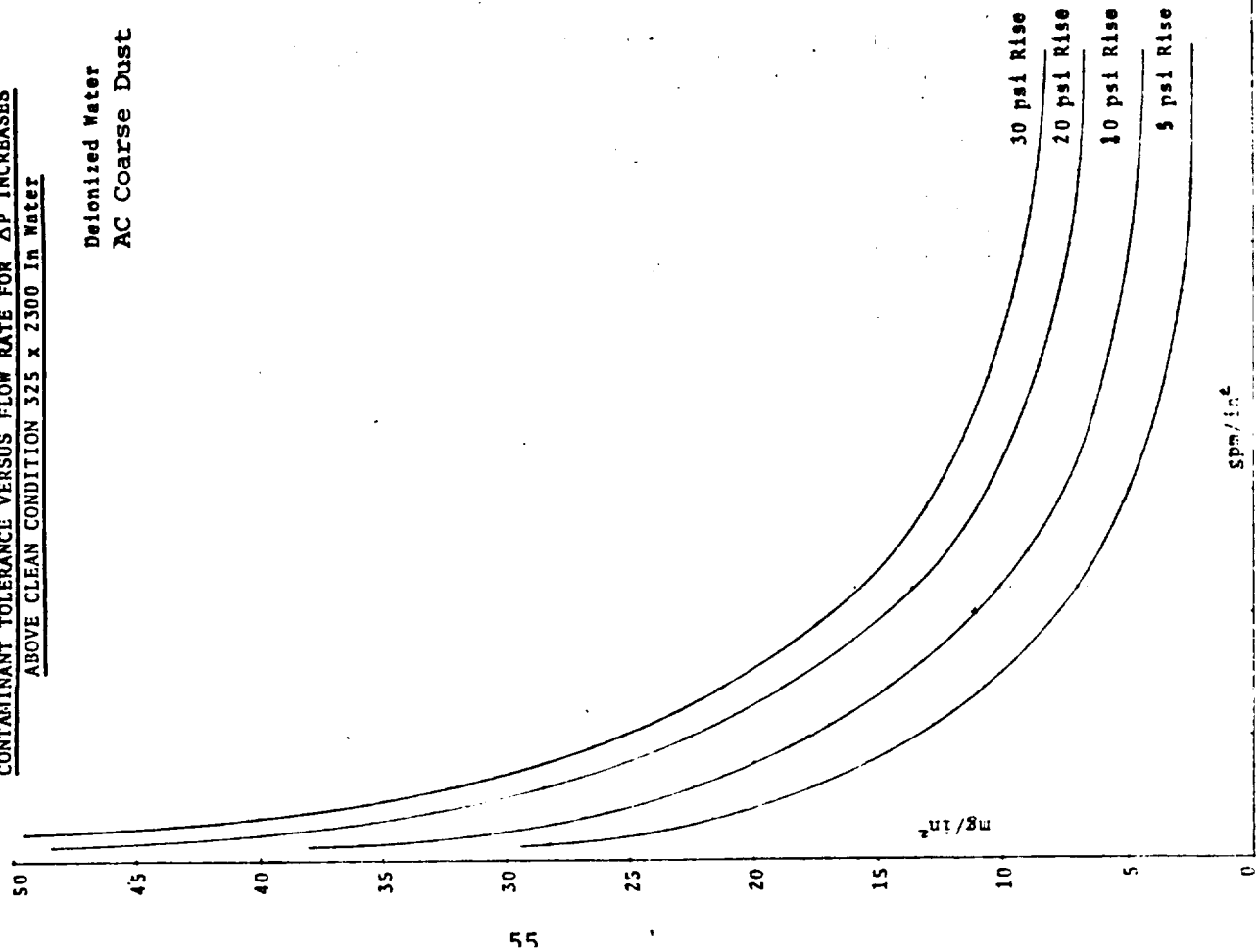


FIGURE 66  
CONTAMINANT TOLERANCE VERSUS FLOW RATE FOR ΔP INCREASES  
ABOVE CLEAN CONDITION 325 x 2300 in Water



The use of AC Coarse Dust contaminant is justified solely by the fact that it is readily available and consistent in composition, certainly not because it is representative of contaminants found in spacecraft systems. Therefore, the contaminant tolerance data obtained by testing the various media must be considered to provide relative evaluations only, and cannot be assumed to accurately predict service life of a filter in a system containing contaminants of a different type or particle size distribution.

To illustrate the effect on contaminant tolerance caused by varying the type of contaminant, tests were conducted on a typical fine filter material, 325 X 2300 TDDW, with a glass bead rating (GBR) of 10 microns. All tests were run at a unit flow rate of 2.2 GPM/in<sup>2</sup> using de-ionized water. The following contaminants were used. AC Coarse Dust; AC Fine Dust - a material similar to AC Coarse Dust, but classified to produce a greater percentage of particles in the smaller size ranges; AC Coarse Dust with iron pyrites added; Polyphenolene Oxide (PPO); and a NASA - WSTF supplied contaminant designated "Mixture 310-FTP."

#### AC Coarse Dust

This material has been described earlier. See Figure 65 for contaminant tolerance.

#### AC Fine Dust

This material is also supplied by General Motors Corporation, and consists of Natural Arizona Dust, classified to produce a greater percentage of particles in the smaller size ranges. Figure 67 shows the contaminant tolerance with AC Fine Dust.

#### AC Coarse Dust with Iron Pyrites, or With Zinc Sulfide

This material is supplied by Particle Information Service, Palo Alto, California, and consists of AC Dust, reclassified to replace all particles over 40 microns in size with an equal weight of iron pyrite or zinc sulfide crystals in the appropriate size ranges. This material is commonly used at the NASA - WSTF to provide a source of easily identifiable particles. Although the mixture is originally made up with all the substitute material in the size ranges above 40 microns, there is a marked tendency for the crystals to break up and, thus, provide considerably more fine particles (and less of the larger particles) than would be present in AC Coarse Dust alone. The mixture, thus, presents a contaminant with a particle size distribution somewhere between the AC Coarse and AC Fine Dusts. See Figure 68 for contaminant tolerance.

#### Polyphenolene Oxide

The "PPO" material has been considered as internal tank insulation for liquid cryogenic propellants. It is a relatively hard "foam" material, supplied in sheets or blocks. Samples were abraded together to provide a contaminant which could be typical of that caused by installing the material inside a cryogenic tank. In general, the particle size distribution was predominantly in the large size ranges, with most of the particles over 100 microns in size and up to 1000 microns. See Figure 69 for contaminant tolerance.

#### NASA - WSTF "Real System Contaminant" (Mixture 310-FTP)

This material was supplied in a small quantity by the NASA - WSTF. During earlier programs at the facility, system filters were back-flushed to obtain material representative of typical spacecraft fluid system contaminant. The material obtained in this manner was examined microscopically and chemically and a small amount of contaminant was "manufactured" with characteristics similar to those of the material obtained from the filters. There were many fibers, shreds of Teflon, chips of braze material, stainless steel particles, etc. The particle size distribution was predominantly in the larger sizes, with many fibers present. The

**FIGURE 68**  
**CONTAMINANT CAPACITY OF 325 x 2300 TWILLED DUTCH**  
**DOUBLE WEAVE WIRE CLOTH**  
 Fluid: Deionized Water @ 74 - 75°F Flow: 2.2 gpm/in<sup>2</sup>

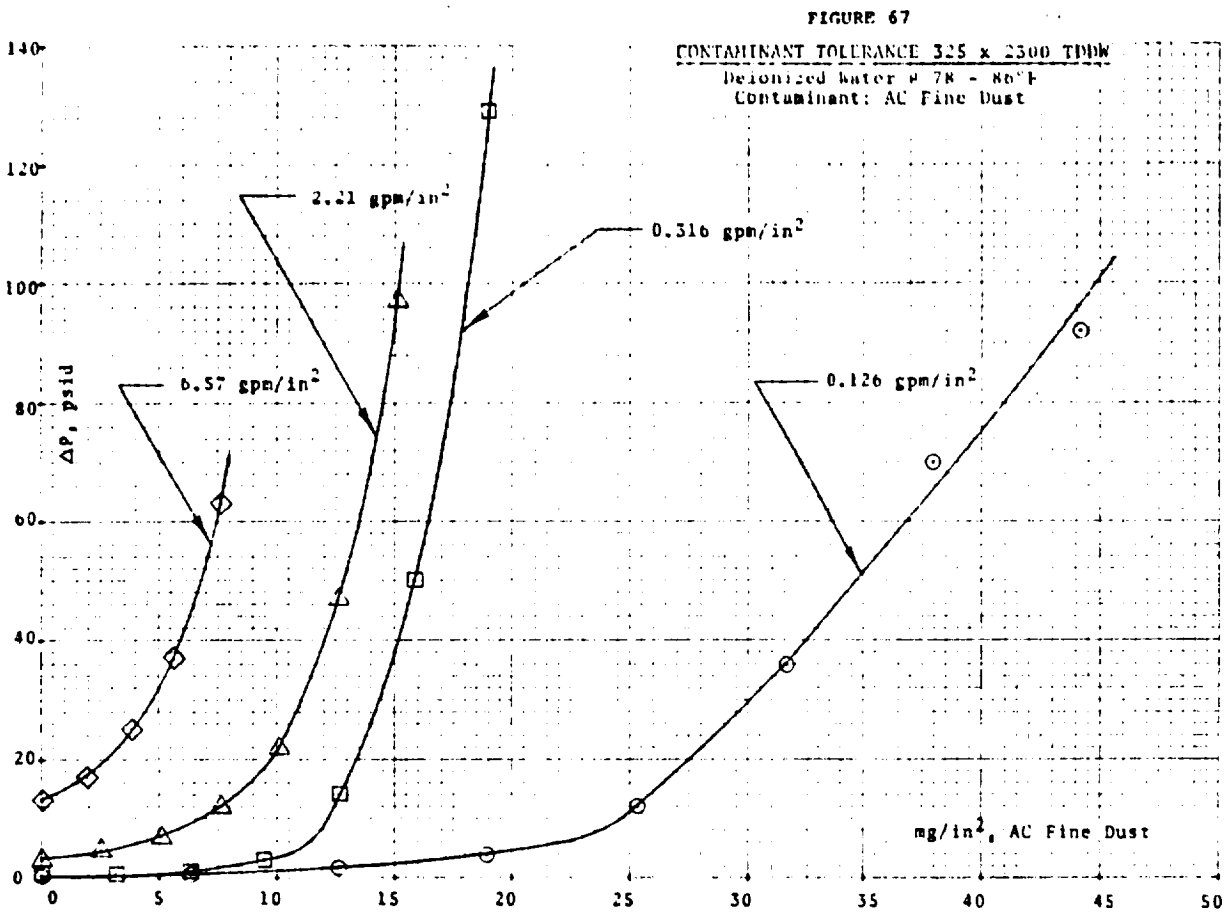
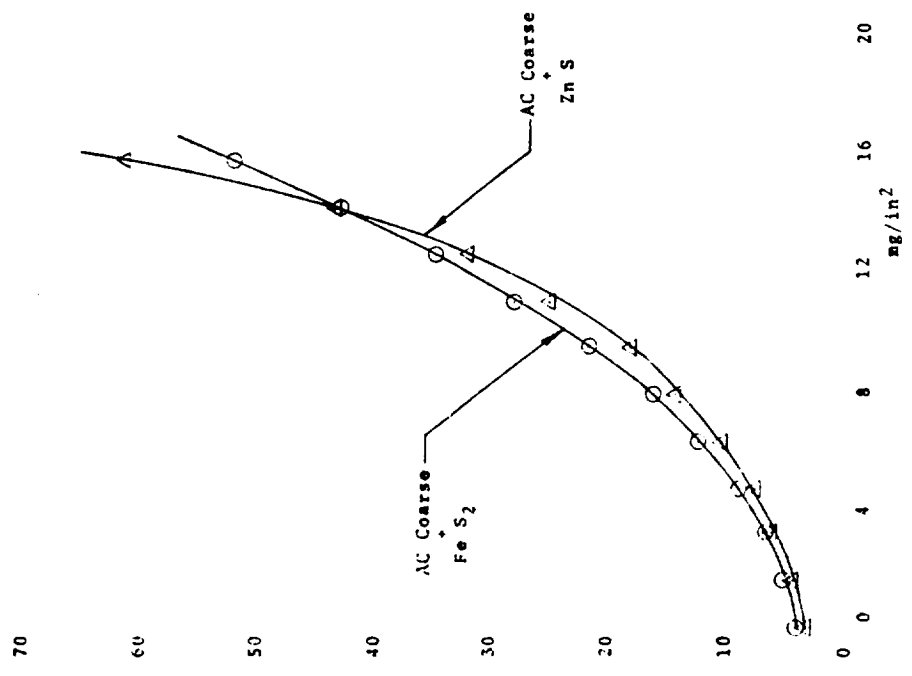


FIGURE 69

CONTAMINANT TOLERANCE OF 325 x 2300 TDDM

Fluid: Deionized Water  
Contaminant: PPO (Polychloroene Oxide)

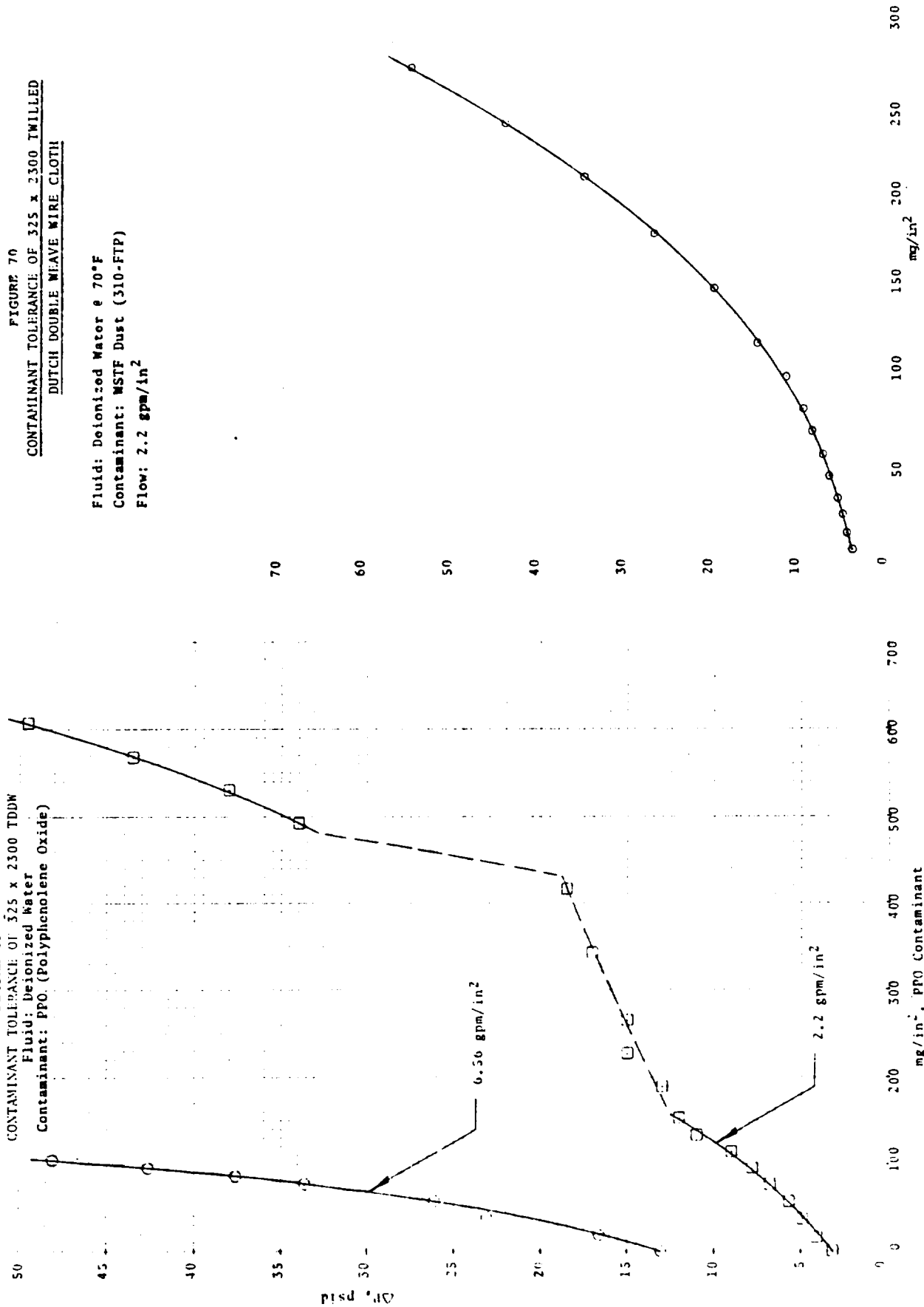
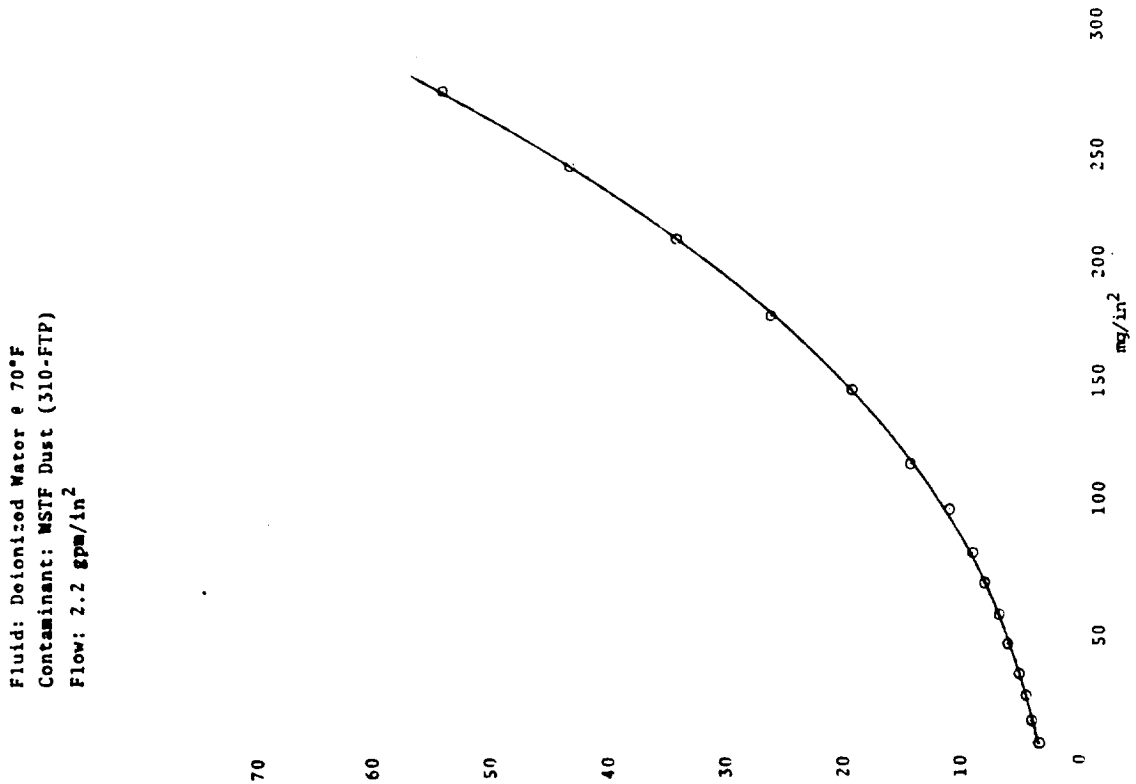


FIGURE 70

CONTAMINANT TOLERANCE OF 325 x 2300 TWILLED

DUTCH DOUBLE WEAVE WIRE CLOTH

Fluid: Deionized Water @ 70°F  
Contaminant: MSTF Dust (310-FTP)  
Flow: 2.2 gpm/in<sup>2</sup>



following table shows the particle size distribution by weight per cent in mixture 310-FTP.

TABLE 11  
PARTICLE SIZE DISTRIBUTION AND CONTENT MIXTURE 310 FTP  
WEIGHT PER CENT

| Component             | Size Range (Microns) |       |       |        |       | Total  |
|-----------------------|----------------------|-------|-------|--------|-------|--------|
|                       | 0-37                 | 37-44 | 44-74 | 74-250 | 250   |        |
| Stainless Steel Chips | 2.73                 | 0.25  | 0.51  | 7.34   | 21.01 | 31.84  |
| Sand                  | 2.73                 | 0.25  | 0.51  | 9.18   | 35.02 | 47.68  |
| Plastic Chips         | 0.91                 | 0.08  | 0.17  | 1.84   | 0.00  | 3.00   |
| Fibers                | 0.00                 | 0.00  | 0.00  | 0.00   | 14.01 | 14.01  |
| Rust ( $Fe_3O_4$ )    | 2.73                 | 0.25  | 0.51  | 0.00   | 0.00  | 3.47   |
| Total                 | 9.09                 | 0.82  | 1.69  | 18.36  | 70.05 | 100.00 |

The contaminant tolerance curve obtained with the WSTF mixture is shown in Figure 70.

Figure 71 graphically illustrates the wide contaminant tolerance variation of the typical fine filter media when tested with the various contaminants. The three AC Coarse Dust contaminants provide the least contaminant tolerance; the material containing the largest number of small particles provides the lowest contaminant tolerance. The contaminants containing mostly large particles (PPO) and many fibers mixed with large particles (WSTF contaminant) exhibit very large values of contaminant tolerance.

In the case of the PPO and WSTF contaminants, a filter cake built up on the filter media, and there was little evidence of "plugging" of the individual pores. This is indicated by the straight, sloping line of the plot, as compared to the rapidly changing slope of the other curves.

The wide variation in results dependent upon type of contaminant used, emphasizes the fact that data obtained under this program, in regard to contaminant tolerance, is only relative. One filter medium can be compared to another, but the real design data, so necessary for optimizing filter design to protect a fluid system without undue weight or envelope penalties, have not been finalized. Some knowledge of the type and particle size distribution to be expected in the spacecraft operational fluids is essential for real filter design optimization.

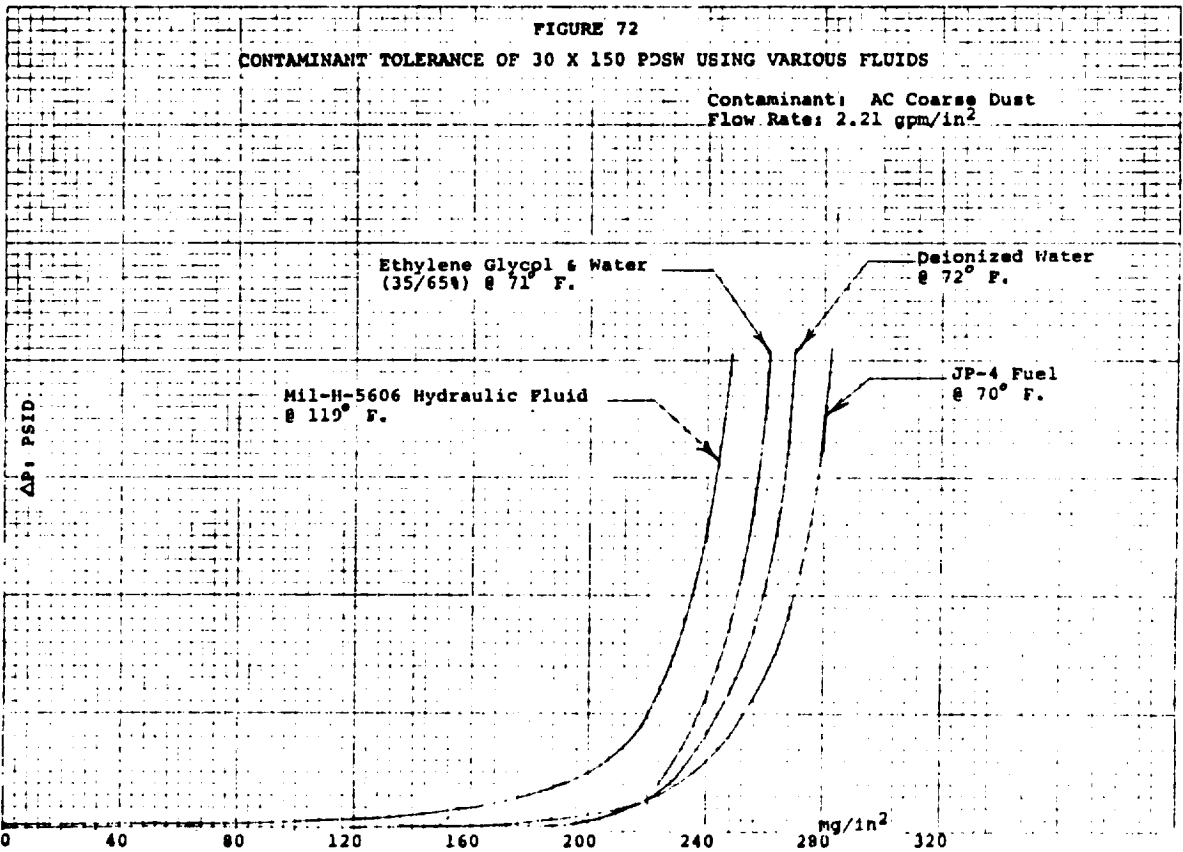
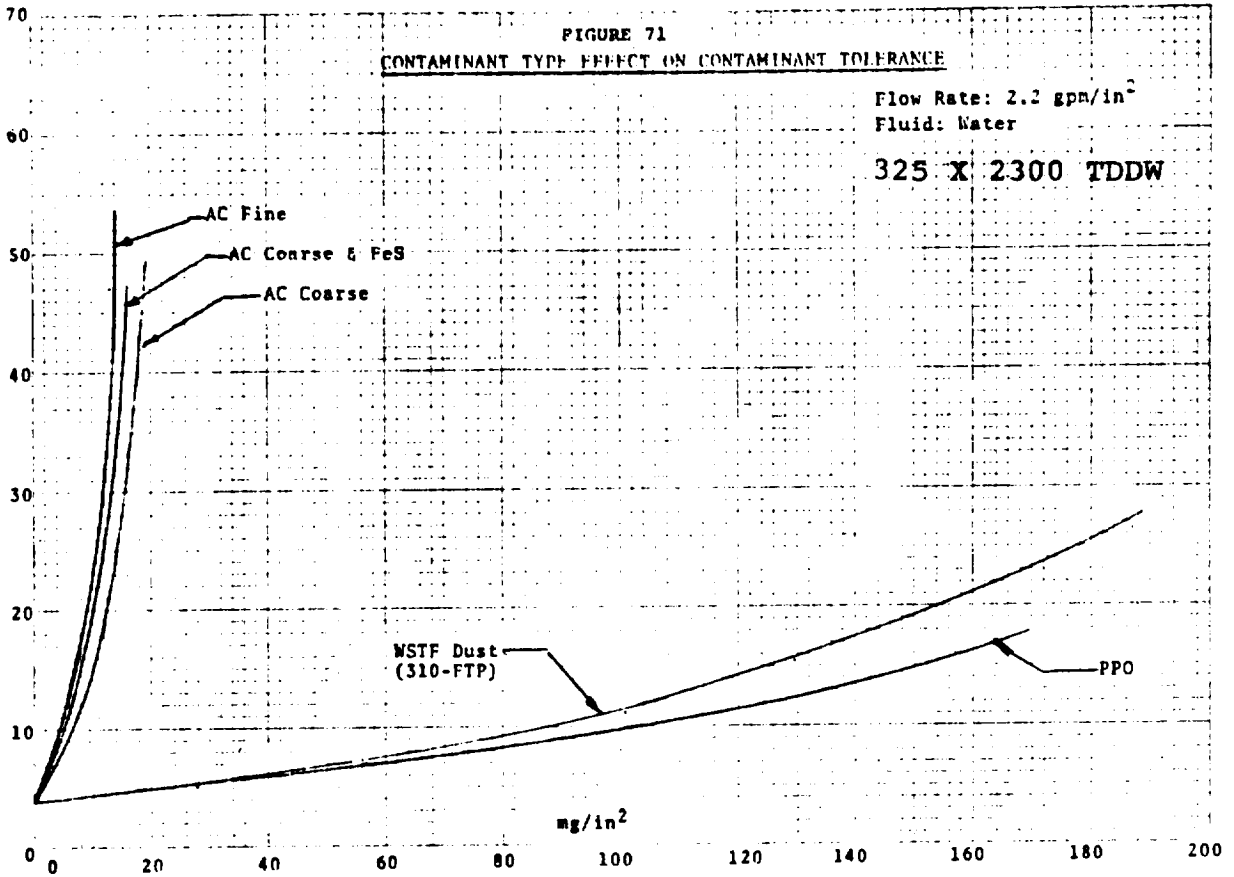
If it is assumed that actual system contaminant will be similar to AC Coarse or AC Fine Dust, and this assumption is accepted in present day design, then the resultant filter design will undoubtedly be heavier and larger than necessary to accomplish the specified mission service life, if the real contaminant resembles the material supplied by the NASA - WSTF.

#### e) Effect of Fluid Characteristics on Contaminant Tolerance

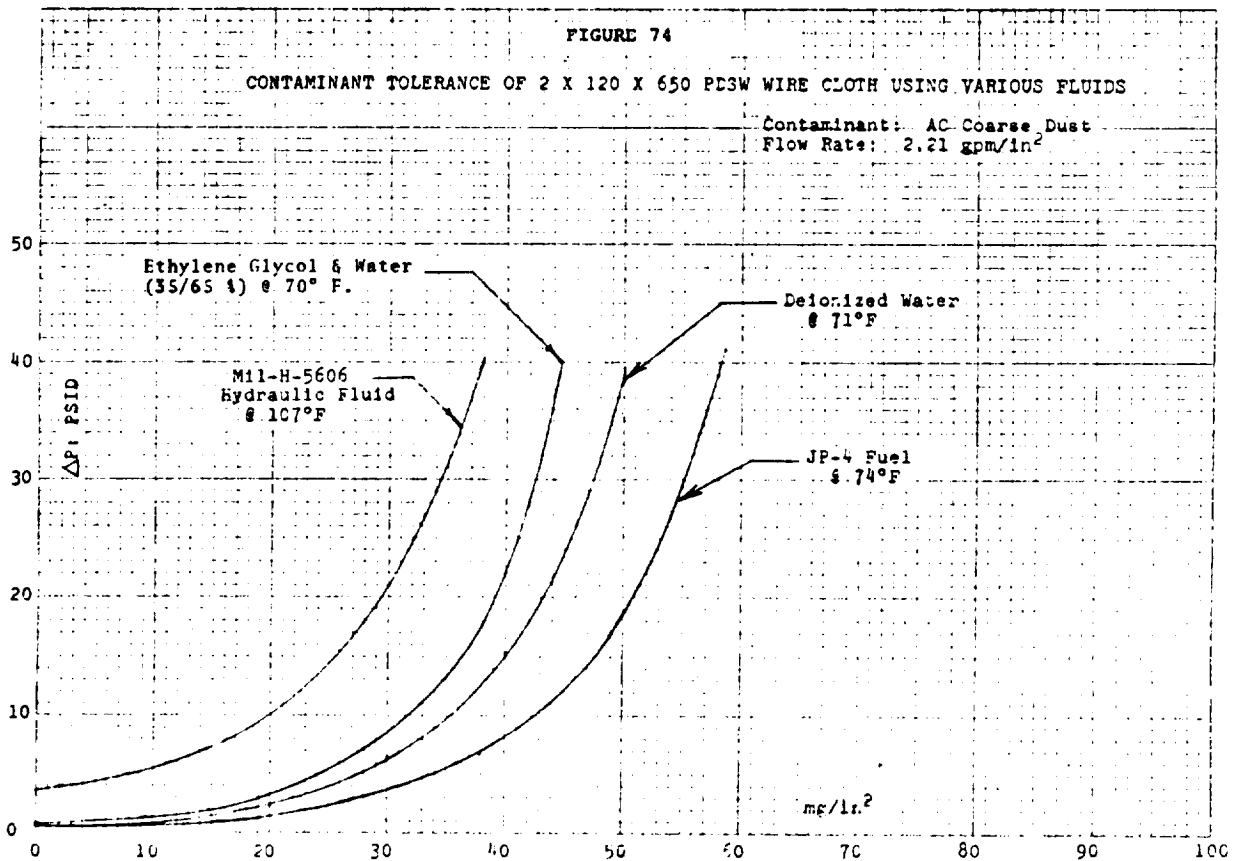
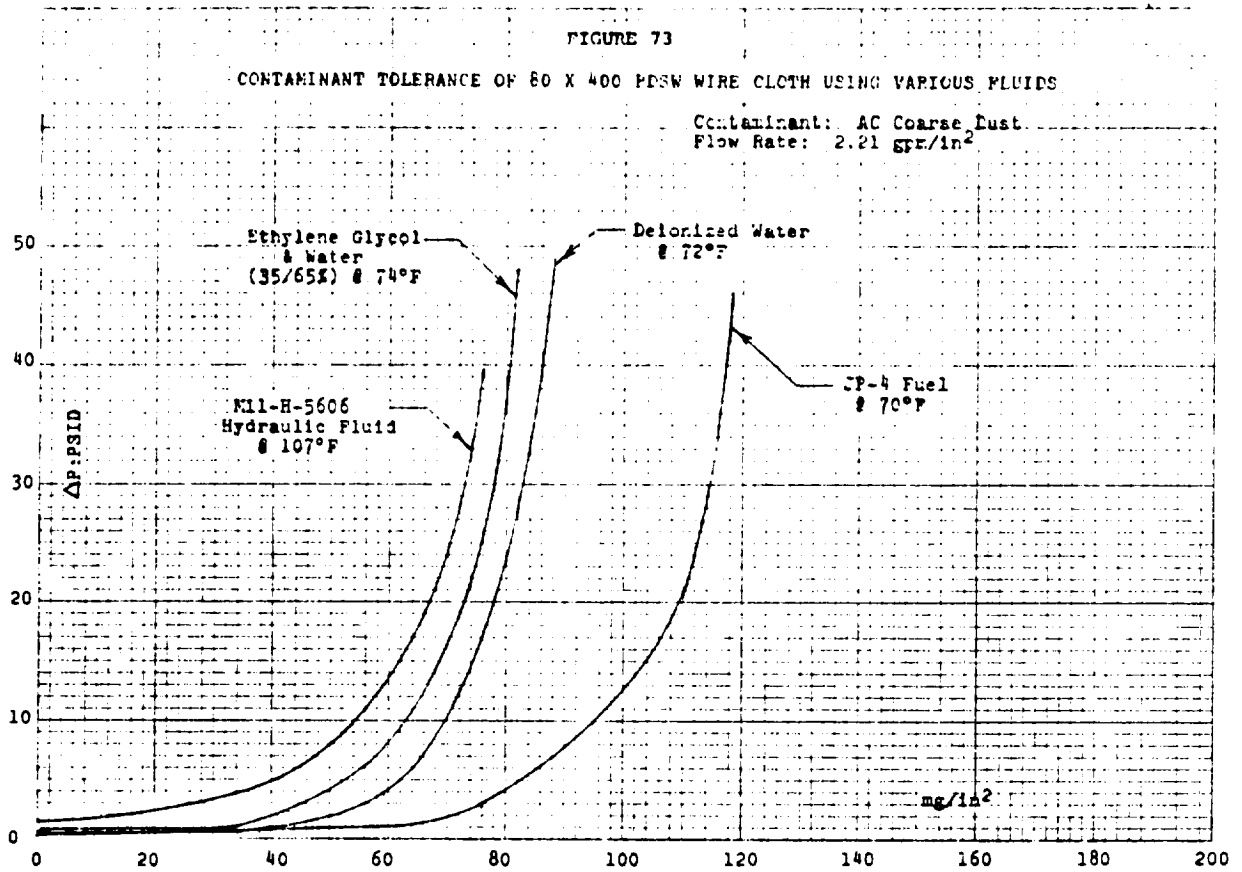
The density (specific gravity) and the viscosity of the operating fluid both affect the contaminant tolerance characteristics of the various media, just as they affect the flow resistance. Both increasing density and increasing viscosity will cause a decrease in contaminant tolerance.

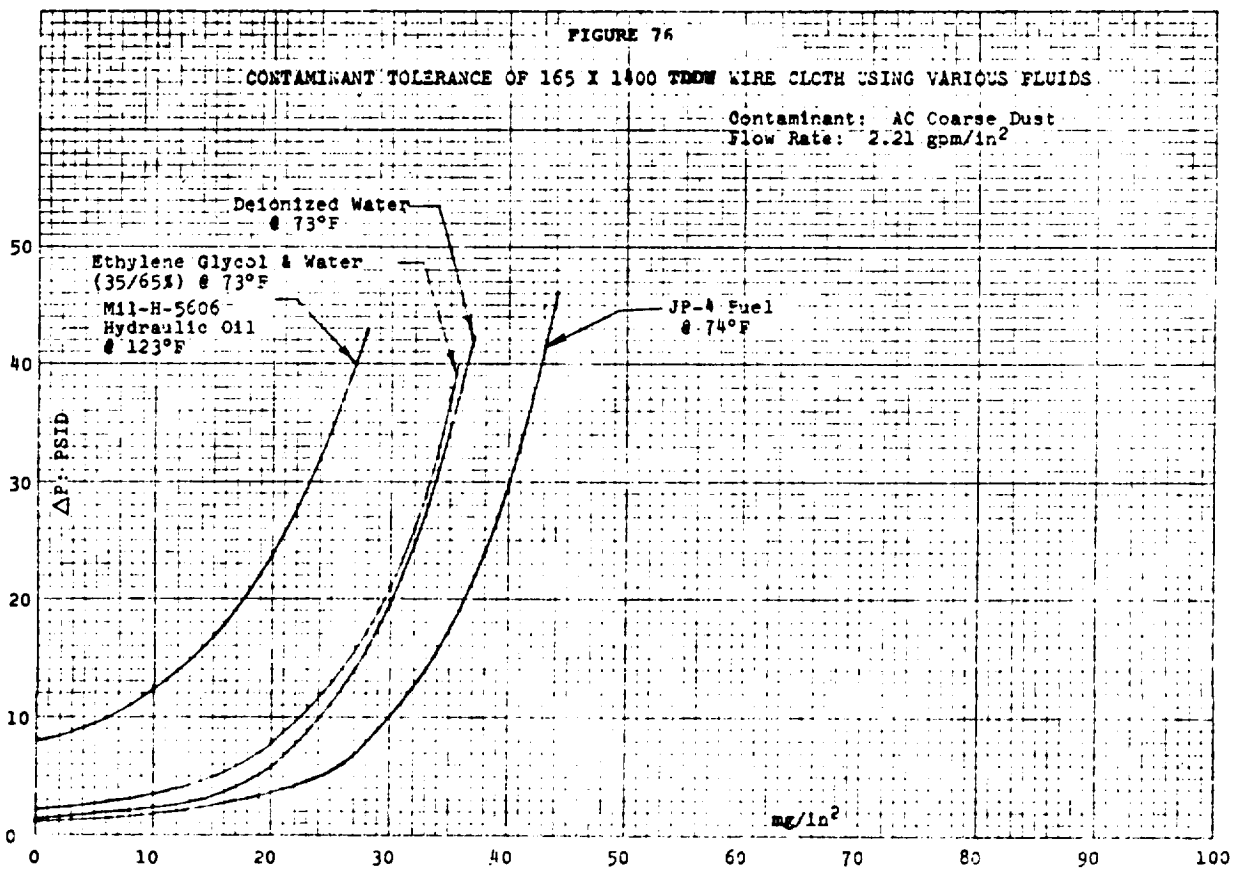
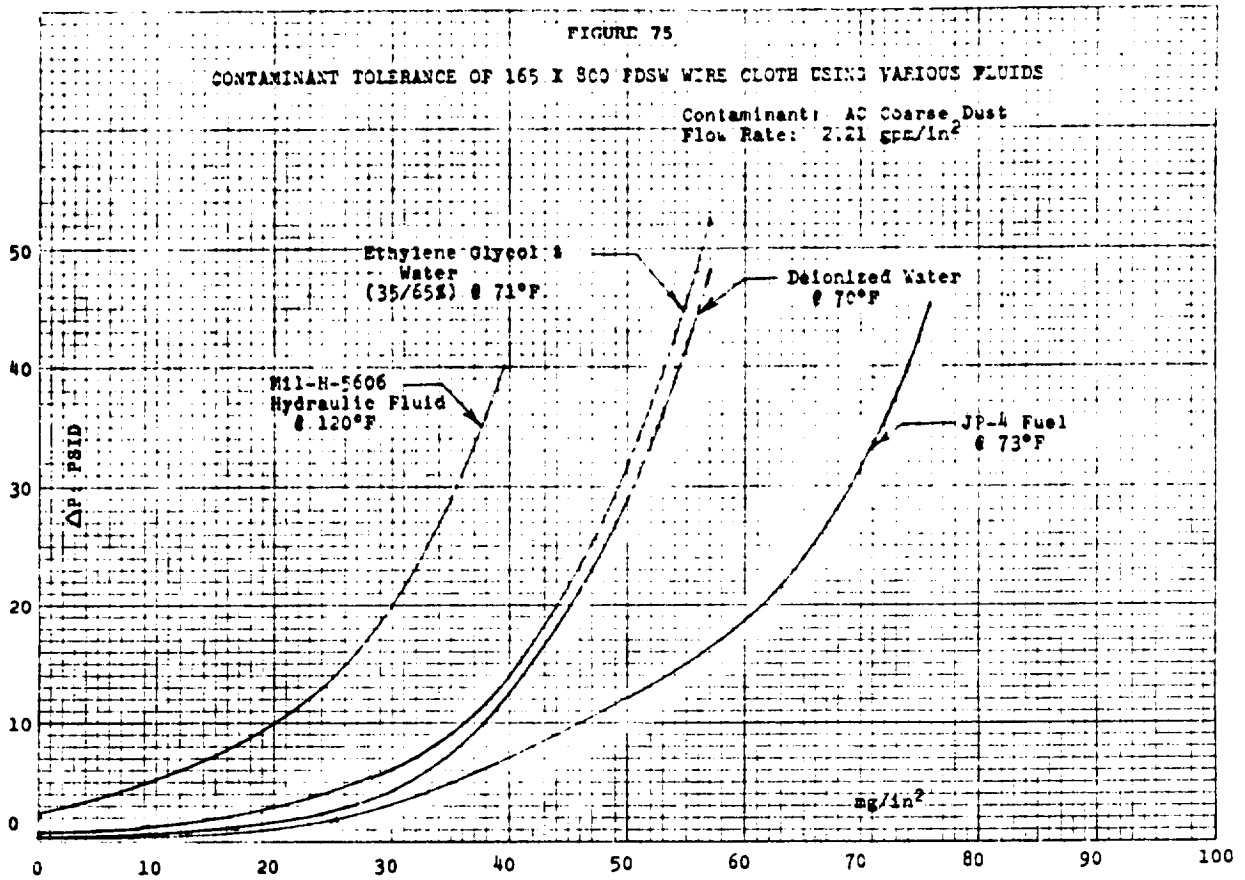
Figures 72 through 77 illustrate the fluid effect graphically. These figures show the contaminant tolerance curves of both PDSW and TDDW media at a unit flow rate of 2.21 GPM/in<sup>2</sup>, using four different liquids. Individual graphs and tables of data are contained in the Appendix.

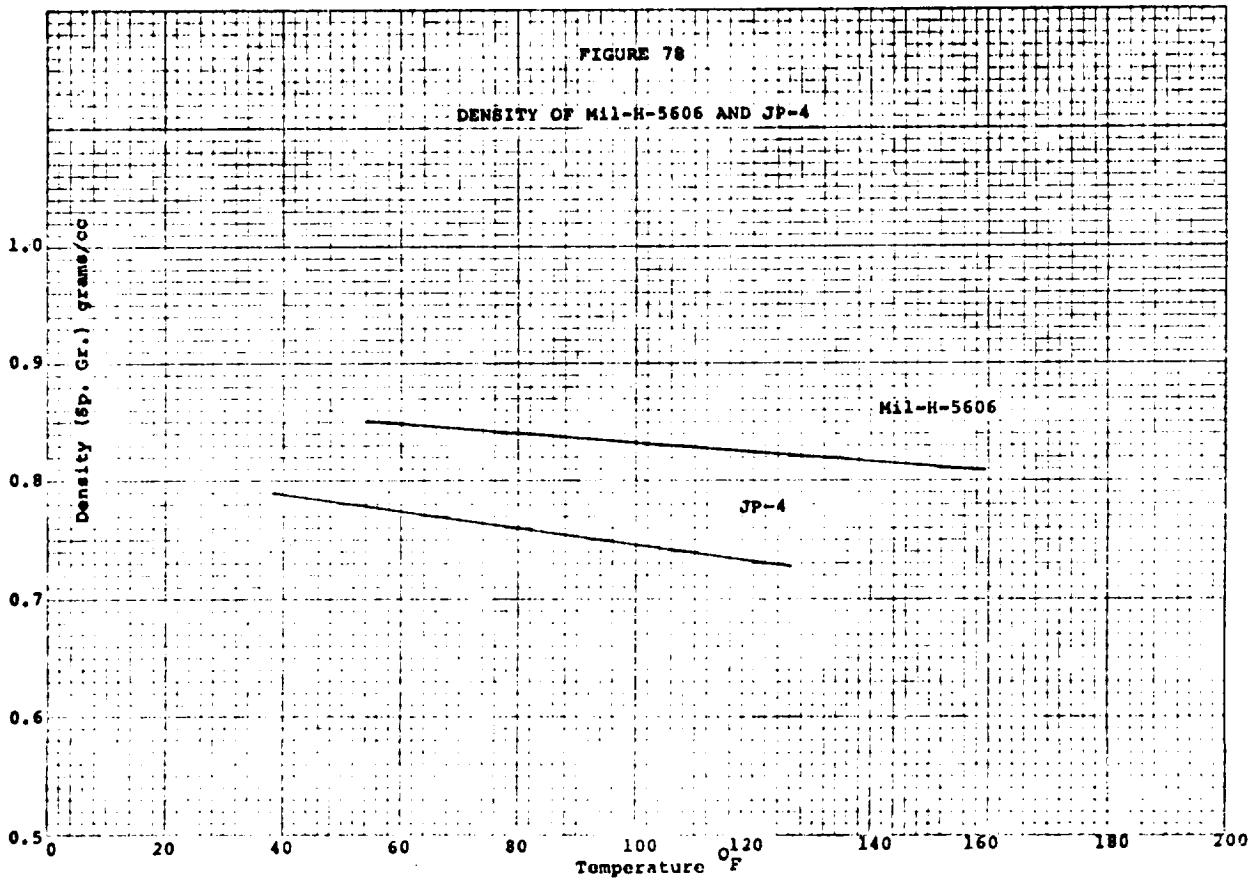
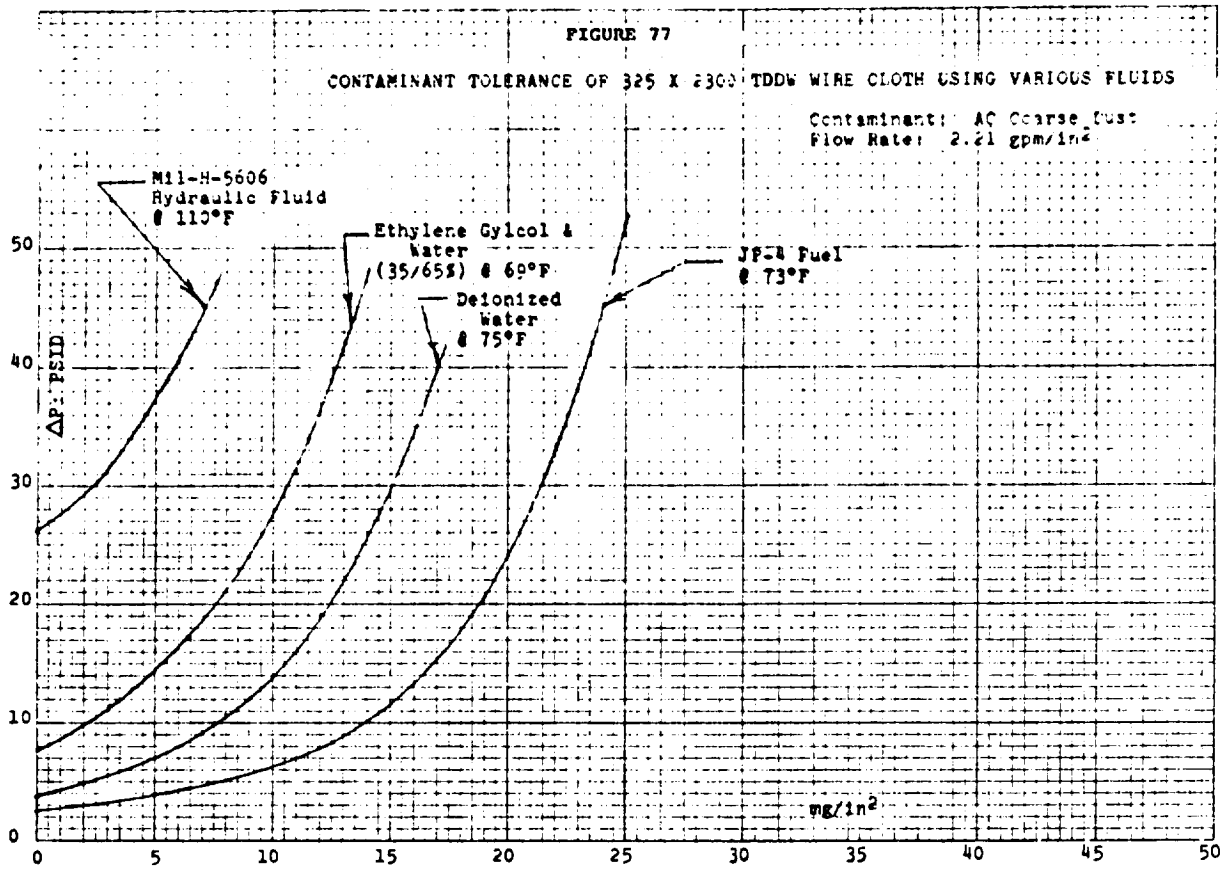
As the specific gravity of the JP-4 fuel and the Mil-H-5606 hydraulic fluid are nearly the











same, these curves can be used to show the extreme effect of viscosity.

Table 12 summarizes the weight of contaminant required to cause an increase of 10 psi above the clean differential pressure for each of the media, for both Mil-H-5606 and JP-4 fluids. In addition, the viscosities are shown at the actual test temperatures, as well as the viscosity ratio and contaminant tolerance ratios. Specific gravities are not shown, but for the temperatures involved, the Mil-H-5606 and JP-4 are approximately 0.82 and 0.70 specific gravities, respectively. Figures 78 and 79 show the average densities and viscosities as a function of temperature for Mil-H-5606, JP-4, and water. The fact that the various tests were not run at the same temperatures for the individual fluids, distorts the data somewhat, but it can be seen that within each type of media, PDSW and TDDW, the effect of viscosity is more pronounced in the media with the finer micron ratings. In addition, the more complex media with more tortuous flow paths, TDDW, shows a greater viscosity effect than the PDSW media.

When one inspects the basic flow equations for these media, as described in Section 3,8, it is apparent that the relative values of the "b" constant, compared to the "a" value, is also an indication of the degree to which viscosity will affect the contaminant tolerance. Within any one grade of medium, the ratio of the values of b/a will determine the relative effect of viscosity on contaminant tolerance. The greater the b/a ratio, the more susceptible the media will be to changes in viscosity of the operating fluid.

#### f) Effect of Element Configuration

Pleating of filter media is a common and accepted method of providing a large area of filter medium, in order to reduce the envelope size of a filter element. The porous medium is convoluted to form pleats of the desired height, which are compressed, so as to provide equal pleat spacing and allow the formation of a cylinder, or cone, of a required size. Eight times more filter area can be provided in a cylinder, than if the filter medium is simply rolled to form without pleating.

This additional surface area results in a higher contaminant tolerance of a filter element than would be predicted on the basis of filter area ratio alone, since the fluid now flows through the medium at a much lower unit flow rate, thus providing higher contaminant tolerance for each square inch of medium.

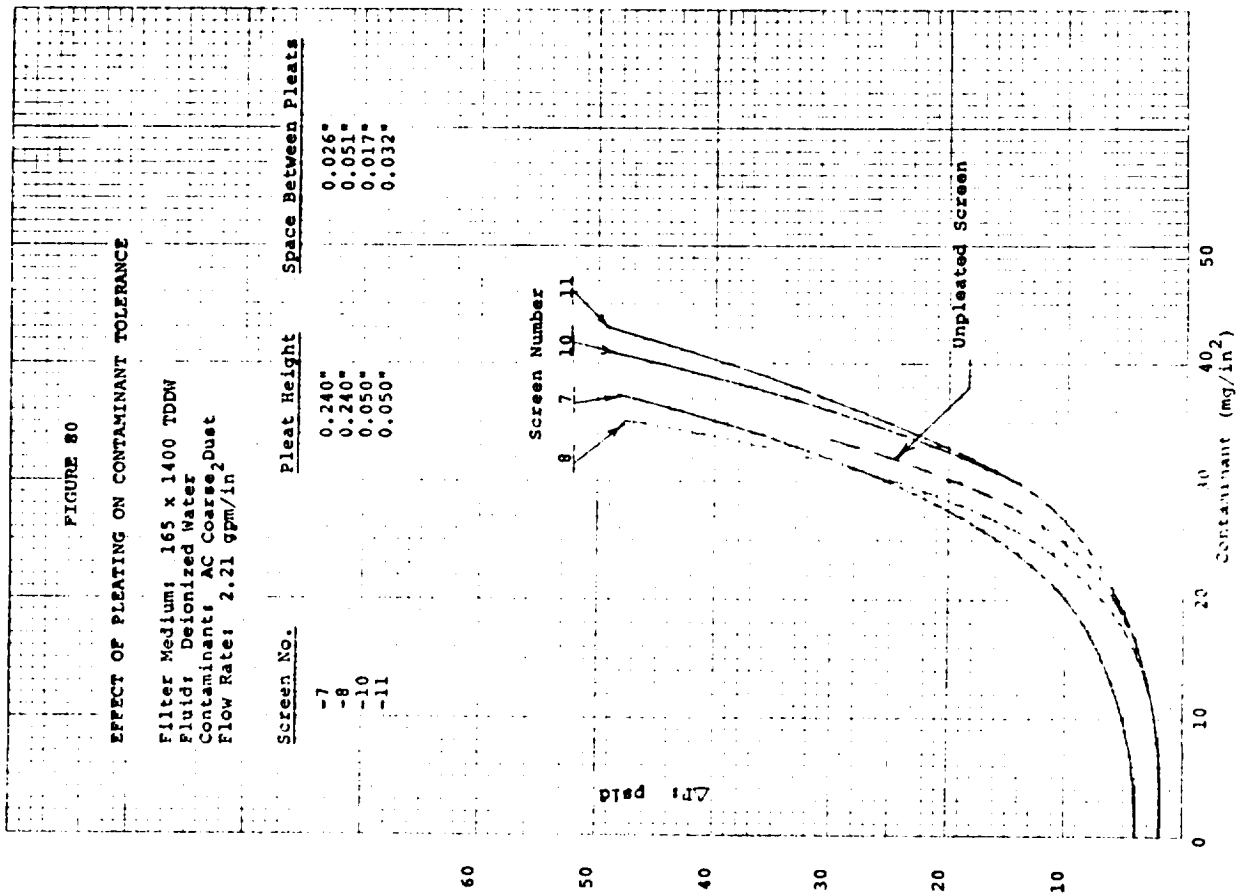
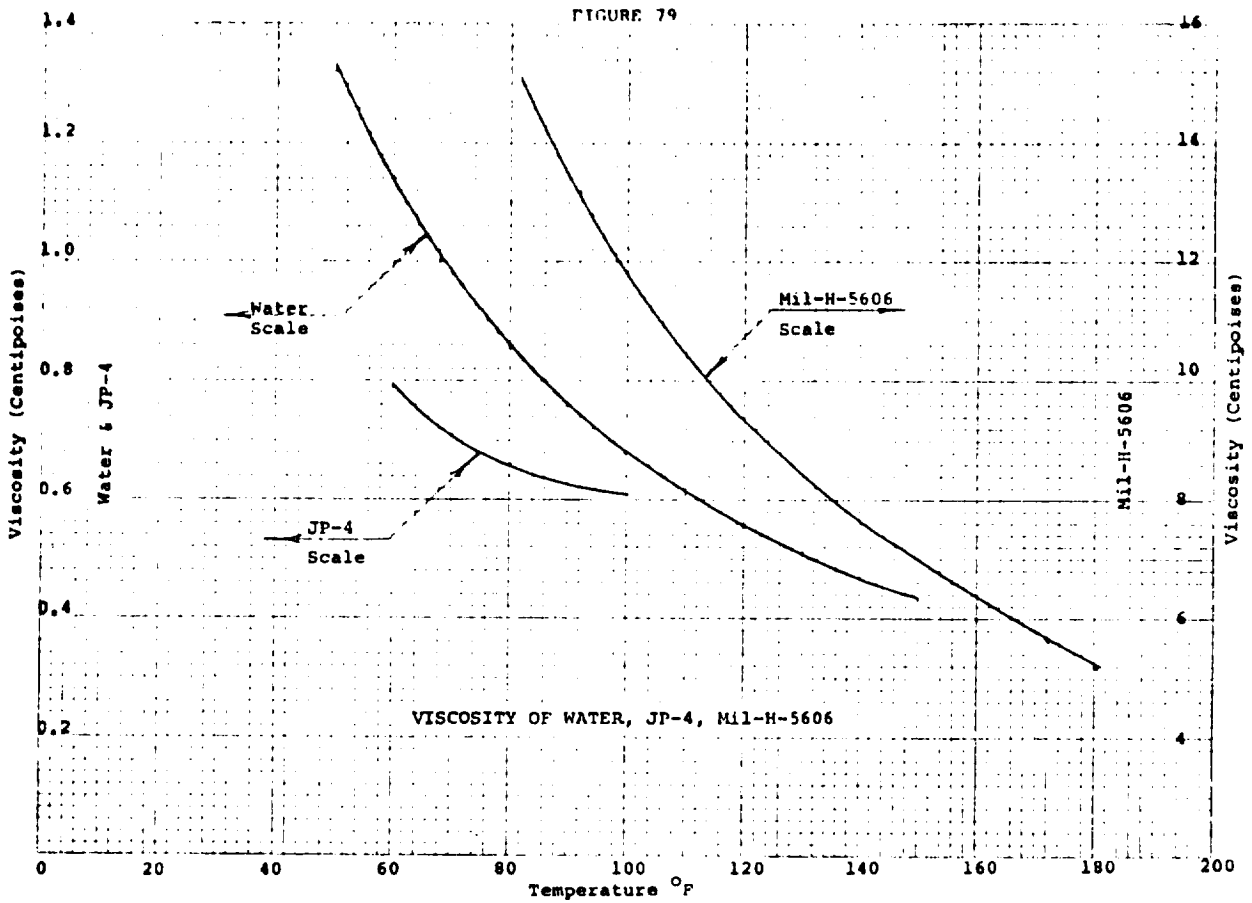
Thus, to compare a simple cylinder of filter medium to a pleated cylinder of the same size, but with five times the screen area, the unit flow rate through the pleated screen is only 1/5 that of the unpleated medium. This can easily result in a doubling of the contaminant tolerance of each square inch of medium. When this factor is multiplied by 5, an overall contaminant "capacity" of 10 times the simple "wrap-around" cylinder can result.

To determine the possible effect on the porous media caused by pleating, several samples of 165 X 1400 Twilled Dutch Double Weave wire cloth were pleated to different heights and pleat spacing. These samples were then fitted into a holder, and contaminant tolerance tests were conducted using deionized water and AC Coarse Dust. The system flow rate was adjusted for each sample to provide a unit flow rate of 2.21 GPM/in<sup>2</sup> of screen in the specimen.

Figure 80 shows the contaminant tolerance curves for four samples with pleat heights of from .050" to .240", and pleat spacings of from .017" to .051". A curve obtained from previous tests showing the contaminant tolerance of flat, unpleated screen is also shown for comparison. The curves for the various pleat configuration compare with the flat screen data within 10%, and this is the approximate repeatability of this type of test. It is apparent, therefore, that within the pleat height and spacing relationships shown, there is no adverse

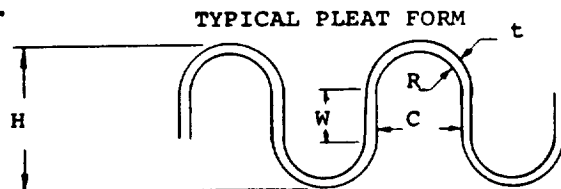
TABLE 12  
CONTAMINANT TOLERANCE INDEX DATA (10 PSI) FOR VARIOUS MEDIA AND FLUIDS

| Medium   | Micron Rating (GBR) | Contaminant Tolerance for 10 psi rise at 2.21 gpm/in <sup>2</sup> (mg/in <sup>2</sup> ) |      | Viscosity (Centipoises) (Test Conditions) | C/T Ratio $\frac{JP-4}{MIL-H-5606}$ | Viscosity Ratio $\frac{MIL-H-5606}{JP-4}$ | b/a Ratio | Fig. No. (Ref.) |
|--|---------------------|---|------|---|-------------------------------------|---|-----------|-----------------|
|  |                     | MIL-H-5606  | JP-4 |   |                                     |   |           |                 |
| PDSW<br>30 x 150<br>80 x 400<br>2 x 120 x 650<br>165 x 800 | 105                 | 222   | 254  | 9.4<br>.71                                | 1.15                                | 13.2                                      | 1.38      | 70              |
|  | 39                  | 57  | 96   | 10.8<br>.71                               | 1.67                                | 15.2                                      | 2.6       | 71              |
|  | 19                  | 25  | 44   | 10.8<br>.685                              | 1.77                                | 15.7                                      | 2.7       | 72              |
|  | 18                  | 24  | 47   | 9.3<br>.69                                | 2.0                                 | 15.2                                      | 4.4       | 73              |
| TDDW<br>165 x 1400<br>325 x 2300                           | 20                  | 16  | 31   | 9.1<br>.685                               | 1.95                                | 13.3                                      | 5.4       | 74              |
|  | 10                  | 4.7   | 15.5 | 10.4<br>.69                               | 3.33                                | 15.1                                      | 7.6       | 75              |



effect caused by pleating.

It is of critical importance, however, that in planning the element configuration, the designer does not provide too close a pleat spacing, especially when deep pleats are to be employed, as all the fluid that passes through the pleat walls must then pass through the linear orifice formed by adjacent pleats. As the commonly used Twilled Dutch Double Weave and Plain Dutch Single Weave materials all have approximately 8 to 10 per cent open area, it appears logical that the space between the pleats should not be so close as to provide less flow area than that provided by the screen. The following shows an example of a method for calculating the minimum pleat space which will provide a flow area at least equal to that of the screen.



- H = Pleat Height
- R = Internal Pleat Radius
- t = Screen thickness
- C = Clearance between pleats
- W = Pleat wall height

All fluid passing through the walls and outside curve of the pleat must eventually pass through the flow passage formed by the inner walls of the pleat. At the bottom curve of the pleat, the fluid will pass through directly, and is not further restricted.

- Let  $A_s$  = screen area subject to fluid which must pass through area denoted C.
- and  $\eta$  = per cent open orifice area of screen expressed decimally
- and  $A_o$  = open orifice area of screen
- and L = length of pleat - assume 1 inch

$$A_s = 2(H-2R-2t) + \pi(R+t)$$

$$A_s = 2H - 0.86(R+t)$$

$$A_o = \eta A_s$$

$$A_o = \eta [2H - 0.86(R+t)]$$

For the area provided at C to equal  $A_o$ :

$$C = \eta [2H - 0.86(R+t)]$$

$$\text{and } R = \frac{C}{2} = \frac{\eta [2H - 0.86(R+t)]}{2}$$

$$R + 0.43\eta R = \eta (H - 0.43t)$$

$$R = \frac{\eta (H - 0.43t)}{1 + 0.43\eta}$$

$$\text{and } C = \frac{2\eta (H - 0.43t)}{1 + .43\eta}$$

These relationships may be used to calculate the pleat radius and clearance which will provide optimum flow between the pleat walls of a typical medium. For example,

Screen: 165 x 1400 TDDW

Thickness, t: 0.0058

Pleat Height, H: 0.150

For 165 X 1400 TDDW, the % open orifice area, , is 9.3%.

$$R = \frac{0.093 [(0.150) - (0.43 \times 0.0058)]}{1 + (0.43 \times 0.093)}$$

$$R = 0.013$$

$$C = 2R = 0.026$$

For pleat height of 0.150", the calculated pleat radius and clearance would be 0.013" and 0.026" respectively.

The pleat clearance described above applies to the spaces at the inside of a cylindrical element, and should be made larger when the screen is pleated to allow for the "tightening" of the pleats at the inside, when the pleated screen is formed into a cylinder.

From the equation presented, it can be seen that the required pleat clearance is a function of the per cent orifice area of the medium used. Following, are the per cent limiting orifice areas applicable for Twilled Dutch Double Weave and Plain Dutch Single Weave media.

TABLE 13  
TOTAL AREA FRACTION OF LIMITING ORIFICES TDDW AND PDSW

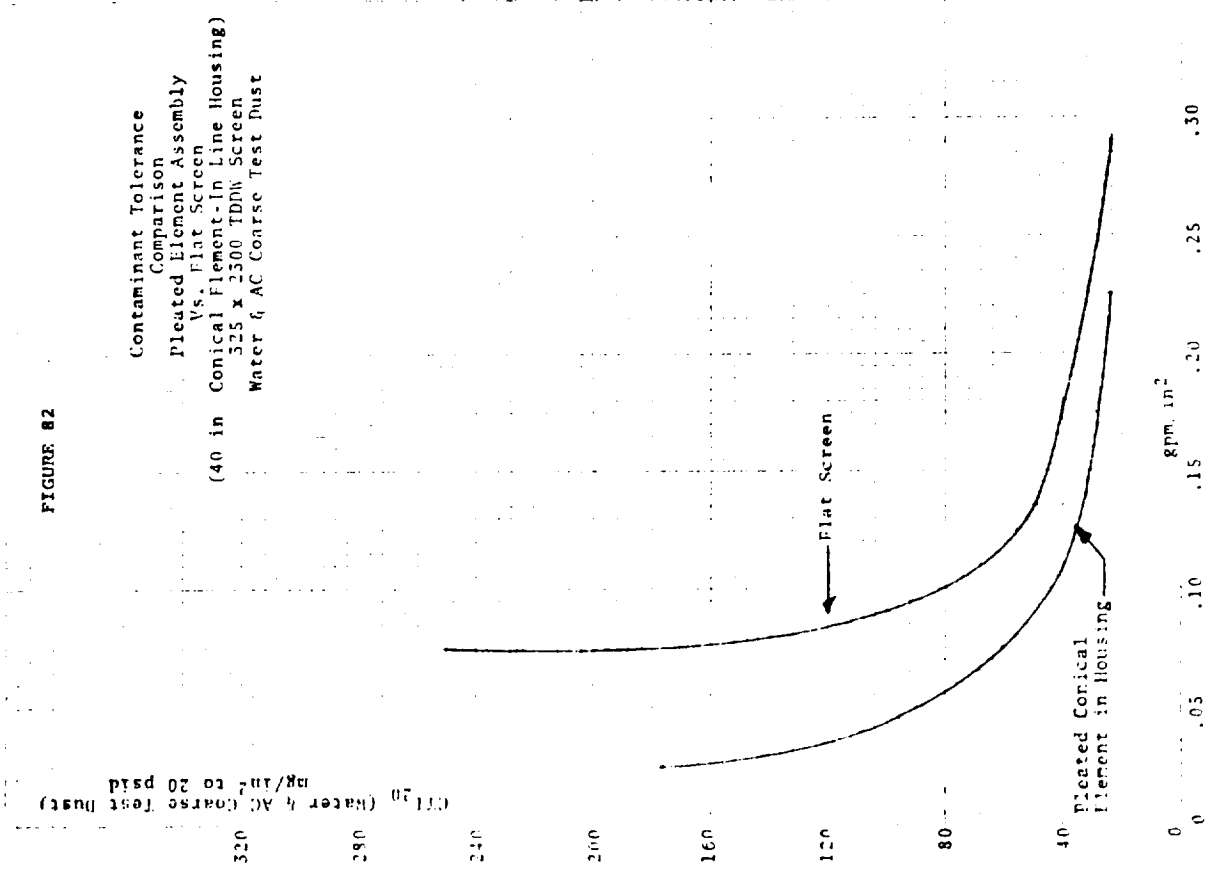
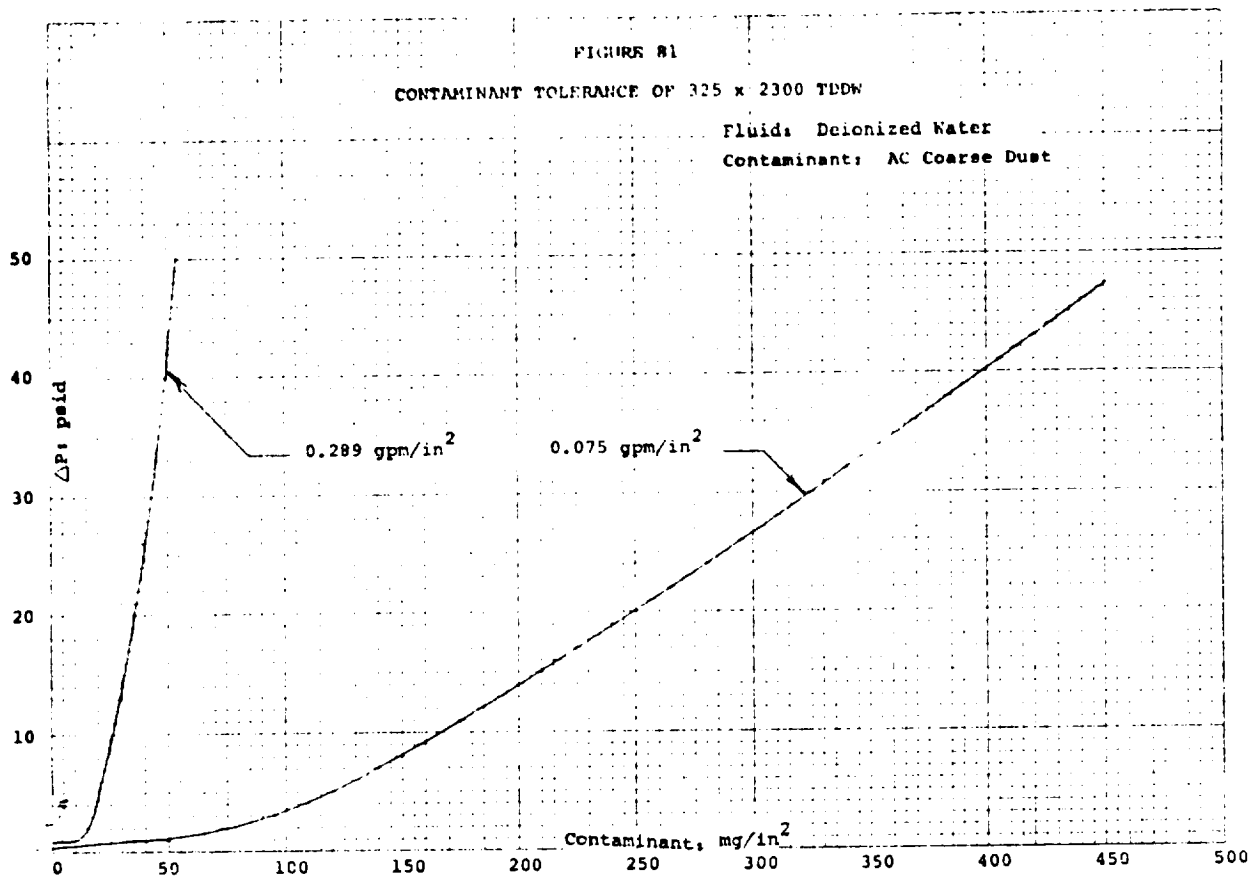
| <u>Twilled Dutch Double Weave</u> |                          | <u>Plain Dutch Single Weave</u> |                          |
|-----------------------------------|--------------------------|---------------------------------|--------------------------|
| <u>Grade</u>                      | <u><math>\eta</math></u> | <u>Grade</u>                    | <u><math>\eta</math></u> |
| 30 X 250                          | 7.4%                     | 30 X 150                        | 19.6%                    |
| 30 X 370                          | 9.9%                     | 30 X 160                        | 19.2%                    |
| 40 X 550                          | 11.2%                    | 80 X 400                        | 17.6%                    |
| 80 X 700                          | 7.6%                     | 165 X 800                       | 17.0%                    |
| 165 X 1400                        | 9.3%                     | 180 X 900                       | 19.6%                    |
| 325 X 2300                        | 7.1%                     | 2 X 120 X 650                   | 12.0%                    |
| 450 X 2750                        | 6.3%                     | 2 X 150 X 800                   | 12.6%                    |

While a calculation, such as shown above, will develop internal pleat spacings, or clearance, which will not further restrict flow beyond the worst restriction caused by the screen, itself, it is important that the external spacings also be considered in light of the effect caused by contaminant build-up on the screen surface.

When a filter is used at unit flow rates of 0.3 GPM/in<sup>2</sup> of filter media and above, a relatively small amount of contaminant collected on the screen face will cause the pressure drop to increase quite rapidly. When the unit flow rate through the medium is reduced to low values, such as 0.07 GPM/in<sup>2</sup> as is commonly accomplished by providing large amounts of screen in the filter element, the contaminant tolerance increases substantially.

Figure 81 shows contaminant tolerance curves for 325 X 2300 Twilled Dutch Double Weave wire cloth at unit flow rates of 0.289 GPM/in<sup>2</sup> and 0.075 GPM/in<sup>2</sup> using AC Coarse Dust and water. If a 20 psi pressure drop is assumed to be the maximum allowable for a particular filter, it can be seen that the amount of screen (square inches of porous medium) and the flow rate through the filter determines total amount of contaminant which can be ingested by the element without exceeding the allowable pressure drop. If the design flow rate is 3 GPM, and only 13.5 square inches of screen are used for the element, the unit flow rate through the screen will be 0.289 GPM/in<sup>2</sup> and a contaminant ingestion of 35 mg/in<sup>2</sup> of screen will cause a pressure drop of 20 psi. If 40 square inches of screen are used, the unit flow rate through the screen will be 0.075 GPM/in<sup>2</sup>, and contaminant in the amount of 250 mg/in<sup>2</sup> will develop the same pressure drop. Thus, the additional screen not only provides a much better contaminant tolerance, but also a large multiplier in determining the total contaminant which





can be exposed to the filter element. In the first case, the total contaminant will be  $13.5 \times 35 = 472$  milligrams, and for the second case, the total contaminant will be  $40 \times 250 = 10,000$  mg. By providing three times the screen area, over 20 times the contaminant ingestion is achieved.

While the theory applicable to the above calculation is sound, based on contaminant tolerance tests on flat, unpleated screen, actual pleated filter elements do not perform in complete accordance with the flat screen data. The most significant reason is that, in the case of the pleated element, the contaminant cake which forms on the upstream face of the screen not only tends to block the pores, but can also block the flow passage between pleats.

The density of AC Coarse Dust is approximately 1.3 grams per cubic centimeter, and it can be shown that 100 milligrams per square inch of screen will form a cake approximately .0048" thick. Thus, if all the AC Coarse Dust is trapped on the face of the mesh, which occurs on both pleat walls, the clearance between pleats will be reduced by .0096". With a pleat clearance space of 0.030, a common design selection, complete blockage of the flow passage will occur with a contaminant concentration of approximately  $300 \text{ mg/in}^2$  of medium.

In order to increase the contaminant tolerance for an element of a specific diameter, the designer often increases the number of pleats so that additional screen can be incorporated. The increased number of pleats decreases the pleat spacing, however, and the advantage of the extra screen may not be realized.

It is important that the designer allow additional space between the pleats to allow the cake thickness to form without undue blocking of the flow passages between pleats.

Figure 82 shows a comparison between data on the amount of contaminant required to produce a pressure drop of 20 psid, with water and AC Coarse Dust, at various flow rates between a flat, unpleated sample of 325 X 2300 TDDW wire cloth and a full size conical element in an in-line housing as shown in Figure 83. There were 40 square inches of screen in the conical element, and the pleat clearance varied from approximately 0.030" at the large end, to 0.010 at the small end of the cone.

Inspection of Figure 82 shows that at the higher flow rates where the contaminant tolerance to 20 psid is relatively low, the pleated element compares quite well with the flat screen data. At the lower flow rates, however, the pleated element does not perform as well as would be expected, and this is caused primarily by the serious blocking of the flow passages between pleats. At a flow rate of  $.075 \text{ GPM/in}^2$ , the pressure drop of 20 psi was reached with only  $67 \text{ mg/in}^2$  in the case of the pleated element, while it took  $250 \text{ mg/in}^2$  for the flat screen to develop the same pressure drop. The  $67 \text{ mg/in}^2$  caused a cake to form on the pleated element screen approximately 0.003" thick. This represents a 0.006" total blockage, or 30% of the 0.020" clearance at the midpoint of the conical element.

When a porous medium must operate at high unit flow rates, or with viscous fluids which provide low contaminant tolerance values, the flow passage blocking is usually not a serious consideration, but at very low unit flow rates and low viscosity fluids, where contaminant tolerance is high, the pleat spacing must be increased to allow maximum performance. This applies primarily to the fine grades of surface filtration media where nearly all the contaminant is trapped on the surface. Depth media which "absorb" the contaminant internally, and coarse media which allow much of the fine contaminant particles to pass through, do not form as much surface cake thickness, and for these materials the above analysis does not apply.

Nearly all data obtained in this program was based on tests using AC Coarse Dust contaminant, and it has been shown that contaminant type has a major effect on performance of porous media.

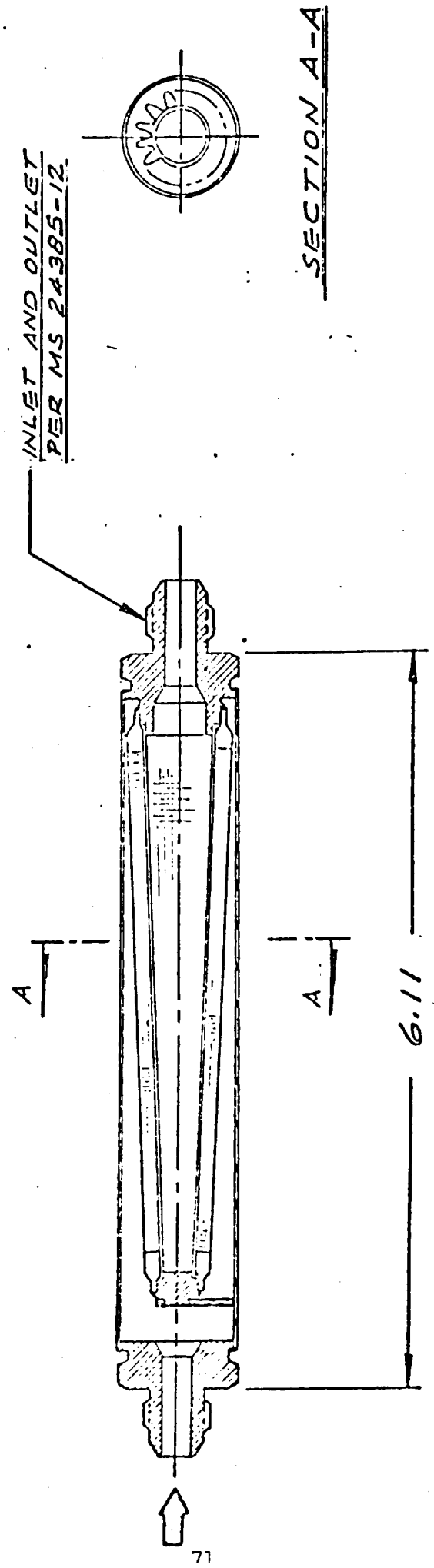


FIGURE 83  
 325 x 2300 TDDW WIRE CLOTH PLEATED CONICAL FILTER  
 (Ref: Dwg. No. 15267-556)

The characteristics of AC Coarse Dust probably do not represent those of "real" system contaminants found in operational fluids and, therefore, the conclusions formed from these test data can be used only for design guides.

### 3.7 FILTER MEDIA TESTS - FILTRATION RATINGS

#### 3.7.1 General Criteria

The filtration rating of a porous medium is an expression of the size of particles which can pass through the medium and, therefore, determine the degree of protection which a filter provides for downstream components. System designers and contamination control engineers usually define this parameter as the longest dimension of any particle observed in a sample of fluid taken from a system operating at rated flow. The filter industry, however, grade their products in terms of "Absolute" filter ratings. This rating certainly sounds reassuring and has led many a system designer to conclude that the filter he selected will, indeed, protect the system or its components from all particles larger than the "absolute" rating. Unfortunately, the term "Absolute Rating" only means that the filter will allow no spherical particles larger than the rated "Absolute" size to pass through the filter under steady flow conditions. In other words, only the second largest dimension of contaminant particles is controlled by the "absolute" rating, while the longest dimension is ignored together with any particles entrapped on the downstream side of the filter medium and released under dynamic flow conditions.

It is obvious, therefore, that a different means of expressing filtration rating is needed if uniform terminology is to be achieved between system designers and filter manufacturers. This has been recognized by NASA - JSC already, most notably in Specification MSC-SF-F-0044, where filters are rated in terms of "Maximum Particle Size" (MPS) which controls the longest (maximum) dimension of any particulate contaminant allowed downstream of a filter.

For the purposes of this report, two different ratings have been employed, the GBR, or Glass Bead Rating, which is equivalent to the "Absolute" Rating, but more definitive, and the MPR, or Maximum Particle Size Rating, as used in MSC-SE-F-0044. The two ratings can also be combined, for example, 10 x 25, where 10 is the GBR and 25 the MPR.

A number of different tests to determine the filtration rating of the various porous media, evaluated during this program, were conducted. These are described below.

#### 3.7.2 Retention Index Tests

Contaminant tolerance tests performed with four grades of Twilled Dutch Double Weave wire cloth, 325 X 2300, 165 X 1400, 80 X 700 and 30 X 250, showed increasing tolerance as the absolute filter rating (GBR) increases. The material with larger pore size allows a greater percentage of the graded contaminant to pass through initially, thus, prolonging the differential pressure rise.

To determine the degree of retention of contaminant offered by each of the four grades of Twilled Dutch Double Weave media, screen samples were dried and weighed prior to conducting contaminant tolerance tests. Weighed amounts of contaminant, AC Coarse test dust, were added upstream at a series of constant flow rates. After each test, the test system was purged with nitrogen to remove all liquid and partially dry the contaminated screen media. The screen sample was carefully removed from the sample holder, dried and weighed.

The retention index for each sample at each flow rate was calculated as follows:

$$\text{Retention Index} = \frac{100 \times [(\text{Wt. of Contaminated Screen}) - (\text{Wt. of Clean Screen})]}{\text{Wt. of Contaminant Added}}$$

Tests were conducted at three flow rates on four grades of Twilled Dutch Double Weave media, 30 X 250, 80 X 700, 165 X 1400 and 325 X 2300. AC Coarse Dust Contaminant was added until a pressure differential across the medium of approximately 50 psi was attained. The data from these tests is contained in Table 14. Figure 84 shows a plot of the retention indices for each medium as a function of the unit flow rate.

Retention index provides a comparative measure of the filter media's efficiency in trapping and holding contaminant. The test results presented in Figure 84 indicate an overall, or average, "efficiency" in that contaminant was added until a  $\Delta P$  of approximately 50 psid was attained at each flow rate. Because contaminant tolerance is a function of medium and flow rate, a consistent weight of contaminant was not added for each screen nor for each flow rate.

The clean screen, initially, functions at its lowest efficiency. The amount of contaminant passing through is highest when the filter media is clean and open. When contaminant builds up on the upstream face of the media, the transmission decreases, as the contaminant acts as a "pre-coat" and improves the efficiency of the screen media. As the  $\Delta P$  rises, the overall retention index increases approaching 100% when the filter media  $\Delta P$  approaches infinity. Thus, the retention index shown in Figure 84 must be used with caution. The curves, however, indicate a sharp upward curve as the flow rate decreases below approximately 1 to 2 GPM/in<sup>2</sup>. This is caused by the low fluid velocity with lower carrying power being unable to drive the contaminant through the media.

The apparent anomaly shown in Figure 84, where the retention index for the 325 X 2300 media appears lower than that for the 165 X 1400 media at high flow rates, illustrates the necessity for adding the same quantity of contaminant for all tests. In the tests from which this figure was derived, more contaminant was added in testing the 165 X 1400 than was added for the 325 X 2300 by a factor of 3 at 6.57 GPM/in<sup>2</sup>. This was done in order to develop the maximum  $\Delta P$ , so the initial low retention for the 165 X 1400 was masked by the additional contaminant added at the higher  $\Delta P$  when the "efficiency" was high, due to the "pre-coat" effect.

To avoid the possible distortion of data, inherent in testing to a consistent pressure differential which required differing weights of contaminant for each medium, a second series of tests were run in which a consistent weight of contaminant was added without regard to the resultant pressure differential. Table 15 shows the retention index for the previous four grades of Twilled Dutch Double Weave, wherein 4.48 milligrams per square inch of medium was injected using water at a flow rate of 6.57 GPM/in<sup>2</sup>. As might be expected, the order of retention index is in reverse order to micron-rating, the finest grade of medium having the highest retention index. Similar tests were conducted on the four grades of TDDW media, using AC Fine Dust and water at each of three unit flow rates, 0.126, 2.21 and 6.57 GPM/in<sup>2</sup>. The data from these tests is shown in Table 16. With all media, the retention index at 6.57 GPM/in<sup>2</sup> is considerably less than that observed with AC Coarse Dust at the same flow rate. The AC Fine Dust contains a much larger percentage of very fine particles than the AC Coarse Dust. Prior to partial clogging of the media, a greater percentage of the contaminant passed through, thus lowering the retention index. It is interesting to note the much greater clogging effect caused by the AC Fine Dust. The pressure differential resulting from the addition of 4.5 milligrams of AC Fine Dust at 6.57 GPM/in<sup>2</sup> was much larger than observed using AC Coarse Dust.

Finally, a series of retention index tests were conducted on five grades of Plain Dutch Single Weave media, 30 X 150, 80 X 400, 165 X 800, 180 X 900 and 2 X 120 X 650. AC Coarse Dust was injected, with water, at 2.21 GPM/in<sup>2</sup> of screen. Sufficient contaminant was added to create

TABLE 14  
RETENTION INDEX OF TWILLED DUTCH DOUBLE WEAVE WIRE CLOTH

| Grade Of Cloth               | Flow Rate                    |      | Temp. °F  | Total Dirt Add mg. | Highest Net Δ <sup>o</sup> psid | Retention Index % |
|------------------------------|------------------------------|------|-----------|--------------------|---------------------------------|-------------------|
|                              | gpm/in <sup>2</sup>          | gpm  |           |                    |                                 |                   |
| 30 x 250<br>TDDW<br>GBR 100  | .126                         | 0.2  | 73-74     | 316.5              | 60.22                           | 43.63             |
|                              | .126                         | 0.2  | 79        | 306.6              | 43.15                           | 32.39             |
|                              | .126                         | 0.2  | 78.5      | 296.5              | 49.04                           | 41.35             |
|                              | .317                         | 0.5  | 73.5-74   | 281.3              | 50.35                           | 35.73             |
|                              | .317                         | 0.5  | 75-75.5   | 284.5              | 57.60                           | 31.21             |
|                              | 2.21                         | 3.5  | 75        | 284.9              | 86.72                           | 25.03             |
|                              | 2.21                         | 3.5  | 75        | 268.2              | 87.30                           | 24.61             |
|                              | 2.21                         | 3.5  | 75        | 265.2              | 60.60                           | 21.61             |
|                              | 6.57                         | 10.4 | 79-79.5   | 246.2              | 86.20                           | 22.05             |
|                              | 6.57                         | 10.4 | 77-85     | 237.3              | 50.28                           | 19.39             |
| 80 x 700<br>TDDW<br>GBR 35   | .126                         | 0.2  | 73.5      | 166.2              | 52.30                           | 85.38             |
|                              | .126                         | 0.2  | 75        | 189.6              | 46.81                           | 86.29             |
|                              | .317                         | 0.5  | 72-73     | 126.3              | 55.61                           | 72.84             |
|                              | .317                         | 0.5  | 74-75     | 142.2              | 67.70                           | 75.95             |
|                              | .317                         | 0.5  | 78.5-79   | 124.6              | 52.70                           | 76.81             |
|                              | 2.21                         | 3.5  | 78.5-77.5 | 83.8               | 64.28                           | 64.98             |
|                              | 2.21                         | 3.5  | 77-77.5   | 82.4               | 59.54                           | 66.50             |
|                              | 6.57                         | 10.4 | 77        | 53.9               | 42.28                           | 58.81             |
|                              | 6.57                         | 10.4 | 78.5-80.5 | 54.0               | 45.10                           | 61.20             |
|                              | 165 x 1400<br>TDDW<br>GBR 20 | .126 | 0.2       | 77-79              | 319.1                           | 51.42             |
| 2.21                         |                              | 3.5  | 76.5      | 59.9               | 52.82                           | 80.63             |
| 2.21                         |                              | 3.5  | 75        | 64.5               | 68.64                           | 80.47             |
| 2.21                         |                              | 3.5  | 75        | 64.4               | 71.07                           | 82.76             |
| 6.57                         |                              | 10.4 | 75.5      | 34.7               | 47.90                           | 82.42             |
| 6.57                         |                              | 10.4 | 77-77.5   | 36.7               | 49.10                           | 79.84             |
| 325 x 2300<br>TDDW<br>GBR 10 |                              | .126 | 0.2       | 75                 | 146.85                          | 57.42             |
|                              | .126                         | 0.2  | 75        | 177.05             | 56.12                           | 98.16             |
|                              | .317                         | 0.5  | 70-71     | 85.9               | 68.6                            | 98.6              |
|                              | .317                         | 0.5  | 72-73     | 85.1               | 64.6                            | 96.0              |
|                              | .317                         | 0.5  | 73        | 85.5               | 89.1                            | 97.6              |
|                              | .317                         | 0.5  | 75-76     | 84.35              | 73.1                            | 99.8              |
|                              | 2.21                         | 3.5  | 76.5      | 35.2               | 58.54                           | 87.78             |
|                              | 2.21                         | 3.5  | 76        | 35.1               | 57.87                           | 86.04             |
|                              | 6.57                         | 10.4 | 75-77.5   | 16.0               | 48.90                           | 76.88             |
|                              | 6.57                         | 10.4 | 77-80.5   | 16.0               | 46.25                           | 77.50             |

Fluid: Deionized Water  
Contaminant: AC Coarse Dust

TABLE 15  
RETENTION INDEX OF TDDW WIRE CLOTH

Fluid: Deionized Water  
Contaminant: AC Coarse Dust

| Grade Of Screen | Flow Rate gpm/in <sup>2</sup> | Dirt Add mg/in <sup>2</sup> | ΔP Rise psid | Retention Index % | Micron Rating (GBR) |
|-----------------|-------------------------------|-----------------------------|--------------|-------------------|---------------------|
| 30 X 250        | 6.57                          | 4.48                        | 0            | 30.4              | 100                 |
| 80 X 700        | 6.57                          | 4.48                        | 0.5          | 61.5              | 35                  |
| 165 X 1400      | 6.57                          | 4.48                        | 1.0          | 93.0              | 20                  |
| 325 X 2300      | 6.57                          | 4.48                        | 9.0          | 97.5              | 10                  |
| 30 X 370        | 2.21                          | 227                         | 177          | 26                | 95                  |
|                 | 2.21                          | 202                         | 80.5         | 24                |                     |
| 40 X 550        | 2.21                          | 120                         | 71           | 38                | 70                  |
|                 | 2.21                          | 130                         | 97           | 41                |                     |

FIGURE 84

Retention Index -  
325 x 2300 TDDW  
165 x 1400 TDDW  
80 x 700 TDDW  
30 x 250 TDDW

AC Coarse Test Dust  
Water  
50 psid Maximum  $\Delta P$

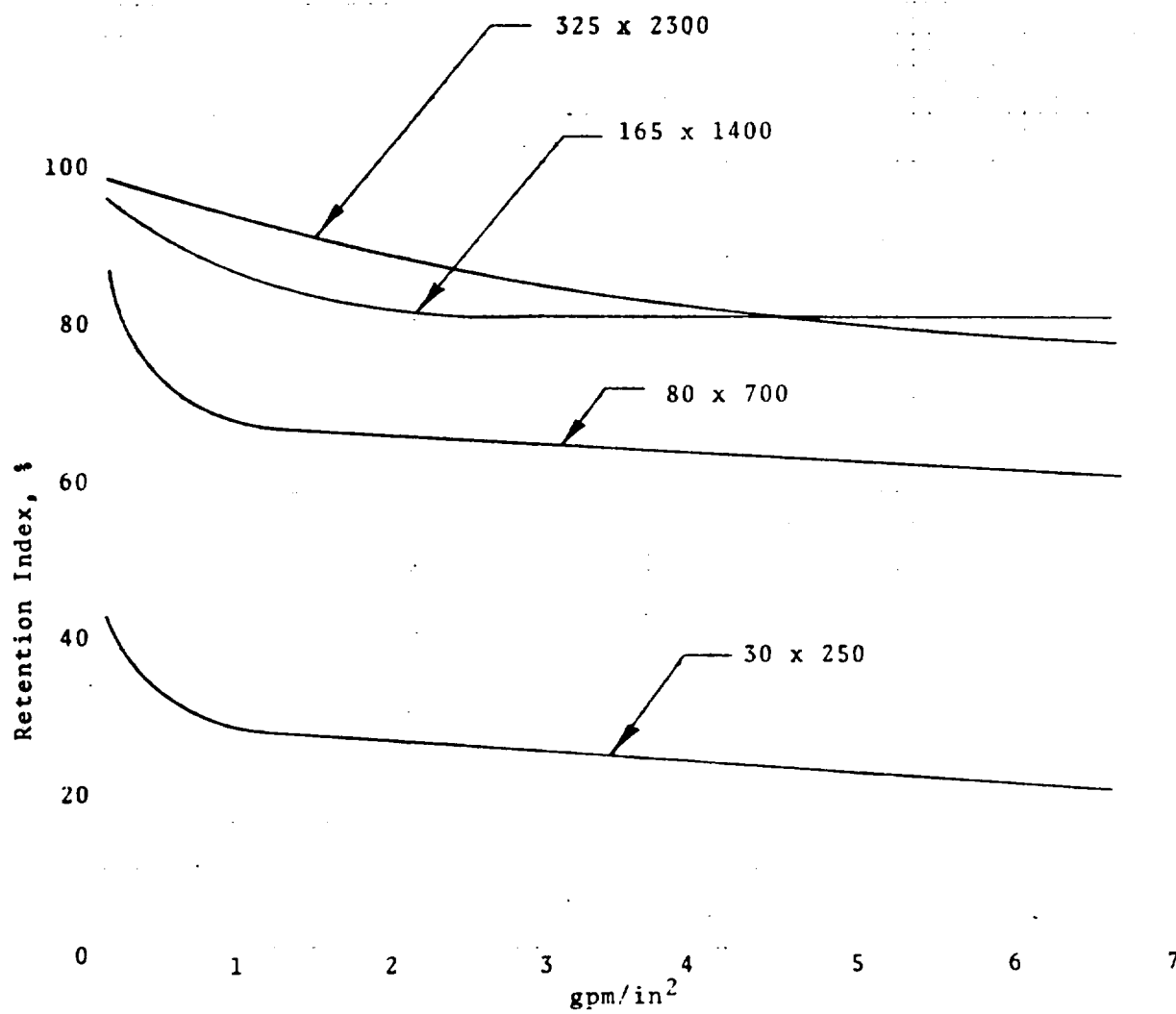


TABLE 16

## RETENTION INDEX OF TDDW WIRE CLOTH

Fluid: Deionized Water  
 Contaminant: AC Fine Dust

| Grade Of Screen | Flow Rate<br>gpm/in <sup>2</sup> | Dirt Add<br>mg/in <sup>2</sup> | $\Delta P$ Rise<br>psid | Retention<br>Index<br>% | Micron<br>Rating<br>(GBR) |
|-----------------|----------------------------------|--------------------------------|-------------------------|-------------------------|---------------------------|
| 80 X 700        | 0.126                            | 39.9                           | 0.5                     | 38                      | 35                        |
|                 | 2.21                             | 10.0                           | 1.4                     | 15                      |                           |
|                 | 6.57                             | 4.5                            | 10                      | 23                      |                           |
| 165 X 1400      | 0.126                            | 39.9                           | 44                      | 67                      | 20                        |
|                 | 2.21                             | 10.0                           | 2.8                     | 45                      |                           |
|                 | 6.57                             | 4.5                            | 11                      | 42                      |                           |
| 325 X 2300      | 0.126                            | 39.9                           | 94                      | 87                      | 10                        |
|                 | 2.21                             | 10.0                           | 18                      | 73                      |                           |
|                 | 6.57                             | 4.5                            | 28                      | 68                      |                           |

TABLE 17

## RETENTION INDEX OF PLAIN DUTCH SINGLE WEAVE WIRE CLOTH

Fluid: Deionized Water<sub>2</sub>  
 Flow Rate: 2.21 gpm/in<sup>2</sup>  
 Contaminant: AC Coarse Dust

| Grade Of Screen                | Dirt Add<br>mg/in <sup>2</sup> | $\Delta P$ Rise<br>psid | Retention<br>Index (%) | Micron<br>Rating (GBR) |
|--------------------------------|--------------------------------|-------------------------|------------------------|------------------------|
| 30 X 150                       | 275                            | 79                      | 21                     | 105                    |
|                                | 260                            | 56                      | 19                     |                        |
| 80 X 400                       | 80                             | 55                      | 65                     | 39                     |
|                                | 80                             | 61                      | 68                     |                        |
| 165 X 800                      | 60                             | 61.5                    | 83                     | 18                     |
|                                | 60                             | 64.5                    | 83                     |                        |
| 180 X 900                      | 70                             | 81                      | 72                     | 17                     |
|                                | 70                             | 80                      | 83                     |                        |
| 2 X 120 X 650<br>(Double Warp) | 60                             | 84                      | 81                     | 19                     |
|                                | 60                             | 82                      | 82                     |                        |



a large pressure differential across the media. Again, the retention indices fall in order of micron ratings (GBR), the smallest micron ratings having the largest retention index. This data is presented in Table 18. It can be seen that the retention indices for the PDSW media are roughly equivalent to those for the TDDW media, with the same micron rating (GBR). This comparison is summarized below.

TABLE 18  
RETENTION INDEX OF DUTCH WEAVE MEDIA

| Medium             | Filter Rating<br>(GBR) microns | Retention Index at<br>2.21 GPM/in <sup>2</sup> Water<br>and With AC Coarse Dust<br>§ |
|--------------------|--------------------------------|--|
| 30 X 250 TDDW      | 100                            | 24   |
| 30 X 150 PDSW      | 105                            | 20   |
| 80 X 700 TDDW      | 35                             | 66   |
| 80 X 400 PDSW      | 39                             | 67   |
| 165 X 1400 TDDW    | 20                             | 81   |
| 165 X 800 PDSW     | 18                             | 83   |
| 2 X 120 X 650 PDSW | 19                             | 82   |

### 3.7.3 Transmission Tests

Each type and grade of porous medium may be assigned a Glass Bead Rating, meaning the diameter of the largest hard spherical particle which can be transmitted. This rating is determined by flowing a mixture of glass beads through the media and collecting and filtering the effluent. Microscopic examination of the filter pad determines the largest bead diameter. In a normally contaminated fluid system, however, the particulate matter is seldom spherical, and elongated particles whose second and third dimensions are less than the glass bead rating may be transmitted. As particle size is customarily designated by the longest dimension, an obvious conflict exists between the glass bead rating and the "largest particle rating."

A good example of the confusion that exists in providing filter ratings for porous media is provided when the case of square weave cloth is considered. The structure of this medium is that of ordinary "window screen" wherein the wire size and spacing determines the size of the square pores. 100 X 100 mesh wire cloth with wire diameter of 0.0045 provides square openings 140 microns on a side. As a 140 micron diameter circle can be inscribed within this area, the glass bead rating for this material would be 140 microns. It is readily apparent, however, that a rod shaped particle 140 microns in diameter, with infinite length, could conceivably pass through this medium. Thus, while 100 X 100 X .0045 square mesh cloth possesses a legitimate glass bead rating, no maximum particle size rating can be assigned.

The controlling factor in the relationship between glass bead rating and maximum particle size rating is the degree of tortuosity of the flow paths along with the size and shape of the largest restricting pore. The more tortuous paths will prevent transmission of elongated particles to a degree determined by the curvature of the flow paths.

In order to determine the maximum dimension of particles transmitted through a medium, tests were conducted wherein a readily identifiable contaminant containing particles of various size and shape was added to the fluid upstream of the test specimen. The effluent was collected, filtered through a membrane filter and examined microscopically. Only the identifiable contaminant was considered, thus, eliminating the possibility of large particles from the system downstream of the test specimen providing erroneous results. The test contaminant was a mixture of AC Coarse Dust with fluorescing zinc sulfide particles added. The test procedure for determining transmission is contained in the Appendix with the Contaminant Tolerance Test procedure. The test contaminant was originally used by NASA - WSTF for particle transmission studies, and is supplied by Particle Information Service, Los Altos, California. The preparation is originally made by removing all particles over 40 microns in size from a quantity of AC Coarse Dust and substituting the zinc sulfide crystals in the micron size ranges of 40 - 80 and 80 - 200 in the same weight per cent as in the original AC Coarse Dust mixture. Certification of particle size range and composition supplied with the material showed the following:

TABLE 19  
COMPOSITION AND SIZE DISTRIBUTION OF AC COARSE DUST  
ZINC SULFIDE MIXTURE

| <u>Weight Per Cent</u> | <u>Composition</u> | <u>Particle Size Range<br/>(microns)</u> |
|------------------------|--------------------|--|
| 12 ± 2                 | AC Coarse Dust     | 0 - 5                                    |
| 12 ± 3                 | AC Coarse Dust     | 5 - 10                                   |
| 14 ± 3                 | AC Coarse Dust     | 10 - 20                                  |
| 23 ± 3                 | AC Coarse Dust     | 20 - 40                                  |
| 30 ± 3                 | Zinc Sulfide       | 40 - 50                                  |
| 9 ± 3                  | Zinc Sulfide       | 80 - 200                                 |

Substituting zinc sulfide for the larger particles of AC Coarse Dust permits simple microscopic observation of transmitted particles, as zinc sulfide fluoresces orange when viewed with ultraviolet light.

Prior to conducting these tests, samples of the contaminant mixture were mixed with water (2.5 mg in 500 ml water) and poured onto a 0.45 micron millipore filter pad. A vacuum was applied on the downstream side of the pad. The pad was then placed between two (2) glass slides and viewed under ultra-violet light. Considerable numbers of particles under 40 microns were observed, indicating that the particle distribution was different from that presented above. This discrepancy is due, undoubtedly, to break-up of the zinc sulfide particles in handling. This phenomenon of having smaller than 40 micron particles is advantageous, however, as it permits the same visual techniques for obtaining transmission data for the finer mesh screens as for the coarse.

Tests were conducted on 6 grades of Twilled Dutch Double Weave and 5 grades of Plain Dutch Single Weave media. The tests were run using deionized water at flow rates of 6.57 and 2.21 GPM/in<sup>2</sup>. The results of the tests are shown in Table 20.

TABLE 20  
LARGEST PARTICLES OF ZINC SULFIDE TRANSMITTED  
THROUGH VARIOUS FILTER MEDIA

Fluid: Deionized Water

Contaminant: AC Coarse Dust and ZnS

| Type of Media | Grade of Cloth | Flow Rate GPM/in <sup>2</sup> | Largest Particle Microns (Zinc Sulfide) | Media Glass Bead Rating ( $\mu$ ) | Transmission Index |
|---------------|----------------|-------------------------------|---|-----------------------------------|--------------------|
| TDDW          | 325 X 2300     | 6.57                          | 10 X 10                                 | 10                                | 1.0                |
|               | 165 X 1400     | 6.57                          | None                                    | 20                                | ---                |
|               | 80 X 700       | 6.57                          | 50 X 91                                 | 40                                | 2.3                |
|               | 30 X 250       | 6.57                          | 125 X 125                               | 100                               | 1.25               |
|               | 40 X 550       | 2.21                          | 87 X 161                                | 70                                | 2.3                |
|               | 30 X 370       | 2.21                          | 112 X 124                               | 100                               | 1.2                |
| PDSW          | 30 X 150       | 2.21                          | 90 X 174                                | 95                                | 1.8                |
|               | 80 X 400       | 2.21                          | 62 X 99                                 | 40                                | 2.5                |
|               | 165 X 800      | 2.21                          | None                                    | 18                                | ---                |
|               | 180 X 900      | 2.21                          | 31 X 62                                 | 17                                | 3.6                |
|               | 2 X 120 X 650  | 2.21                          | 20 X 36                                 | 19                                | 1.9                |

Examination of Table 20 shows that two media transmitted no zinc sulfide particles of any size, but as both of these media have glass bead ratings below the theoretical smallest zinc sulfide particle (40 microns) it can only be concluded that there were no small particles of zinc sulfide in the test contaminant used for these screens.

The fact that both the 80 X 700 and 30 X 250 TDDW media transmitted a particle whose second largest dimension is approximately 20 per cent larger than the glass bead ratings is understandable when one considers the shape of the pores in this material. The opening is in the form of a skewed triangle and the glass bead rating is theoretically the diameter of the inscribed circle. A properly shaped particle with width more than this circle diameter and length controlled by tortuosity alone could conceivably pass through. Thus, it is difficult to assign absolute values to transmission indices, but the approximate value of 2.5

seems applicable to both types of media. Thus, for TDDW and PDSW media, the maximum size particle capable of transmission is approximately 2.5 times the glass bead rating.

#### 3.7.4 Bubble Point Tests

The bubble point test is a non-destructive means of determining the size of the largest pore in a porous medium. The detailed procedure is described in the Society of Automotive Engineers (SAE) document ARP 901. Briefly, the procedure consists of wetting the medium under test with a liquid of known surface tension and then determining the air pressure required to force a bubble of gas through the wetted pores. The pressure required is a function of the pore shape, pore size and the surface tension of the test liquid. Any liquid may be used so long as it will "wet" the porous medium. Customarily, ethyl or isopropyl alcohol is used. It is essential that the porous medium be clean and grease-free to facilitate the wetting action and the formation of a liquid film across the pores. The larger the pore, the less pressure will be required to break the liquid film and allow a bubble of gas to exit the pore. Obviously, the largest pore will allow a bubble or a stream of bubbles to form at the lowest pressure. Thus, the pressure at which this occurs is known as the initial bubble point.

In practice, the test screen is immersed in, or covered with the test liquid. The immersion depth is measured and recorded as the hydrostatic head of immersion which acts against the pressure applied to force the gas through the medium.

After the medium is thoroughly wet, a gas pressure (using air or nitrogen) is applied beneath the specimen ( a special holder or fixture is used for flat screen tests) and the pressure is slowly increased until the first bubble or stream of bubbles is observed. The air pressure is recorded in units of inches of water column.

As explained in SAE ARP 901, the observed bubble point pressure for a given medium is a function of pore size, shape and liquid surface tension. As even carefully controlled samples of test liquid may have differing surface tension values, it is necessary to measure the surface tension (dynes/cm) and convert the observed results into a "Standard Bubble Point," which assumes a liquid surface tension of 21.15 dynes per cm. Conversion of the observed bubble point data to a "Standard Bubble Point" is accomplished as follows:

$$\text{S.B.P.} = \frac{(\text{O.B.P.} - dh) \times 21.15}{\text{ST}}$$

S.B.P. = Standard Bubble Point

O.B.P. = Observed Bubble Point

21.15 = "Standard" surface tension (dynes/cm)

S.T. = Surface tension of test liquid (dynes/cm)

d = specific gravity of test liquid

h = depth of immersion (inches)

Having converted the observed bubble point into a standard bubble point, taking into account the immersion depth and actual surface tension, the Standard Bubble Point is related to equivalent glass bead rating (GBR) by the factor 207 for Twilled Dutch Double Weave and Plain Dutch Single Weave media.

The mathematical expression for converting the observed bubble point pressure into equivalent glass bead rating of Twilled Dutch Double Weave and Plain Dutch Single Weave media is as follows:

- G.B.R. =  $\frac{207 \times S.T.}{21.15 \times (P-dh)}$
- G.B.R. = Glass Bead Rating (microns)
- 207 = Standard Bubble Point Factor (TDDW, PDSW Only)
- 21.15 = Standard Surface Tension (dynes/cm)
- P = Pressure for First Bubble to Appear ("H<sub>2</sub>O)
- S.T. = Surface Tension of Test Liquid (dynes/cm)
- d = Specific Gravity of Test Liquid
- h = Depth of Immersion of Test Media in Test Liquid (inches)

Table 3, which lists the physical properties of the various media, contains a column listing the corrected, or Standard Bubble Point, for the various media tested. This information is of value other than for determining the largest pore size in a given medium. Design of liquid acquisition devices, or bubble traps, used for separation of gases from liquids requires knowledge of the pressure at which gas will break through the medium. If the surface tension of the design liquid is known, the bubble point pressure at which gas breakthrough will occur is found as follows.

For media with pore shapes markedly different from the Dutch Weave materials, a conversion factor can be determined by conducting a glass bead test wherein a mixture of beads of various diameters is placed in liquid suspension and forced through the medium. Filtration of the effluent with subsequent microscopic examination will determine the glass bead rating of the medium. Having previously determined the initial bubble point, and converting to a Standard Bubble Point as described earlier, the micron rating (GBR) conversion factor can be determined by multiplying the Standard Bubble Point value by the diameter (in microns) of the largest bead found.

$$\text{Conversion Factor} = \text{Largest Bead Dia. (microns)} \times \text{S.B.P. (inches of water)}$$

For each pore shape medium, the conversion factor can be used to convert Standard Bubble Point values to Glass Bead Ratings for other media grades with larger or smaller pores.

$$\text{Bubble Point (New Liquid)} = \frac{\text{S.B.P.} \times \text{S.T. (New Liquid)}}{21.15}$$

S.B.P. = Standard Bubble Point (inches of water)

S.T. = Surface Tension (dynes/cm)

In conjunction with the data on flow resistance, practical design of a surface tension device, or gas trap, consists of supplying sufficient area of porous medium so that the pressure differential across the medium at design flow rate will never exceed the calculated bubble point pressure for the operational liquid. Thus, gas entrained in the liquid will not penetrate the medium, while liquid will pass freely.

### 3.7.5 Boiling Pressure Test

A measure of the primary flow pore size of the Twilled Dutch Double Weave media may be obtained in a manner similar to the Initial Bubble Point Test. The procedure for conducting the Boiling Pressure Test is presented in the Appendix. Essentially, the procedure consists of wetting the media with a fluid of known surface tension, and then forcing nitrogen gas through the wetted pores. The surface tension of the fluid in the pores resists gas flow. The amount of resistance is a measure of the equivalent pore size. By measuring flow rate of the gas as the pressure is slowly increased, a point will be reached at which there is a sudden large increase in flow rate with no appreciable increase in pressure. It is this

point, at which a great percentage of flow pores are opening nearly simultaneously, that "boiling pressure" is reached.

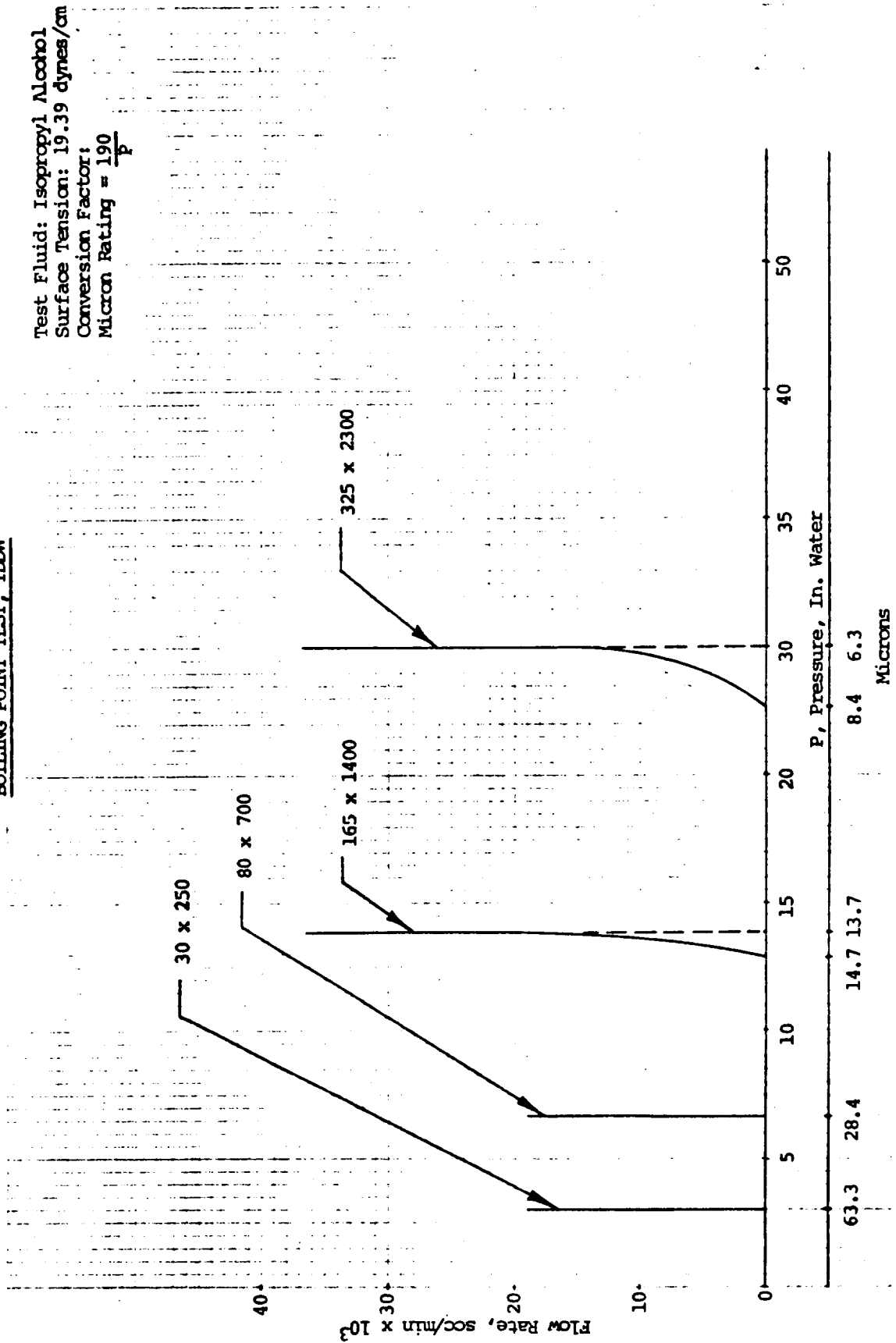
Conversion of the inlet gas pressure at boiling point to equivalent primary micron rating may be accomplished as in the Initial Bubble Point Test, by dividing the inlet pressure into a factor whose value is a function of the surface tension of the test liquid.

Figure 85 shows the plotted data of flow rate vs. inlet pressure for the four grades of Twilled Dutch Double Weave media. The point at which flow first begins is known as the Initial Bubble Point, and is a measure of the largest pore size. Where the curve rises nearly vertically showing increased flow at constant pressure, that pressure is the "boiling" point. In the case of the 30 X 250 and 80 X 700, the primary pore size is very nearly the same as the largest pore. The 165 X 1400 exhibits a slightly larger deviation, while the 325 X 2300 shows a greater pore size distribution between the initial bubble point and the boiling pressure point.

FIGURE 85

BOILING POINT TEST, TDDW

Test Fluid: Isopropyl Alcohol  
 Surface Tension: 19.39 dynes/cm  
 Conversion Factor:  $\frac{190}{P}$   
 Micron Rating =  $\frac{190}{P}$



### 3.8 FORMULATION OF MATHEMATICAL MODELS

#### 3.8.1 Flow Resistance - Liquids

The primary goal of this portion of the contract was to develop mathematical characterization of various filter media so that design trade-offs could be conducted and performance predicted.

A preliminary investigation of work accomplished by others indicated nearly all tests had been conducted with hydraulic fluids. Mathematical expressions had been developed such as the flow equation published by R.F. Church, et al, in an article entitled, "The Mechanics of Wire Cloth Filter Flow," appearing in the October, 1965 edition of Hydraulics and Pneumatics. The equation expressed flow rate in terms of the physical characteristics of the medium, the viscosity of the test liquid and the resultant pressure drop:

$$Q = \frac{0.87 \times 10^{-4} \phi D^2 A_c \Delta P}{\mu t}$$

Where: Q = Flow Rate, GPM  
 $\phi$  = Porosity of Medium =  $\frac{\text{Void Volume}}{\text{Bulk Volume}}$   
D = Capillary Diameter, microns  
 $A_c$  = Cross Sectional Area of Medium Exposed to Flow, in<sup>2</sup>  
 $\Delta P$  = Pressure Drop Across Medium, psi  
 $\mu$  = Dynamic Viscosity, centipoise  
t = Thickness of Medium, inches

The O.S.U. equation, when plotted on log-log graph paper, produces a straight line with a slope of 45°. Thus, the equation and graph indicated a linear relationship between flow rate and pressure drop.

As the work planned under this contract was related to propellant type fluids, with viscosities of much lower values than that of hydraulic oil, it was decided that water would be a more appropriate and representative test fluid.

The first flow resistance tests conducted were with 325 X 2300 Twilled Dutch Double Weave wire cloth using water, and it was immediately apparent that the O.S.U. equation was not going to be applicable for water due to the fact that the graph of the pressure drop vs. flow rate did not produce a straight line on log-log paper. The graph appeared to be a curve with a slope of approximately 45° at the low flow rates increasing to 63-1/2° at the highest flow rates. The comparison between the O.S.U. equation and the actual test data for the 325 X 2300 medium is shown in Figure 86, and the actual test data for the 325 X 2300 medium is shown in Figure 87.

So that the performance curves, for samples of different exposed areas, could be compared, the flow rate is expressed as GPM/in<sup>2</sup> of medium, or "unit flow rate."

An excellent review of early work accomplished in the development of flow resistance equations is contained in The Physics of Flow Through Porous Media, by A.E. Sheidegger, University of Toronto Press, 1963. The following is excerpted from this source.

Some of the earliest work on the development of the theory for laminar flow through homogeneous porous media was performed by Darcy in 1856, in which seepage flow of an incompressible liquid through a homogeneous filter bed of height, h, was measured and the following relationship developed:

$$Q = \frac{KA(\Delta P)}{t}$$



FIGURE 86

FLOW RESISTANCE CURVE COMPARISON  
 EMPIRICAL DATA VS O.S.U. EQUATION  
 325 X 2300 TDDW With Water @ 73°F

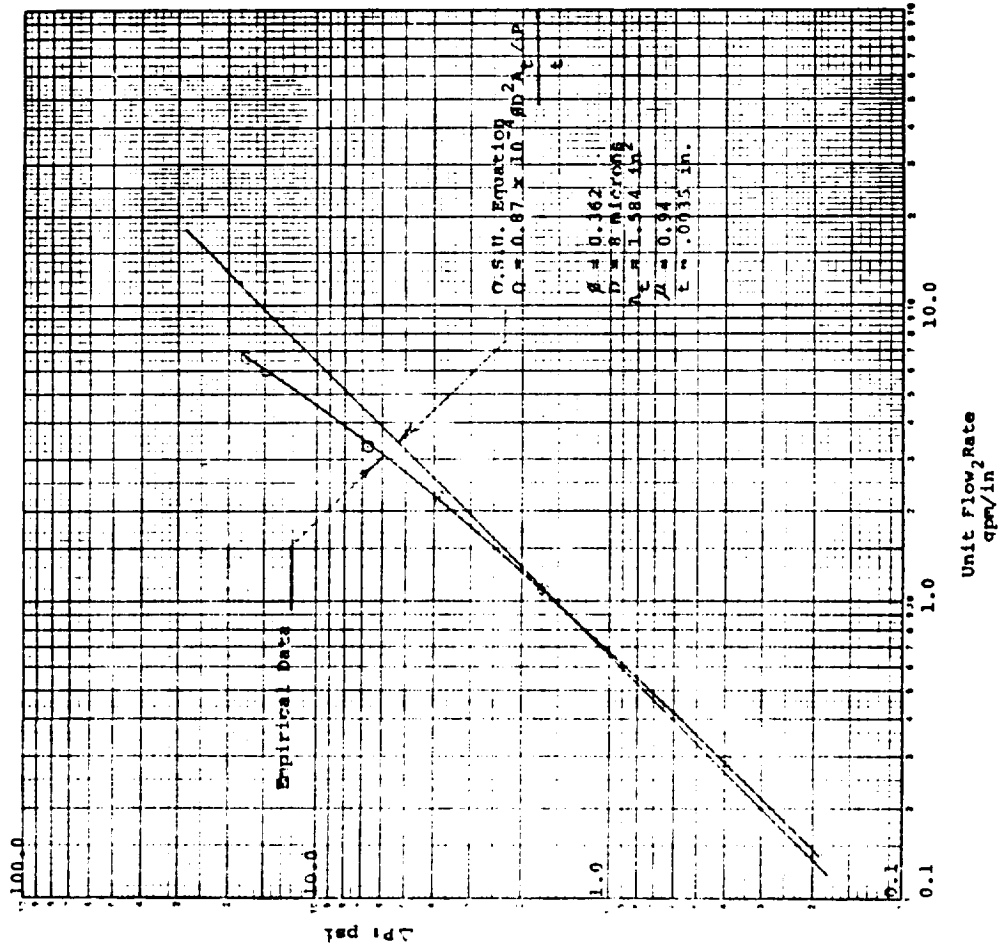
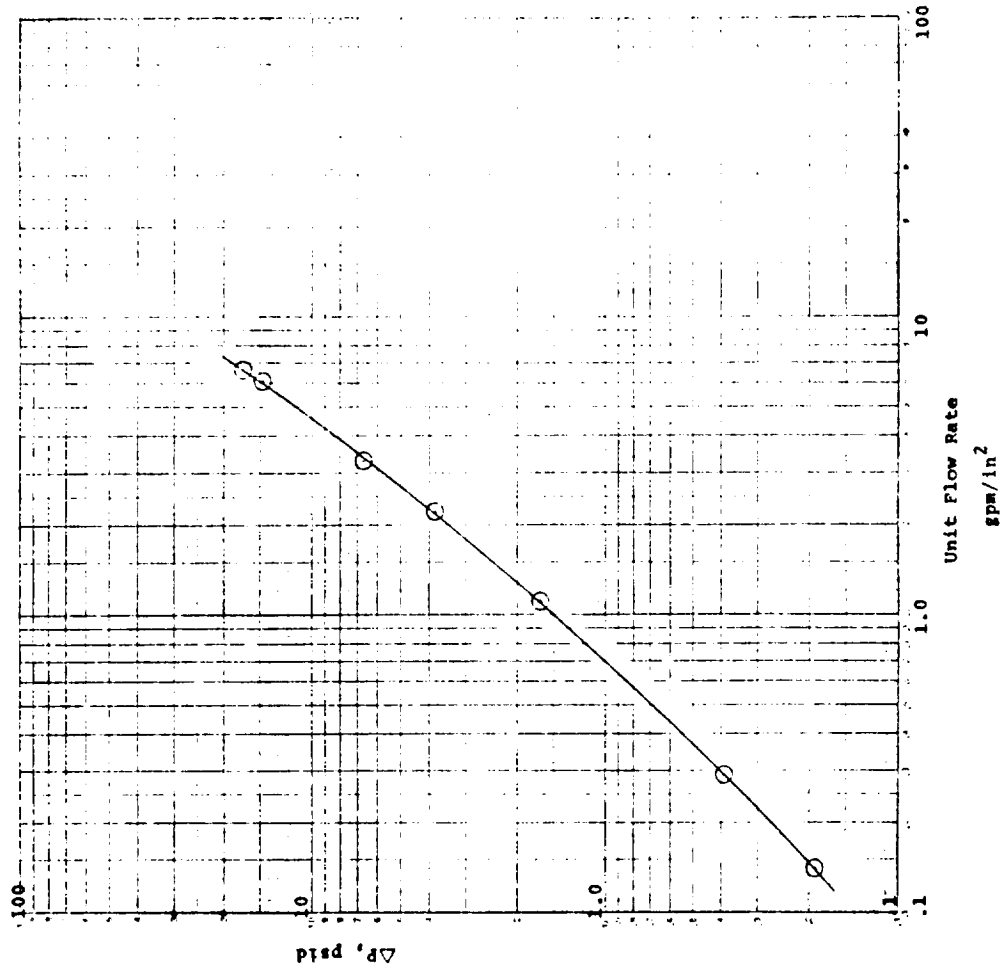


FIGURE 87

FLOW RESISTANCE OF 325 X 2300 TWILLED DUTCH DOUBLE WAVE WIRE CLOTH  
 Deionized Water @ 73 - 74 F



Where: Q = Flow Rate (volume divided by time)  
 K = A Constant Depending on the Properties of the Fluid and the Porous Medium  
 A = Exposed Cross Sectional Flow Area  
 ΔP = Pressure Loss Through the Medium  
 t = Thickness of the Medium

It is apparent that the above expression is similar to the O.S.U. equation and represents a linear relationship between flow rate and pressure drop for any given filter medium.

As early as 1900, investigators such as Forchheimer suggested that Darcy's Law was only valid for very low flow velocities, and that the equation for flow should contain a second order term in the velocity:

$$\Delta P/\Delta X = aq + bq^2$$

and later by adding a third order term to provide a better fit to experimentally determined curves:

$$\Delta P/\Delta X = aq + bq^2 + cq^3$$

In the above equations the pressure drop correlation is written for the linear case (linear dimension x); ΔP is the pressure (neglecting gravity); q is the seepage or flow velocity, and a, b and c are thought to be constants.

Another method of expressing the relationship between unit flow rate and pressure drop to provide a fit to experimentally developed curves was postulated by Missbach (A. Missbach, 1937, Listy Cukrovar 55,293) who set  $\Delta P/\Delta X = aq^m$ , with m undetermined between 1 and 2. The exact value of the exponent m, however, was noted to vary from case to case so that no universal correlation could be achieved.

An extremely popular correlation has been that between Reynold's Number, Re, and friction factor. Unfortunately, all such correlations are subject to limitations as the Reynold's Number significantly depends upon a definition of pore diameter which cannot be achieved properly.

Lindquist (1933) came to the conclusion that Darcy's Law was valid for Reynold's Number less than 4, and Kling (1940) claimed Darcy's Law would hold true for Re up to 10.

At the low Reynold's numbers (under 500) which apply to the flow rate ranges which are under consideration, it stands to reason that nonlinearly (in the flow - pressure drop correlations) is due to the emergence of inertia effects in laminar flow and not the onset of "turbulence." Curvature of the flow channels, for example, will cause nonlinear effects even at very low Reynold's Numbers.

To illustrate the very low Reynolds number associated with flow through typical porous media, Reynolds number values are calculated below for two typical grades of wire cloth at the highest unit flow rates used for testing in this program, 6.5 GPM per square inch of medium.

$$Re = \frac{4VR\rho}{\mu}$$

$$\text{Velocity at Screen Face, } V_1 = \frac{6.5 \text{ gal}}{\text{min} \times \text{in}^2} \times \frac{\text{ft}^3}{7.48 \text{ gal}} \times \frac{\text{min}}{60 \text{ sec}} \times \frac{144 \text{ in}^2}{\text{ft}^2}$$

$$V_1 = 2.09 \text{ ft/sec}$$

For 100 X 100 X 0.0045 square mesh, Open Area = 30.3%

$$\text{Velocity through "orifices," } V = \frac{2.09}{.303} = 6.90 \text{ ft/sec}$$

$$\text{Hydraulic Radius, } R = \frac{\text{Area}}{\text{Perimeter}} = \frac{(0.0055)^2}{4 \times .0055} \times \frac{\text{ft}}{12 \text{ in}} = 0.000115 \text{ ft}$$

For water at 100° F, ρ = 62.0 lb/ft<sup>3</sup>, μ = 0.000457 lb/ft/sec

1 - 2

$$Re = \frac{4VR\rho}{\mu} = \frac{4(6.90)(0.000115)(62.0)}{0.000457} = 431$$

For 325 X 2300 Twilled Dutch Double Weave, with 10 micron "diameter" openings and 7.1 per cent open area, the Reynolds number under identical conditions is as follows:

$$v = \frac{2.09}{0.071} = 29.5 \text{ ft/sec}$$

$$R = \frac{\pi(.0004)^2}{4\pi(.004)(12)} = 0.0000083 \text{ ft}$$

$$Re = \frac{4 \times 29.5 \times 0.0000083 \times 62.0}{0.000457} = 133$$

The following table shows Reynolds numbers for Hydraulic Oil and Water at typical test temperatures, for the two media.

TABLE 21  
REYNOLDS NUMBER THROUGH FILTER MEDIA

| Filter Medium                    | Flow Rate GPM/in <sup>2</sup> | Reynolds Number Through Screen |        |            |        |
|----------------------------------|-------------------------------|--------------------------------|--------|------------|--------|
|                                  |                               | Water                          |        | Mil-H-5606 |        |
|                                  |                               | @68°F                          | @100°F | @68°F      | @100°F |
| 100 X 100 Plain Square Wire Mesh | 6.5                           | 294                            | 431    | 14         | 21     |
| 325 X 2300                       | 6.5                           | 91                             | 133    | 4.3        | 6.5    |

From the above, it can be seen that the nonlinear effects observed in the flow resistance tests cannot be attributed to "turbulence" as normally defined, Reynolds number above 2000, and that pressure drop prediction or calculation could be better accomplished if Reynolds number need not be considered in the calculations.

For the purpose of this contract, it was decided that the most simple flow equation which would provide a reasonable fit to experimentally obtained data should be used as the basic relationship; and for this reason, the correlation  $\Delta P = aQ^2 + bQ$  was chosen, where:

- $\Delta P$  = Pressure Drop, psi
- a, b = Constants
- Q = Unit Flow Rate, GPM/in<sup>2</sup> of Medium

Inspection of the first and second order terms of velocity (GPM/in<sup>2</sup>) show resemblance to the Darcy - Weisbach turbulent flow equation for pressure drop through an orifice.

$$\Delta P = \frac{W}{2g} \left[ \frac{Q_1}{C_D A_O} \right]^2$$

- $\Delta P$  = Pressure Drop, lb/ft<sup>2</sup>
- W = Fluid Density, lb/ft<sup>3</sup>
- g = 32.2 ft/sec<sup>2</sup>
- Q<sub>1</sub> = Flow Rate, ft<sup>3</sup>/sec
- A<sub>O</sub> = Orifice Cross Sectional Area, ft<sup>2</sup>
- C<sub>D</sub> = Discharge Coefficient

and the Hagen - Poisuille law for laminar flow through a conduit:

$$\Delta P = \frac{32 VL\mu_m}{gD^2}$$

- $\Delta P$  = Pressure Drop, lb/ft<sup>2</sup>
- $V$  = Velocity of Flow, ft/sec
- $D$  = Diameter of Circular Flow Path, ft.
- $L$  = Length of Flow Path, ft
- $\mu_m$  = Fluid Absolute Viscosity, lb/ft/sec
- $g$  = 32.2 ft/sec<sup>2</sup>

The path through which flow occurs in typical screen types of filtration media may be considered to have two distinctly different characteristics. Initially, the fluid enters a relatively large opening formed by adjacent wires at the upstream side of the screen. The fluid then passes through a relatively small opening formed by the geometrical relationship of the wires in the specific type of weave of the medium. This smaller opening determines the filtration rating of the medium and may be considered to be the "orificing" portion of the flow path. The fluid then enters a larger area at the downstream side of the screen identical to that at the upstream side.

The total pressure drop across the screen type media may thus be considered to consist of two components, one representing the kinetic energy loss through the orifices and curved passages, and one representing the viscous drag pressure loss through the "pipe-like" inlet and outlet portions of the flow path.

Further substantiation for the use of the simplified flow equation, and the similarity to the equations for orifice and conduit flow, is apparent from the equation for flow through porous media suggested by Greenberg and Weger, "An Investigation of the Viscous and Inertial Coefficients for the Flow of Gases Through Porous Sintered Metals with High Pressure Gradients," Chemical Engineering Science, Pergamen Press Ltd., London, England, 1960, Volume 12.

$$\frac{dP}{dX} = \alpha\mu V + \beta\rho V^n$$

- Where
- $\alpha$  and  $\beta$  are Constants
  - $\mu$  is a Viscosity Coefficient
  - $\rho$  is a Density Coefficient
  - $V$  is Velocity of the Fluid
  - $dP/dX$  is the Pressure Gradient Through the Medium
  - $n$  is a Constant with Value Between 1 and 2

Thus, the simple basic equation of flow resistance,  $\Delta P = aQ^2 + bQ$ , suggests that the total pressure drop across the medium consists of two components. The  $aQ^2$  term represents the kinetic energy loss due to "turbulence" or, more likely, the emergence of inertia effects in laminar flow, while the  $bQ$  term represents the "viscous" energy loss. The "Q" term, it should be noted, is expressed as volume per unit area per unit time and, thus, represents velocity of flow.

The value of the constant "a" is a function of the smallest cross sectional area of the "orifices" in the medium, the number of "orifices," a screen orifice coefficient and the density of the fluid.

The value of the constant "b" is a function of the average cross sectional area of the flow conduits, the number of flow conduits, the length and tortuosity of flow paths and the vis-

cosity of the fluid.

To empirically determine the value of the constants "a" and "b" in the flow resistance equation, samples of each medium were installed in a test fixture and deionized water was flowed through the media at various flow rates while measuring the pressure drop across the media. The test data was reduced to GPM/in<sup>2</sup> of media and pressure drop in terms of psi for each flow rate.

This data was then plotted on log - log paper and the values of "a" and "b" were determined by choosing two flow rates on the curve, noting the corresponding values for  $\Delta P$  and Q, and solving the two equations for two unknowns. This procedure can be illustrated by the following example.

Figure 87 shows the relationship for  $\Delta P$  and Q for 325 X 2300 Twilled Dutch Double Weave wire cloth using deionized water at 73° - 74° F.

Choosing a unit flow rate of 1 GPM/in<sup>2</sup>

$$1.5 = a(1)^2 + b(1)$$

At a unit flow rate of 6 GPM/in<sup>2</sup>

$$14.8 = a(6)^2 + b(6)$$

Solving the two equations for the values of "a" and "b":

$$a = 0.19 \text{ and } b = 1.31$$

The values of 0.19 and 1.31, for "a" and "b" respectively, provide the flow equation  $\Delta P = 0.19Q^2 + 1.31Q$ . This is the equation for the curve shown in Figure 87.

However, it is desirable that the values of "a" and "b" be determined for a hypothetical fluid with specific gravity and viscosity both equal to unity. This will provide a "basic" equation which, for any given medium may be modified to suit any other liquid simply by multiplying the value of "a" by the specific gravity of the new fluid and multiplying "b" by the viscosity (centipoises) of the new fluid.

The values of the constants determined above are for water at 74° F. At this temperature, the specific gravity may be taken as 1.0 and the viscosity is 0.9. Thus, the "basic" values of "a" and "b" become 0.19 divided by 1.0, and 1.31 divided by 0.9, or 0.19 and 1.45 respectively. The "basic" flow resistance equation for 325 X 2300 Twilled Dutch Double Weave wire cloth may be written:  $\Delta P = 0.19Q^2 + 1.45Q$ .

As noted earlier, the O.S.U. flow equation, like Darcy's Law, expressed a linear relationship between unit flow rate and pressure drop. It is readily apparent from inspection of the O.S.U. equation, which contains a fluid viscosity term, that it is equivalent to the second term, bQ, of the basic two-constant equations.

It is understandable that the O.S.U. work with hydraulic fluid, a liquid of relatively high viscosity and low density, would lead to a single term, first order relationship between unit flow rate and pressure drop. As in the work conducted under this contract, the equation for flow was developed from empirical test data, and within the practical flow rate regime, up to 6 or 7 GPM per square inch of medium, the plotted data for hydraulic fluid produces practically a straight line at 45° slope on log - log paper. Thus, a linear relationship between unit flow rate and pressure drop is indicated.

The change in shape of the flow resistance curve, between data collected in water tests compared to similar data obtained in tests with hydraulic fluid, can be explained by examination of the basic flow equation and the modified equation representing the flow resistance with

Mil-H-5606 hydraulic fluid. The basic flow equation for the 325 X 2300 Twilled Dutch Double Weave wire cloth is  $\Delta P = .19Q^2 + 1.45Q$ . This represents the flow resistance relationship with a liquid of specific gravity of 1.0 and a viscosity of 1 centipoise. As noted earlier, the equation can be modified for any other liquid by multiplying the "a" and "b" values by the specific gravity and viscosity respectively of the new liquid.

Thus, for Mil-H-5606 hydraulic fluid, with a specific gravity of 0.8 and a viscosity of 10 centipoises at a typical temperature of 115° F., the flow equation would be  $\Delta P = 0.15Q^2 + 14.5Q$ . Here, the first order term, 14.5Q, has become so large in comparison to the second order term, .15Q<sup>2</sup> for the lower unit flow rates of up to 5 or 6 GPM/in<sup>2</sup>, that the viscous drag term predominates and masks the kinetic energy term. The flow equation for hydraulic fluid will produce essentially a straight line with slope of approximately 45° when plotted on log - log paper.

#### Calculation of Flow Constants from Physical Characteristics of the Media

The method described earlier for determining the equation of flow resistance for various media is empirical in that actual test data must be obtained using a sample of each medium and a liquid of known density and viscosity.

If, as stated earlier, the aQ<sup>2</sup> portion of the flow resistance equation is equivalent to the equation for flow through an orifice and the bQ portion is equivalent to the Hagen - Poisuille law for laminar flow, then it should be possible to calculate values for the flow resistance constants from the physical characteristics of the various media.

The characteristic shape of the flow path for the Plain Square Weave media consists of the inlet side "collection area" formed by adjacent wires. The path becomes smaller toward the center of the screen forming the "orifice" and then enlarges again at the outlet side.

This simple construction is the least complex of the various media tested, and the similarity of the regularly shaped square openings to a set of orifices is readily apparent. The correlation of the aQ<sup>2</sup> term in the flow resistance equation to the equation for pressure drop through an orifice can now be shown. The physical characteristics of Plain Square Weave media are shown in Table A-1 in the Appendix.

The Darcy - Weisbach equation for pressure drop through an orifice states:

$$\Delta P = \frac{W}{2g} \left[ \frac{Q_1}{C_D A_O} \right]^2$$

Where:  $\Delta P$  = Pressure Drop, lb/ft<sup>2</sup>  
 $W$  = Fluid Density, lb/ft<sup>3</sup>  
 $g$  = 32.2 ft/sec<sup>2</sup>  
 $Q_1$  = Flow Rate, ft<sup>3</sup>/sec  
 $A_O$  = Orifice Area, ft<sup>2</sup>  
 $C_D$  = Discharge Coefficient

The equivalent portion of the flow resistance equation states:

$$\Delta P = aQ^2$$

Where:  $\Delta P$  = Pressure Drop, lb/in<sup>2</sup>  
 $a$  = Dynamic Flow Coefficient  
 $Q$  = Unit Flow Rate, GPM/in<sup>2</sup>

In order to relate the two equations it is necessary to provide identical terms and units.

The total flow area of the screen medium is equal to the area of each individual pore multiplied by the number of pores. The ratio of this total flow area to the area of medium exposed to flow is expressed as "per cent orifice area,"  $\eta$ .

Thus:

$$A_0 = \frac{A \eta}{144}$$

Where:  $A_0$  = Total Orifice Area,  $\text{ft}^2$   
 $A$  = Exposed Screen Area,  $\text{in}^2$   
 $\eta$  = Per Cent Orifice Area, decimal

or

$\eta$  = Number of Pores/ $\text{in}^2$  of Screen Surface x  $\text{in}^2$  Area per Pore

And:

$$Q_1 = \frac{AQ}{(7.48)(60)}$$

Where:  $Q_1$  = Flow Rate,  $\text{ft}^3/\text{sec}$   
 $A$  = Area of Screen,  $\text{in}^2$   
 $Q$  = Unit Flow Rate through Screen,  $\text{GPM}/\text{in}^2$   
 7.48 = Gal/ $\text{ft}^3$  Conversion  
 60 = Seconds/min Conversion

The expressions shown for  $A_0$  and  $Q_1$  may be substituted in the orifice flow equation:

$$\Delta P = \frac{W}{2g} \left[ \frac{AQ}{(C_s)(7.48)(60)} \times \frac{144}{A \eta} \right]^2 \frac{1}{144}$$

$$\Delta P = \frac{WQ^2}{(300.37C_s)^2}$$

Where:  $\Delta P$  = Pressure Drop,  $\text{lb}/\text{in}^2$   
 $W$  = Fluid Density,  $\text{lb}/\text{ft}^3$   
 $Q$  = Unit Flow Rate,  $\text{GPM}/\text{in}^2$   
 $\eta$  = Orifice Area, decimal per cent  
 $C_s$  = Screen Coefficient

Also, from the flow resistance equation:

$$\Delta P = aQ^2$$

Therefore:

$$aQ^2 = \frac{WQ^2}{(300.37C_s)^2}$$

and

$$a = \frac{W}{(300.37C_s)^2}$$

The screen coefficient,  $C_s$ , may be evaluated by inspection of empirical test data and is found to have an average value of 0.65 for the four square weave media.

Table 22 shows a comparison between the calculated and empirically determined values for the dynamic flow constant,  $a$ , for the four plain square weave media.

Other media of differing construction and orifice shape will have different values for the screen constant,  $C_s$ , than that determined for the Plain Square Weave media.

TABLE 22  
CALCULATED VS. EMPIRICAL VALUES FOR FLOW CONSTANT, "a"

| Media<br>(Mesh Count) | Clear<br>Opening<br>(inches) | Per Cent<br>Open Area<br>$\eta$ | Thickness<br>t (inches) | $C_s$ | "a"<br>Calc. | Empir. |
|-----------------------|------------------------------|---------------------------------|-------------------------|-------|--------------|--------|
| 100 X 100             | 0.0055                       | 30.3                            | 0.009                   | 0.65  | 0.017        | 0.011  |
| 150 X 150             | 0.0041                       | 37.4                            | 0.0052                  | 0.65  | 0.012        | 0.013  |
| 200 X 200             | 0.0029                       | 33.6                            | 0.0042                  | 0.65  | 0.015        | 0.015  |
| 250 X 250             | 0.0024                       | 36.0                            | 0.0032                  | 0.65  | 0.013        | 0.016  |

The similarity of the "bQ" term in the flow resistance equation to the Hagen - Poissuille law for pressure drop through a conduit can be illustrated by correlating the two and determining the screen characteristics corresponding to the terms in the Hagen - Poissuille equation which states:

$$(1) \quad \Delta P = \frac{32VL\mu_m}{gD^2}$$

Where:

- $\Delta P$  = Pressure Drop, lb/ft<sup>2</sup>
- V = Velocity of Flow, ft/sec
- L = Length of Flow Path, ft
- $\mu_m$  = Absolute Viscosity of Fluid, lb/ft/sec
- D = Diameter of Circular Flow Path, ft.
- g = 32.2 ft/sec<sup>2</sup>

To compare the bQ terms of the flow resistance equation to the Hagen - Poissuille law, it is necessary to determine and define similar terms and express them in a measurable fashion. Various constants of proportionality will be used in the discussion to handle conversion of inconsistent units.

The equivalent effective circular diameter of the total screen flow passages is difficult to measure in the more complex weaves such as Twilled Dutch Double Weave wire cloth, so the following method was used to obtain an approximation of this equivalent diameter.

Calculate the total volume of a sample of area, A, in<sup>2</sup>.

$$(2) \quad \text{Volume} = A \times t \text{ in}^3$$

Where:

- A = Area of Sample, in<sup>2</sup>
- t = Thickness of Sample, in

Determine calculated weight if solid material.

$$(3) \quad \text{Calculated Weight} = \text{Volume} \times \text{Density}$$

Weight expressed in lbs  
Volume expressed in in<sup>3</sup>  
Density expressed in lbs/in<sup>3</sup>

Weigh the screen sample and determine void fraction.



$$(4) \quad \beta = 1 - \frac{\text{Actual Weight}}{\text{Calculated Weight if Solid}}$$

Determine the average effective length of flow passage.

$$(5) \quad l = t \times \tau$$

$l$  = Average Flow Passage Length, in  
 $t$  = Screen Thickness, in  
 $\tau$  = Tortuosity Factor

Calculate Total Area of flow passages.

$$(6) \quad A_C = \frac{\text{Total Flow Passage Volume}}{\text{Average Flow Path Length}}$$

$$A_C = \frac{A \times t \times \beta}{l}$$

$$A_C = \frac{At\beta}{t\tau} = \frac{A\beta}{\tau}$$

The total flow passage area can also be expressed as the area of the average flow path multiplied by the number of flow paths.

$$(7) \quad A_C = \frac{\pi d^2}{4} \times N_a$$

Where:  $d$  = Diameter of Average Capillary  
 $N_a$  = Number of Capillaries in Total Screen Area,  $A$  in<sup>2</sup>

Relating expressions (6) and (7)

$$(8) \quad \frac{A\beta}{\tau} = \frac{\pi d^2}{4} N_a$$

Solving for  $d^2$

$$(9) \quad d^2 = \frac{4A\beta}{\pi\tau N_a}$$

This expression may be simplified by considering  $A$  equal to 1 square inch and  $N_a$  equal to the number of flow passages in 1 square inch of medium.

Then

$$(10) \quad d^2 = \frac{4\beta}{\pi\tau N_1}$$

Where:  $N_1$  = Number of Flow Passages per Square Inch of Medium

In the Hagen - Poissuille law, the term  $V$  represents velocity in units of ft/sec. In the term  $bQ$  of the flow equation, the term  $Q$  is really a measure of velocity in that it represents volume per unit time per unit area, GPM/in<sup>2</sup>. Using a constant of proportionality  $C_1$ , the velocity of flow through the capillaries of the filter medium can be written:

$$(11) \quad V = C_1 \left[ \frac{Q_v}{A_C} \right]$$

Where:  $V$  = Velocity of Flow, ft/sec  
 $Q_v$  = Flow Rate, gal/min  
 $A_C$  = Total Flow Passage Area, in<sup>2</sup>

For consistency,  $C_1$  must have the units of  $\frac{\text{ft-min-in}^2}{\text{sec-gal}}$

and, therefore, the value of  $C_1$  is:

$$(12) \quad C_1 = \frac{1}{(60 \text{ sec/min})(4.329 \times 10^{-3} \text{ gal/in}^3)(12 \text{ in/ft})}$$

$$C_1 = 0.3208 \frac{\text{ft-min-in}^2}{\text{sec-gal}}$$

To express velocity,  $V$ , in terms of the flow rate and characteristics of the filter medium, equation (6) may be substituted into (11):

$$(13) \quad V = \frac{C_1 Q_v \tau}{A\beta}$$

As the term  $Q$  in the flow equation is expressed as  $\text{GPM/in}^2$ , the value  $Q$  may be substituted for  $\frac{Q_v}{A}$ , thus:

$$(14) \quad V = \frac{C_1 Q \tau}{\beta}$$

Where:  $Q$  = Flow Rate/ $\text{in}^2$  of Medium,  $\text{GPM/in}^2$   
 $\tau$  = Tortuosity Factor  
 $\beta$  = Void Fraction

Both  $L$ , the length of flow path, and  $D$  the diameter of the circular flow path, in the Hagen Poissuille law (equation 1) are expressed in feet, while the equivalent values of  $l$  and  $d$  for the screen are expressed in inches. In addition, from equation (5),  $l = \tau t$ .

Converting the  $L$  and  $D$  terms to match the equivalent screen parameters:

$$L = \frac{\tau t}{12}$$

and

$$D = \frac{d}{12}$$

and

$$(15) \quad \frac{L}{D^2} = \frac{\tau t}{d^2} \times 12 \frac{\text{in}}{\text{ft}}$$

Also, the term  $\mu_m$  in equation (1) has the units of  $\text{lb}_m/\text{ft}/\text{sec}$ . This may be converted to units of centipoises as follows:

$$\text{Centipoise} = (\text{lb}_m/\text{ft}/\text{sec})(6.72 \times 10^{-4})$$

Substituting this conversion value for viscosity, the value of  $L/D^2$  from (15) and the value of  $V$  from (14) into equation 1 gives:

$$(16) \quad \Delta P = \left[ \frac{(32)(C_1)(12)(6.72 \times 10^{-4})}{32.17} \right] \left[ \frac{Q\tau^2 t \mu}{\beta d^2} \right]$$

Where:  $t$  and  $d$  are expressed in inches,  $\mu$  is expressed in centipoises,  $Q$  is expressed as  $\text{GPM/in}^2$ .

$$\text{Setting: } C_2 = \frac{32C_1(12)(6.72 \times 10^{-4})}{32.17}$$

$$(16a) \quad \Delta P = \frac{C_2 Q r^2 t \mu}{\phi d^2}$$

Where:  $C_2$  has units of  $\frac{\text{min-in}^3 \text{lb}_f}{\text{gal-ft}^2 \text{-centipoise}}$

In equation (10) it was determined that:

$$d^2 = \frac{4\phi}{\pi r N_1}$$

Where:  $N_1$  equals the number of flow passages per square inch of medium.

Substituting equation (10) into (16a):

$$(17) \quad \Delta P = \left[ \frac{C_2 Q r^2 t \mu}{\phi} \right] \left[ \frac{\pi r N_1}{4\phi} \right]$$

$$\Delta P = \left[ \frac{C_2 \pi}{4} \right] \left[ \frac{r^3 t \mu N_1}{\phi^2} \right] \times Q$$

From the expression,  $\Delta P = bQ$ , it can be seen that the value for  $b$  is as follows:

$$(18) \quad b = \left[ \frac{C_2 \pi}{4} \right] \left[ \frac{r^3 t \mu N_1}{\phi^2} \right]$$

Again, for simplicity:

$$(19) \quad b = \frac{K r^3 t \mu N_1}{\phi^2}$$

Where:  $K = \frac{C_2 \pi}{4} = \frac{(32)(.3208)(12)(6.72 \times 10^{-4})\pi}{(32.17)(4)}$

$$(20) \quad K = 2.021 \times 10^{-3}$$

$K$  has the units of  $C_2$ , or  $\frac{\text{min-in}^3 \text{-lb}_f}{\text{gal-ft}^2 \text{-centipoise}}$

The units of  $b$  in equation (19) may now be determined:

$t$  is expressed in inches  
 $\mu$  is expressed in centipoises  
 $N_1$  = number per square inch  
 $r$  and  $\phi$  are dimensionless

$$b = \text{inches} \times \text{centipoises} \times \frac{1}{\text{in}^2} \times \frac{\text{lb}_f \text{min-in}^3}{\text{ft}^2 \text{-gal-centipoise}} = \frac{\text{in}^2 \text{-lb}_f \text{-min}}{\text{ft}^2 \text{-gal}}$$

and  $bQ = \frac{\text{in}^2 \text{-lb}_f \text{-min}}{\text{ft}^2 \text{-gal}} \times \frac{\text{gal}}{\text{min-in}^2}$

$$bQ = \text{lb/ft}^2$$

But, it is desired that  $bQ$  be expressed in units of pounds/in<sup>2</sup>, therefore, dividing the value of  $K$  shown in equation (20) by  $\frac{144 \text{ in}^2}{\text{ft}^2}$  will provide the proper units for  $bQ$ .

$$K_0 = \frac{K}{144} = \frac{2.021 \times 10^{-3}}{144}$$

$$(21) \quad K_0 = 1.403 \times 10^{-5}$$

In summary, the value for b may be stated as follows:

$$(22) \quad b = \frac{K_0 \tau^3 t \mu N_1}{\phi^2}$$

Where:

- $K_0$  =  $1.403 \times 10^{-5}$
- $\tau$  = Tortuosity Factor, dimensionless
- $t$  = Thickness, inches
- $\mu$  = Viscosity of Liquid, centipoise
- $N_1$  = Number of Major Flow Passages per Square Inch of Medium
- $\phi$  = Void Fraction, dimensionless

For square weave wire cloth, the flow path length varies considerably across the square opening. At the corners, the path length is equal to the thickness of the screen, while at the midpoint of the opening, the flow path approaches the thickness of one wire only, or one half the thickness. Good approximations of the value for the b term in the flow equation can be obtained in the case of the coarser weaves by using the decimal per cent open area value for the void fraction in the equation (22). The value of  $\tau$  for the plain square weave media is assumed to be 1.0.

Table 23 shows the comparison between the calculated and empirically determined values of b for the four plain square weave media. These are "basic" values for a liquid of 1.0 cp viscosity.

TABLE 23  
CALCULATED VS. EMPIRICAL VALUES FOR FLOW CONSTANT "b"

| Media<br>(Mesh Count) | Thickness<br>(Inches) | Open Area<br>(Decimal Per Cent) | Calculated<br>b | Empirical<br>b |
|-----------------------|-----------------------|---------------------------------|-----------------|----------------|
| 100 X 100             | 0.009                 | 0.30                            | 0.014           | 0.011          |
| 150 X 150             | 0.0052                | 0.37                            | 0.012           | 0.011          |
| 200 X 200             | 0.0042                | 0.33                            | 0.019           | 0.011          |
| 250 X 250             | 0.0032                | 0.36                            | 0.022           | 0.017          |

For all of the plain square weave media, the values for the viscous drag flow constant, b, are quite small because of the short path and lack of tortuosity.

For the more complex weaves, such as Plain Dutch Single Weave and Twilled Dutch Double Weave, the viscous drag contribution to the total pressure drop becomes comparatively large, and the value of the constant, b, rises accordingly.

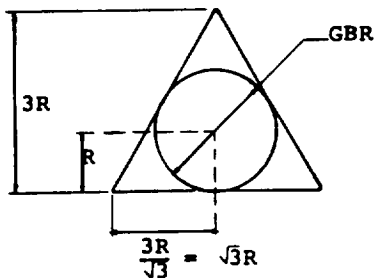
The flow paths for Plain Dutch Single Weave media consist of rectangular "collection" areas formed by adjacent shute wires and the longitudinal warp wires. The number of individual rectangular openings per square inch of medium is equal to the product of the number of warp and shute wires per linear inch. These rectangular openings rapidly narrow toward the center of the screen, and two triangular openings at right angles to the rectangular path is formed

by the crossing shute wires. This triangular opening is the "orifice" portion of the flow path. The fluid must turn 90°, pass through the triangular opening, where it enters another rectangularly shaped opening on the reverse side of the media. The fluid then turns 90° back to the original direction of flow and exits the screen.

For Twilled Dutch Double Weave media, the flow path is even more complex. Again, rectangular "collector" openings are formed at the inlet side of the screen. These openings are formed by the shute wires only. The path narrows rapidly toward the center of the medium, and divides into two triangular openings at 90° to the entrance path. The fluid passes through these "orifice" openings, turns 90° back to the original direction, and then 90° in a reverse direction through another triangular opening where it enters a rectangularly shaped area identical to that on the inlet side. Here, the fluid makes another 90° turn and exits the screen. There are, thus, two triangular orifices in series in the flow path. The number of main entrance and exit paths per square inch of medium is equal to one fourth the product of warp and shute wires, while the number of orifice pairs is equal to one half the product of warp and shute wires.

The calculated values for the constants "a" and "b" are determined for the Plain Dutch Single Weave and Twilled Dutch Double Weave media by using the formulae developed earlier. In both of these more complex media, the number of "orifice type" pores which affect the determination of the value for the dynamic flow constant "a" is expressed in terms of the actual mesh count of the media, while the area of the "orifices" is expressed in terms of the filtration rating of the screen.

For convenience, the area of an individual "orifice" can be approximated in terms of the "glass bead rating" of the media. In the case of the triangular shaped orifices of the TDDW and PDSW media, the relationship between orifice area and GBR can be simplified by assuming the pore shape to be that of an equilateral triangle. (In reality, the pore more closely resembles a skewed isocoles triangle which is most difficult to accurately describe).



$$\begin{aligned} \text{Area of Triangle} &= \frac{(2\sqrt{3}R)(3R)}{2} \\ &= 3\sqrt{3}R^2 \\ &= 3\sqrt{3} \left(\frac{\text{GBR}}{2}\right)^2 \\ &= 1.30(\text{GBR})^2 \end{aligned}$$

The total area of the orifices in a square inch of media can be found by multiplying the number of orifices per square inch by the individual orifice area. Thus, for the two Dutch Weave and the Square Weave media:

| Medium   | Orifices per in <sup>2</sup>                                  | Area of Orifice       |
|----------|---|-----------------------|
| TDDW     | $\frac{\text{Shute Wires/in} \times \text{Warp Wires/in}}{2}$ | 1.30 GBR <sup>2</sup> |
| PDSW     | (Shute Wires/in x Warp Wires/in) x 2                          | 1.30 GBR <sup>2</sup> |
| PSW, TSW | Shute Wires/in x Warp Wires/in                                | GBR <sup>2</sup>      |

As stated earlier, the value of the dynamic flow constant can be expressed as follows:

$$a = \frac{W}{(300.37C_s)^2}$$

Where:  $W$  = Fluid Density, lb/ft<sup>3</sup> (62.4 for "basic" value of "a")  
 $\eta$  = Total Orifice Area, decimal per cent  
 $C_g$  = Screen Coefficient

The total orifice area per square inch of media,  $\eta$ , is the orifice area fraction of the surface area of the media. The value of the screen constant,  $C_g$ , varies depending on the shape of the orifice. The following values for  $C_g$  provide excellent correlation between the empirical and calculated values for the dynamic flow constant, "a", for the various media.

| <u>Type of Medium</u>                                    | <u>Value of <math>C_g</math></u> |
|--|----------------------------------|
| Plain Square Weave                                       | 0.7                              |
| Plain Dutch Single Weave &<br>Twilled Dutch Double Weave | 0.86                             |

Values for  $\eta$ , the orifice fraction, for the three media are found as follows:

| <u>Type of Medium</u>      | <u>Orifice Fraction</u>                 |
|----------------------------|---|
| Plain Square Weave         | $(GBR)^2 (W_c \times S_c)$              |
| Plain Dutch Single Weave   | $1.3(GBR)^2 (W_c \times S_c) \times 2$  |
| Twilled Dutch Double Weave | $1.3(GBR)^2 \frac{(W_c \times S_c)}{2}$ |

Where: GBR = Glass Bead Rating, inches  
 $W_c$  = Warp Wires per Linear Inch  
 $S_c$  = Shute Wires per Linear Inch

Table 24 presents the physical characteristics of the Dutch Weave media necessary for calculation of the value of the flow constant "a" and a comparison between calculated and empirical values.

When calculating the value of the viscous drag coefficient "b" for the Dutch Weave media, the equation developed earlier may be used for good approximations. This equation is:

$$b = \frac{K_0 \tau^3 t \mu N_1}{\beta}$$

Where:  $K_0$  =  $1.403 \times 10^{-5}$   
 $\tau$  = Tortuosity Factor, dimensionless  
 $t$  = Thickness of Medium, inches  
 $\mu$  = Viscosity of Liquid, centipoises  
 $N_1$  = Number of Major Flow Passages per Square Inch of Medium  
 $\beta$  = Void Fraction, dimensionless

The simplicity of the flow path and the number and degree of directional changes has a marked effect on the viscous drag portion of the total pressure drop through the media. This effect is reflected in the value of the "b" flow constant. Variations in the type of the flow path are accounted for in the value of  $\tau$ , the tortuosity factor.

The number of major flow paths,  $N_1$ , per square inch of medium is not necessarily the same as the number of "orifices" used in calculating  $\eta$ , the total orifice area. Table 25 shows the value to be used for  $\tau$  and the number of major flow passages per square inch of medium for the three types of wire cloth.

TABLE 24

PHYSICAL PROPERTIES OF DUTCH WEAVE WIRE CLOTH  
 RELATIVE TO CALCULATION OF FLOW CONSTANT "a"  
 FOR LIQUIDS WITH DENSITY OF 62.4 #/ft<sup>3</sup> (SP. GR. = 1.0)

| GRADE OF WIRE CLOTH | ACTUAL MESH COUNT PER INCH<br>W <sub>c</sub> x S <sub>c</sub> | GLASS BEAD RATING (GBR) MICRONS | GLASS BEAD RATING INCHES | ORIFICE AREA η <sub>s</sub>                              | VALUES OF "a" FOR FLUID OF 1.0 SP. GR. CALCULATED | EMPIRICAL             |
|---------------------|---|---------------------------------|--------------------------|--|---|-----------------------|
|                     |   |                                 |                          | 1.3 (GBR) <sup>2</sup> W <sub>c</sub> S <sub>c</sub> / 2 | a = (300.37C <sub>s</sub> ) <sup>2</sup> / W      | C <sub>s</sub> = 0.86 |
| <b>TDDW</b>         |   |                                 |                          |  |   |                       |
| 30 x 250            | 30 x 250  | 100                             | 0.0039                   | 7.4  | 0.171   | 0.16                  |
| 30 x 370*           | 30 x 370*   | 95                              | 0.0037                   | 9.9  | 0.095   | 0.09                  |
| 40 x 550*           | 40 x 550*   | 70                              | 0.0028                   | 11.2   | 0.075   | 0.08                  |
| 80 x 745            | 80 x 745  | 35                              | 0.0014                   | 7.6  | 0.162   | 0.15                  |
| 165 x 1400          | 165 x 1350  | 20                              | 0.0008                   | 9.3  | 0.108   | 0.09                  |
| 325 x 2300          | 325 x 2100  | 10                              | 0.0004                   | 7.1  | 0.186   | 0.19                  |
| 450 x 2750*         | 450 x 2750*   | 7                               | 0.00028                  | 6.3  | 0.236   | 0.24                  |
| <b>PDSW</b>         |   |                                 |                          |  |   |                       |
| 30 x 150            | 30 x 150  | 105                             | 0.0041                   | 19.6   | 0.024   | 0.021                 |
| 30 x 160            | 30 x 162  | 100                             | 0.0039                   | 19.2   | 0.025   | 0.024                 |
| 80 x 400            | 76 x 397  | 39                              | 0.0015                   | 17.6   | 0.030   | 0.027                 |
| 165 x 800           | 165 x 790   | 18                              | 0.00071                  | 17.0   | 0.032   | 0.027                 |
| 180 x 900           | 180 x 930   | 17                              | 0.00067                  | 19.6   | 0.024   | 0.024                 |
| 2 x 120 x 650       | 2 x 120 x 680   | 19                              | 0.00075                  | 12.0   | 0.064   | 0.046                 |
| 2 x 150 x 800       | 2 x 150 x 810   | 16                              | 0.00063                  | 12.6   | 0.059   | 0.046                 |

Where:  
 W = 62.4 lb/ft<sup>3</sup>  
 GBR = Glass Bead Rating, inches  
 W<sub>c</sub> = Warp bount, wires per inch  
 S<sub>c</sub> = Shute count, wires per inch  
 C<sub>s</sub> = Screen Constant  
 η<sub>s</sub> = % Orifice Area (decimal)

TABLE 25

EMPIRICAL VALUES OF TORTUOSITY FACTOR AND NUMBER OF MAJOR FLOW PATHS FOR VARIOUS MEDIA

| <u>Type of Medium</u>      | <u><math>\tau</math></u> | <u><math>N_1</math></u>    |
|----------------------------|--------------------------|----------------------------|
| Plain Square Weave         | 1.0                      | $W_c \times S_c$           |
| Plain Dutch Single Weave   | 1.9                      | $W_c \times S_c$           |
| Twilled Dutch Double Weave | 2.7                      | $\frac{W_c \times S_c}{4}$ |

Where:  $W_c$  = Warp Wires per Linear Inch  
 $S_c$  = Shute Wires per Linear Inch

The void fraction,  $\beta$ , may be determined by weighing a screen sample of known volume and comparing this weight to the calculated weight of a solid sample of equal volume.

$$\beta = 1 - \frac{\text{Weight of Sample}}{\text{Weight Calculated if Solid}}$$

The value of  $\beta$  will vary for every screen type and grade as it is a function of the number and size of wires used to weave the material.

Table 26 presents the physical characteristics of the Dutch Weave media necessary for calculating values of the viscous drag constant "b" and a comparison between calculated and empirical values. The value of  $\mu$ , the viscosity of the fluid is taken as 1.0 centipoise in the calculation to provide "basic" values for the constant "b".

During this program, liquid flow resistance tests were conducted within the unit flow rate range of 0.1 to 6.5 GPM/in<sup>2</sup> on seven grades of Plain Dutch Single Weave, seven grades of Twilled Dutch Double Weave, one grade of Twilled Dutch Single Weave, four grades of Twilled Square Weave, and nine grades of Plain Square Weave wire mesh. In addition, flow resistance tests were conducted on four grades of Plain Square Weave synthetic (nylon or polyester) media, four Porous Membranes (Millipore proprietary material) and six grades of sintered metal fiber (Dynalloy - X) media.

From the flow resistance curves obtained for the above materials, the liquid flow resistance equations were developed. All follow the general form,  $\Delta P = aQ^2 + bQ$ , where "a" and "b" are constants dependent on media characteristics and are directly related to specific gravity and viscosity respectively of the test liquid.

Table 27 shows the "basic" flow equation for each of the materials tested. The values shown for the "a" and "b" constants are for a liquid of 1.0 specific gravity and 1.0 centipoise viscosity. The flow resistance equation for any liquid is developed by multiplying the "basic" value of "a" by the liquid specific gravity and multiplying the "basic" value of "b" by the liquid viscosity in centipoises.

In addition to the basic flow equations for each media shown in Table 27, the glass bead rating is shown for the Dutch Weave wire meshes, the Porous Membranes, and the Sintered Metal Fiber media. For the Plain Square Weave and Twilled Square Weave materials the nominal, or average, size of the square opening is shown. No maximum glass bead rating is assigned to these media, due to the fact that the strands comprising the weaves are not driven together, and strand shift can occur creating larger openings than the particular weave would supply if all strands were equally spaced. The figures shown for Glass Bead Rating in Table 27 for all the square weave media do not, therefore, represent the diameter of the largest hard spher-



TABLE 26

PHYSICAL PROPERTIES OF DUTCH WEAVE WIRE CLOTH  
RELATIVE TO CALCULATION OF FLOW CONSTANT "b"  
FOR LIQUIDS OF VISCOSITY OF 1.0 CENTIPOISE

| GRADE OF WIRE CLOTH | ACTUAL MESH COUNT PER INCH | THICKNESS OF WIRE CLOTH INCHES t | VOID FRACTION $\beta$ | VALUE OF "b" FOR LIQUID OF VISCOSITY 1.0 CENTIPOISE CALCULATED | EMPIRICAL                    |
|---------------------|----------------------------|----------------------------------|-----------------------|--|------------------------------|
|                     |                            |                                  |                       | $b = \frac{K_0 r^3 \mu t N_1}{\beta^2}$                        | $K_0 = 1.403 \times 10^{-5}$ |
|                     |                            |                                  |                       |  | $r = 2.7$                    |
|                     |                            |                                  |                       |  | $N_1 = \frac{W S c}{4}$      |
|                     |                            |                                  |                       |  | $\mu = 1.0 \text{ CP}$       |

TDDW

|            |            |        |       |       |      |
|------------|------------|--------|-------|-------|------|
| 30 x 250   | 30 x 250   | 0.028  | 0.424 | 0.080 | 0.08 |
| 30 x 370   | 30 x 370   | 0.0225 | 0.476 | 0.076 | 0.06 |
| 40 x 550   | 40 x 550   | 0.0157 | 0.502 | 0.09  | 0.07 |
| 80 x 700   | 80 x 745   | 0.0098 | 0.449 | 0.20  | 0.20 |
| 165 x 1400 | 165 x 1350 | 0.0058 | 0.388 | 0.59  | 0.49 |
| 325 x 2300 | 325 x 2100 | 0.0035 | 0.362 | 1.26  | 1.45 |
| 450 x 2750 | 450 x 2750 | 0.0025 | 0.371 | 1.55  | 1.66 |

$K_0 = 1.403 \times 10^{-5}$

$r = 1.9$

$N_1 = W_c \times S_c$

$\mu = 1.0 \text{ CP}$

$$b = \frac{K_0 r^3 \mu t N_1}{\beta^2}$$

PDSW

|               |               |        |      |       |       |
|---------------|---------------|--------|------|-------|-------|
| 30 x 150      | 30 x 150      | 0.023  | 0.59 | 0.029 | 0.029 |
| 30 x 160      | 30 x 162      | 0.020  | 0.62 | 0.024 | 0.030 |
| 80 x 400      | 76 x 397      | 0.009  | 0.58 | 0.078 | 0.070 |
| 165 x 800     | 165 x 790     | 0.004  | 0.60 | 0.140 | 0.119 |
| 180 x 900     | 180 x 930     | 0.0036 | 0.61 | 0.157 | 0.132 |
| 2 x 120 x 650 | 2 x 120 x 680 | 0.005  | 0.62 | 0.103 | 0.125 |
| 2 x 150 x 800 | 2 x 150 x 810 | 0.004  | 0.59 | 0.135 | 0.153 |

TABLE 27  
BASIC FLOW RESISTANCE EQUATIONS FOR VARIOUS MEDIA

| Media Type                            | Media Grade                   | Glass Bead Rating* |                               | Basic Flow Resistance Equation (Liquids)<br>(Q = gpm/in <sup>2</sup> of Medium) ( $\Delta P$ = psi)<br>$\Delta P = aQ^2 + bQ$ |
|---------------------------------------|-------------------------------|--------------------|-------------------------------|---|
|                                       |                               | Microns            | Inches                        |   |
| Plain Square Weave Wire Mesh          | 18x18x.017                    | 980                | 0.0386                        | $\Delta P = 0.0063Q^2$  |
|                                       | 24x24x.010                    | 805                | 0.0317                        | $\Delta P = 0.0048Q^2$  |
|                                       | 50x50x.008                    | 305                | 0.0120                        | $\Delta P = 0.0096Q^2$  |
|                                       | 60x60x.007                    | 246                | 0.0097                        | $\Delta P = 0.011Q^2$   |
|                                       | 80x80x.0055                   | 178                | 0.0070                        | $\Delta P = 0.011Q^2$   |
|                                       | 100x100x.0045                 | 140                | 0.0055                        | $\Delta P = 0.011Q^2 + .011Q$   |
|                                       | 150x150x.0026                 | 101                | 0.0041                        | $\Delta P = 0.013Q^2 + .011Q$   |
|                                       | 200x200x.0021                 | 74                 | 0.0029                        | $\Delta P = 0.015Q^2 + .011Q$   |
|                                       | 250x250x.0016                 | 61                 | 0.0024                        | $\Delta P = 0.016Q^2 + .017Q$   |
|                                       | Twilld Square Weave Wire Mesh | 400x400x.0010      | 38                            | 0.0015  |
| 508x508x.00098                        |                               | 25                 | 0.00098                       | $\Delta P = 0.015Q^2 + 0.050Q$  |
| 635x635x.00079                        |                               | 20                 | 0.00079                       | $\Delta P = 0.016Q^2 + 0.055Q$  |
| 850x850x.00055                        |                               | 16                 | 0.00063                       | $\Delta P = 0.013Q^2 + 0.072Q$  |
| Plain Square Weave Synthetic Material | ASTM-100-149                  | 149                | 0.0059                        | $\Delta P = 0.03Q^2$  |
|                                       | 102x102x.0039                 |                    |                               |   |
|                                       | PE-7-140-105                  | 132                | 0.0041                        | $\Delta P = 0.017Q^2 + .006Q$   |
|                                       | 143x143x.0029                 |                    |                               |   |
|                                       | ASTM-200-74                   | 102                | 0.0029                        | $\Delta P = 0.019Q^2 + .014Q$   |
|                                       | 210x210x.0020                 |                    |                               |   |
|                                       | PE-7-200-74                   | 74                 | 0.0029                        | $\Delta P = 0.06Q^2 + .034Q$  |
|                                       | 223x223x.0016                 |                    |                               |   |
|                                       | ASTM-230-62                   | 62                 | 0.0024                        | $\Delta P = 0.047Q^2 + .019Q$   |
| 242x242x.0017                         |                               |                    |                               |   |
| PE-7-230-62                           | 62                            | 0.0024             | $\Delta P = 0.019Q^2 + .009Q$ |   |
| 249x249x.0016                         |                               |                    |                               |   |
| NITEX44                               | 44                            | 0.0017             | $\Delta P = 0.054Q^2 + .009Q$ |   |
| 300x300x.0055                         |                               |                    |                               |   |
| Plain Dutch Single Weave              | 30x150                        | 105                | 0.0041                        | $\Delta P = 0.021Q^2 + .029Q$   |
|                                       | 30x160                        | 100                | 0.0039                        | $\Delta P = 0.024Q^2 + 0.030Q$  |
|                                       | 80x400                        | 39                 | 0.0015                        | $\Delta P = 0.027Q^2 + 0.070Q$  |
|                                       | 165x800                       | 18                 | 0.00071                       | $\Delta P = 0.027Q^2 + 0.119Q$  |
|                                       | 180x900                       | 17                 | 0.00067                       | $\Delta P = 0.024Q^2 + 0.132Q$  |
|                                       | 2x120x650                     | 19                 | 0.00075                       | $\Delta P = 0.046Q^2 + 0.125Q$  |
|                                       | 2x150x800                     | 16                 | 0.00063                       | $\Delta P = 0.046Q^2 + 0.153Q$  |
| Twilld Dutch Double Weave             | 30x250                        | 100                | 0.0039                        | $\Delta P = 0.16Q^2 + 0.08Q$  |
|                                       | 30x370                        | 95                 | 0.0037                        | $\Delta P = 0.09Q^2 + 0.06Q$  |
|                                       | 40x550                        | 70                 | 0.0028                        | $\Delta P = 0.08Q^2 + 0.07Q$  |
|                                       | 80x700                        | 35                 | 0.0014                        | $\Delta P = 0.15Q^2 + 0.20Q$  |
|                                       | 165x1400                      | 20                 | 0.0008                        | $\Delta P = 0.09Q^2 + 0.49Q$  |
|                                       | 200x1400                      | 15                 | 0.0006                        | $\Delta P = 0.13Q^2 + 0.58Q$  |
|                                       | 325x2300                      | 10                 | 0.0004                        | $\Delta P = 0.19Q^2 + 1.45Q$  |
|                                       | 450x2750                      | 7                  | 0.00028                       | $\Delta P = 0.24Q^2 + 1.66Q$  |
| Twilld Dutch Single Weave             | 120x600                       | 33                 | 0.0013                        | $\Delta P = 0.02Q^2 + 0.11Q$  |
| Dynalloy Sintered Metal Fiber Felt    | X-3                           | 3                  | 0.000012                      | $\Delta P = 0.35Q^2 + 9.65Q$  |
|                                       | X-4                           | 5                  | 0.00020                       | $\Delta P = 0.40Q^2 + 3.6Q$   |
|                                       | X-5                           | 10                 | 0.0004                        | $\Delta P = 0.80Q^2 + 1.2Q$   |
|                                       | X-7                           | 20                 | 0.0008                        | $\Delta P = 0.05Q^2 + 0.35Q$  |
|                                       | X-11                          | 40                 | 0.0016                        | $\Delta P = 0.05Q^2 + 0.20Q$  |
|                                       | X-13                          | 80                 | 0.0032                        | $\Delta P = 0.06Q^2 + 0.06Q$  |
| Porous Membranes                      | SC8                           | 8                  | 0.00031                       | $\Delta P = 0.04Q^2 + 7.95Q$  |
|                                       | SM5                           | 5                  | 0.00020                       | $\Delta P = 0.50Q^2 + 12.0Q$  |
|                                       | AA0.8                         | 0.8                | 0.000031                      | $\Delta P = 2.76Q^2 + 40.2Q$  |
|                                       | AA0.45                        | 0.45               | 0.000017                      | $\Delta P = 41.9Q^2 + 167.0Q$   |

NOTE 1: For Square Weave media, possible wire shift will increase glass bead rating above values shown. Ratings shown for these media are the sizes of the square openings with all strands equally spaced.

ical particle (glass bead) which can pass through the medium, as is the case with all the other media shown, but does indicate the dimension of the sides of the square pore if all strands are equally spaced and at right angles to each other.

In addition, it will be noted that for the coarse grades of Plain Square Weave media, the  $bQ$  term is missing from the equation. This apparent omission is caused by the fact that the flow resistance curves with water form a straight line with a slope of 2 on log - log paper. The equation of such a curve is  $\Delta P = aQ^2$ . In actuality, the  $bQ$  term undoubtedly exists, but the value of "b" is so small that the flow tests conducted with water did not disclose its value. The equations shown are, therefore, only approximate.

The sintered metal fiber media is sold under the trade name, Dynalloy X, and is an improved version of the same type of material originally called Brunspore, and reported on during the test program. The Dynalloy X provides a very homogeneous matrix of various size stainless steel fibers felted in random lay, compressed to a pre-determined density and sintered together. The choice of fiber mix and sheet density controls the micron rating of the material.

Figures 88, 89 and 90 show the calculated flow resistance curves for 325 X 2300 TDDW, 165 X 1400 TDDW and 80 X 400 PDSW, respectively, with Mil-H-5606, JP-4, ethylene glycol - water (35%/65% by weight) and deionized water. Superimposed on the calculated curves are the data points obtained during actual test. Figure 91 shows the same data as obtained at WSTF using liquid nitrogen as the test fluid. Test data tables are contained in the Appendix.

The "basic" flow equation is shown at the top of each figure, and the values of the "a" and "b" flow constants have been modified by multiplying their basic values by the specific gravity and viscosity (centipoises) of the individual test fluids. The equation applicable to each calculated curve is shown. The specific gravity and viscosity for the glycol - water mixture was measured at a single temperature, 75° F, and were 1.044 and 2.32, respectively. Figures 78 and 79 showed the specific gravity and viscosity of water, JP-4 and Mil-H-5606 hydraulic oil as a function of temperature.

FIGURE 88  
TEST DATA COMPARISON  
TO

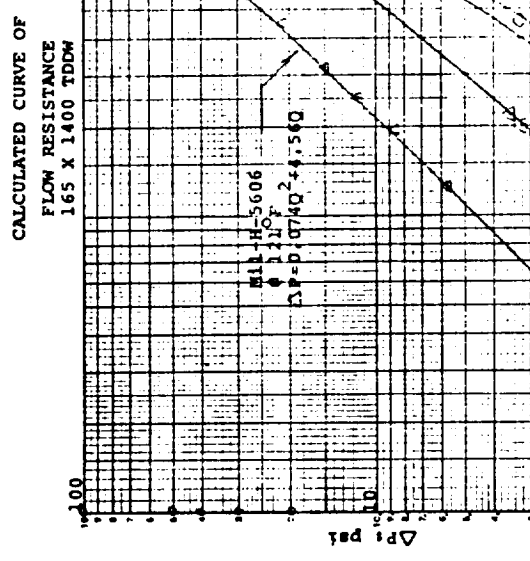


FIGURE 89  
TEST DATA COMPARISON  
TO

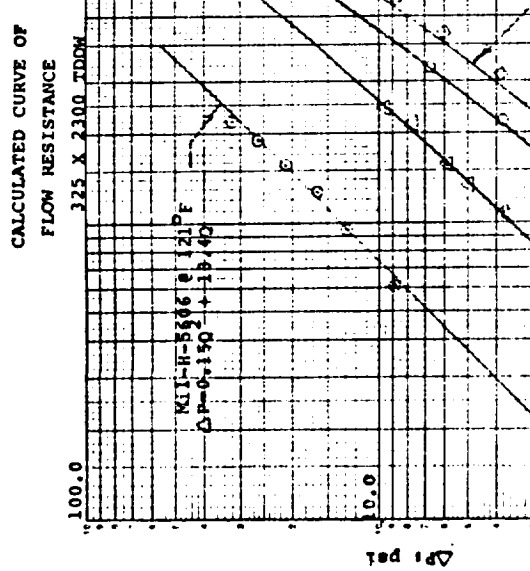


FIGURE 90

TEST DATA COMPARISON

TO

CALCULATED CURVE OF  
FLOW RESISTANCE  
80 X 400 PDSW

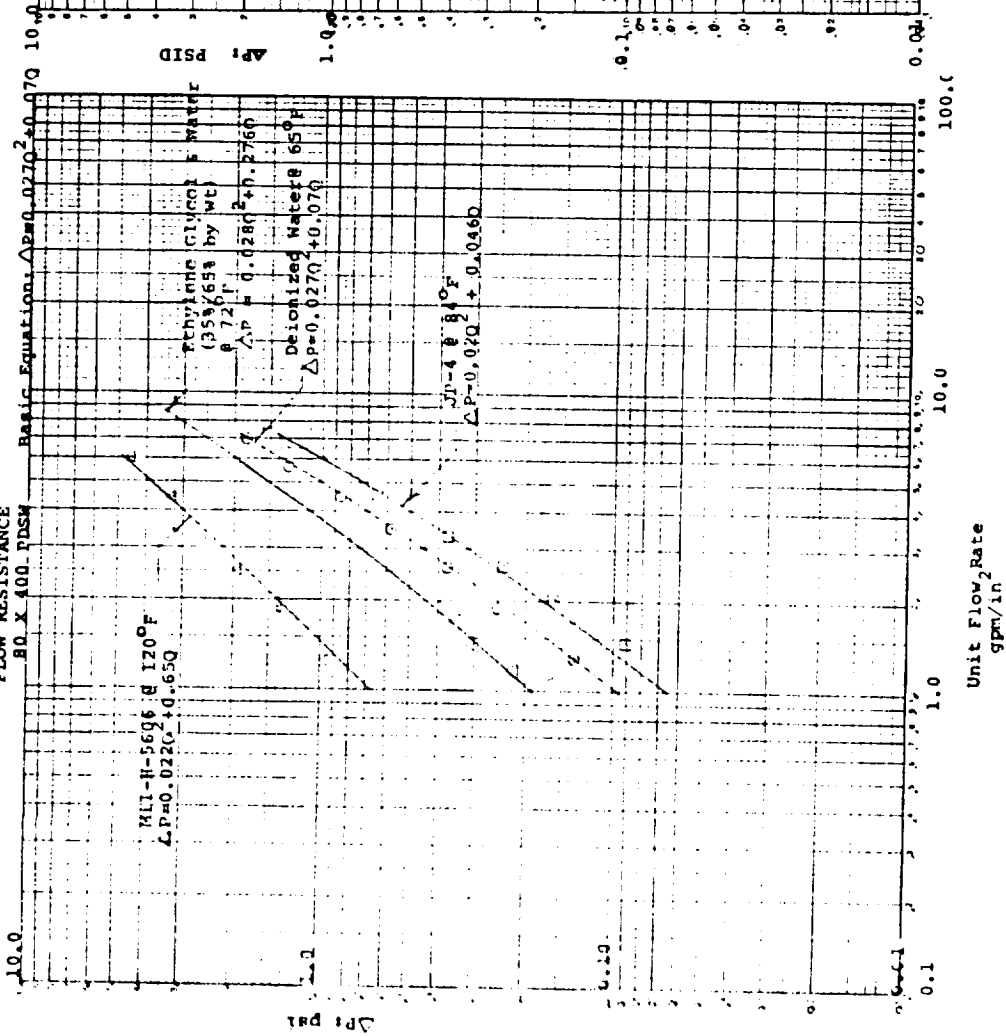
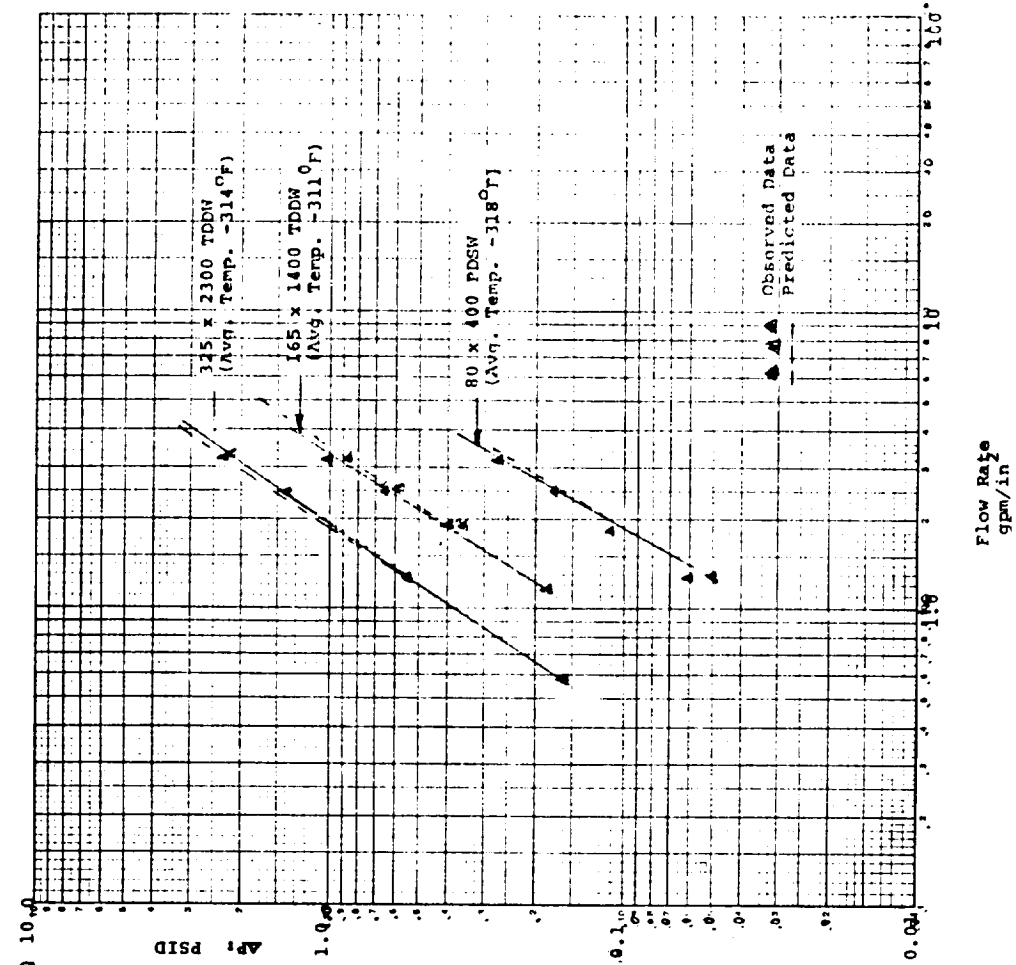


FIGURE 91

TEST DATA COMPARISON TO CALCULATED CURVES

FLOW RESISTANCE LIQUID NITROGEN



### 3.8.2 Flow Resistance Tests - Gas

Tests were conducted with various grades of Twilled Dutch Double Weave wire cloth using nitrogen, oxygen, helium and hydrogen gases. When the flow rate, in terms of actual cubic feet per minute at flow conditions per square inch of screen (ACFM/in<sup>2</sup>) was plotted against pressure drop through the screen, a relatively straight line was obtained on log - log paper. The curve obtained for gas at low density showed, not only lower values, but also a lesser slope than that obtained with gas at higher density. Thus, the equation for flow resistance appeared to be in the form  $\Delta P = aQ^n$ , where "a" is a flow constant dependent on screen geometry, Q is expressed as ACFM/in<sup>2</sup> (with units of velocity) and n is dependent on density.

A similar resultant change in slope with increasing densities can be achieved, however, when the flow resistance equation is expressed in terms equivalent to those used for liquid flow,  $\Delta P = aQ^2 + bQ$ . Here, "a" is a constant dependent on screen geometry and gas density, "b" is dependent on screen geometry and gas viscosity and Q represents the actual flow velocity ACFM/in<sup>2</sup>. This equation will produce a slight curve when plotted on log - log paper with the curve slope approaching 45° at low unit flow rates and increasing to approximately 63° at the higher flow rates.

Although the curves for flow resistance were plotted as straight lines, the equation  $\Delta P = aQ^2 + bQ$  plot falls quite well within the data point scatter. Further justification for the use of the second order equation for flow resistance of gas is apparent when the curves for the fine weave, 325 X 2300 TDDW is compared to the coarser weave material, 30 X 250 TDDW. At the same gas densities, the slope of the curves for the coarser weave material is higher than for the fine material. This parallels the data obtained using liquids where the viscosity effect on pressure drop is greater on the fine weaves than on the coarse weaves.

Assuming the general form of the flow resistance equation for gases is  $\Delta P = aQ^2 + bQ$ , the relationship may be determined empirically by conducting a flow resistance test with the medium and gas of interest, and plotting pressure drop vs. ACFM/in<sup>2</sup> on log - log paper. As in the case of liquid flow, two points may be selected on the curve and two mathematical relationships in the form  $\Delta P = aQ^2 + bQ$  may be written. These relationships may then be solved simultaneously for the two unknown constants "a" and "b". In order for both "a" and "b" to have real values, it is, of course, necessary that the slope of the curve be more than 1.0 and less than 2.0. As the slope of the plotted data increases markedly with increasing gas density, the test pressure may be chosen to provide a curve of intermediate slope.

Using the data shown in Figures 92 through 95 for flow resistance of nitrogen through four grades of TDDW media, the flow equations representing the plotted data were determined. In all cases, the 50 psia curves were used as they fell well within the 45° to 63-1/2° range, providing slopes greater than 1.0 and less than 2.0.

Following are the empirically derived flow resistance equations representing the 50 psia curves for the four media.

TABLE 28  
FLOW RESISTANCE EQUATIONS FOR NITROGEN GAS @ 50 PSIA & 78° F

| <u>Media</u> | <u>Flow Resistance Equation for Nitrogen @ 50 psia Inlet and 78° F</u> |
|--------------|--|
| 325 X 2300   | $\Delta P = .021Q^2 + .117Q$   |
| 165 X 1400   | $\Delta P = .013Q^2 + .047Q$   |
| 80 X 700     | $\Delta P = .0155Q^2 + .022Q$  |
| 30 X 250     | $\Delta P = .0247Q^2 + .007Q$  |

**FIGURE 92**  
**FLOW RESISTANCE OF 325 x 2300 TWILLED DUTCH DOUBLE WEAVE WIRE CLOTH**  
 Fluid: Gaseous Nitrogen

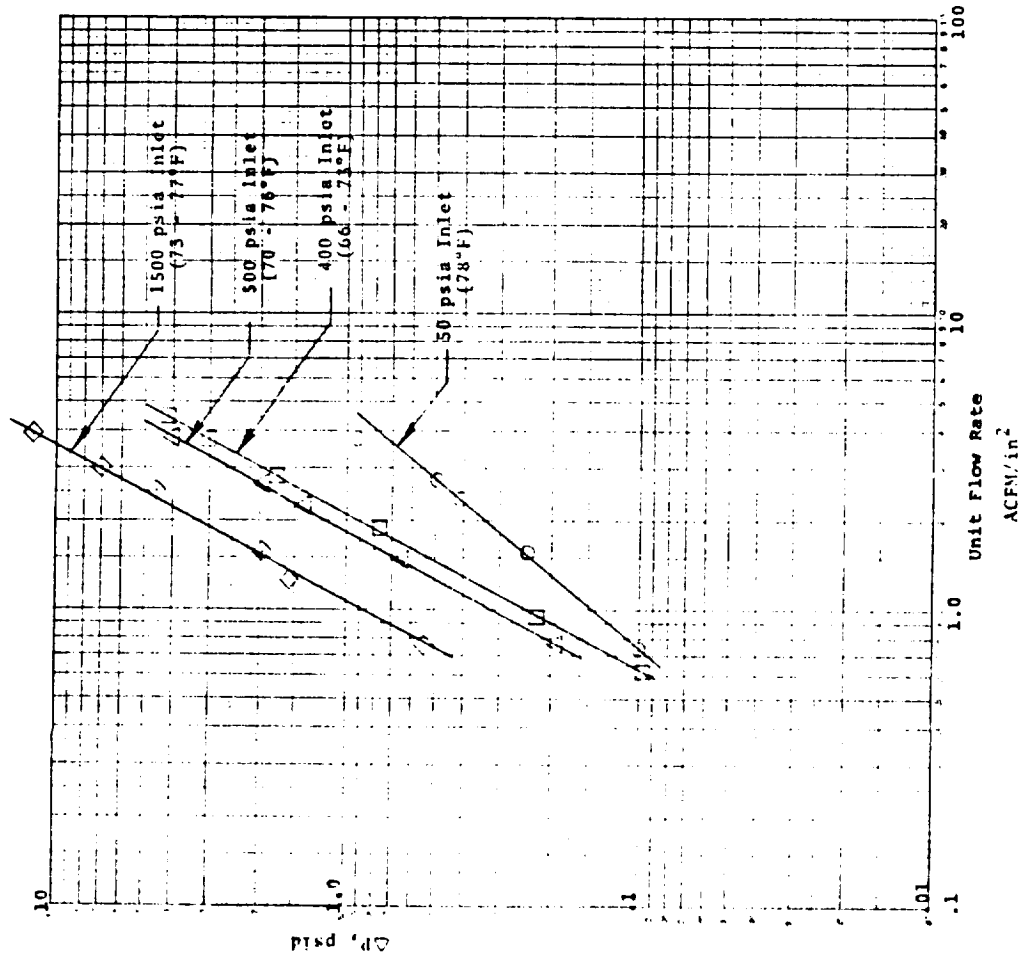


**FIGURE 93**  
**FLOW RESISTANCE OF 165 x 1400 TWILLED DUTCH DOUBLE WEAVE WIRE CLOTH**  
 Fluid: Gaseous Nitrogen

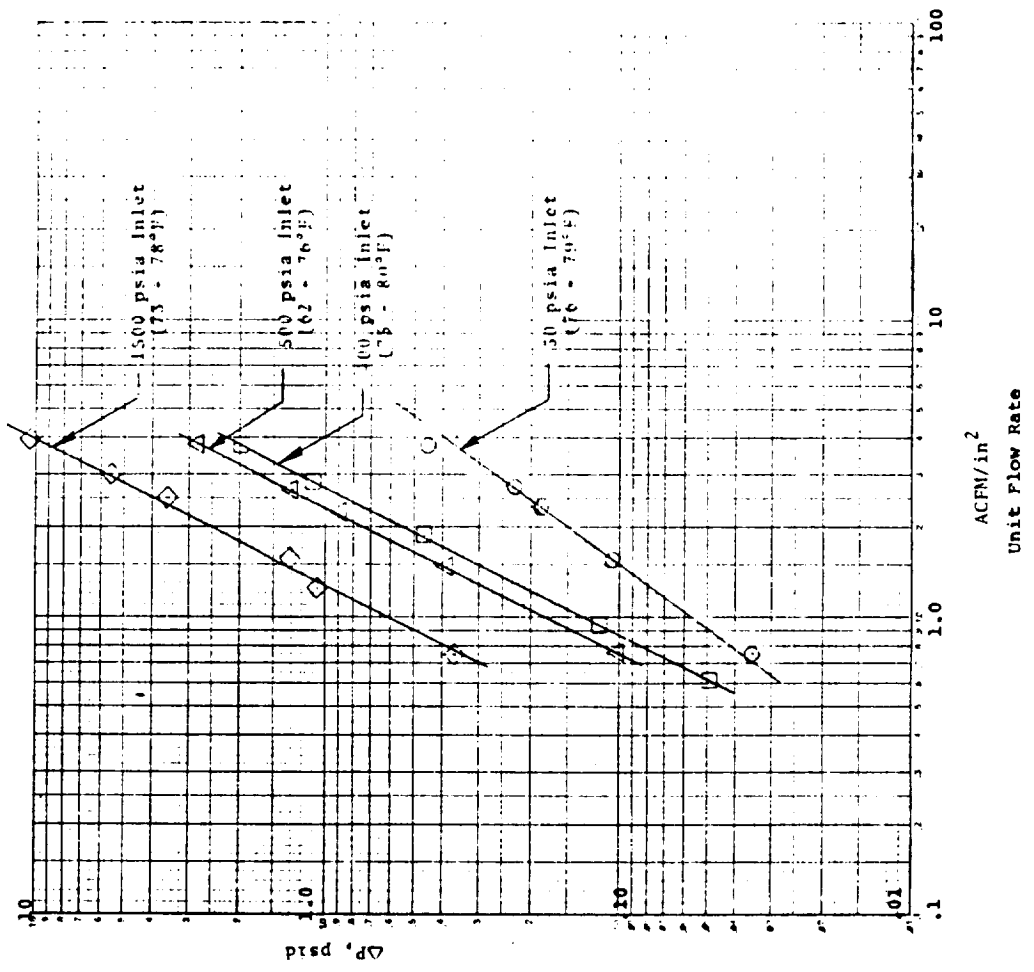


FIGURE 94  
 FLOW RESISTANCE OF 80 x 700 TWILLED DITCH DOUBLE WEAVE WIRE CLOTH

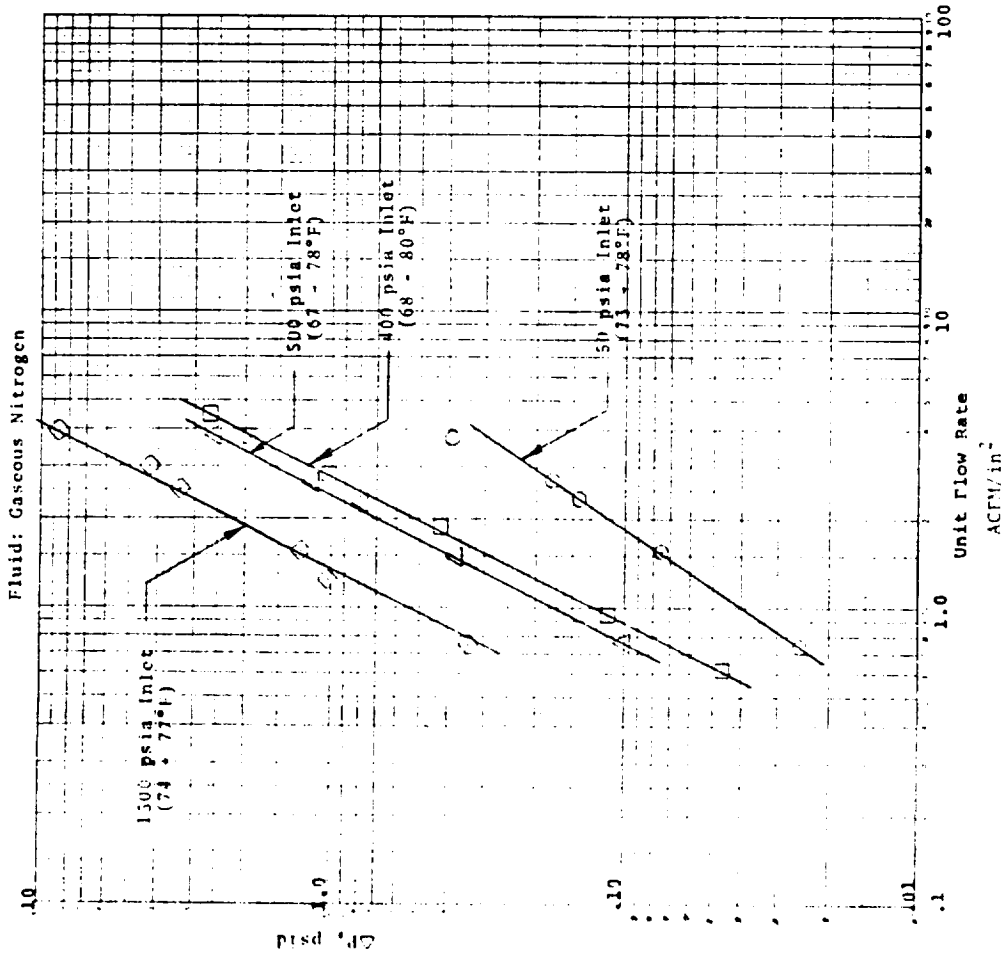
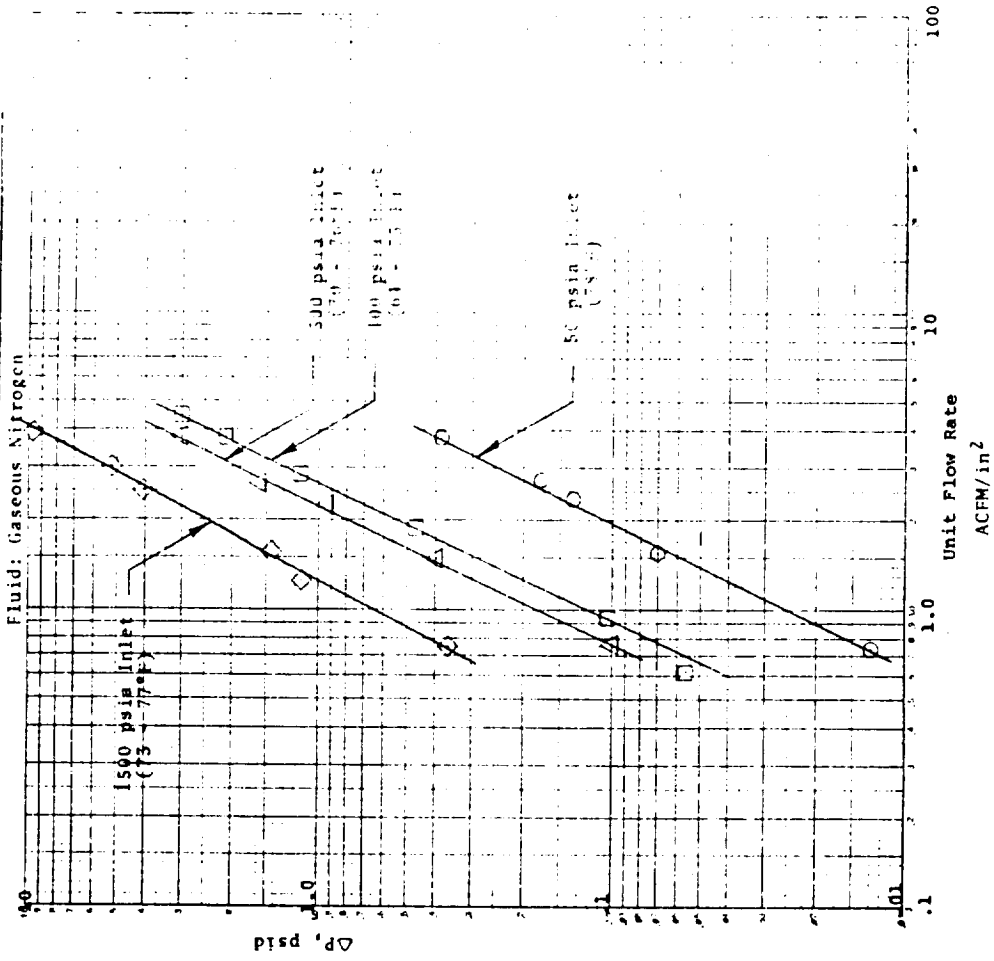


FIGURE 95  
 FLOW RESISTANCE OF 30 x 250 TWILLED DITCH DOUBLE WEAVE WIRE CLOTH





As these equations describe only the actual test conditions of 50 psia inlet pressure, 78° F and nitrogen gas, it is necessary to convert the values of "a" and "b" to some basic reference so that they may be easily modified to represent a different gas or different test conditions. By dividing the value for "a" determined earlier by the density of the nitrogen at 50 psia and 78° F, a "basic" value for this flow constant can be obtained. It is only necessary to multiply this "basic" value by the density of the gas at the new test conditions to develop the value for "a" at those conditions.

Similarly, the values for "b" determined earlier may be divided by the viscosity (in centipoises) of the nitrogen at 50 psia and 78° F to provide a "basic" value for "b". For a new gas, at any temperature, the viscosity of the gas at the new conditions may be multiplied by the "basic" value of "b" to determine the "b" value at the new conditions. This may be illustrated using the flow formulae determined earlier for the four TDDW media using nitrogen gas at 50 psia and 78° F.

At these conditions, the density of the nitrogen is 0.242 lb/ft<sup>3</sup> and the value for the viscosity of nitrogen at 78° F is 0.0175 centipoises.

Dividing each of the values for "a" by 0.242, and each of the values for "b" by 0.0175, the following "basic" equations result.

TABLE 29  
BASIC FLOW RESISTANCE EQUATIONS FOR GAS

| Medium<br>(TDDW) | Basic Flow Resistance Equation (for gas of<br>density 1 lb/ft <sup>3</sup> and viscosity of 1.0 centipoise) |
|------------------|---|
| 325 X 2300       | $\Delta P = 0.087Q^2 + 6.7Q$  |
| 165 X 1400       | $\Delta P = 0.055Q^2 + 2.67Q$   |
| 80 X 700         | $\Delta P = 0.062Q^2 + 1.26Q$   |
| 30 X 250         | $\Delta P = 0.010Q^2 + 0.40Q$   |

To illustrate the method of converting the "basic" equation to predict the pressure drop through one of the media using a different gas, the following example develops the flow resistance equation for 165 X 1400 TDDW using hydrogen gas at 400 psia inlet pressure and 75° F. Figure 96 shows the viscosity of various gases as a function of temperature for use in converting the "basic" equations to specific gas use.

$$\text{Density of hydrogen at 14.7 psia and } 60^\circ\text{F} = .0052 \text{ lb/ft}^3$$

$$\text{Density at 400 psia and } 75^\circ\text{ F} = (0.0052) \left[ \frac{400}{14.7} \right] \left[ \frac{520}{535} \right] = 0.1375 \text{ lb/ft}^3$$

$$\text{Value for "a" at test conditions} = (0.055)(0.1375) = 0.0075$$

$$\text{Viscosity of hydrogen at } 75^\circ\text{ F} = 0.0087 \text{ centipoises}$$

$$\text{Value for "b" at test conditions} = (2.67)(.0087) = 0.023$$

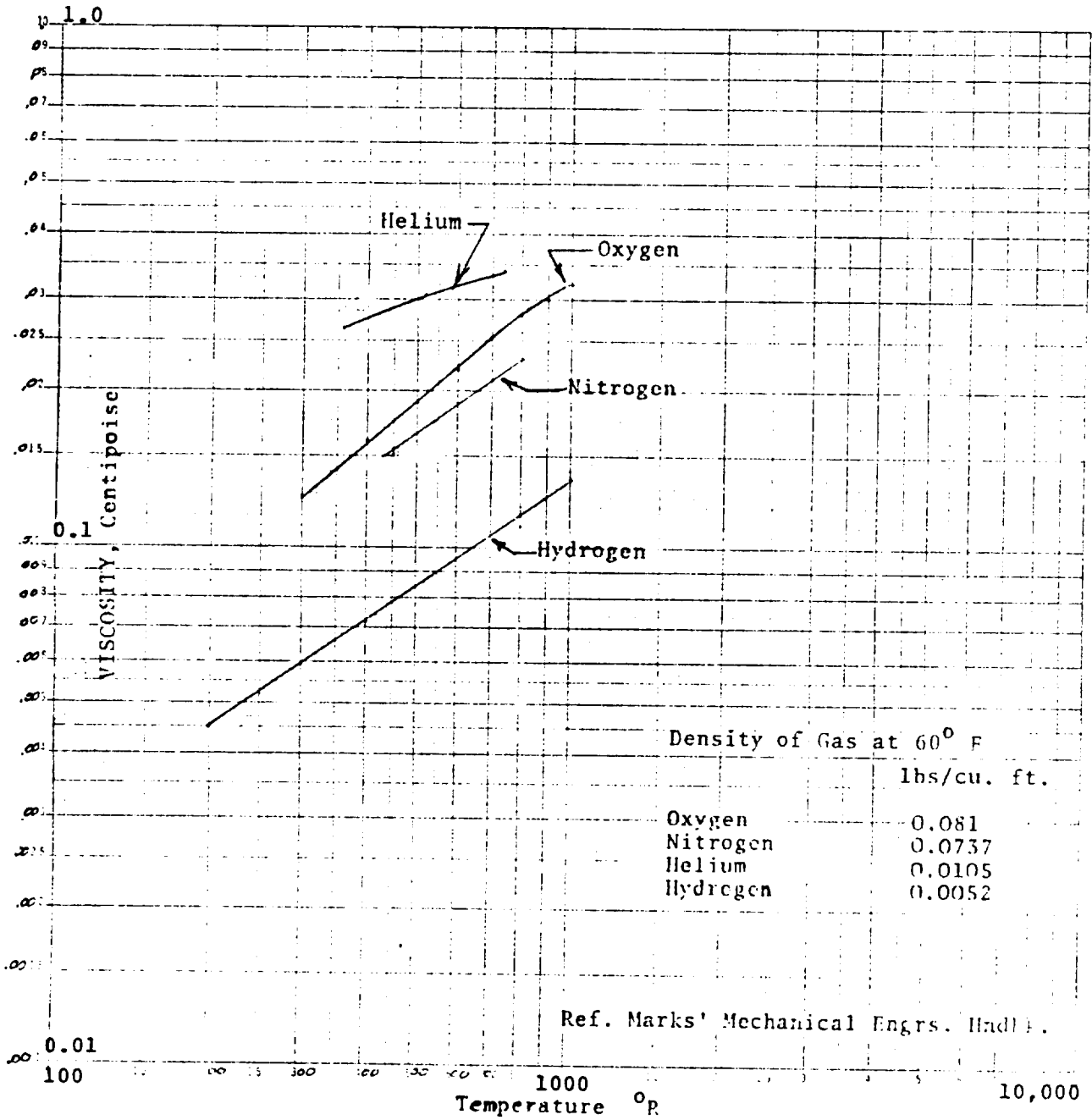
The flow resistance equation for 165 X 1400 TDDW wire cloth flowing hydrogen gas at 400 psia inlet pressure and 75° F. may now be written:

$$\Delta P = 0.0075Q^2 + .023Q$$

Where:  $\Delta P$  = Pressure drop, psid  
 $Q$  = Unit Flow Rate, ACFM/in<sup>2</sup>

This equation agrees with observed test data on hydrogen within 10% throughout the entire flow curve. A similar calculation for the flow equation for hydrogen at 50 psia and 62° F agrees

FIGURE 96  
 VISCOSITY OF GASES



with the test data even more closely.

The validity of the assumption that the flow resistance equation follows the form,  $\Delta P = aQ^2 + bQ$ , appears to be confirmed in that the flow equation was developed from oxygen tests and modified to suit a gas with entirely different characteristics. The use of empirical solutions to determine the flow resistance equation requires rather accurate determination of the original data, and gas flow testing presents several difficulties, all of which can have a serious effect on the data and the resultant values for the flow constants in the formulae.

The greatest problem lies in the ability to accurately measure the very low pressure drops experienced at the flow rates used for the tests. An error of only 0.1 psi in measurement can lead to serious percentage errors when the pressure drop is on the order of 0.5 psid. Also, the temperature during test must be held constant and the inlet pressure to the screen sample must not vary. Variations in flow rate during the test can also lead to large errors.

Most importantly, however, is the fact that a "tare" value on the system is run prior to inserting the test screen in the test fixture. This tare value is subtracted from the "gross" value of pressure drop with the test screen in place to determine the "net" pressure drop across the screen. As the net pressure drop values are small, the tare and gross are of the same magnitude, and subtracting one from the other can provide great errors in the "net" value.

For these reasons, the flow formulae developed for the four filter media should not be treated as absolute or exact equations. They do, however, provide very good correlations to the observed test data within the range of pressures and flow rates employed in this program.

Figures 97, 98, 99 and 100 show the calculated flow resistance curves and appropriate curve equations for four Twilled Dutch Double Weave media, 325 X 2300, 165 X 1400, 80 X 700 and 30 X 250, each with four gases, oxygen, nitrogen, helium and hydrogen, all at approximately 400 psia. The "basic" flow resistance equation, developed from the 50 psia nitrogen flow resistance curves and converted to unit density ( $\text{lb}/\text{ft}^3$ ) and unit viscosity (CP) is shown for each medium. The equations shown for each gas have been converted from the basic equation by multiplying the "a" and "b" basic constants by the density in pounds per cubic foot and viscosity in centipoises for each gas at the stated conditions of pressure and temperature. The curves for viscosity and the standard densities for the various gases were shown in Figure 96. Superimposed on the graphs for each gas are actual test data points obtained during flow resistance tests. Tables of test data are contained in the Appendix.

A reasonable correlation between test data and calculated values is obtained for the high pressure nitrogen and oxygen gases with all screens. The hydrogen data points agree very well for the 325 X 2300 TDDW medium, and within approximately 0.1 psi for the other screens. The helium data points appear to be consistently low for all screens. It is possible that the characteristics of helium are such that it does not behave as a perfect gas, thus, accounting for the imperfect data point correlation.

As neither the 50 psia curves from which the basic equation was derived, nor the data points themselves, were obtained at a constant pressure or temperature, the accuracy of the derived basic equation and the superimposed data points are subject to error. In addition, the relatively low pressures associated with gas testing are difficult to measure accurately. As noted earlier, the relatively large "tare" pressure value also contributes to possible errors in "net" pressure drop determination.

FIGURE 97

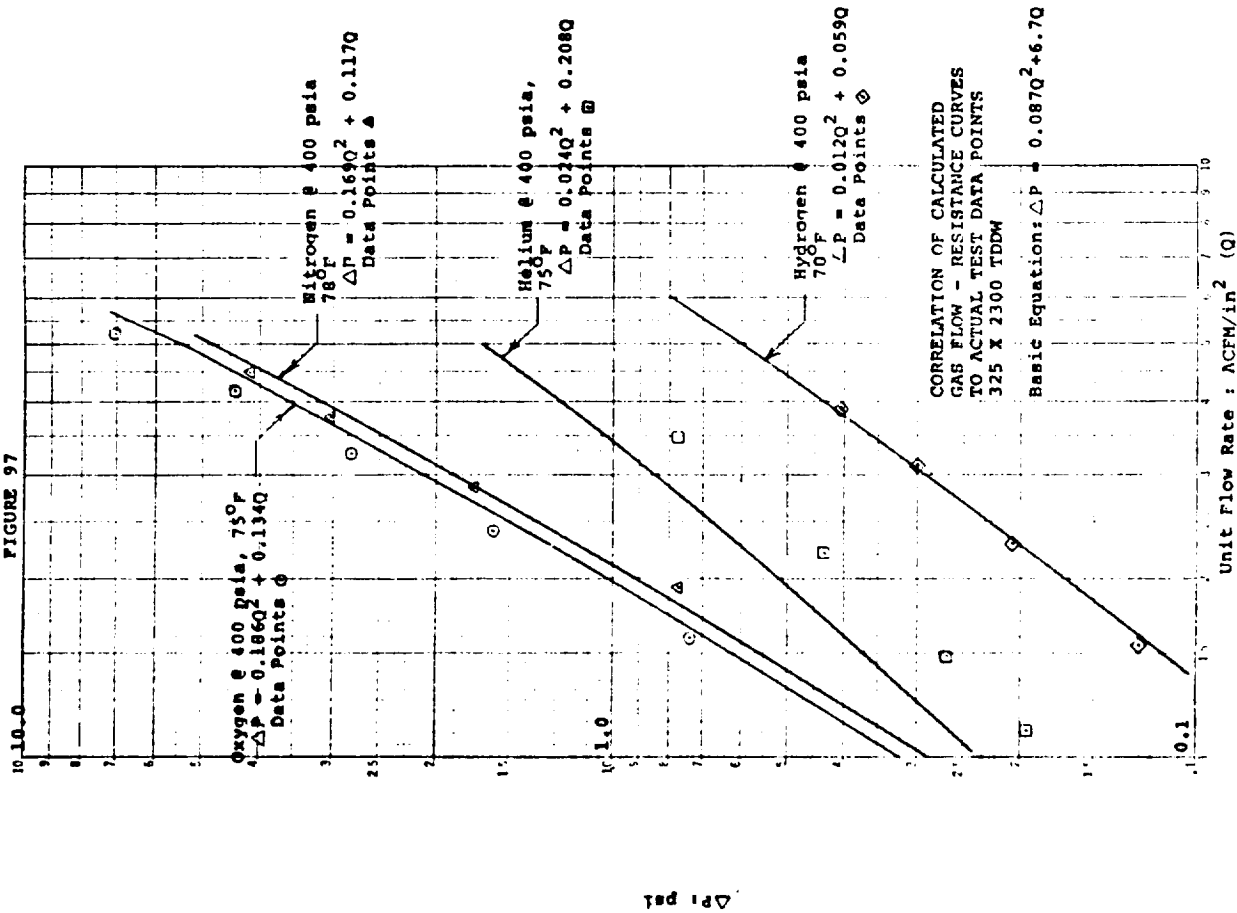


FIGURE 98

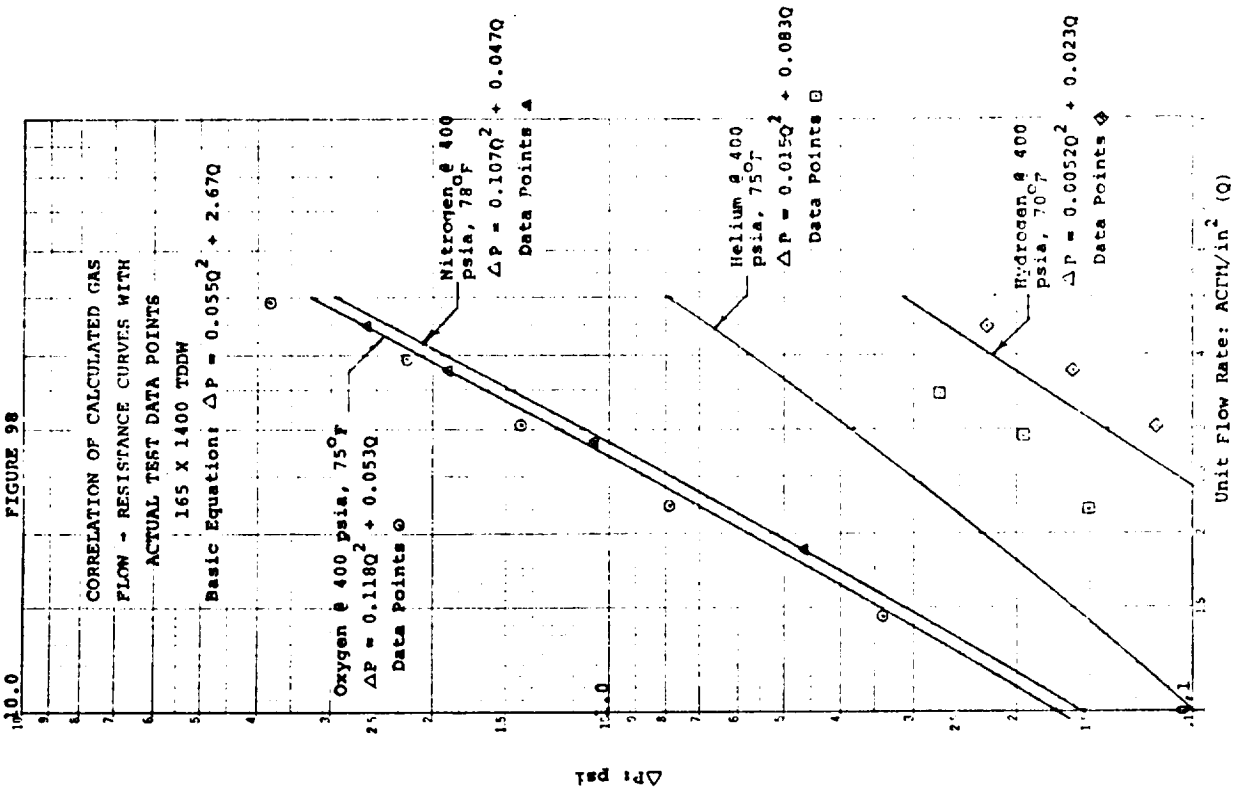


FIGURE 99

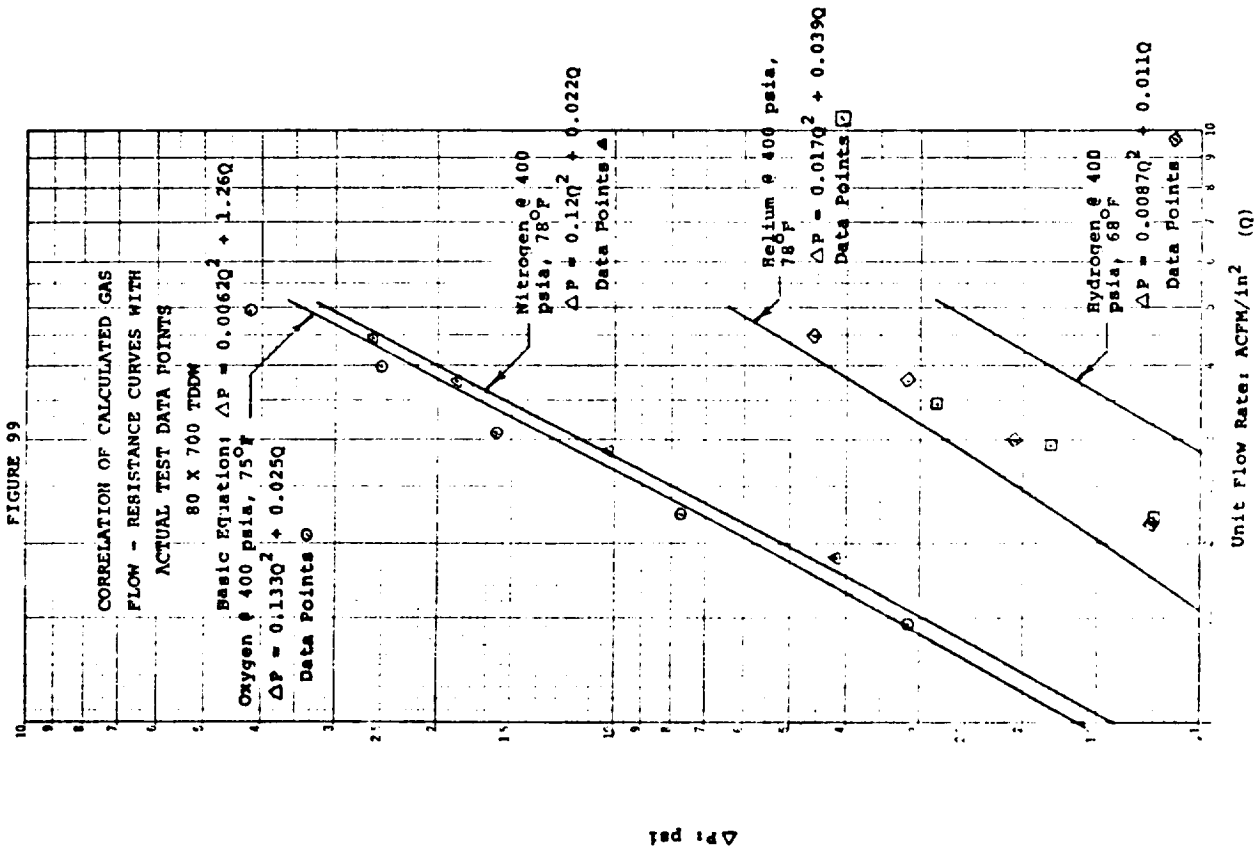
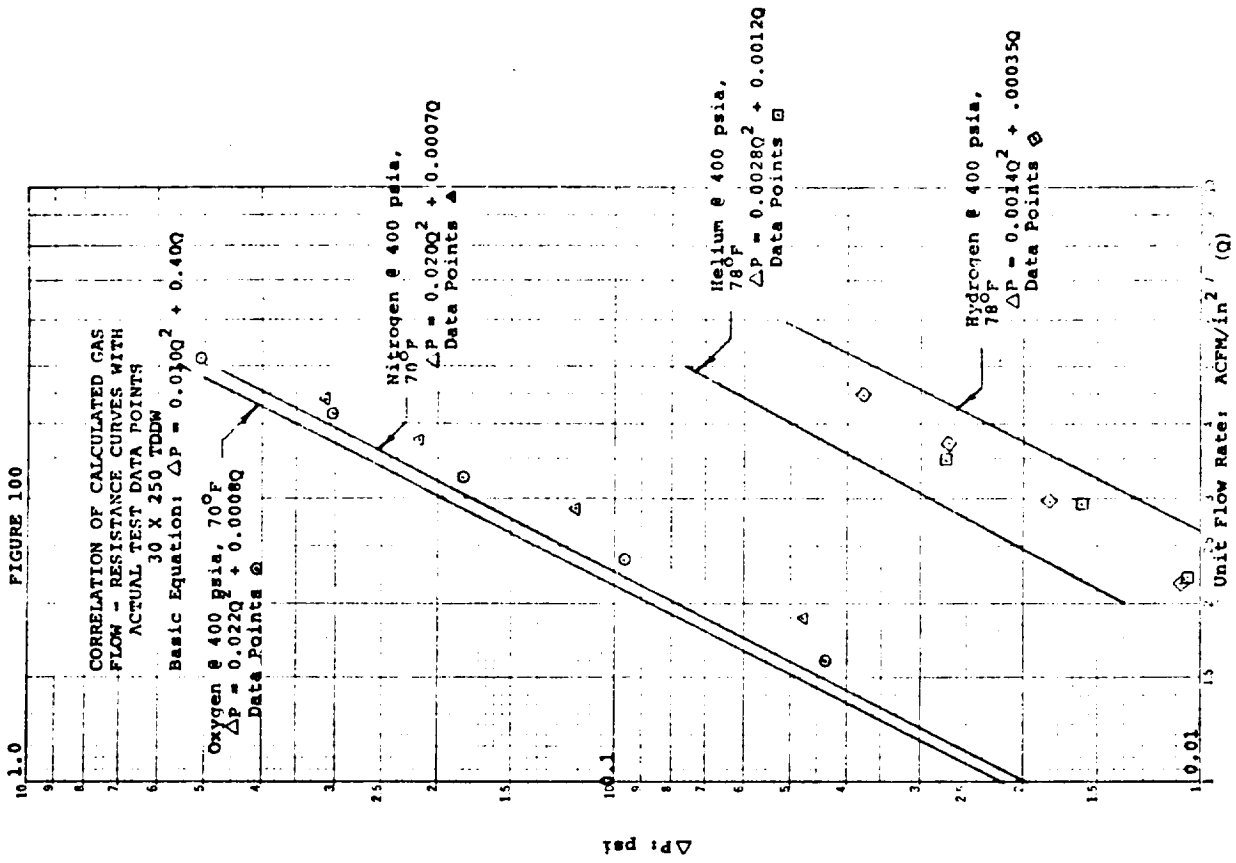


FIGURE 100



### 3.9 FILTER PERFORMANCE DESIGN GUIDES

#### 3.9.1 Specific Flow Index

Although the slopes of the flow resistance curves are not identical for all filter media at any particular pressure drop or unit flow rate, a useful method of relating the flow resistance of the various media is obtained by expressing the flow resistance as a "Specific Flow Index," SFI, (that unit flow rate which will develop a pressure drop of 1 psi across the medium). In this manner, each type and grade of porous medium will provide a single datum point which can be used in conjunction with other characteristics of the medium, such as glass bead rating or contaminant tolerance indices.

#### 3.9.2 Class Bead Rating vs. Specific Flow Index

Figure 101 is a composite graph showing the relationship between specific flow resistance and glass bead rating for several filter media. It is apparent that the specific flow index is related not only to the glass bead rating, but also to the type of medium. While the size of the flow pores controls the glass bead rating, the size, length, number and degree of tortuosity of the flow passages all influence the flow resistance and the specific flow index. Thus, it can be seen that there is a wide difference in specific flow indices between the various types of media, even though the glass bead filter ratings are equivalent. Of the materials shown in Figure 101, all are surface type filter media, with the exception of the Dynalloy X sintered metal fiber, which is a depth type medium. It can be seen that the fine grades of Dynalloy X fall between the Millipore Membranes and the Twilled Dutch Double Weave wire cloth materials, while the coarser grades show specific flow indices higher than the Twilled Dutch Double Weave. This is due to the fact that the depth type media glass bead rating is obtained by a combination of fiber size and density (pore size) and depth or thickness of the material. The media offering the most favorable flow characteristics (least flow resistance or highest specific flow index) are the square weave (plain or twilled), the Plain Dutch Single Weave, sintered metal fiber, and the Twilled Dutch Double Weave. The Dynalloy X sintered metal fiber shows a slightly better specific flow index than that of the Twilled Dutch Double Weave media in glass bead ratings above 20 microns, while the TDDW has a higher index in the ratings below 20 microns.

#### 3.9.3 Contaminant Tolerance Index

In addition to providing particle size control (maximum particle size or glass bead rating) porous media exhibit varying ability to tolerate contaminant. In general, the contaminant tolerance is controlled by the size and number of exposed flow pores per unit surface area of the medium and the degree of tortuosity of the flow paths.

The contaminant tolerance characteristics of the various media are usually shown in the form of plotted curves in which the data points are obtained by adding weighed increments of contaminant while flowing fluid at a constant rate and measuring the resultant effect on differential pressure across the screen. A typical curve begins with a relatively flat section until sufficient contaminant has been added to produce a "plugging" effect on the pores of the medium. The curve then sweeps upward with rapidly rising pressure differential as more contaminant is added. Each type of contaminant, as well as each type of fluid, will produce its own particular curve with a specific medium. The flow rate, of course, has a very significant effect on the relationship between pressure drop and contaminant weight added.

A convenient method of expressing relative values for contaminant tolerance is to determine the weight of contaminant which will provide a specific increase in pressure differential



FIGURE 101

GLASS BEAD RATING VS. SPECIFIC FLOW INDEX  
VARIOUS MEDIA

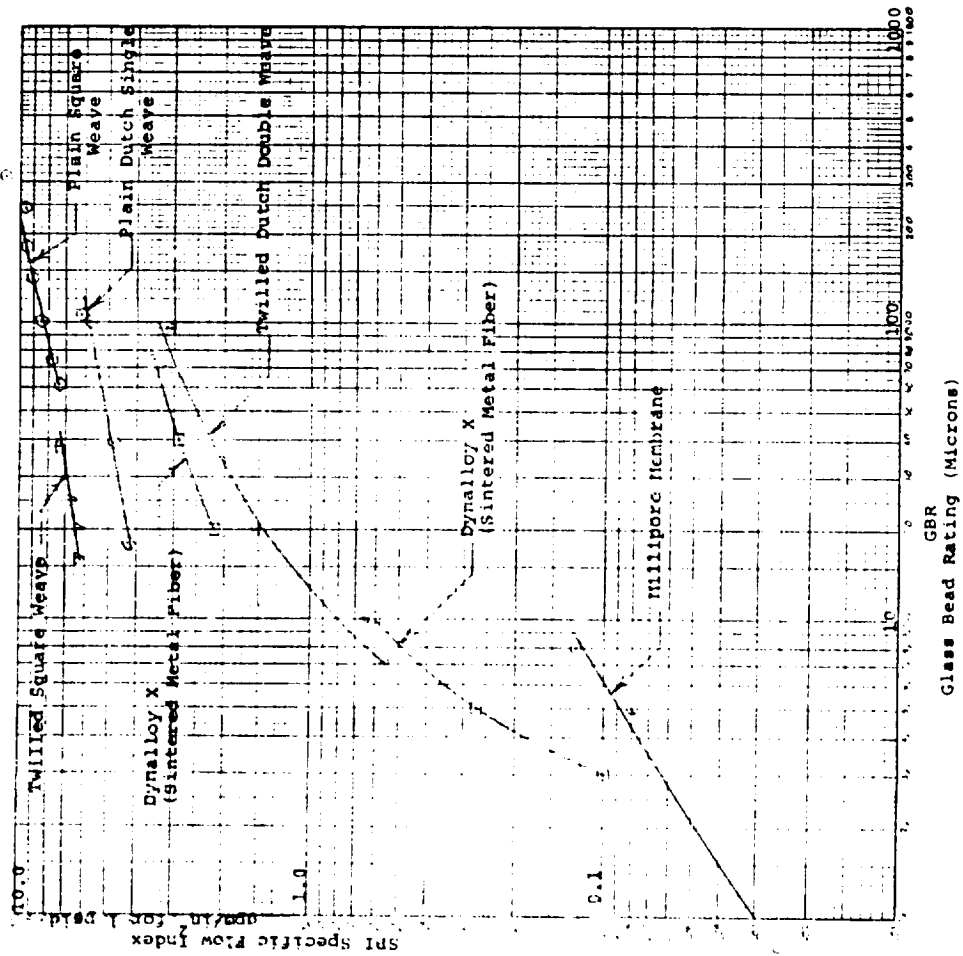
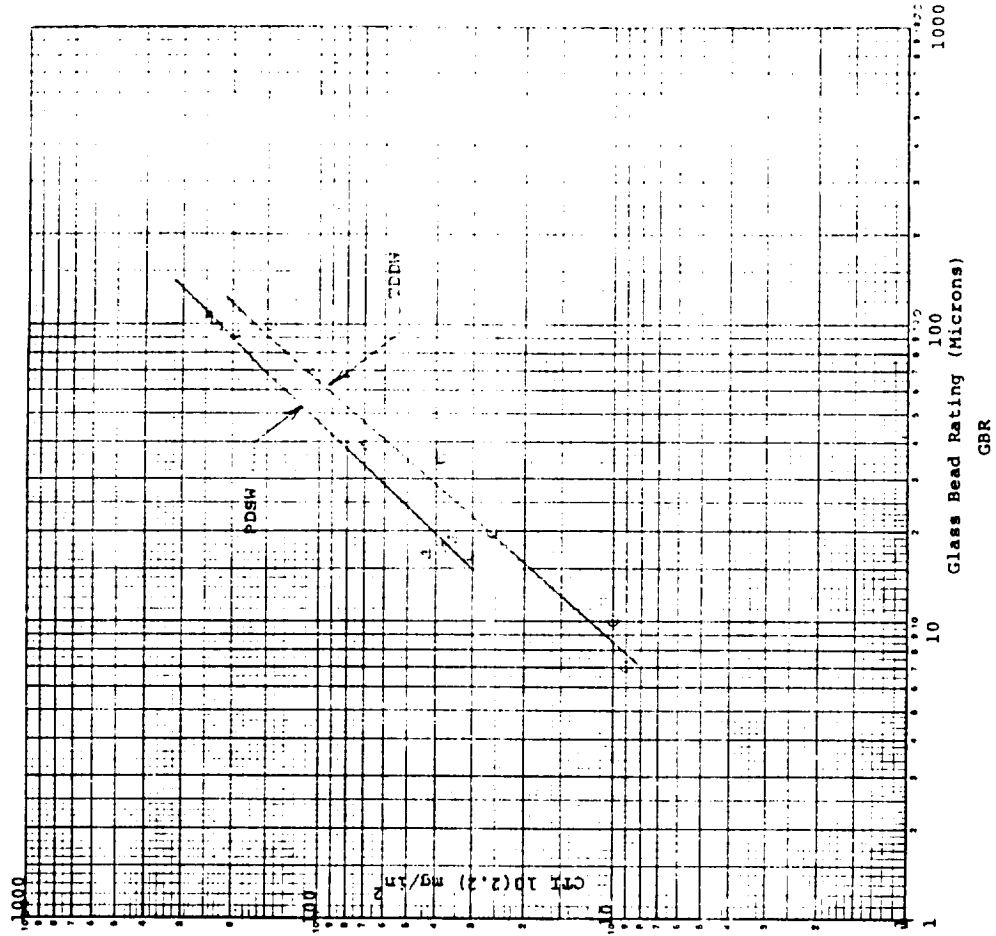


FIGURE 102

GLASS BEAD RATING VS. CONTAMINANT TOLERANCE INDEX 10(2.2)  
FOR 10 PSI RISE AND 2.2 gpm/in<sup>2</sup>  
WITH WATER AND AC COARSE DUST





above that of the uncontaminated medium with a specific fluid at a specific flow rate and with a specific contaminant. The following discussion assumes the fluid to be water, and the contaminant to be AC Coarse Dust. For each medium and flow velocity, a specific contaminant tolerance index can be determined such as C.T. 20(2.21). This indicates that the amount of contaminant introduced will cause the pressure drop across the medium to rise 20 psi above that in the uncontaminated condition at a flow rate of 2.21 GPM per square inch using water. CT 10 (0.289), would represent the weight of AC Coarse Dust to cause a 10 psi increase at a flow rate of 0.289 GPM/in<sup>2</sup> with water.

As the micron ratings of the media affect the amount of contaminant which can pass through, the relative contaminant tolerance characteristics of different media should be compared at equivalent micron ratings. From the curves for the various media at a flow rate of 2.21 GPM/in<sup>2</sup> using water and AC Coarse Dust, C.T. 10(2.21) indices were determined and plotted against Glass Bead Ratings (GBR) for the TDDW and PDSW media in Figure 102. Figure 103 shows similar comparisons for C.T. 10(0.29) for these two types of media.

It is readily apparent from the graphs that at all comparable glass bead ratings, the PDSW media have a greater contaminant tolerance than the TDDW. By comparing the graphs of Figures 102 and 103, it can be seen that as the unit flow rate (GPM/in<sup>2</sup>) decreases, the C.T.I. increases.

In both Figures, the PDSW media show higher contaminant tolerance indices than the TDDW media. As the indices consider only the rise of pressure differential above clean conditions, rather than the total pressure drop, the higher flow resistance of the TDDW does not account for the lower C.T.I.'s. It is the fact that the more tortuous flow paths of the TDDW are more effective in trapping particles smaller than the glass bead rating (GBR) of the media that causes the lower tolerance to the contaminant. Again, it must be remembered that the ability of a medium to allow particles smaller than its GBR to pass through will provide a higher contaminant tolerance. As the PDSW and the TDDW have approximately the same number of pores per square inch of surface area, it is the effectiveness of the TDDW in trapping particles, many of which would pass through the PDSW, that causes the lower contaminant tolerance index.

This type of presentation allows a comparison and estimate of service life for the various media. While the PDSW media provide good control of maximum particle size, and appear to be ideally suited for spacecraft filter applications, the TDDW media may be more desirable for interface (GSE) filtration where filter size and pressure drop are not as critical, and where filtration of a much larger percentage of fine particles is most desirable. For even greater retention of fine particles, the sintered metal fiber felt media, Dynalloy X, offers great advantages.

#### 3.9.4 Contaminant Tolerance Index vs. Specific Flow Index

Figure 104 combines the information shown in Figures 102 and 103, and illustrates for both TDDW and PDSW media, the relationship between their Specific Flow Resistance and Contaminant Tolerance Index, 10(2.2).

The shapes of the curves for the two media indicate that as SFI increases (due to increasing micron rating of the media), the CTI also rises, but much more rapidly for the PDSW than for the TDDW. Again, this is caused by the more open nature of the PDSW flow passages. The tortuosity of the passages of the TDDW remains effective in trapping the smaller particles of AC Coarse Dust until the micron rating of the TDDW approaches 100 microns GBR (250 microns maximum particle size). At this point, the TDDW flow pores are so large that the tortuosity effect is minimized and the slope of the TDDW curve approaches that of the PDSW. Within the

FIGURE 103

GLASS BEAD RATING VS. CONTAMINANT TOLERANCE INDEX 10(0.29)  
FOR 10 PSI RISE AND 0.29 gpm/in<sup>2</sup>

WITH WATER AND AC COARSE DUST

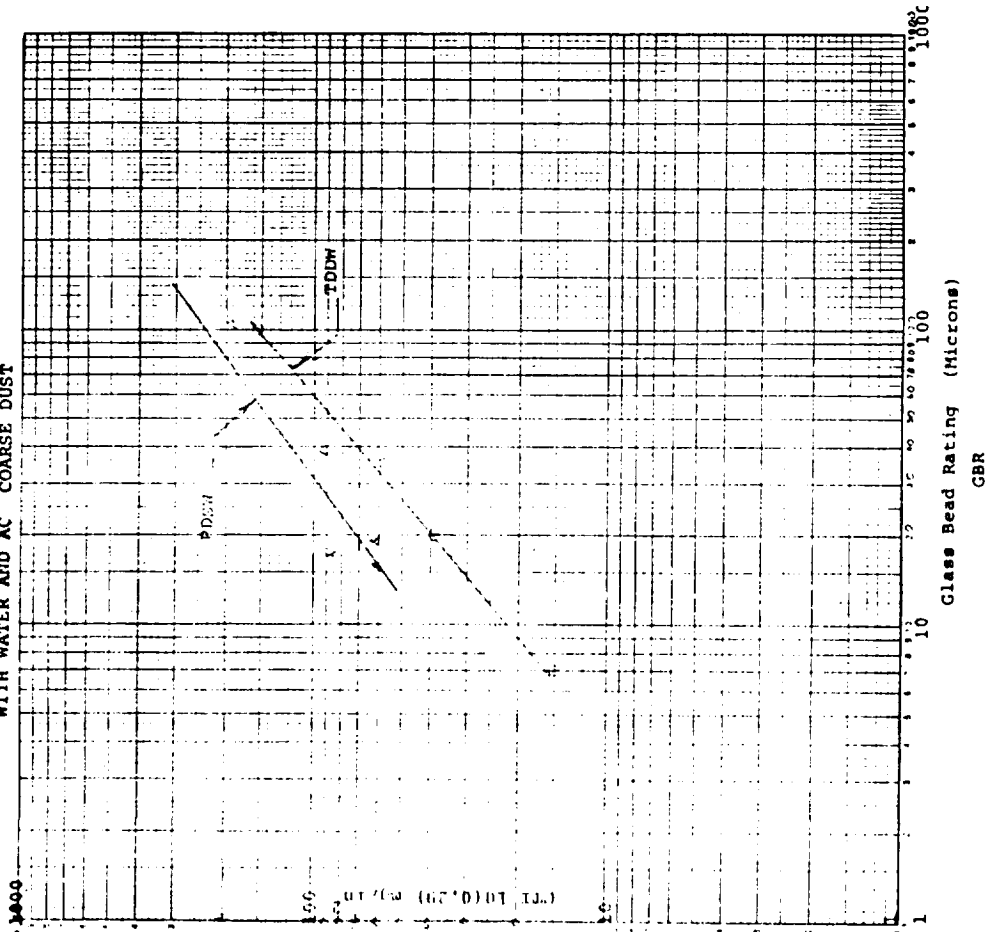
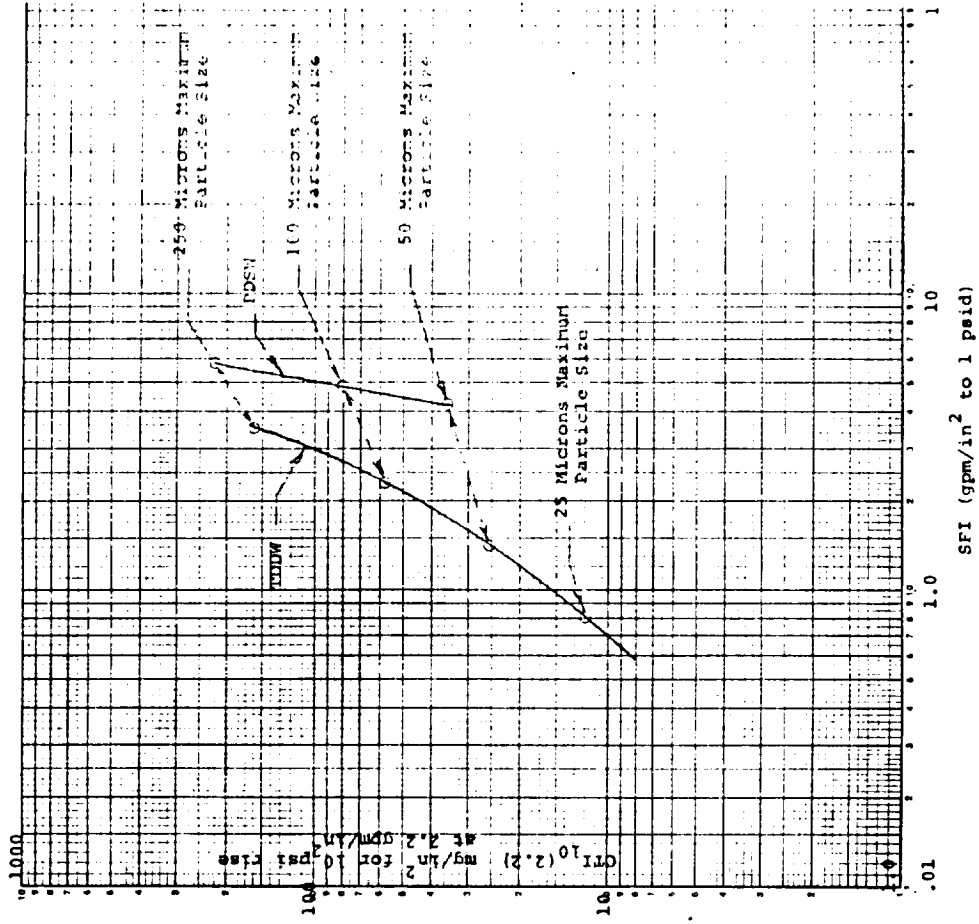


FIGURE 104

CONTAMINANT TOLERANCE INDEX 10(2.2) VS. SPECIFIC FLOW INDEX

WITH WATER AND AC COARSE DUST



micron ratings of the media tested, however, the PDSW evidences a consistent advantage over the TDDW media. The noted points on both curves denote equivalent micron ratings (maximum particle size) for the two media.

Keeping in mind that the contaminant tolerance is not a measure of the contaminant "held" by the medium, but can also reflect the amount of particulate matter passing through, the much sharper rise in CTI with increasing SFI for the PDSW media is not surprising.

Again, the PDSW shows the most favorable characteristics for spacecraft filtration, but the ability of the TDDW media to trap a greater percentage of fine particles must be considered when designing filters for spacecraft loading interfaces or general GSE applications where the additional filter size and weight can be tolerated.

### 3.9.5 Filter Area Requirements

While the equations for flow resistance allow the filter designer to select the proper area of medium to provide the desired pressure drop in an uncontaminated condition, it is necessary to increase this minimum area of medium so that a known amount of contaminant can be ingested without causing the pressure differential across the medium to rise beyond some maximum value.

Figures 105 and 106 show sets of curves for TDDW and PDSW media, respectively, which relate the total weight of contaminant, the flow rate, the filtration rating and the area of media which will cause a rise of 10 psi differential pressure above the clean condition. The data points from which these curves were constructed were obtained from the contaminant tolerance curves for each medium, by determining, at each of several unit flow rates, the weight of AC Coarse Dust which would cause a rise of 10 psi differential pressure.

The reciprocal of the unit flow rate ( $\text{in}^2$  per GPM) was then plotted against the product of this value times the contaminant tolerance ( $\text{in}^2/\text{GPM} \times \text{mg}/\text{in}^2 = \text{mg}/\text{GPM}$ ). The family of contaminant tolerance curves for 325 X 2300 TDDW medium can be used as follows to show the values.

TABLE 30  
CONTAMINANT FLOW FACTOR VS. AREA FLOW FACTOR: 325 X 2300 TDDW

| Unit Flow Rate<br>(GPM/ $\text{in}^2$ ) | Unit Flow Rate<br>( $\text{in}^2$ /GPM) | Contaminant Flow Factor<br>Unit Contaminant Capacity<br>for 10 psi Rise (mg/ $\text{in}^2$ ) | Area Flow Factor<br>$\text{in}/\text{GPM} \times \text{mg}/\text{in}^2$<br>(mg/GPM) |
|---|---|--|---|
| 0.136                                   | 7.35                                    | 36   | 264.6   |
| 0.289                                   | 3.46                                    | 26.5   | 91.7  |
| 2.21                                    | 0.45                                    | 10   | 4.5   |
| 6.63                                    | 0.15                                    | 6.8  | 1.02  |

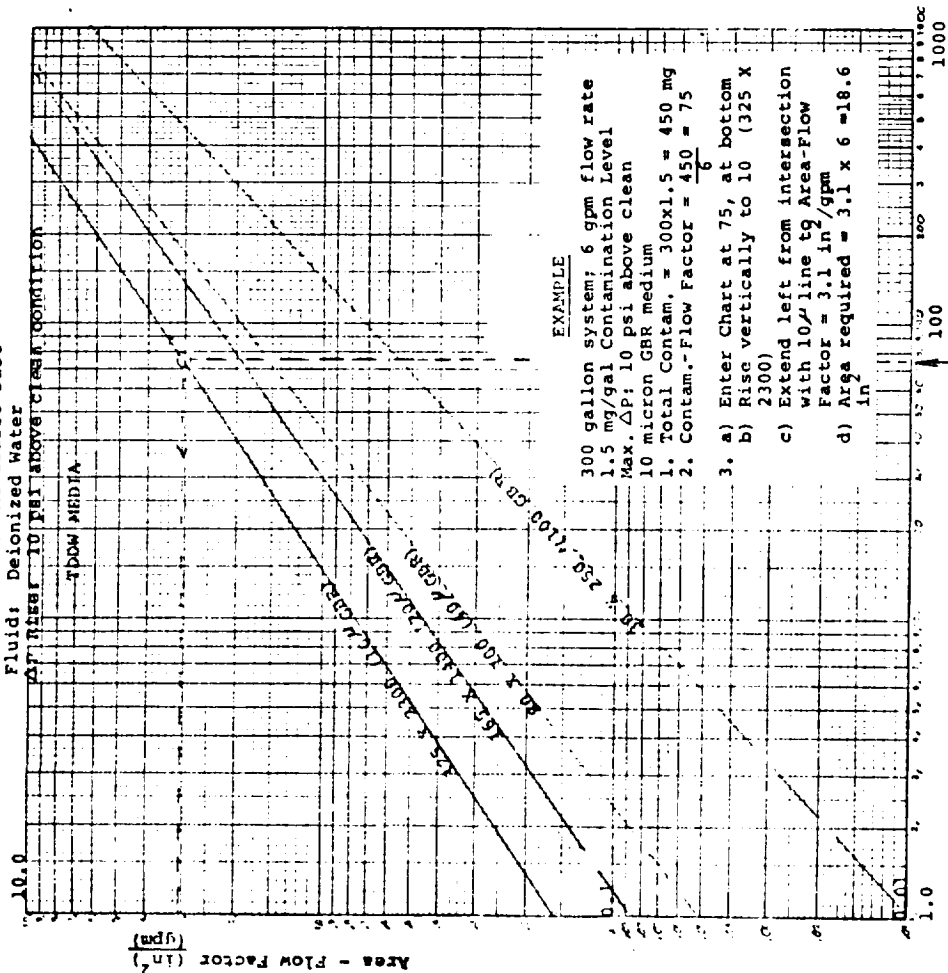
When the data points of column 2 are plotted on log - log paper against those of column 4, a nearly straight line results. The curves, of course, apply only to the fluid (water) and contaminant (AC Coarse Dust) which were used to obtain the original contaminant tolerance curves, but separate curves can be generated for each selected rise in differential pressure, fluid type and contaminant.

To use the information, the designer first determines the total amount of contaminant to be ingested by the filter medium. As the flow rate (GPM) through the filter is assumed to be known, the value of Total Weight of Contaminant/GPM can be determined. The type of medium, TDDW or PDSW, controls which figure is used, and the glass bead rating (GBR) desired deter-

FIGURE 105

AREA REQUIRED FOR SPECIFIC  
FILTRATION REQUIREMENTS

Contaminant: AC Coarse Dust  
Fluid: Deionized Water  
 $\Delta P$  Rise: 10 psi above clean condition



EXAMPLE

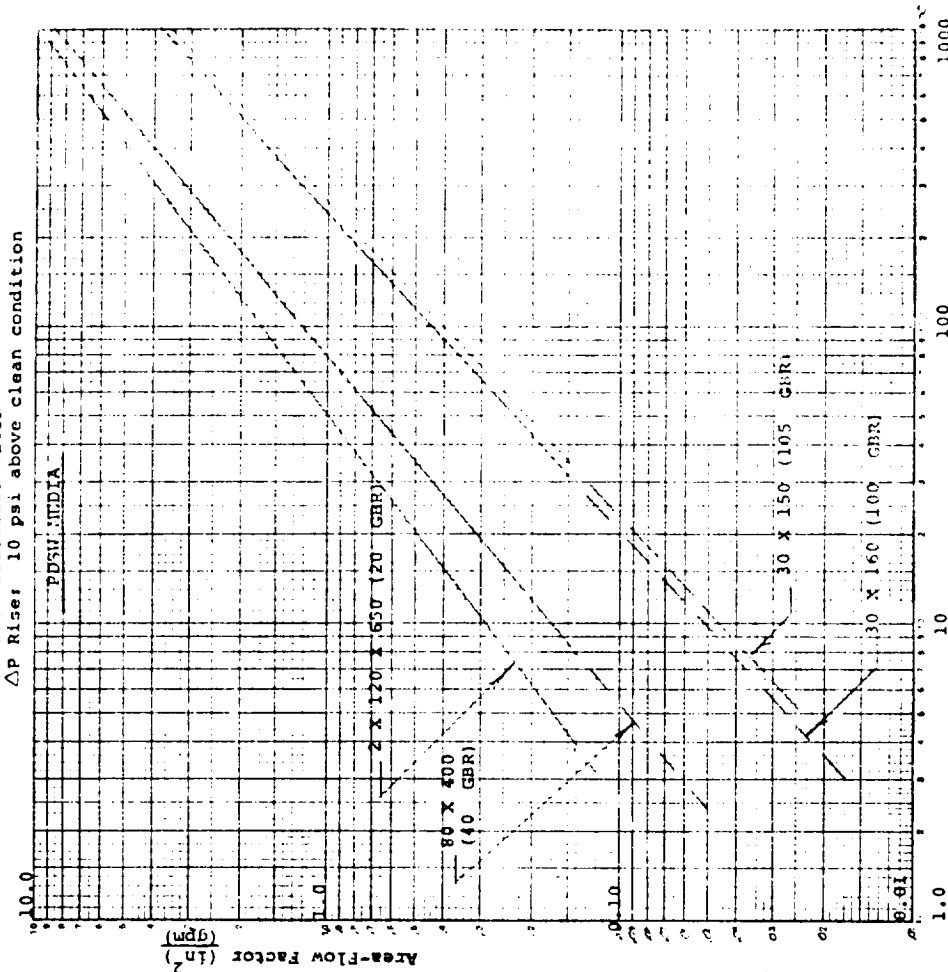
- 300 gallon system; 6 gpm flow rate
- 1.5 mg/gal Contamination Level
- Max.  $\Delta P$ : 10 psi above clean
- 10 micron GBR medium
- 1. Total Contam. =  $300 \times 1.5 = 450$  mg
- 2. Contam.-Flow Factor =  $\frac{450}{6} = 75$
- 3. a) Enter Chart at 75, at bottom
- b) Rise vertically to 10 (325 X 2300)
- c) Extend left from intersection with 10<sup>th</sup> line to Area-Flow Factor = 3.1 in<sup>2</sup>/gpm
- d) Area required =  $3.1 \times 6 = 18.6$  in<sup>2</sup>

Contaminant-Flow Factor  
 $\frac{\text{Total Contaminant Weight (mg)}}{\text{Flow Rate (gpm)}}$

FIGURE 106

AREA REQUIRED FOR SPECIFIC  
FILTRATION REQUIREMENTS

Contaminant: AC Coarse Dust  
Fluid: Deionized Water  
 $\Delta P$  Rise: 10 psi above clean condition



Contaminant-Flow Factor  
 $\frac{\text{Total Contaminant Weight (mg)}}{\text{Flow Rate (gpm)}}$

mines which specific curve will be used.

The chart is entered at the abscissa at value of Contaminant Flow Factor (mg/GPM) previously determined. A line is drawn vertically to an intersection of the appropriate filter medium line. From this intersection, a horizontal line is drawn to the left, to the Area - Flow Factor Value (in<sup>2</sup>/GPM) The Area - Flow Factor is then multiplied by the system Flow rate (GPM) to provide the area (square inches) of medium required.

Obviously, an infinite number of curve sets can be drawn for each medium, depending on the value of the rise in differential pressure above clean condition selected. And again, the designer must remember that the values shown are for water and AC Coarse Dust as fluid and contaminant, respectively. Other fluids and/or other contaminants will produce entirely different values.

The area of medium for a filter must be sufficient to ingest the expected system contaminant without exceeding some maximum permissible rise in differential pressure. The "clean pressure drop" characteristic of any porous medium is a momentary value, and it is of practical interest only in establishing the minimum pressure drop that will ever be experienced in service at the system flow rate.

As fluid flows through the medium particulate contaminant is removed and the pressure differential across the medium will increase, slowly at first, and then at a constantly increasing rate. The most important design criterion is that the filter provides the protection required for contaminant sensitive components throughout the system service life without exceeding the maximum allowable rise in pressure differential.

Once the total area of medium required for contaminant ingestion is known, the clean pressure drop can be determined from the flow resistance equation,  $\Delta P = aQ^2 + bQ$ , where the value of Q is Gallons per Minute per square inch of medium. The total pressure drop for the contaminated unit is then the sum of the clean pressure drop and the maximum allowable rise in differential pressure selected.

The curves of contaminant tolerance for the various media can be used in another manner to produce a secondary generated curve showing the relationship between unit flow rate (GPM/in<sup>2</sup>) and "contaminant loading" (mg/in<sup>2</sup>) to produce a given rise in differential pressure. Again, 325 X 2300 TDDW, at four flow rates with water and AC Coarse Dust, is used as an example. For each unit flow rate, the weight of contaminant per square inch of medium to create a rise of four selected values is read from the curves.

TABLE 31  
CONTAMINANT TOLERANCE INDEX FOR 325 X 2300 TDDW

| Unit Flow Rate<br>GPM/in <sup>2</sup> | Contaminant Tolerance<br>mg/in <sup>2</sup> |             |             |             |
|---------------------------------------|---|-------------|-------------|-------------|
|                                       | 5 psi rise                                  | 10 psi rise | 20 psi rise | 30 psi rise |
| 6.63                                  | 2.3   | 4           | 6.8         | 8.3         |
| 2.21                                  | 6.8   | 10          | 13.4        | 15.9        |
| 0.289                                 | 21.8  | 26.7        | 34.3        | 40.2        |
| 0.136                                 | 27.5  | 36          | 48.7        | 59.5        |

The above data points for each column of pressure differential rise are plotted on log - log paper in Figure 107. A set of four curves results showing the relationship between contaminant tolerance and unit flow rate for each pressure differential rise value, 5, 10, 20 and 30 psi.

This type of curve can also be used for filter design when the total weight of contaminant and the flow rate are known, but it involves a series of "trial and error" selections of area to find the unit flow rate and contaminant tolerance values which intersect at the proper differential pressure rise curve.

Figures 108 through 114 show contaminant tolerance vs. unit flow rate for several grades of TDDW and PDSW media.

### 3.10 FILTER DESIGN OPTIMIZATION

#### 3.10.1 Filter Configurations

As a result of work performed under this program, the design of filters for use in Space Shuttle applications can be optimized so that a minimum number of filter types, or configurations, commensurate with the filtration requirements can be established.

Three specific filter assembly types will satisfy the various applications for subsystem filtration. In order to avoid unnecessarily large and heavy filters installed in the spacecraft, it is proposed that all fluids be filtered at the loading interfaces to a high level of cleanliness. The onboard filters will then be required to ingest only the contaminants generated by operating components and by installation or replacement of components or subsystems. Furthermore, the filter media used in the onboard filters should be selected to provide the lowest level of filtration acceptable to the components of each system or subsystem. As contaminant tolerance has been shown to be a function of the filtration rating of the media, the coarser filters of equivalent size will provide longer service life. An analysis of component sensitivity will determine the particle size control required to protect the component from contamination - related failure. In addition, contaminant generation studies of operating components will determine the amount, size and type of contaminant to which the filters will be exposed.

The three major types, or classes, of filter assemblies are as follows:

#### Type I: GSE/Spacecraft Interface Filter

This unit will be coupled as close as possible to the ground half of the disconnect coupling used for loading fluids into the spacecraft. Its size will be dependent on loading rates, and the filter medium rating will be 10 microns (GBR) maximum, (25 microns maximum particle size). The filter media used for these filters should also be capable of removing a large percentage of particles of smaller size than the maximum filter rating. A typical configuration for the Type I filter assembly is shown in Figure 115.

#### Type II: Onboard System Filter

This unit will be located in the main system line, preferably downstream of the major contaminant generating component. Its construction can be similar to that of the Type I, or it can be such that information is provided relative to the existing contaminant level of the system, changes to the contaminant level and remaining (unexpended) life of the filter. Filters of the latter type have been developed under this program and are described in the section on "Prototype Filter Development."

#### Type III: Component Filters

As a result of sensitivity tests conducted with the component, the level of contaminant, in terms of maximum particle size, which will cause malfunction of the component can be determined. A filter, sized to the flow rate and degree of protection (filtration rating) required by the component, should be located immediately upstream or as an integral part of the

FIGURE 108  
CONTAMINANT TOLERANCE VS. UNIT FLOW RATE  
FOR  $\Delta P$  INCREASE ABOVE CLEAN CONDITION

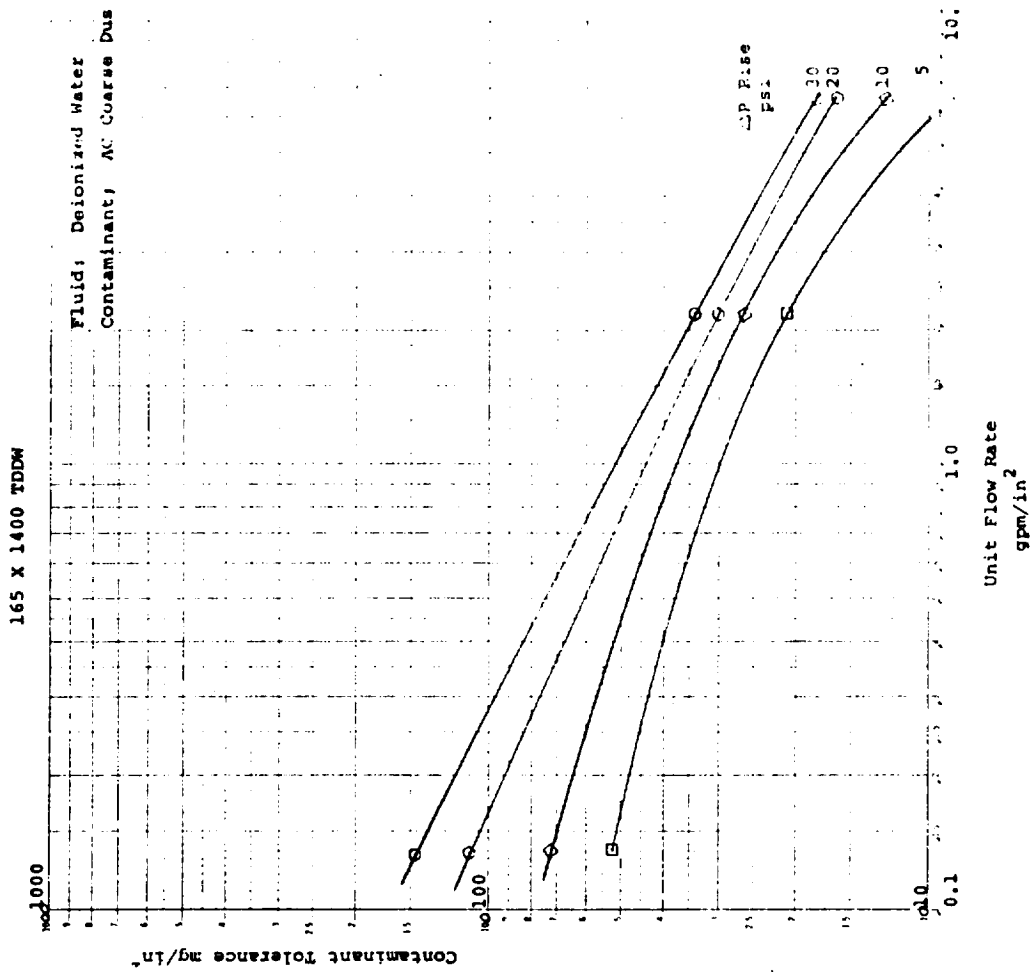


FIGURE 107  
CONTAMINANT TOLERANCE VS UNIT FLOW RATE  
FOR  $\Delta P$  INCREASE ABOVE CLEAN CONDITION

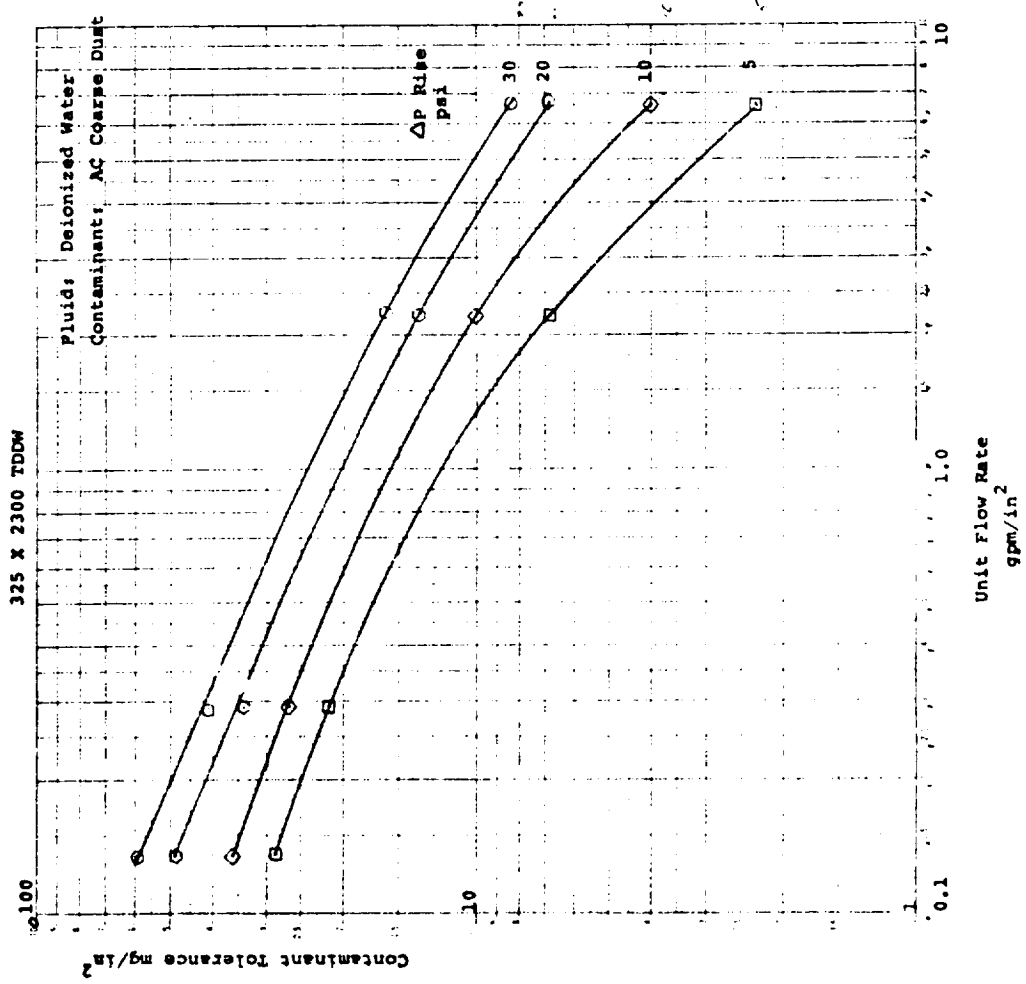


FIGURE 110  
 CONTAMINANT TOLERANCE VS. UNIT FLOW RATE  
 FOR  $\Delta P$  INCREASE ABOVE CLEAN CONDITION  
 30 X 250 TDDW

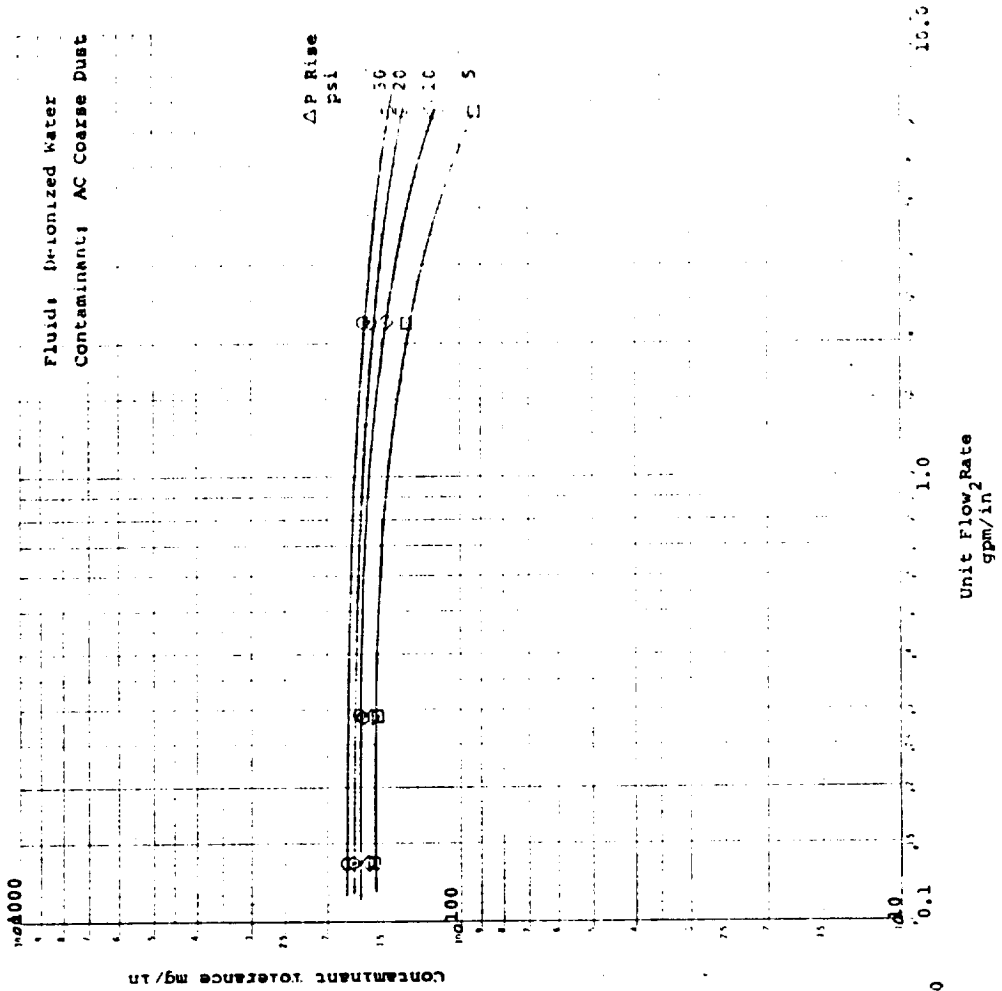


FIGURE 109  
 CONTAMINANT TOLERANCE VS. UNIT FLOW RATE  
 FOR  $\Delta P$  INCREASE ABOVE CLEAN CONDITION  
 80 X 700 TDDW

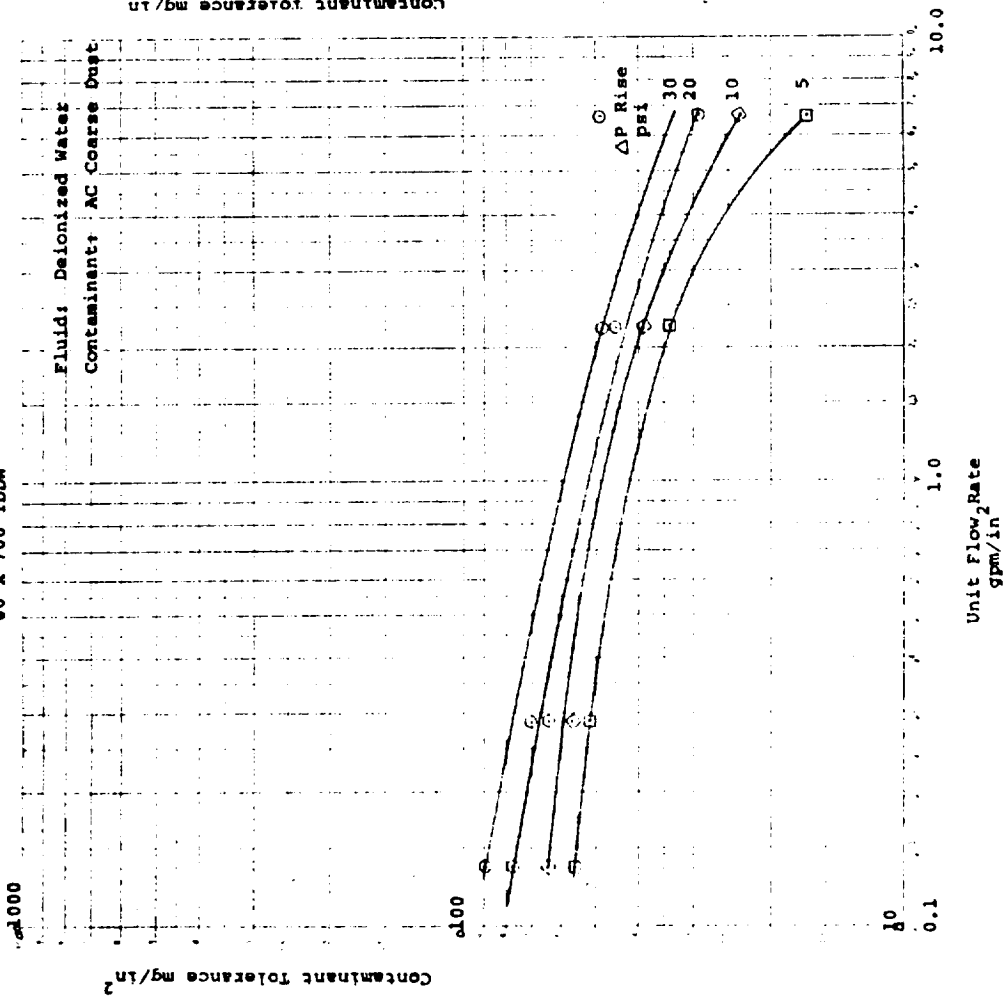




FIGURE 111

CONTAMINANT TOLERANCE VS UNIT FLOW RATE  
FOR  $\Delta P$  INCREASE ABOVE CLEAN CONDITION

80 X 400 PDSW

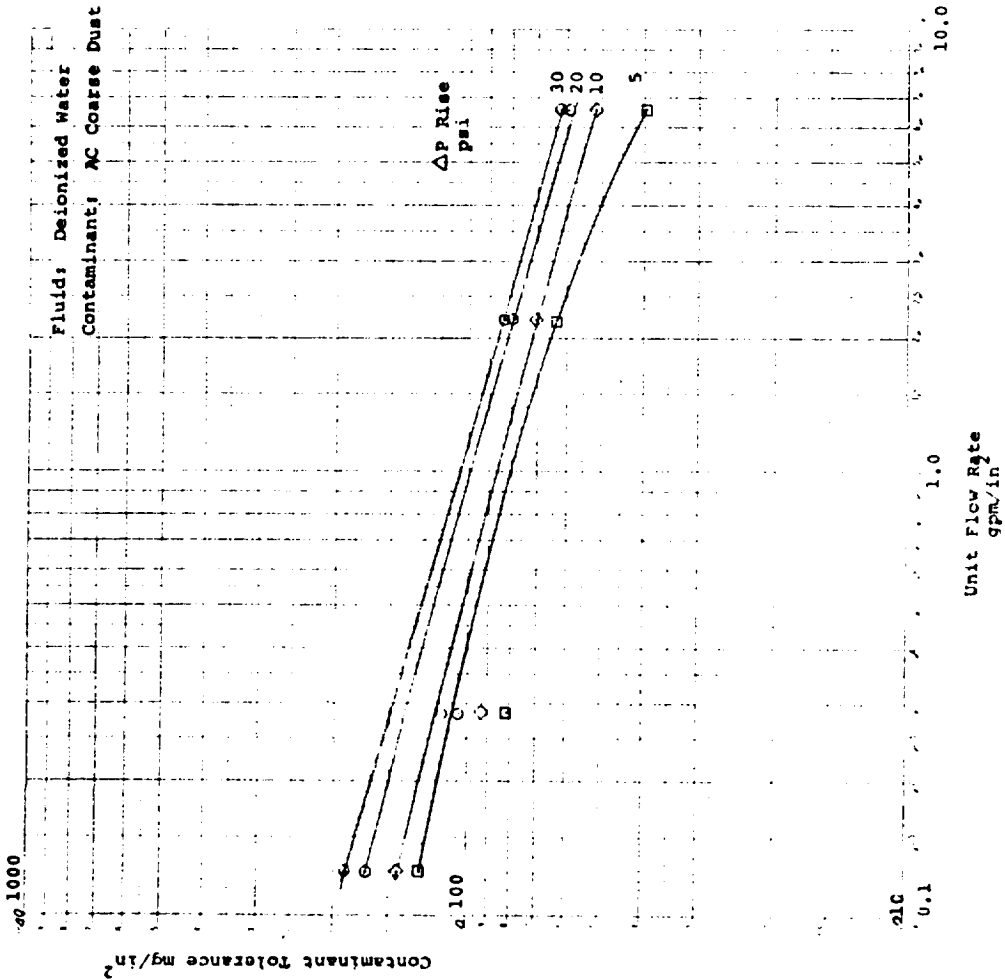


FIGURE 112

CONTAMINANT TOLERANCE VS UNIT FLOW RATE  
FOR  $\Delta P$  INCREASE ABOVE CLEAN CONDITION

2 X 120 X 650 PDSW

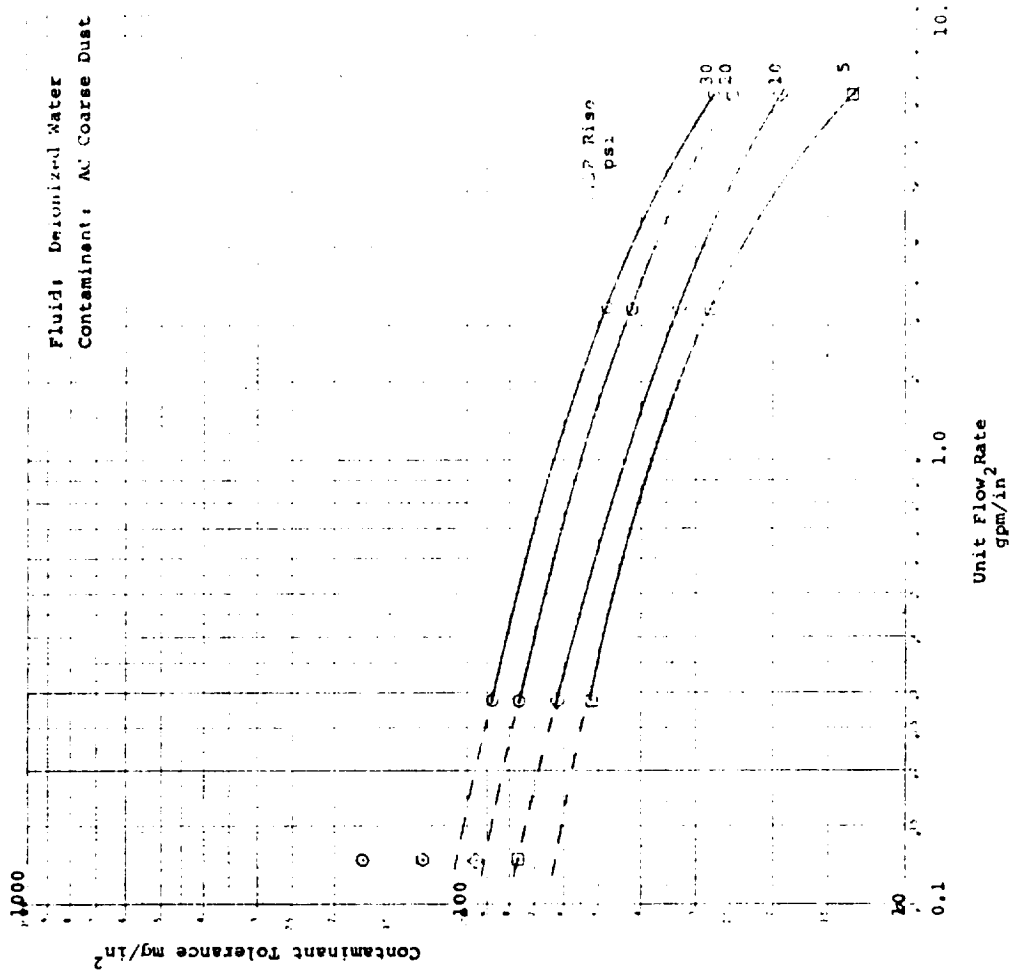


FIGURE 113  
 CONTAMINANT TOLERANCE VS UNIT FLOW RATE  
 FOR  $\Delta P$  INCREASE ABOVE CLEAN CONDITION

30 X 160 PDSW

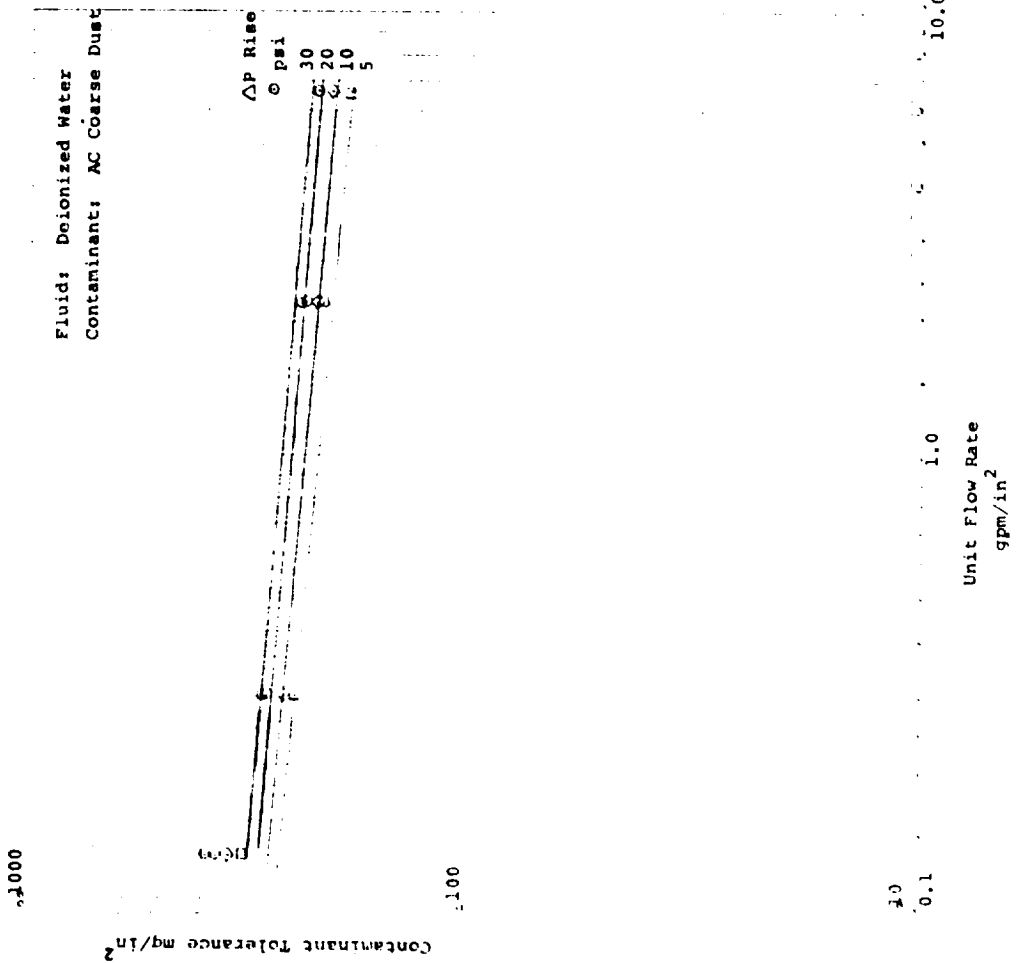
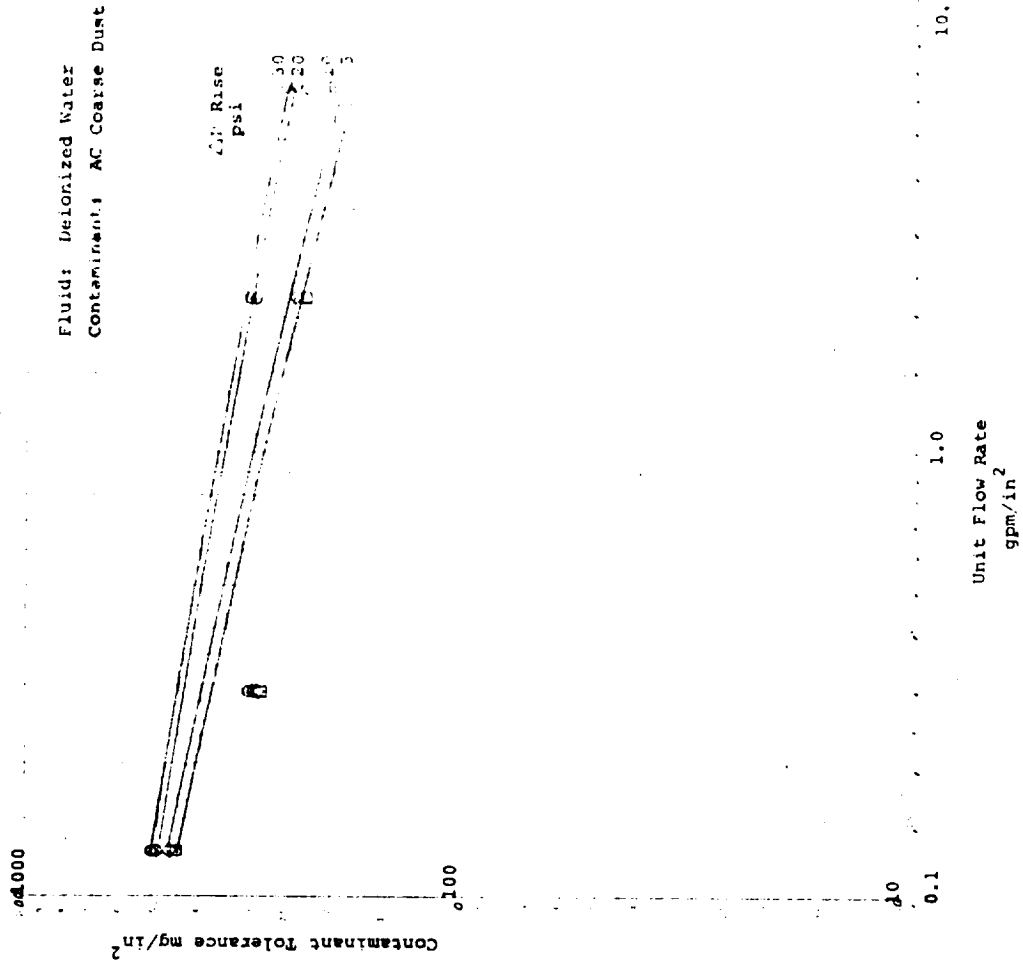


FIGURE 114  
 CONTAMINANT TOLERANCE VS UNIT FLOW RATE  
 FOR  $\Delta P$  INCREASE ABOVE CLEAN CONDITION

30 X 150 PDSW



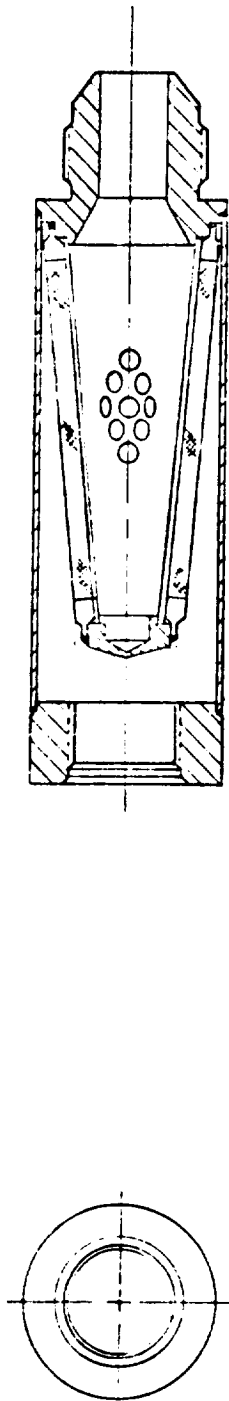


FIGURE 115

TYPE I

SPACECRAFT/GSF INTERFACE FILTER

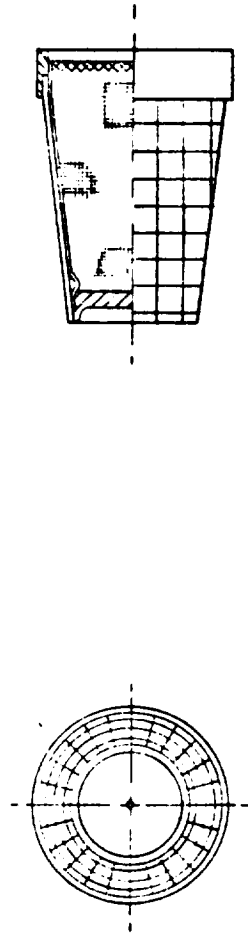


FIGURE 116

TYPE III

COMPONENT FILTER

component. It will be of relatively small size, and its configuration may be a simple disc (pleated or flat) or a conical unit as shown in Figure 117.

Installation and use of the three basic types of filters described will assure removal of harmful contaminants from the three primary sources, supplied fluids, component-generated and maintenance or assembly-introduced.

### 3.10.2 Filter Media

As the medium used for filter elements will be selected after the required level of protection is determined, it is not possible to recommend specific grades of media for the various subsystems at this time. However, the filter media recommended for various maximum particle size control can be listed. Table 32 shows the recommended media for various applications based on the best combination of minimum flow resistance, particle size control and contaminant tolerance.

TABLE 32  
RECOMMENDED FILTER MEDIA

| Filter Type | Micron Rating<br>GBR<br>Microns | Maximum Particle<br>Size<br>Microns | Medium                                  |
|-------------|---------------------------------|-------------------------------------|---|
| I           | 10                              | 15                                  | Dynalloy X-5                            |
|             | 10                              | 25                                  | 325 X 2300 TDDW                         |
|             | 20                              | 50                                  | 165 X 1400 TDDW &<br>2 X 120 X 650 PDSW |
|             | 40                              | 100                                 | 80 X 700 TDDW &<br>80 X 400 PDSW        |
| II          | 100                             | 250                                 | 30 X 250 TDDW &<br>30 X 160 PDSW        |
| III         | 10                              | 25                                  | 325 X 2300 TDDW                         |
|             | 20                              | 50                                  | 2 X 120 X 650 PDSW                      |
|             | 40                              | 100                                 | 80 X 400 PDSW                           |
|             | 100                             | 250                                 | 30 X 160 PDSW                           |

NOTE: The PDSW media will provide equivalent particle size control with lower pressure differential, but will trap a lower percentage of finer particles than the TDDW media.

The foregoing table lists three types of media and grades recommended for the great majority of filter applications. Each has its own advantages and disadvantages which the designer must consider for the individual application. A summary of these performance parameters follows.

#### Dynalloy X-5

A depth medium with relatively high pressure differential in the clean condition. Although rated at 10 microns (GBR), the very tortuous flow paths provide excellent control of elongated particles and the material will ingest a very large percentage of particles in the lower micron sizes. Contaminant tolerance is excellent.

#### Twilled Dutch Double Weave

The four grades all offer good control of maximum particle size, due to their rather tortuous flow paths. As the wires are driven together tightly, there is excellent control of opening

size. The flow resistance is moderate, but the contaminant tolerance is relatively low. A fair degree of filtration is obtained in the smaller size ranges.

#### Plain Dutch Single Weave

These are very free flowing media and are recommended for use where a larger percentage of fine particles can be tolerated. The shute wires are driven up tight and there is excellent control of pore size. The flow resistance characteristics are very good. These media are recommended for the great majority of applications due to the good combination of low flow resistance and high contaminant tolerance.

#### Other Media

The recommended media cover the range of 15 to 250 microns maximum particle size control (10 to 100 microns GBR). There are many applications where protection against very large particles is the only requirement, such as injection plate filters. For these applications, the Square Weave media are recommended. They are relatively strong and offer good control of two dimensions of particles. They have the lowest flow resistance for any micron rating (GBR) and very high contaminant tolerance due to their ability to pass fine particles through.

The particular mesh to be recommended is, of course, a function of the degree of protection required. Plain Square mesh media are available with square openings as fine as 60 microns on a side. The wires are not driven together, so it is quite probable that there will be a variation in pore size. However, there is little difference in flow resistance from the 100 X 100 mesh to the 250 X 250 mesh, so the designer can provide a "safety factor" by choosing a medium finer than required without penalizing the system pressure drop.

For filtration applications considered in this program, the range of from 10 to 100 microns GBR is considered adequate to meet the maximum particle size fluid cleanliness requirements of from 25 to 250 microns. The Dutch Weave media provide relatively positive control of maximum pore size with a rather small deviation from the mean pore size. The sintered metal fiber media provide equivalent cut-off ratings, but the larger deviation of mean pore size from maximum pore size provides filtration characteristics which allow a much larger percentage of fine particles to be trapped within the matrix.

For special filtration applications requiring closer control of particulate matter below 25 microns maximum dimension, the finer grades of sintered metal fiber media should be considered. The finest grade, Dynalloy X-3, can provide control down to approximately 8 microns (3 microns GBR), while the membrane materials will control down to very low (0.5 microns) levels. The membranes, however, possess neither the strength nor the environmental compatibility of the metallic media.

#### 3.10.3 Filter Cleanliness

Although this test is also conducted on most other aerospace components as a routine matter, the conduct of the test on a filter requires special equipment and techniques and, therefore, is regarded as being unique with respect to filters.

There are a number of different cleanliness test methods which are employed to determine the initial cleanliness of a filter; however, it should be noted here that any filter cleanliness evaluation test method not employing ultrasonic energy (such as the "Flow-through" test or the so-called "vibraflush" method) do not provide high enough energy levels to release built-in contaminants. As a consequence, these tests are practically meaningless except where gross contamination is present. The only useful method which provides an indication of the true cleanliness level of a filter consists of repetitive cycles of first subjecting the

filter to an ultrasonic vibration field and then flowing a predetermined increment of fluid (usually 100 or 500 ml) through the filter until the total specified sample amount (usually 500 or 2,500 ml) has passed through a downstream membrane-type filter and been examined under a microscope. Specific details for conducting this test are contained in ARP 599. Particle counting methods and techniques are described in ARP 598.

A full definition of the test parameters should include the following:

- (a) Whether the test is to be conducted from the outside to the inside of the filter element, in the reverse direction, or in both directions. This is determined by the flow direction of the filter.
- (b) The total volume of the sampling fluid on which the count is to be based and the incremental volumes withdrawn. ARP 599 specifies 2000 ml total volume and 500 ml increments.
- (c) The allowable number of particles in each of at least two ranges. This test should always be conducted as the final acceptance test since it is meant to be a cleanliness verification test.

### 3.11 PROTOTYPE FILTER DEVELOPMENT

During this program, a new type of filter was designed and constructed based on concepts developed by Wintec prior to the start of this contract.

Current designs of liquid and gas filters have a limited life owing to their finite contaminant capacity. That portion of the system pressure drop attributable to the filter increases exponentially as the unit nears its maximum capacity. At this point, either a valve is actuated to by-pass the filter or the downstream pressure capability is severely limited. The condition is alleviated by shutting the system down to clean the filter element or by replacing the element. Because of the wide variations in system fluid cleanliness, the operational life of a filter can never be predicted. The end of the useful life period is normally indicated by a "pop-up" differential pressure switch or by a differential pressure gauge. Both of these instruments require frequent monitoring which is inconvenient in most cases and impossible in remote, inaccessible installations.

The problem of providing a continuing means of removing system contamination and maintaining a low pressure drop has been solved by the design of a unique device known as the Sequential Strip Filter. The assembly and cross sectional views of this filter are shown in Figure 117.

The filter (1) senses increasing pressure drop and uses this to compress a bellows (2). The compression of the bellows stores energy in a spring (3) until a predetermined pressure drop level is reached. At this point, the bellows and spring are released. The relaxation of the spring is used to move a clean area of screen into position across the fluid stream. In section BB, the clean screen is shown in position (4) across the flow aperture (5). The dirty screen is taken up on a wind up spool (6) and the clean screen is stored on a cartridge spool (7). The number of "franes" of screen used is shown on a mechanical indicator (8). This indication can readily be converted to an electrical signal, capable of remote read out.

There are several unique features inherent in the design of this filter assembly. A large contaminant capacity is provided with a very low pressure drop range. The pressure drop monitoring device and the screen advance mechanism are internal to the filter assembly. No external power source is required.

The application of the Sequential Strip Filter to contaminant removal is obvious, but there is an additional advantage to its use in that it can be used to monitor fluid cleanliness

within a system. The rate of screen "frame" advance is directly proportional to the amount of contamination in the system. If the screen advance rate increases significantly, this is a direct indication of component degenreation and possible failure upstream of the filter assembly.

In addition, the number of frames used, or conversely, the number of unused frames of filter media, provides an accurate measurement of the remaining filter "life."

A drawing of this filter is included in this report as Figure 117.



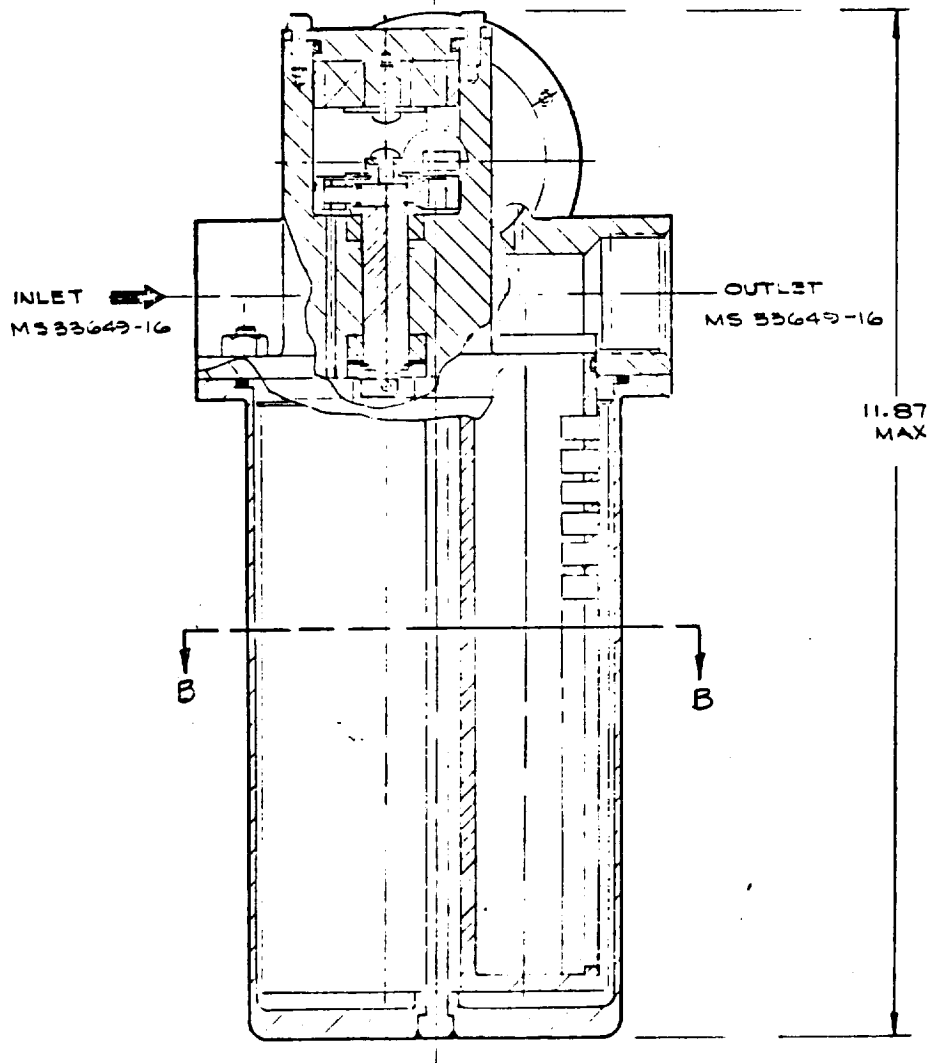
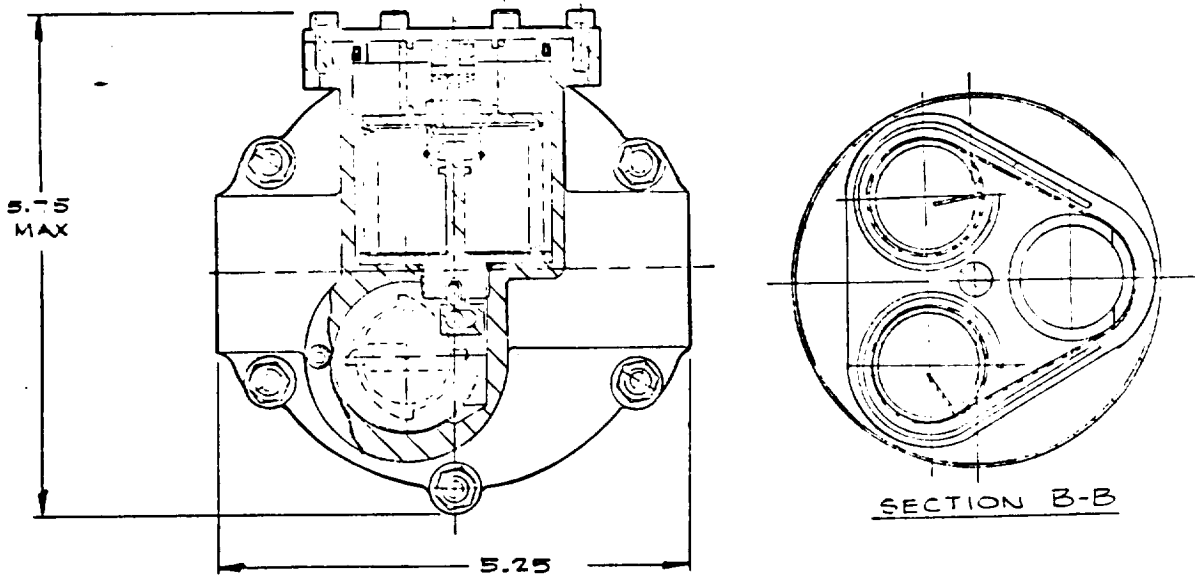


FIGURE 117  
PROTOTYPE SEQUENTIAL STRIP FILTER

## SECTION 4

### CONTAMINATION GENERATION AND SENSITIVITY TESTS

#### 4.1 CONTAMINANT GENERATION TESTS

The investigation conducted under this phase of the program are described in a separate Volume (Volume III) of this report.

The abstract of Volume III, Section A is, however, reproduced below.

Contaminant Generation Studies were conducted at the component level using two different methods, radioactive tracer technique and gravimetric analysis test procedure. Both of these were reduced to practice during this program. In the first of these methods, radioactively tagged components typical of those used in spacecraft were studied to determine their contaminant generation characteristics under simulated operating conditions. Because the purpose of the work was 1) to determine the types and quantities of contaminants generated and 2) to evaluate improved monitoring and detection schemes, no attempt was made to evaluate or qualify specific components. The components used in this test program were, therefore, not flight hardware items. Some of them had been used in previous tests; some were obsolete; one was an experimental device. They were supplied for the purpose of these tests by NASA and NASA contractors.

In addition, to the component tests, various materials of interest to contaminant and filtration studies were irradiated and evaluated for use as autotracer materials. These included test dusts, plastics, valve seat materials, and bearing cage materials.

In all, five components were tested. These included:

- Two types of solenoid valves,
- An augmented spark igniter valve assembly,
- A hydraulic actuator,
- A bearing test device.

These components were selected because they were representative of the basic motions involved in wear, i.e., sliding surfaces, rotating motion, impact, etc.

The test procedure involved operating the component a predetermined number of cycles in a test loop. A circulating fluid removed contaminants for collection on filter screens. Either water, hydraulic fluid, or liquid nitrogen was used. Nuclear detection techniques were used to determine the type and quantity of contaminants collected on the filters.

With these techniques, it was possible to make on-line measurements of contaminant generation. In most cases, the source of the contaminant could be identified, i.e., "valve body," "bearing race," etc. Sensitivity was quite good using these methods, since test results indicated that 10 micrograms of typical contaminant materials can be detected with ease. Using more sophisticated techniques, the limit of detectability can be extended to 1 nanogram, but there seems to be no practical incentive to do so for the purposes of these tests.

#### 4.2 CONTAMINANT SENSITIVITY TESTS

The tests conducted under this phase of the program are contained in Volume III, Section B of this report.

## SECTION 5

### CONTAMINATION MANAGEMENT PLAN

The proper selection of a filter medium and the size and configuration of a filter are functions of the degree of protection required by contaminant sensitive components and total quantity of contaminant to be ingested. It is, therefore, necessary for design optimization that these parameters be known. Filters of the proper size and micron ratings may then be placed intelligently within the fluid system.

As the filter must ingest all the contaminant within a fluid system during its service life, it is essential that contamination control methods be implemented which will minimize the amount of contaminant introduced unnecessarily into the system.

The following Contamination Management Plan recommends the requirements for contamination control that will provide the necessary design information, determine the degree of protection required from the filter, the optimum size and location of filters and prevention of the introduction of extraneous contaminant into the system.

## CONTAMINATION MANAGEMENT PLAN

### 1.0 SCOPE

This document establishes the general contamination management requirements for flight vehicle and associated ground support equipment for the shuttle program. The contractor shall generate an overall contamination management plan and implement approved procedures for meeting the requirements of this document.

### 2.0 CONTAMINATION CONTROL

#### 2.1 General Requirements

Contamination Control procedures shall be generated on the basis of the functional performance reliability requirements of each system and its individual operating components. Predicted contaminant generation and sensitivity characteristics shall be a prime consideration at the components procurement level. Target limits shall be specified in all procurement specifications. Filters shall be installed as required to protect each operating component throughout its full service cycle.

#### 2.2 Contaminant Generation of Components

The contractor shall submit a plan for determining the contaminant generation characteristics of shuttle components. This information shall be obtained during component development test. Size, quantity and type of particulate matter generated by the component under operating conditions, and as a result of post fluid exposure, shall be recorded. The objective of the generation tests shall be to establish the predicted contaminant level and type of contaminant that will be added into the fluid by the component, and to determine its wear-in point. The test plan shall specify the operating conditions and number of cycles required for wear-in and total service life.

#### 2.3 Contaminant Sensitivity of Components

The contractor shall submit a plan for determining the contaminant sensitivity of operating components to particulate matter in the operational fluid. The sensitivity characteristics may be expressed in terms of component life expectancy as a function of contaminant size and quantity levels in the fluid or in terms of the life expectancy as a function of an upstream filter micron rating. The objective of the sensitivity tests shall be to establish the coarsest filter rating required to assure acceptable component life. The test plan shall specify the contaminant level of the test fluid, the operating conditions and the number of cycles during the test.

#### 2.4 Filter Application and Location

The contractor shall select the appropriate standard filtration rating, and establish the size and location of filters required to provide contamination protection for the operating components. The filters shall be designed to provide the filtration ratings determined, necessary in component sensitivity tests, to provide the required degree of contamination control. Each filter shall also be designed to provide service life determined necessary on the basis of contaminant generation tests of upstream components. Filters which cannot provide sufficient surface area to protect a component throughout its intended service life cycle shall be designed so as to be removable without removing the component itself. Protective strainers shall be installed both upstream and downstream of all sensitive operating components to protect them from con-

tamination introduced during maintenance and repair. All onboard interface connections subject to disconnect - connect as a normal function shall be provided with filters located immediately downstream of the interface. All filters shall be procured in accordance with NASA MSC, Specification SE-F-0044.

### 3.0 CONTAMINATION PREVENTION

#### 3.1 General Requirements

Prime considerations in the design of components, subsystems and systems shall be to minimize entrapment areas and to assure that contaminants can be readily removed by flushing operations without disassembly.

#### 3.2 Surface Cleanliness Levels

The contractor shall establish the required cleanliness levels, methods of cleanliness verification, and packaging for the various components, subsystems and systems. Cleanliness levels shall be verified during acceptance testing.

#### 3.3 Assembly and Disassembly Methods

The contractor shall establish contamination prevention procedures to preserve the cleanliness of cleaned items prior to, during and after assembly into systems. Assembly methods shall be established which will not add contamination to the system. Disassembly and reassembly procedures shall also be generated so as to minimize introduction of contaminants during replacement or maintenance.

#### 3.4 Test Fluid Control

The contractor shall require that all test and flushing fluids be filtered to a level such as the largest particle in the fluid is less than half the size of the largest particle determined to be detrimental to the most sensitive component. In addition, the number of particles in the smaller size ranges shall be no more than 10% of the allowable quantity specified for the cleanliness level of the component, subsystem or system. The contractor shall also generate a method of coding all components with regard to flush fluid compatibility.

#### 3.5 Interface Filter Requirements

All test, flushing and/or loading interface connections shall contain an interface filter located immediately upstream of the connecting point and shall be closely coupled to the ground half. The interface filter micron rating shall be equal to or finer than the finest filter in the system, and the filter shall be in accordance with NASA Specification SE-F-0044.

### 4.0 REFERENCES

The following documents may be used as a reference for implementing the requirements of this document.

4.1 NAS 9-11264 - Final Report, "Cryogenic Filter Study"

4.2 NASA MSC Specification SE-F-0044.

## SECTION 6

### CONCLUSIONS AND RECOMMENDATIONS

The following conclusions and recommendations can be formulated as a result of the effort performed under this program.

1) The four standardized grades of stainless steel wire cloth filter media selected during this program (Table 1) represent the optimum state-of-the-art filtration performance capability in terms of positive particle size cut-off, minimum flow resistance and maximum service life per unit area.

It is recommended that they be adopted as standard media for all space shuttle systems.

2) Using these standardized media basic fluid cleanliness levels with maximum particle size cut-off ratings of 25, 50, 100 and 250 microns can be reliably and continuously produced by means of installing filters within fluid systems. The standardized media selected on the basis of extensive tests in most shuttle systems satisfy the fluid cleanliness requirements of NASA JSC Specification SE-S-0073. Fluid Cleanliness level requirements for a given system should be based on the contaminant sensitivity of its operating components. It was demonstrated during this program that the degree of protection required for an operating component can be determined by conducting contaminant sensitivity tests using the four standardized filter media.

In the absence of such test data, it is recommended that the fluid system cleanliness levels of NASA Specification SE-S-0073 be adopted as minimum baseline requirements.

3) The mathematical formulations developed during this program (Table 27) provide a basis for predicting the differential pressure per unit area of filter medium at any flow rate and for any given fluid whose viscosity and density are known. These formulae can be used to determine the amount of surface area required in a filter for a given initial pressure drop. The rate of differential pressure build-up during the service life of a filter is influenced by many factors most of which were categorized and quantified during this program. The main influence bearing parameter was found to be the particle size composition of the contaminant or type of dirt introduced into the filter. It was demonstrated during this program that accurate performance data concerning the amount, size and type of contaminant generated by operating components can be determined by conducting wear analysis tests using a radioactive tracer technique.

In the absence of such test data, it is recommended that each filter installation be analyzed in terms of total duty cycle cleanliness levels in order to make certain that the filter is adequately sized.

4) The reliability requirements of filtration devices necessitate the establishment of controls over the physical/chemical characteristics of the wire cloth medium, as well as over the manufacturing processes and cleanliness levels employed during fabrication.

It is recommended that all filters used on the Shuttle program be procured in accordance with the requirements of NASA JSC Specification SE-F-0044 which defines all necessary parameters of medium selection, filter sizing, manufacturing environment and quality control.

SECTION 7  
REFERENCES

7.1 TERMINOLOGY AND DEFINITIONS

**BOILING PRESSURE TEST:** The boiling pressure test, often called "open bubble point" or "mean flow pore size" test, is an extension of the bubble point test and is used as a nondestructive method of measuring the average, or mean, pore size of a filter.

**CLEANLINESS LEVEL:** Same as contamination level.

**COLLAPSE PRESSURE:** The maximum differential pressure which the filter element assembly must be able to withstand without collapse and continue to meet the filtration requirement.

**CONTAMINANT TOLERANCE:** The minimum weight of standard contaminant which can be added at the inlet of a filter under specified flow, fluid temperature and pressure conditions before the pressure loss exceeds a maximum allowable value.

**CONTAMINANT TOLERANCE INDEX:** The weight, in milligrams, of a specified particulate contaminant (e.g. AC Coarse Dust) which will cause a specified rise of pressure differential across one square inch of filter medium at a specified unit flow rate (GPM/in<sup>2</sup>) of particular fluid.

**CONTAMINANT TRANSMISSION RATING:** The maximum particle size found in a fluid sample taken during contaminant tolerance tests.

**CONTAMINATION LEVEL:** A measure of the particulate contaminant found in a specified volume, usually 100 ml., of fluid sampled from a system at a specific time and location. Contamination levels can be expressed either in terms of quantity of particles in various size ranges, or gravimetrically in terms of milligrams. Occasionally, in determining contamination levels, a differentiation is also made by physical properties, chemical composition or particle shape. In addition, the amount of dissolved material (NVR) is often specified.

**CONTAMINATION TOLERANCE LEVEL:** The maximum particle size, or the contamination level of a fluid system, which cannot be exceeded without affecting the specified performance, reliability or life expectancy of the components of the system.

**DEPTH FILTER:** A filter consisting of a porous material, or combination of materials, with long, often intricate, interstices which trap particulate contaminants within these flow paths.

**DUTCH WEAVE:** A weave wherein the shute wires are of a smaller diameter than the warp. The shute wires are driven up against each other.

**FILTER MEDIUM:** The material, or combination of materials, which are used to remove solids from a fluid stream.

**FILTER RATING, "ABSOLUTE":** The size, in microns, of the largest hard spherical particle (i.e., glass beads) which would be removed by the filter under steady flow (blow-down) conditions.

**FILTER RATING, "MEAN" OR "AVERAGE":** The size, in microns, of the average, or mean, pore diameter of a filter. This rating, though not yet in common usage, can be determined by various standard destructive and nondestructive tests, and is a good indication of the filter's ability to remove particles smaller than its absolute rating, as well as of the particle size to which the filter is most sensitive with respect to clogging.

**FILTER RATING, "NOMINAL":** Nominal ratings attempt to assess the ability of a filter to remove a specified percentage of particles which are smaller than the absolute rating by assigning a "nominal" rating value, which is smaller than the absolute rating.

**FILTERED CONTAMINATION LEVEL:** The cleanliness level of the fluid, as sampled at the outlet of a filter at rated flow and under conditions which simulate system operating conditions. The sample includes all fluid passed through the filter and all particulate matter regard-



less of source.

**FILTRATION EFFICIENCY:** Same as Retention Index.

**GLASS BEAD RATING, (GBR):** Same as Absolute Rating.

**GSE AND FACILITY FILTER:** "Roughing" Filter of adequate surface area to remove gross amounts of contamination over long periods of operation with a minimum service. This type of filter is generally much larger than typical vehicle filters.

**INITIAL BUBBLE POINT:** The air pressure, in inches of water, required to produce the first bubble in a liquid of known surface tension, in which the element is wetted, immersed to a known depth and pressurized with air. The bubble point test is a non-destructive method of verifying the maximum pore size of a filter medium, and is presented in detail in SAE ARP 901.

**INITIAL ELEMENT CLEANLINESS:** The cleanliness level of a new filter, or element, prior to installation as measured per ARP 599.

**INLET FILTER:** A small modular filter, most frequently installed by component manufacturers at the inlet of components, or at test connections leading to the components, for the purpose of protecting the component from harmful contaminants with particular emphasis on the size distribution, rather than the quantity of contaminants to be encountered.

**MASS FLOW CYCLE:** The total throughput, in weight or volume of fluid, which will pass through a filter during an entire Mission Duty Cycle, including check-out of the filter and system.

**MAXIMUM PARTICLE SIZE:** The maximum size measurement of a single solid particle along its longest dimension.

**MEDIA MIGRATION:** The presence of any form of particulate contaminant identifiable as filter material, or the supporting structure in the fluid, which has passed through a filter.

**NON VOLATILE RESIDUE (NVR):** The residue remaining in an evaporated sample of filtered liquid. Generally expressed in milligrams per 100 milliliters of fluid.

**PLAIN DUTCH SINGLE WEAVE (PDSW):** A dutch weave, also known as corduroy or basket weave, with relatively thick warp wires, spaced well apart, and with thinner shute wires passing over one - under one and driven together in a single layer. Light is transmitted at an angle to the face of the cloth. A relatively easy cloth to clean with excellent flow characteristics.

**PLAIN SQUARE WEAVE (PSW):** A square weave, wherein each shute wire passes over one warp and under the next. Ordinary household window screen is an example of PSW.

**PLAIN WEAVE:** A weave in which the shute wires pass over one warp and under the next adjacent warp.

**PRESSURE DROP (CLEAN):** The pressure differential across a clean filter unit including inlet and outlet ports under specified condition of flow rate, temperature, pressure and flow medium. SAE ARP 24 B presents recommended methods in detail.

**PRESSURE DROP AT RATED CONTAMINANT CAPACITY:** The pressure differential across a filter unit, including inlet and outlet ports, after a specified weight of a contaminant having a specified particle size distribution has been added on the inlet side of a filter, under specified condition of flow rate, temperature, pressure, and flow medium.

**RETENTION INDEX:** The percentage of contaminant retained on or within a filter medium when a known amount of specified contaminant is injected upstream of the medium at a specified flow rate of a specified fluid.

**REVERSE DUTCH WEAVE:** A weave wherein the shute wires are of a diameter larger than the warp. All shute wires are driven together.

**SILTING:** Silting is an accumulation of minute particles in the size range normally not counted, of sufficient quantity to cause haze or partial or complete obscuring of gridlines (or any portion of the grid) on a test filter membrane, when observed by the unaided eye or under 40-power magnification. The particles may range in size up to 5 microns.

**SQUARE WEAVE:** A weave in which the shute wires are separated from each other as they cross the warps so that a square opening is formed.

**SURFACE FILTER:** A filter which performs its filtering function by separating particulate contamination at the upstream surface of the media.

**SYSTEM FILTER:** A "Mass Filter" usually installed by the system manufacturer for the purpose of reducing the total system fluid contaminant level input to a point where the component inlet filters can provide adequate protection at the interface to the critical operating components during the mission duty cycle of the system.

**TOTAL CONTAMINANT INPUT:** A gravimetric expression of the amount of particulate contamination entrained in a system fluid which flows through a filter or other components during a Mass Flow Cycle. This value can be calculated empirically by multiplying the gravimetric contamination level by the total volume of fluid passing through the filter and dividing by the volume of the fluid sample upon which the contamination level was based.

**TOTAL FILTERABLE SOLIDS:** The weight of material which can be filtered from a specified volume of fluid using a filter of specified size rating and type, generally 0.45 micron membrane type.

**TRANSMISSION INDEX:** The ratio of maximum particle size of particulate which passes through a filter to the glass bead rating of the filter. The transmission index of a filter medium is related to the tortuosity of the flow paths through the medium.

**TWILLED DUTCH DOUBLE WEAVE (TDDW):** Also known as "micronic" cloth, it is essentially a Twilled Dutch Weave, wherein a double layer of shute wires is woven into the warp by offsetting the shutes. The flow path is quite tortuous, and the cloth is "light tight." The surface is quite smooth. There are twice as many shute wires of the same diameter as in PDSW. This weave has excellent control of glass bead filtration rating and is used for critical filtration applications. It is difficult to clean.

**TWILLED DUTCH SINGLE WEAVE (TDSW):** A dutch weave with a single layer of shute wires which overlap each other slightly. Each shute wire passes over two-under two. This weave is usually not as tight as PDSW and is not usually used where glass bead filtration rating is critical. It has excellent flow characteristics, and will transmit light at an angle to the face of the cloth.

**TWILLED SQUARE WEAVE (TSW):** A square weave wherein each shute wire passes over two and under two warp wires. This weave is usually used when wire diameters are small to avoid the relatively sharp bends associated with over one-under one construction. Weaves finer than 250 X 250 are usually of twilled construction.

**TWILLED WEAVE:** A weave in which the shute wires pass over two consecutive warp wires, then under two consecutive warps.

**UNIT FLOW RATE:** The flow rate through a filter medium divided by the area of medium exposed to flow.

**USEFUL SERVICE LIFE:** The time, in terms of volume of fluid or hours of system performance, before a filter develops a pressure differential due to contaminant build-up, which adversely affects the performance of an operating component of the system.

**VEHICLE INTERFACE FILTER:** A final filter frequently installed as an assembly with the ground half of a quick disconnect, or at the end of a flex hose, in order to control the cleanliness of fluids entering the vehicle during flushing, check-out, purging or loading operations. The major emphasis of this filter is placed on filter cleanliness, in order to assure fluid cleanliness reliability without the need for continuous monitoring or sampling.

**WARP WIRES:** The strands of a filter cloth which are set-up in the loom prior to weaving the fill wires. The warp wires run the length of the finished screen.

## 7.2 LIST OF PUBLICATIONS

| <u>Ref. No.</u> | <u>Title and Author</u>  |
|-----------------|--|
| 1               | <u>High Performance Wire Cloth Filters</u> , Joseph Wiley, Jr.   |
| 2               | <u>Adding Ultrafine Filters to Aircraft Hydraulic Systems</u> , F.E. Bishop  |
| 3               | <u>How Lockheed Keeps Contamination Out of Hydraulic Systems During the Manufacture of Large Cargo Aircraft</u> , Stanley F. Reid  |
| 4               | <u>The Mechanics of Wire Cloth Filter Flow</u> , Royce F. Church, Ernest C. Fitch, Robert E. Reed, and Roger H. Tucker   |
| 5               | <u>Synthetics - Flow of Fluids in Filter Cloths</u> , A. Ruchton, D.J. Green, H.E. Khoo  |
| 6               | <u>Filtration and Separation Technology in Eastern Europe</u> , Dr. Peter Buentzschel  |
| 7               | <u>Membrane Filters for Control of Contamination</u> , Ahmad El Hindi  |
| 8               | <u>Auditing Microscopic Particle Analysis</u> , M.C. Miyaji  |
| 9               | <u>Formal Description of Ultrafiltration</u> , E.N. Lightfoot  |
| 10              | <u>Delivery of Clean, Dry, Thermally Stable Jet Fuel to Supersonic Aircraft by In-Field Catalytic Filtration</u> , Arnold M. Leas  |
| 11              | <u>Inorganic Fiber Fabrics</u> , John Goodrich   |
| 12              | <u>Flexing Fatigue of Glass-Fiber Filter Cloth</u> , R.E. Hicks and W.G.B. Mandersloot   |
| 13              | <u>Military Fuels Decontamination</u> , L.L. Stark   |
| 14              | <u>Sand Filterbeds</u> , Kou-ying, John L. Cleasby   |
| 15              | <u>The Method of Calculation for Non Uni-dimensional Filtration</u> , Mompei Shirato, Kazumasa Kobayashi   |
| 16              | <u>Diesel Fuel Filtration</u> , L.A. Yemel'yenov   |
| 17.             | <u>Experimental Investigation on the Relationship Between the Separation Efficiency of a Nonclogging Fiber Filter and Its Porosity</u> , Pavel Gruner                          |
| 18              | <u>Developments in Membrane Processes</u> , J.W. Carter  |
| 19              | <u>High Viscosity Polymer Melt Filtration</u> , Robert R. Biemer, Nicholas Nickolaus   |
| 20              | <u>Filterability of Distillate Fuels - Effect of Fuel Viscosity and Related Factors</u> , A.J. Chiantella, J.E. Johnson  |
| 21              | <u>The Separation of Water from Oil by the Principle of Coalescence</u> , Clifford H. May  |
| 22              | <u>Advances in Filtration Theory</u> , R.L. Baird  |
| 23              | <u>Verification of Particulate Cleanliness Levels in Fluid Systems</u> , Milt W. McKenzie  |
| 24              | <u>Filtering System for Aerospace Water Reclamation</u> , Klaus Feindler   |
| 25              | <u>Filtration Up to Spacecraft Requirements</u> , Dr. David B. Pall, President   |
| 26              | <u>New Approaches to Contaminant Control in Spacecraft</u> , Eric E. Auerbach, Sid Russell   |
| 27              | <u>Hydraulic Fluid Contamination Study</u> , N.F. Robinson   |
| 28              | <u>Fluid Contamination Survey of 143rd Naval Aircraft Hydraulic Systems</u> , Douglas Aircraft Co., Inc.   |
| 29              | <u>Hydraulic System Contamination</u> , James W. Parker  |
| 30              | <u>Decontamination of Hydraulic Fluids and Dynamic Hose Study</u> , Systems Engineering Group  |
| 31              | <u>Cigarette Filter Tips</u> , U.S. Patent Office  |
| 32              | <u>Automatic Plating - Solution Filter Changes it Own Media</u>  |
| 33              | <u>AEC/NASA Symposium on Contamination Control - Current and Advanced Concepts in Instrumentation and Automation</u>   |
| 34              | <u>Proceedings of the OAR Research Application Conference</u> , U.S. Air Force   |
| 35              | <u>Model for Predicting Pressure Drop and Filtration Efficiency in Fibrous Media</u> , Lloyd Spielman, Simon L. Green  |
| 36              | <u>Rarefied Gas Flow Through Ultra-fine Filtering Media</u> , T.E. Scott, M.W. Milligan  |
| 37              | <u>Technical Data Manual and Design Guide for the Control of Particulate Contamination in Aerospace Fluid Systems by Means of Controlled Filtration</u> , (Wintec Corp., 1/69) |

38 Apollo Fluid Systems Cleanliness Evaluation (10/12/65)  
39 The Maturing Concept of Keeping Clean, Space Age News, 11/68  
40 Contamination Control, J.W. Parker, USAF  
41 Effect of Contamination on Servovalves, George F. Meagher, Moog Inc., 2-62  
42 An Analog Simulation of the Effect of Particle Contamination on Electrohydraulic Servovalve Performance, H.J. Pritchard, Jr., 7/66  
43 Calculating Pressure Drop in Compressed Air Systems, D.G. Faust  
44 Various Test Methods for Identification of Fibrous Contaminants, P.H. Dutch, 10/2/62  
45 Filtration and the Aircraft Industry, P.A. Smith  
46 Realistic Filtration Levels Set for Hydraulic Servosystems, Hydraulic/Pneumatic Power and Control/ Product Engineering, 2-12-68  
47 Filtration Media, Which One Does Which Job Best? Charles Snow, 10/61  
48 Fluid Storage and Deterioration, Leo E. Gatzek and R.F. Connolly  
49 Jet Fuel Contamination and Its Removal, C.L. Aubrey  
50 Media and Filtration Mechanics, Ting C. Tao, 3/23/66  
51 Particle Counting, A Breakthrough In, R.F. Connelly, 7/64  
52 Microscopic Sizing and Counting Techniques Using Globe and Circle Methods, R.D. Cadle  
53 The Nature and Behavior of Contaminant Particulate Matter, J. Wray  
54 A Method For Measuring Solid Particulate Matter in Fluids, R.L. Snuggs, Jr.  
55 Porous Metals, Fluid Flow Through, L. Green, Jr., and Polduwez, T.  
56 Porous Media, Dispersion-Permeability Correlation in, Journal of the Hydraulics Division of ASCE, 3/63  
57 Sensors: Industry, Aerospace Redesign Filters to Cope with Clogging, Product Engineering 2/12/68  
58 Wire Gauzes, A Correlation of the Resistance to Air Flow of, P. Grootenhuis  
59 Wire Mesh in Flow Research, Dr. Walter Wuest, 2/62  
60 Mathematical Models for the Flow and Filtration Characteristics of Multi-Layered Wire Cloth Filter Media, R.H. Tucker, OSU  
61 Concepts on Description of Contamination Levels, OSU, 10/67  
62 Fluid Contamination Project, Report No. 4, OSU  
63 Correlation of Hydraulic Component Contamination Tolerances with Filtration Capabilities, Dr. E.C. Fitch, Jr., OSU  
64 Contamination Levels and Tolerances in Hydraulic Systems, E.C. Fitch, Jr., OSU  
65 Filtration Mechanics Project, NASA/OSU/1967/1968  
66 The Mechanics of Wire Cloth Filter Flow, Royce F. Chruch, Ernest C. Fitch, Robert E. Reed, Roger H. Tucker, OSU, 1965  
67 Calibration of the Model PC-202 HIAC Automatic Particle Counter, NASA Filtration Mechanics Project  
68 Study of Filtration Mechanics and Sampling Techniques, OSU  
69 The Development and Verification of Theoretical Models and the Performance of Wire Cloth Filter Media, R.E. Tucker, OSU  
70 Proceedings - Fluid Power Research Conference, OSU, 7/25 - 26/67  
71 Study in the Field of Fluid Contamination and the Feasibility of Employing a Sonic Method for the Removal of Foreign Materials, A.G. Comer, O.L. Burchett, Joel Gilbert, 8/59, OSU  
72 Effects of Vibrations on Filtration, R.E. Reed, OSU, 10/66  
73 The Mechanics of Wire Cloth Filter Flow, R.F. Church, E.C. Fitch, R.E. Reed, R.H. Tucker, OSU, 10/65  
74 Contamination Factors, Determination of Hydraulic, In the Development of an Aircraft Weapons System, William N. Bickel, NAR  
75 Contamination - Stock Mix of Apollo RCS System Contaminants

- 76 Particle Evaluation, Dr. Charles J. Rebert, NAR
- 77 Particulate Matter Characterization, Laboratory Manual, For North American Aviation, Inc.
- 78 B-70 Contamination Experiment...Influence of Contamination in the YJ93-GE-3 Engine Fuel System, Morris G. Hocutt, NAR
- 79 Contamination Control, Philosophy for, For Aerospace Vehicle Fluid System Components, G. Vern Von Vihl, The Martin Company
- 80 Sensors, Contamination, Martin Marietta Corp.
- 81 Design and Development of a 1000 F. Hydraulic System, Part 1, Investigation, William E. Mayhew, WADC, 7/69
- 82 Drag Devices, Investigation to Determine the Feasibility of Using Inflatable Balloon Type for Recovery Applications in the Transonic Supersonic and Hypersonic Flight Regime, Part II, Mach 4 to Mach 10 Feasibility Investigation, W.C. Alexander, WADC, 12/62
- 83 Aerospace Hydarulic Systems, A Problem in, Which Can be Improved by Proper GSE and Better Operations Practices, James W. Parker, WADC
- 84 Contamination Level in Flight Control Systems, Criteria For, Vernon R. Schmitt, WADC, 10/66
- 85 Advanced Valve Technology, Kenneth D. May, NASA
- 86 Contamination Control Handbook, Sandia Laboratories, NASA, 2/69
- 87 Contamination Control and Its Importance to Manned Space Flight, Charles F. Warnock, NASA
- 88 Contamination Control Research and Development Program, Quarterly Status Report, D.T. Norton, and J.S. Koonce, NASA, 12/17/64
- 89 Handbook for Contamination Control on the Apollo Program, NASA, 8/66
- 90 Monograph, Liquid Rocket Lines, Bellows, Flexible Hose, and Filter Design Criteria, C.M. Daniels, Rocketdyne
- 91 Pre-Cleaning Filters, Contamination Report, W.A. Riehl, and Hawkins, C., NASA
- 92 Investigation of Propellant Valve Leakage Phenomena in Apollo Service Module Reaction Control System Rocket Engine, George J., Petino, Jr., NASA
- 93 Interim Summary Report on the NASA-MSC-WSTF Filter Test Program, 3/31/70, TR-121-013
- 94 General Specification, Filters Wire Cloth Type, NASA-MSC Specification SE-F-0044
- 95 Specification, Spacecraft Chemical and Fluid Cleanliness Requirements, NASA-MSC Specification C-6B, 6/27/67
- 96 Engineering Evaluation Test Report TR-161 For Grumman Aircraft Engineering Company, Covering LM, GSE, Propellant Loading Final Filters, Wintec Corporation, 4-17-68
- 97 Design Report - Cluster Filter Element, Marquardt Corp.
- 98 Post Testing HR-3P Propellant Filters LSC 310-125-1B, LSC-310-125-1B, J. Duzich, Grumman Aircraft, 8/29/67
- 99 Report on a Contaminant Loading Test Plan for Evaluation Fluid Components in Relation to Acceptance Cleanliness Levels, J.R. Esquerre, Grumman Aircraft, 9/11/64
- 100 Results of Cleanliness Test on Three Apollo Filters, P/N NA5-28156, J. Keller, Rocketdyne
- 101 Dirt Holding Capacity Test, NA5-28156 Apollo Propellant Valve Inlet Filter, J.P. Keller, Rocketdyne, 10/11/65
- 102 Results of Vibration on Three Apollo Propellant Valve Filters, P/N NA5-28156, J.P. Keller, Rocketdyne, 10/11/65
- 103 Sampling Dynamic Fluid Systems, John A. Mitchell
- 104 Survey of Conatmination in Rocket Propulsion Fluid Systems, G.F. Tellier, J.W. Lewellen, H. Standke, Rocketdyne, 11/67
- 105 Orifice Screen: Final Report Development of Screen-Protected Orifices for the Atlas MA-5 Propulsion System, Rocketdyne, 8/27/65
- 106 Investigation of the Formation and Behavior of Clogging Material in Earth and Space Storable Propellants, TRW, 11/69

- 107 The Theory of the Design of Rotary Filamentary Filters for the Continuous Removal of Particulate From Fast Flowing Gases, B.W. Soole, TRW
- 108 Aircraft Fuel Filtration, Peter A. Reiman and Arthur D. Little, Inc.
- 109 Development of High Flow Hydraulic System Filters, Peter A. Reiman and Arthur D. Little, Inc., 7/65
- 110 Filtration in Modern Fluid Systems, Bendix Filter Division, 9/64
- 111 Filtration: Gravimetric Conversion of Particle Count Data, Fred W. Cole, Bendix Filter Division, 2/68
- 112 Particle Count Rationalization, Fred W. Cole, Bendix Filter Division, 3/66
- 113 Filter Ratings and Particle Count Rationalization, Fred W. Cole, Bendix Filter Division, 3/66
- 114 Proceedings, 6th Annual Technical Meeting and Exhibit, American Association of Contamination Control
- 115 Filtration Level, Determining the Optimum, D.V. Basham, ASME
- 116 Flow and Filtration Characteristics of Wire Cloth, R.H. Tucker, Peter Dransfield, R.E. Reed, ASME, 8/68
- 117 Hydrogen Gas on Metals at Ambient Temperature, Effects of, J.R. Campbell, Battelle Memorial Institute, 11/56
- 118 Porous Materials, Evaluation of, for Boundary-Layer Control, David E. Debeau, Battelle Memorial Institute, 11/56
- 119 Fluid Contamination: Source, Definition and Control, Tadamasa Yoshiki, SAE
- 120 GUARD... Garrett Unified Automated Reliability Data System, Garrett Aircsearch
- 121 Filter Evaluation Program Addendum, Marquardt Corporation
- 122 Strainer Tests: Valve Inlet Strainer Pressure Drop Tests for the Apollo SM/RCS Propellant Control Valve, H.H. Deboe, Marquardt Corporation, 7/67
- 123 How to Select the Filter for Your Application, Purolator
- 124 A Glossary of Filtration Terms, Purolator, 4/63
- 125 Fluid Power Design Forum "Contamination Effects on Servovalves: Is It Really Still a Problem?" Jack Williams, APM
- 126 Effect of Contamination on Fluid System Components, Pall Corporation
- 127 Evaluating Fluid-Filtering Media, Charles H. Hacker, APM
- 128 The Meaning of Fluid Filter Ratings, John A. Farris, APM, 4/65
- 129 New Approach to Selecting Fluid System Filtration, John A. Farris, APM
- 130 Pressure Differential Across Filter Element, Methods of Measuring or Observing, Circle Seal Development Corp.
- 131 Rated Flow of Filter Elements, APM
- 132 A Systematic Approach to Obtaining Meaningful Contamination Data From System Fluid Samples, Erwin A. Kirnbauer, APM, 11/64
- 133 Evaluation of the Acceleration Produced by the Filter Element Tap Test Contamination Measurement Method, Erwin A. Kirnbauer, APM, 1/63
- 134 Transpiration Cooling Through Rigimesh Sintered Woven Wire Sheet, Martin G. Kurz, APM, 3/64
- 135 What About Automatic Particle Counters? D.R. Walker, McDonnell Douglas Astronautics Company, 5/69
- 136 Automatic Particle Counters for Hydraulic Fluids, Part I, Calibration, D.R. Walker McDonnell Douglas Astronautics Company, 5/63
- 137 Hydraulic Filters: Clean Fluid for Hydraulic Systems, D.R. Walker, McDonnell Douglas Astro. Co.,
- 138 Filtration Study: Studies on Filters for Missile Hydraulic System, W.A. Riehl and Hawkins, C., ABMA, 6/60
- 139 Contamination Effects, Servos: Effects of Servovalve Contamination: Hydraulic and Valve Forces, H.L. Huggett, ASTM, 11/62
- 140 Valve Assembly - Solenoid, Fuel Report of Tests On, Aerotest Laboratories, Inc. 8/64
- 141 The Physics of Flow Through Porous Media, A.E. Scheidegger, University of Toronto Press, 1957